UNIVERSITY OF LIVERPOOL

HIV-1 persistence during ART

Thesis submitted in accordance with the requirements of
The University of Liverpool for the degree of Doctor in Philosophy

By

Alessandra Ruggiero

June 2016

Declaration of Authorship

I declare that except where indicated by specific reference in the text, this work is my own work. Work done in collaboration with, or with the assistance of other, is indicated as such and acknowledged.

……

Alessandra Ruggiero

June 2016

Acknowledgments

I wish to express my gratitude to everyone that helped and supported me through my PhD experience. First, I would like to thank my primary supervisors Prof. Anna Maria Geretti for giving me the opportunity of joining her research group and for guiding me through the whole process. Thank you to my second supervisor Dr. Georgios Pollakis for his constant and useful feedback and support.

I wish to thank all patients and the ERAS team for their contribution; the Immunology Diagnostic Service of the Royal Free Hospital for the immunology tests; Dr Mark Hopkins at the Royal Liverpool University Hospital for CMV and EFV testing; Dr. Matthew Strain, Mr Stephen Lada and Prof. Douglas Richman for performing the 2-LTR circular HIV-1 DNA assays. I am grateful to Prof. Linos Vandekerckhove for allowing me to spend some time with his group at the University of Gent and achieve competence in the Alu-gag assay; thanks also to Dr. Ward De Spiegelaere for his guidance. Thank you to Dr. Alessandro Cozzi-Lepri for the help on data analysis. Thank you also to the SSAT team for patient's recruitment.

I am very grateful to Prof. Bill Paxton for the scientific discussions on my project and for the invaluable support during my PhD and during my writing up.

I would like to thank all my "ex-colleagues" from the Geretti group for their untiring support over the years. I would like to thank Maria and "my" student Lydia for their contribution to produce data on total and integrated HIV-1 DNA; the research technicians for generating soluble markers and virology data for the ERAS study.

Thank you to my friends: the "Cool Ronald Ross" group for the limitless support and a special thank you to Lindsay and Jordan for the language-related help. Thank you to my Italian friends in Liverpool and in Italy for their love and support.

Last but not least I thank my family: my parents, my sister and her husband, my nephews, my mother and sister in law. Thank you to my husband Giovanni, this work is dedicated to you above everyone else for your limitless love, support and patience.

Abstract

HIV-1 persistence during ART

Alessandra Ruggiero

Antiretroviral therapy (ART) suppresses HIV viremia, but it does not eliminate the stable cellular reservoir of integrated viral DNA that is generated early during infection. As a consequence, low levels of HIV are detected in patients with consistent viral suppression (HIV-1 RNA<50 copies/ml) in CD4 cells in different body compartments including plasma, peripheral cells and CD4 T-cell subsets.

We first explored the levels of HIV-1 RNA below the cut-off of clinical assay (HIV-1 RNA load<50 copies/ml, herein referred to as 'residual viremia') in a group of patients who switched from Atripla to Eviplera due to toxicity. Furthermore, we studied HIV-1 DNA and RNA loads in peripheral blood of patients with stable virological suppression (HIV-1 RNA<50 copies/ml) while being on first line-ART with 1 NNRTI and 2 NRTIs. The measured virological markers included the residual HIV-1 RNA load in plasma quantified by an ultrasensitive assay; total and integrated HIV-1 DNA in both peripheral blood mononuclear cells (PBMC) and the CD4 T-cell subsets using quantitative PCR methods; 2-LTR circular HIV-1 DNA in PBMC using droplet digital PCR assay. Furthermore, a panel of cellular and immunological markers of immune activation, as measured by flow cytometry and ELISA assay respectively, were available for the analysis. Additionally we explored alternative methods to quantify and to study HIV-1 persistence.

In patients that switched from Atripla to Eviplera we observed that overall the patients showed maintained virologic suppression until the end of the observation; however, 4 patients experienced virologic rebound with HIV-1 RNA>50 copies/ml and this was predicted by a progressive increase in residual HIV-1 RNA levels over time.

Patients on suppressive ART were studied with a cross sectional approach and we observed detection of residual HIV-1 RNA and 2-LTR circular DNA in a proportion of patients and total HIV-1 DNA in PBMC the whole study group. Additionally, we found that residual HIV-1 RNA levels and total HIV-1 DNA were associated with sCD27 and CD8+HLA-DR/DP/DQ+ T-cells, respectively. Following setting-up of the Alu-gag qPCR assay, we measured integrated HIV-1 DNA in PBMC and we confirmed the association with $CD8^{+}$HLA-DR/DP/DQ^{+} T-cells.

In the context of assay development, we proposed the Alu-5LTR assay as an alternative to the Alu-gag assay for integrated HIV-1 DNA quantification and preliminary results showed increased sensitivity. Furthermore, we identified and characterized the tools needed to set up an *in vitro* system to study direct and cell-to-cell HIV-1 infection.

Results from my thesis showed the importance of residual HIV-1 RNA monitoring to detect virus rebound. Moreover, patients on suppressive ART for a long period showed HIV detection in plasma and in cells which was associated with high levels of immune activation, suggesting a role for the host immune environment in HIV persistence. In the context of assay developments for more sensitive quantification of integrated HIV DNA reservoir, our proposed Alu-5LTR assay as described in this thesis may be a potential alternative.

TABLE OF CONTENTS

LIST OF FIGURE

LIST OF TABLE

LIST OF ABBREVIATIONS

ABC	Abacavir
AIDS	Acquired immune deficiency syndrome
APC	Allophycocyanin
ART	Antiretroviral therapy
AZT	Zidovudine
BL	Baseline
bp	Base pair
ART	Active antiretroviral therapy
CD4	Cluster of Differentiation 4
CD8	Cluster of Differentiation 8
CDC	Centre for Disease Control and Prevention
CI	Confidence interval
CMV	Cytomegalovirus
CNS	Central nervous system
CSF	Cerebrospinal fluid
Ct	Cycle threshold
CTL	Cytotoxic CD8 T-cells
d4T	Stavudine
DDI	Didanosine
ddPCR	Droplet digital PCR
DMEM	Dulbecco's modified eagle medium
DMSO	Dimethyl sulfoxide
EDTA	Ethylenediaminetetraacetic acid
EFV	Efavirenz
ELISA	Enzyme-linked immune-enzymatic assay
ENV	Envelope
FBS	Fetal bovine serum
FITC	Fluorescein isothiocyanate
FTC	Emtricitabine
Gag	Group specific antigen protein
GFP	Green fluorescent protein
HEK-293	Human Embryonic Kidney 293 cells
HIC	HIV-1 controllers
HIV	Human immunodeficiency virus
HLA	Human leukocyte antigen
hrs	Hours
hs-CRP	High-sensitivity C-reactive protein
IL	Interleukin

INSTI	Integrase strand transfer inhibitor
IQR	Interquartile range
IS	Internation standandard
IUMP	Infectious unit per milliliter
kb	Kilobase
L	Litre
ln	Natural logarithm
LPS	Lipopolysaccharide
LTR	Long terminal repeats
MGB	Minor groove binding
MHC	Major histocompatibility complex
nm	Nanometer
NNRTI	Non-nucleoside reverse transcriptase inhibitor
NRTI	Reverse transcriptase inhibitor
NVP	Nevirapine
OD	Optical density
OFR	Open reading frame
PBMC	Peripheral Blood Mononuclear cells
PBS	Phosphate-buffer saline
PCR	Polymerase chain reaction
PE	R-phycoerythrin
PFA	Paraformaldehyde
PI	Proteinase inhibitor
qPCR	Quantitative PCR
RNAseH	Ribonuclease H
RPMI	Roswell Park Memorial Institute medium
RPV	Rilpivirine
RRE	Rev responsive element
RT	Room temperature
sCD14	Soluble CD14
SIV	Simian Immunodeficiency virus
TAR	Tat responsive elements
TDF	Tenofovir disoproxil
TE buffer	Tris-EDTA buffer
VLS	Viral load suppression
VOA	Viral outgrowth assay
VS	Virological synapses
VSV	Vesicula stomatitis virus
WHO	World health organisation
X^2	Chi-square test
xg	Centrifugal force

CHAPTER 1: General introduction

The human immunodeficiency virus (HIV) is a member of the family Retroviridae, genus of *Lentivirus* (International Committee on Taxonomy of Viruses, 2002). HIV is transmitted through body fluids (blood, sexual fluids, and breast milk) and causes the acquired immunodeficiency syndrome (AIDS). At the end of 2014, 36.7 million people globally were living with HIV-1 and 1.1 million people died from AIDS-related illnesses (UNAIDS, 2016). Although the discovery of HIV dates back to the early 1980s, a vaccine is still not available. Antiretroviral therapy (ART) however effectively suppresses virus replication preventing disease progression and mortality.

1.1 HIV discovery, origin, and genetic diversity

In1981-1982, the Morbidity and Mortality Weekly Report (MMWR) from the Centre of Disease Control and Prevention (CDC) in the U.S. described cases of *Pneumocystis carinii* pneumonia and Kaposi sarcomas (Hymes et al., 1981) occurring among healthy young men, predominantly sexually active homosexuals. In line with the fact that such opportunistic infections were known to be limited to severely immunosuppressed (Walzer et al., 1974) individuals, clinical examination of the patients confirmed that all of them had immune deficiency. Similar clinical conditions were soon reported in Western Europe (Vilaseca et al., 1982, Rozenbaum et al., 1982, Francioli et al., 1982), and not only in men having sex with men, but also in heterosexuals, subjects who had received blood or blood products, and intravenous drugs users. The common denominator was a "cellular-immune dysfunction related to a common exposure" (Centers for Disease, 1981), and in 1982 CDC officially defined the condition as the Acquired immune deficiency syndrome (AIDS).

In 1983, Luc Montagnier and Françoise Barré-Sinoussi from the Pasteur Institute in Paris first isolated a retrovirus from cultures of T lymphocytes derived from a patient with cervical lymphadenopathy, which they named Lymphadenopathy-Associated Virus (LAV) (Barre-Sinoussi et al., 1983). A few months later in 1984, Robert Gallo and colleagues at the National Cancer Institute of Bethesda in the U.S. announced the discovery of a new T lymphotropic virus in patients with AIDS that they named Human T-Lymphotropic Virus type III (HLTV-III). Sero-epidemiological analyses supported the hypothesis that HLTV-III was the etiological agent of AIDS (Popovic et al., 1984). In the same year, Jay Levy's group isolated an AIDS-associated virus (ARV) from 22 patients with AIDS. In 1985, the full genomes from LAV, HTLV-III, and ARV were obtained demonstrating that they were variants of the same virus (Ratner et al., 1985). In May 1986, the International Committee on the Taxonomy of Viruses named the virus the Human Immunodeficiency Virus (HIV).

Later in the same year a second retrovirus was isolated from two West African patients, which were hospitalized in Portugal and France, and presented with AIDS-like clinical features (Clavel et al., 1986). The new virus was called HIV type 2 (HIV-2), while the former was renamed HIV type 1 (HIV-1). In 2008, Luc Montagnier and Françoise Barré-Sinoussi were awarded the Nobel Prize in Physiology or Medicine for the discovery of HIV-1.

HIV-1 is more transmissible and virulent than HIV-2 and as such it is more widely spread globally, whereas HIV-2 has a more limited geographical distribution in West Africa and countries with links to this region. Phylogenetic analysis of viral sequences shows homology between HIV and the simian immunodeficiency virus (SIV) which infects non-human primates including chimpanzees (Hahn et al., 2000) (SIV_{cpz}) and gorillas (SIV_{gor}). Three genetically distinct HIV-1 groups originated by independent zoonotic transmission events of SIV_{cpz} into humans: group M ("major"), group O ("outlier"), and group N ("non-M, non-O") (Ward et al., 2013, Gao et al., 1999). One

additional group named P was identified recently which appears to be more directly related to SIV_{gor}. Group M strains are responsible for the HIV-1 pandemic and nearly 95% of AIDS cases. Group O, N, and P strains are mainly found in Central and West Africa.

HIV-1 group M is further divided into nine subtypes: A, B, C, D, E, F, G, H, J, K that show inter-subtype genetic variability in the *gag* and *env* genes (Geretti, 2006). HIV-1 diversity is mainly caused by fast replication cycle of the virus coupled with the high error prone rate of the reverse transcriptase (RT) enzyme (Preston et al., 1988, Jacobs et al., 2014). Within these subtypes, recombinant forms have been identified by full-length genome sequence and they can be classified either as unique recombinant forms (URFs) or circulating recombinant forms (CRFs). URFs are defined as recombinant viruses that have been found in only one individual or an epidemiologically linked cluster and they do not show evidence of spread; CRFs are recombinant viruses that have been identified in at least three epidemiologically unlinked individuals (Geretti, 2006). Currently, 75 different CRFs have been described (HIV sequence database, 2016).

1.2 The viral life-cycle

1.2.1 Virion structure

Similar to other retroviruses, HIV-1 consists of an enveloped particle approximately 100 nm in diameter (Figure 1.1). The virion envelope (ENV) consists of a lipid bilayer membrane, derived from the host cell, and a viral trimeric envelope protein complex. Each trimeric structure comprises three surface glycoproteins named gp120 and three trans-membrane protein named gp41. Underneath the viral envelope, the matrix protein (Matrix, MA, p17) surrounds the viral capsid, which consists of the major capsid protein (CA, p24) and the nucleocapsid protein (NC, p7p9). The capsid contains two identical

molecules of single stranded RNA and three viral enzymes: protease, integrase, and reverse transcriptase (RT) (Barre-Sinoussi, 1996).

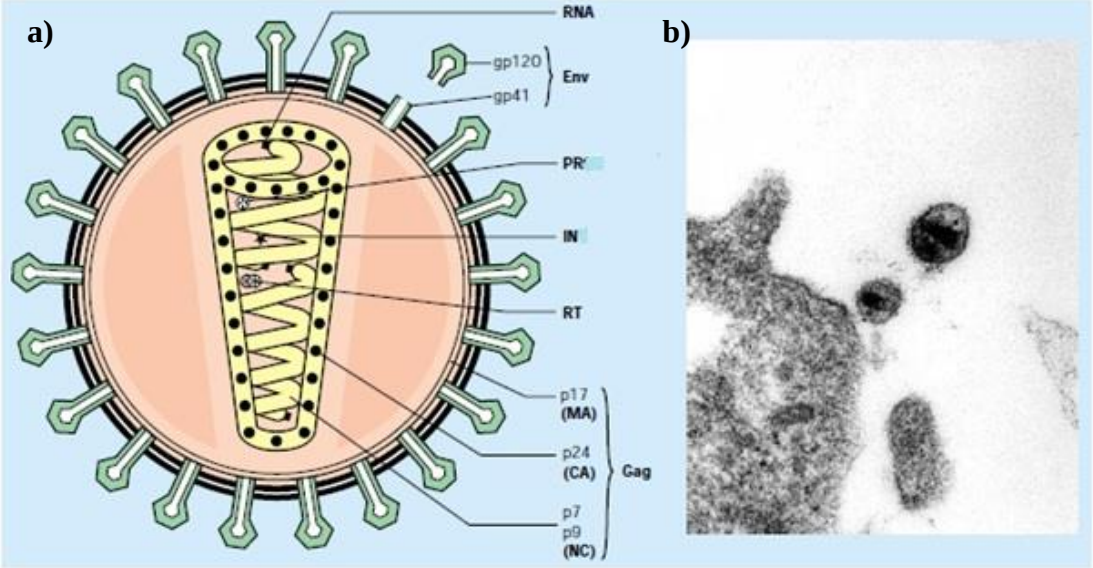

Figure 1.1 Virion structure

(*adapted from Barré-Sinoussi, the Lancet 1996). Schematic picture (a) and electron micrograph (b) of a HIV-1 particle. Env= envelope; PROT = protease; INT= integrase; RT= retro-transcriptase; MA= matrix; CA= capsid; NC= nucleocapsid protein.*

1.2.2 Genome and proteins

The HIV-1 genome is approximately 9.2 kb in size and contains nine open reading frames (ORFs) which encode 15 distinct proteins (Watts et al., 2009). At the two edges of the genome there are two long terminal repeats (LTRs): the 5' LTR contains transcription regulatory factors, while the 3'LTR contains the polyadenylation site. A schematic representation of the viral genome organization is given in Figure 1.2.

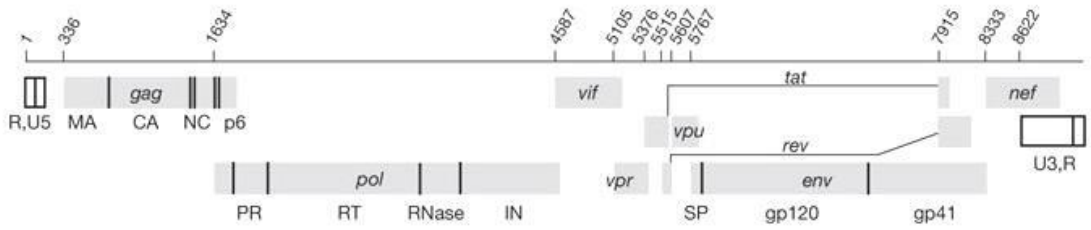

Figure 1.2 HIV-1 Genome

(adapted from JM Watts et al., Nature 2009). The full genome contains 9 open reading frames (ORF): gag, pol, vif, tat, vpu, vpr, rev, env, nef. Grey boxes= ORF; white boxes= LTR as they appear in the virion. MA= Matrix; Ca= capsid; NC= nuscleocapside; PR= protease; RT= retro-transcriptase; IN=integrase; SP= signal peptide.

Three of the nine ORFs encodes for polyprotein precursors that undergo further processing: Gag (p55), Gag-Pol (p160) and Env (glycoprotein, gp160). P55 is cleaved by the viral protease enzyme to produce the matrix, capsid, nucleocapsid, and p6 proteins. These viral proteins are fundamental for virus assembly, as discussed further below in the text.

Gag-Pol precursors encode for the viral enzymes which will be contained into mature viral particles. Some poly-protein undergoes autocatalysis and the first enzyme to be produced is protease, which is responsible for processing the other gag-pol proteins (Pearl and Taylor, 1987, Yang et al., 2012) to yield the RT and integrase enzyme. RT is involved in three enzymatic processes: reverse transcription of the viral RNA into DNA, RNAseH activity to mediate the degradation of the RNA strand in the RNA-DNA duplex (Sarafianos et al., 2009) obtained from the reverse transcription, and DNA polymerase activity to produce a second strand of DNA. RT lacks proof-reading activity, creating a highly favourable condition for HIV genetic evolution during

replication. The integrase enzyme regulates the integration of the linear viral DNA produced by RT into a host chromosome (Li et al., 2011).

The Env precursor gp160 is digested by host furin-like protease (Stein and Engleman, 1990) to produce a typical spike conformation comprising the gp120 sub-unit on the viral surface, which mediates binding of the viral particle to the CD4 receptor and one of several co-receptors on host target cells. Three gp120 glycoproteins are attached non-covalently (Pancera et al., 2010) to three gp41 proteins, which are trans-membrane proteins responsible for the fusion between the virus and the cellular membrane.

The other six ORFs encode for 6 accessory proteins that do not require further processing: tat, rev, vif, vpr, nef, vpu. Tat and Rev are two *trans-activating* proteins. Tat regulates viral genome expression, including transcription of the three polyproteins and synthesis of the full viral genome, by binding the Tat responsive element (TAR) situated within the viral genome. Rev is involved in the export of messenger RNA from the nucleus to cytoplasm. Vif is the viral infectivity factor and it is required for production of infectious virions by inducing degradation of the intracellular APOBEC protein, which exerts antiviral activity by inducing an inactivating hyper-mutation in the HIV-1 genome. Vpr or viral protein R is involved in viral transcription, cell cycle control, infectivity and nuclear import of the HIV-1 DNA pre-integration complex. Nef or negative regulator factor sustains infection by interaction with human cellular functions, including down regulation of the expression of the human leukocyte antigen (HLA) genes that encodes the class I major histocompatibility complex (MHC), thus facilitating viral escape from immune recognition. Vpu protein is known to assist the budding of the newly formed virions from the infected cells membrane.

1.2.1 Virus replication cycle

The HIV-1 replication cycle requires approximately 24 hours to be completed (Perelson et al., 1996) and it includes a series of sequential steps (Figure 1.3).

1.2.1.1 Binding and fusion with host cells

The HIV-1 envelope spikes mediate the initial phases of infection. Gp120 has a high affinity for the CD4 receptor that is expressed on the surface of different cell types including T-cells (Kwong et al., 1998), macrophages, dendritic cells (DC), hematopoetic stem cells, and astrocytes (Iordanskiy et al., 2013). After the binding of gp120 to the CD4 receptor, the envelope spikes regions V1-V2 and V3 region are re-arranged to from a bridging sheet structure that enables the exposure of the co-receptor binding site (Kwong et al., 1998, Liu et al., 2008). Two molecules have been identified as the major co-receptor *in vivo*: the α-chemokine receptor (CXCR4) and the β-chemochine receptor CCR5. Depending on which co-receptor is used to enter the cells, HIV-1 strains can be classified as: CCR5 tropic (R5) if using only the CCR5 co-receptor, CXCR4 tropic (X4) if using only the CXCR4 co-receptor, or dual tropic if using either CCR5 or CXCR4. An HIV-infected individual may show different a mixture of R5, X4 or dual tropic virus and in this case is defined as being mixed tropic (M). Regardless the routes of transmission, R5 tropic viruses are preferentially transmitted and drive the initial phase of HIV infection. Individuals with homozygous genetic defects in the CCR5 receptors (Δ32 deletion) are naturally resistant to HIV infection (Hutter et al., 2009). Co-receptors expression varies depending on cell types; in particular CCR5 is predominantly expressed on the surface of macrophages and a subset of memory CD4 T-cells, whereas CXCR4 is constitutively expressed on many cell type, including CD4 T-cells and macrophages (Este and Telenti, 2007).

Binding of the co-receptor induces a disruption of the interaction between the gp120 and gp41 and results in an extended gp41 conformation (Roche et al., 2015, Roux and

Taylor, 2007). In this extended state, gp41 C-terminal domain is anchored to the viral membrane and the highly hydrophobic N-terminal fusion peptide of gp41 is free to insert into the host cell membrane. This early exposed gp41 conformation is termed pre-hairpin intermediate (PHI) (Sackett et al., 2009). Following insertion into the host cell membrane, the extended gp41 folds back into a stable trimer-of-hairpins in a six-helix bundle (6HB) structure where the C-terminal and the N-terminal domain are in close interaction. This conformational change, called final state hairpin conformation, is needed for the contact between the viral and host membrane (Jiao et al., 2015) resulting in the formation of a fusion pore (Melikyan et al., 2000) through which the viral content is delivered into the cellular cytoplasm.

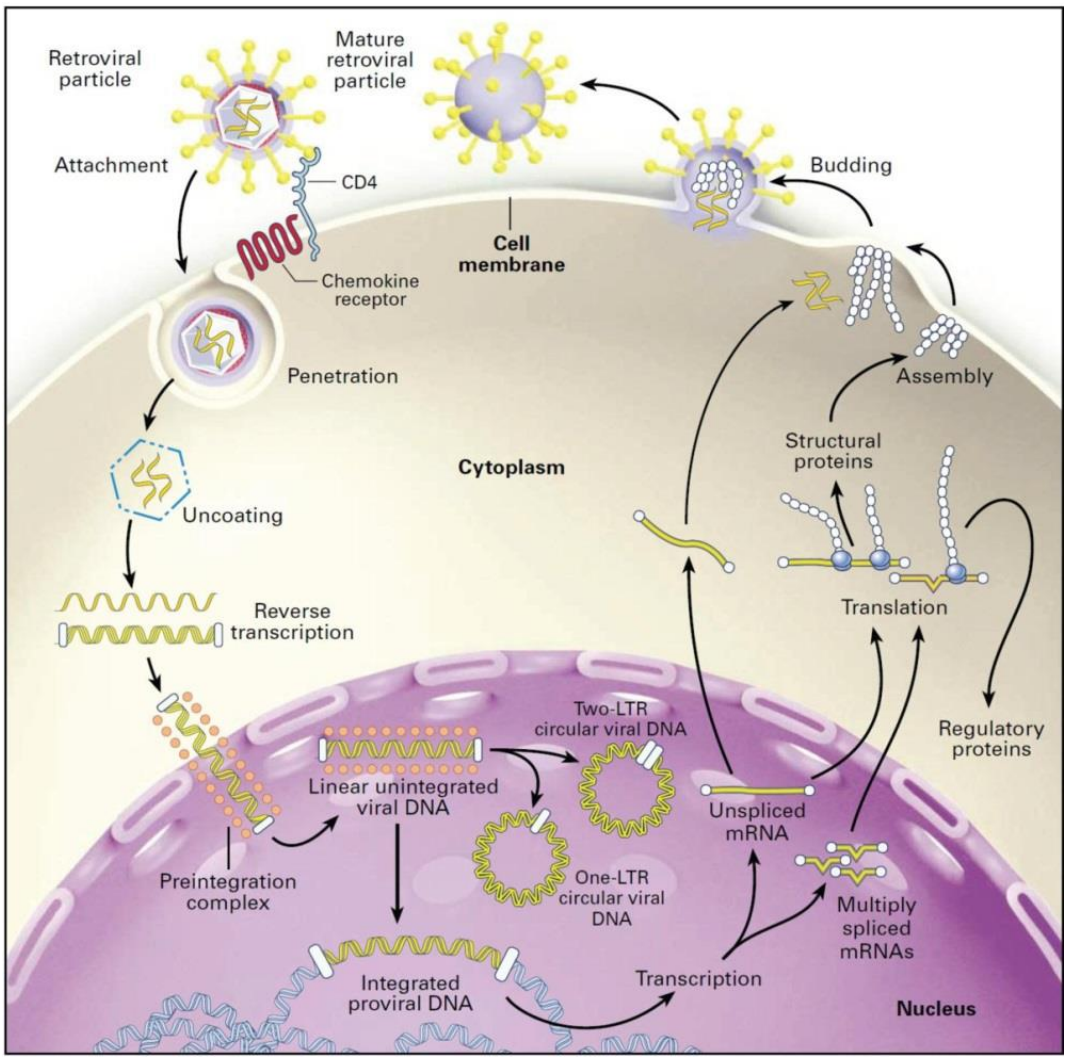

Figure 1.3 HIV-1 cell cycle

Adapted from Pasternak AO et al. 2013 (Pasternak et al., 2013)

1.2.2 Uncoating, reverse transcription and nuclear import

After entering the cells, HIV undergoes uncoating (Ambrose and Aiken, 2014) and the RNA genome and associated enzymes are injected into the cytoplasm. This is followed by reverse transcription of the viral RNA into double stranded DNA prior to import into the nucleus for integration into the host genome. The capsid dissociation occurs in proximity of the nuclear membrane, thus allowing passage of the viral genome through the cytoplasm without intracellular DNA sensors (Rasaiyaah et al., 2013).

As described before, the RT enzyme is responsible for the reverse transcription that initiates with the binding of a host transfer RNA ($tRNA^{Lys3}$) primer to a primer binding site (PBS) situated at the 5' end of the positive single strand viral RNA. Primer binding allows the viral polymerase to copy the 5'into minus DNA viral strand: this step generates DNA/RNA hybrid that acts as substrate for RNase H activity of the RT which degrades the RNA strand, leaving the nascent viral DNA. This DNA sequence includes the repeated sequence of the viral genome (called R, repeat) that are identical at the 5' and 3' end. Therefore, the free nascent viral DNA can bind its complementary sequence at the 3' end of the viral RNA. This step is known as minus strand transfer and it allows the polymerase to continue the elongation of the minus strand viral DNA from the 3' end towards the 5' end. As the DNA synthesis proceeds, RNase H degrades the RNA from RNA/DNA hybrids excluding a specific region called polypurin tracts (PPT). These regions, in particular one situated towards the 3' end of the viral RNA, serve as primers for the synthesis of the positive DNA strand that copies the 5' end including the U3, R and U5 sequence but also the first 18 nucleotides of the $tRNA^{Lys3}$. RNase H partially degrades the tRNA facilitating the exposure of a region at the 3' end of the plus viral DNA that is complementary to the PBS sequence at the 5'end of the minus viral DNA. Following the pairing of the two regions (plus-strand transfer), both the minus and plus DNA strands are extended until the entire DNA is double stranded and with same end sequences containing U3-R-U5 regions (long terminal repeats, LTR).

Migration of the viral DNA towards the nucleus is regulated by the pre-integration complex (PIC) that includes viral (e.g., p17, p24, RT, integrase and vpr) and cellular proteins (Jayappa et al., 2012), which engages nuclear pore proteins (NUP) such as NUP358 and NUP153 to promote the translocation of the viral genome into the nucleus.

1.2.2.1 Virus integration

This reaction happens in three steps which are catalysed by the integrase enzyme, which exhibits two distinct catalytic activities: the 3' processing and the strand transfer (Kvaratskhelia et al., 2014). During the first step, the 3' end of the linear viral DNA is modified to end with a CA_{OH}-3' sequence. The 3-idroxyl group is used by the integrase in the second step during which the integrase generates a cut in the complementary host DNA and covalently binds the 3' ends of the viral DNA to the 5' ends of the target DNA. Following this strand transfer process, the viral and host DNA have unpaired regions of DNA (gaps) that recruits host cellular DNA damage response proteins, including polymerase, nuclease and ligase, which repair these gaps. HIV integration sites are random within the human genome, even though it has been shown that the virus preferentially integrates into actively transcribed genes to ensure efficient gene expression (Marshall et al., 2007). The cellular transcription activator factor LEDGF/p75 has a role in the efficiency of integration by binding both the integrase and the active transcription DNA loci to direct the viral integration in these regions.

A fraction of the linear viral DNA is not integrated and can either become circularised to contain one or two LTR (1- and 2-LTR circular DNA) or can remain linear which then undergoes degradation mediated by the host cell (Butler et al., 2002, Sharkey, 2013). The half-life of these non-integrated forms is still debated, however it is generally accepted that circularised viral DNA is more stable when compared with the linear form and therefore they could be used to track viral persistence.

Integrated HIV DNA, also called *provirus*, has a long half-life and it provides the genetic information for the production of new viral particles, including genomic and messenger RNA.

1.2.2.2 Gene expression

A single strong promoter in the viral 5'LTR region drives viral expression, subjected to regulation by cellular transcription factors that are expressed only when cells are activated (Nabel and Baltimore, 1987). The most important of these transcription factors are the NF-κB factors that bind to the viral genome in two adjacent regions within the 5'LTR. Transcription of viral genes leads to the production of three categories of messenger DNA (mRNA molecules): fully spliced mRNAs that encodes the viral proteins Tat, Rev and Nef, the partially spliced mRNAs that encode for Env and the accessory proteins Vif, Vpr and Vpu and unspliced mRNA that act both as the virion genomic RNA and the mRNA for the Gag/Gag-pro-pol polyproteins. Initial expression produces short fully spliced mRNA that are exported to the cytoplasm by constitutive cellular pathways to generate the viral proteins. Among those, Tat and Rev play key roles in the regulation of HIV-1 genome expression. Tat interacts with a TAR in the 5' end of the nascent HIV-1 transcript and with the positive transcription elongation factor (pTEFb) acts to promote transcript elongation (Cullen, 1991); Rev mediates the transport of the unspliced and partially spliced mRNA from the nucleus to the cytoplasm by interaction with the cellular nuclear export factor CRM1. In the cytoplasm, incompletely spliced mRNA produces Env and the accessory proteins, whereas unspliced mRNA generates the Gag/Gag-pro-pol polyproteins or functions as genomic RNA (Karn and Stoltzfus, 2012).

1.2.2.3 Viral particle assembly, budding and maturation

After the translocation of the viral mRNA into the cytoplasm, viral proteins are synthesized and assembled together to compose the immature viral particle (Freed, 2015). In the rough endoplasmic reticulum (RER), the incompletely spiced mRNA generates the Env spikes composed by gp120 and gp141 which are transported to the secretory pathway to the plasma membrane. In the cytoplasm, the unspliced mRNA is synthesized to produce the Gag-Pol and Gag polyproteins to generate the viral enzymes and the viral proteins that are needed for virus particles assembly. The matrix protein target Gag to the plasma membrane and it is responsible for the incorporation of Env glycoproteins in the virions (Fiorentini et al., 2006). The capsid protein regulates Gag multimerization that will form the conical core of the virion. The NC protein is an RNA binding protein and it recruits the double strand genomic HIV-1 RNA via its interaction with specific sequences at the 5'UTR (Ψ region) in order to coordinate the packaging of the genomic RNA into the virion (Dawson and Yu, 1998). The P6 protein is responsible for the incorporation of Vrp, Vif and Nef. Furthermore, interaction of the p6 domain and the endosomal sorting complex required for transport (ESCRT) mediates the in the release of the virus from the cells, a dynamic process called *budding* (Muller et al., 2002). During budding, the viral protease enzyme promotes the maturation of the viral particle to become an infectious virion. In particular, the Gag precursor is cleaved into the mature matrix, capsid, and nucleocapsid and p6 proteins and this step induces morphological transformation in the virion including the re-organization of CA to form the conical capsid core.

1.2.3 Pathogenesis

In absence of treatment, the course of HIV-1 infection proceeds through three main phases: primary/acute infection, asymptomatic/clinical latency, and the symptomatic phase leading to the development of AIDS as illustrated in Figure 1.4. The symptomatic acute phase is characterized by high viremia, a sharp drop in CD4 T-cell counts,

establishment of reservoirs of latently infected cells, and the development of the anti HIV-1 specific immune response (Douek et al., 2003). This is followed by a drop in viral load and a partial and temporary increase in CD4 T-cell numbers that marks the beginning of a long asymptomatic phase during which the virus production and the CD4 T-cell number decline is slow. When CD4 T-cell count is less than 200 cells/L, the opportunistic tumours and infections that characterize AIDS are established in the patient. The typical rate of progression is such that AIDS and death occur within 10-12 years from initial infection. However, the course of the infection is different from patient to patient and it is driven by a complex interplay between virus replication and host immune responses as described in the following sections.

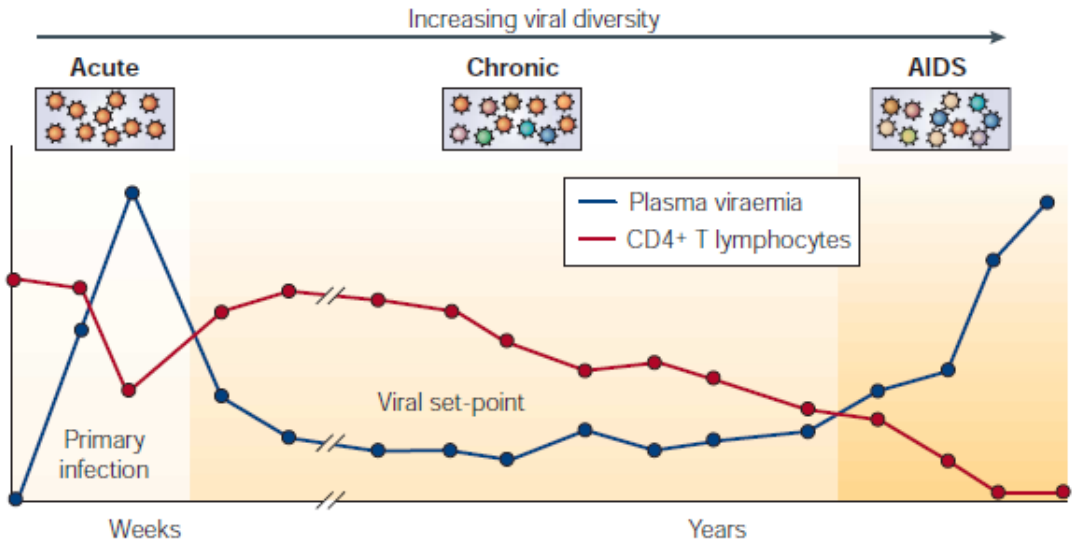

Figure 1.4 Natural course of HIV-1 infection

(adapted from Viviana Simon and David D.Ho 2003, Nature reviews). This figure depicted the reciprocal relationship between plasma HIV load increase and CD4 T-cell loss over the course of infection.

1.2.3.1 HIV transmission and primary infection

HIV can be transmitted via body fluids such as semen, vaginal secretion, blood, and breast-milk. The infection occurs when the virus enters the body via the bloodstream through: shared needles, blood transfusion, damaged skin, mother-to-child transmission during childbirth and via the placenta when transmitted from mother to child during pregnancy. Transmission can also occur through the mucous membranes that cover a variety of body cavities such as conjunctiva, rectum and genital mucosa. Transmission via mucosa can also occur through tissue damage through which HIV can enter. Additionally, these body compartments are highly populated by dendritic cells (DC), macrophages and $CD4^{+}$T cells, all of which express high levels of the CD4 receptor and CCR5 co-receptor and are highly permissive for HIV-1 infection (Keele et al., 2008). As discussed previously R5 virus represents the majority of the transmitted virus. This tropism represents a crucial adaptation of the virus that promotes infection of a subset of effector CD4 T-cells differentiated in lymphoid tissue, which represent a large initial target population (Okoye and Picker, 2013, Brenchley et al., 2004, Picker and Watkins, 2005). Furthermore, the dissemination of HIV throughout the body is also supported by DCs that bind and present HIV to CD4 T-cells. This is a natural immune mechanism that serves to elicit specific immune responses against any pathogens; however in the case of HIV this protective mechanism gives the virus direct access to the CD4 T-cells cells which are its preferred target of infection. HIV-infected T-cells remain sequestered in lymph nodes until a threshold of replication is reached (typically within 2-4 weeks post infection) and subsequently a burst of plasma viremia occurs and the virus is disseminated within days around the body (Weber, 2001). This period is termed primary HIV infection (PHI) and it covers the period between the virus transmission and the completion of the induction of the primary immune response.

1.2.3.2 Plasma viremia and anti-HIV immune response dynamics

Virus transcription in infected cells is positively regulated by cellular factors that bind the HIV-1 LTR and is associated with a high plasma HIV RNA burden that can reach levels that exceed $5x10^6$ copies/ml (Weber, 2001) during the acute phase/primary infection and becomes detectable at around 11 days post-exposure. The viremic peak has been associated with a transient reduction of CD4 T-cells. However, both the plasma viremia burden and the CD4 T-cell loss resolve spontaneously after 2-4 weeks, in association with the presence of a vigorous HIV-1-specific cell-mediated immune response which includes cytotoxic CD8 T-cells (CTL) and CD4 T-helper cells. It is generally accepted that CD4 T-helper cell responses are generally weak during the course of infection, whereas the CTL response seems to be the major effector cells of anti-HIV immune responses (Weber, 2001) and this has been proved by several studies that have reported the presence of HIV genetic variants that can escape from CTL function (Borrow et al., 1994, Phillips et al., 1991). Nonetheless, other mechanisms are believed to be involved in the control of viremia in the initial period following infection. First non-neutralizing antibodies may bind core, matrix and envelope viral proteins and direct virus clearance via Fc receptor mediated mechanism (Weber, 2001). Furthermore, exhaustion of infected CD4 T-cells may reduce virus production without the presence of immune responses (Weber, 2001).

During the following 10-24 weeks the HIV viral load drops to its lowest point known as "set-point". This is different for each patient and is also a predictor of prognosis (Mellors et al., 1996). At this stage, anti-HIV antibody responses are strong and can be detected (seroconversion) and the so-called chronic HIV infection phase/clinical latency phase starts. Over the clinical latency phase, HIV genetic diversity increases to escape from CTL action and its replication is persistent with approximately 10^8 virions produced/day. Interestingly, disease progression is associated with the emergence of X4 tropic virus, normally dual or mixed population, in 50% of untreated patients. It still is not clearly defined if the emergence of X4 variants is a consequence rather than the

cause of disease progression. It has been proposed that the increase in CD4 T-cells expressing CXCR4 in individuals with CD4 counts<400 cells/L may favour the rise of X4 tropic virus (Lin et al., 2005). Of note, this CXCR4 over-expression seems to be mediated by IL-7 produced to induce cell proliferation to compensate for lymphopenia (Brieu et al., 2011, Fiser et al., 2010, Llano et al., 2001). On the other hand clinical studies on patients treated with CCR5 antagonist drugs showed that the appearance of R4 viruses was rapidly outgrown by R5 viruses upon drug discontinuation, indicating a lack of overall advance for X4 viruses when a drug selective pressure is removed (van der Ryst and Westby, 2007).

1.2.3.3 Virus dissemination into target tissues, immune activation and CD4 T-cell loss dynamics

R5-tropic virus dominates acute and chronic infection as described above. Cell targets of primary infection are mainly macrophages, dendritic cells and CD4 T-cells. Studies that tracked HIV-1 viral genotypes in local microenvironment showed that initial propagation of infection is mainly clonal and it is localized in mucosal tissues where cell density is particularly high (Douek et al., 2003). Efficient HIV-1 production and propagation from infected cells to adjacent $CD4^+CCR5^+$ cells is supported by T cell activation that can be mediated by different mechanisms. First, HIV-1 gene products themselves including Nef, Tat, Vpr and Enf can induce T cell-activation independently from T cell receptor pathways; furthermore, the mucosal environment is rich in inflammatory cytokines that can contribute to cell activation (Douek et al., 2003). As result of HIV infection, lymphoid architecture is disrupted as well as the functionality of gut-resident immune cells, e.g. IL-17 and IL-22 producing cells that normally block translocation of opportunistic pathogens that populate the gut lumen (Figure 1.5). Therefore, translocation of microbial products in peripheral blood can in turn induce

monocyte activation that leads to soluble CD14 (sCD14) production. It can also lead to the activation of CD4 and CD8 lymphocytes which results in the expression of activation markers including CD69 (Sousa et al., 2002), CD26, CD38 and the human leukocyte antigen complex HLA-DR/DP/DQ (French et al., 2009) on the surface of these T cells. Similarly there is an increased level of soluble plasma protein expression including neopterin, CD30, CD27 and tumour necrosis factor receptors (sTNFR) (French et al., 2009, Lawn et al., 2001). This generalized status of immune activation increases the damage to the gut barrier which can become independent of virus replication, however immune activation still sustains disease progression and viral production in the absence or presence of treatment (Tincati et al., 2016, Marchetti et al., 2008). In this context, several studies have tried to identify specific markers of immune activation as predictors of disease progression. .

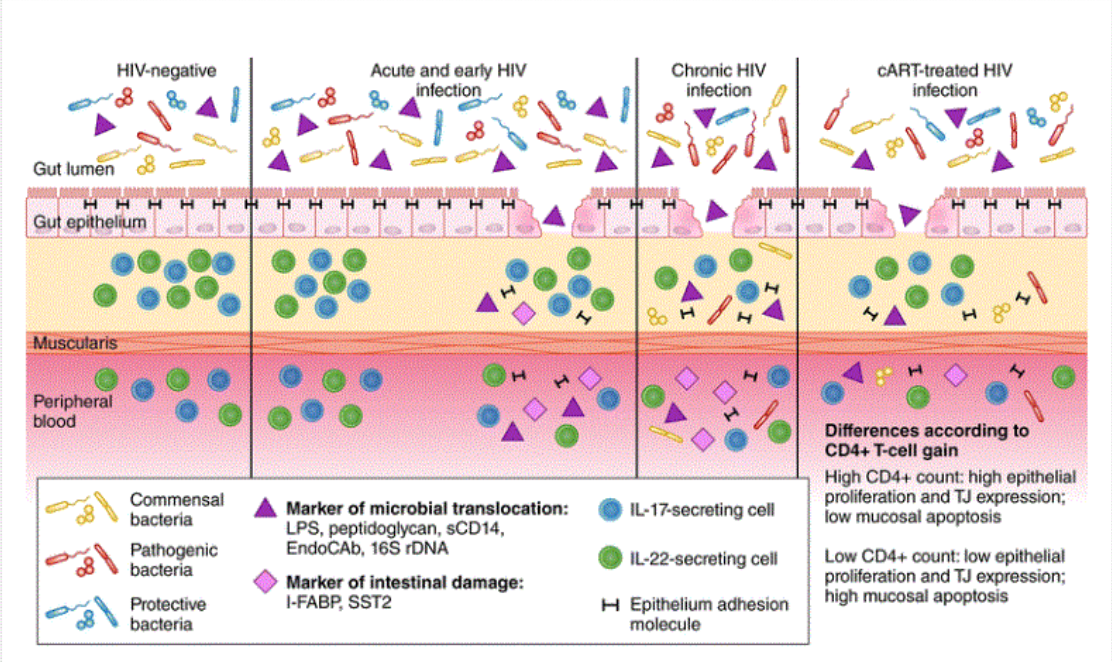

Figure 1.5 GALT damage during HIV-1 infection

Adapted from Tincati C et al 2016. Figure representing the induction of GALT damage during untreated and ART treated HIV-1 infection.

Sandler and colleagues demonstrated that levels of sCD14 and markers of gut epithelial dysfunction, coagulation (D-Dimer) and inflammation (hsCRP and IL-6) correlate with disease progression and mortality in both untreated and treated patients (Sandler et al., 2011). Furthermore, studies have been performed to investigate the clinical significance of the T-cell activation during HIV-1 infection. Among the soluble markers, the soluble CD30 and CD27, two members of the sTNFR family, have been associated with disease progression (Rizzardi et al., 1996, Pizzolo et al., 1994). In the context of cellular markers of immune activation, expression of CD38 and HLA-DR/DP/DQ on CD4 and CD8 T-cells has been described as a strong predictor of disease progression in several studies (reviewed by (Lichtfuss et al., 2011) (Klatt et al., 2013)). Of note, individuals that are naturally capable of controlling HIV-1 progression (long term non-progressors, LNTP) have been found to have lower expression of CD38, HLA-DR/DP/DQ and CD26 (Carbone et al., 2003, Brostrom et al., 1998). The findings of studies on LTNP confirm that higher levels of immune activation might support HIV-1 progression.

Gut damage and microbial translocation are not the only driving forces that support this chronic immune activation: coinfections with other microbes have been implicated as possible responsible factors (Younas et al., 2016). Latent viruses such as Cytomegalovirus (CMV) and Epstein-Barr virus (EBV) reactivated more frequently during HIV infection due to the depletion of $CD4^{+}$T cells and it has been shown that such viruses can drive cell activation during untreated and potentially, treated HIV infection (Klatt et al., 2013, Naeger et al., 2010). In the context of HIV progression, CMV and EBV directly drive CD8 T cell activation and this mechanism contributes to the general immune activation status (Doisne et al., 2004, Paiardini and Muller-Trutwin, 2013). Furthermore, levels of asymptomatic CMV replication in the male genital tract of ART treated HIV-1 infected individuals has been associated with plasma immune inflammation and higher proviral HIV-1 DNA load in peripheral blood mononuclear cells (PBMCs), despite virological suppression.

Chronic immune activation supports disease progression that is associated with rapid and massive CD4 T-cell depletion (mainly of the $CCR5^{+}CD4^{+}$ memory T-cell subset) during acute infection followed by slow and constant T-cell depletion during the chronic phase (Douek et al., 2003). Different mechanisms (Doitsh and Greene, 2016) have been proposed to explain declines in such population. Initially, this depletion was thought to reflect a viral cytopathic effect occurring in productive CD4 T-cell infection (Alimonti et al., 2003). However, while viral production is extensive throughout the course of infection, loss of CD4 T-cell is much slower. This enigma suggests that CD4 T-cell-driven viral cytopathicity alone cannot explain the cell loss and course of disease (Douek et al., 2003). Other studies showed that most of the dying cells in lymph nodes of infected patients were bystander CD4 T-cells that themselves were not actively infected (Finkel et al., 1995). Bystander cell death can be driven by both cellular factors (Herbeuval et al., 2005) (e.g. tumour necrosis factors) and viral factors including HIV-1 Tat, Vpr and Nef which are released by infected cells (Schindler et al., 2006). Moreover, recent studies (Monroe et al., 2014) showed that abortive infection events particularly in resting cells can activate cell suicide as the consequence of the presence of viral DNA within the cells (Munoz-Arias et al., 2015).

Cell depletion towards the end of the chronic phase and the beginning of the AIDS phase has been associated with the emergence of CXCR4 viruses that *in vitro* showed high cytotoxicity for peripheral immature T-cells produced by the thymus to compensate for T-cell loss.

1.3 Antiretroviral drugs

Antiretroviral drugs are classified according to the targeted step in the viral cycle (Figure 1.6). The main targets of antiretroviral therapy are: viral entry by targeting the interaction between HIV and host cell (CCR5 antagonists) and the fusion step (fusion

inhibitors); reverse transcription (nucleoside/nucleotide analogues and non-nucleoside reverse transcription inhibitors, NRTIs and NNRTIs); integration (integrase strand transfer inhibitors, INSTIs) and protease (protease inhibitors, PIs).

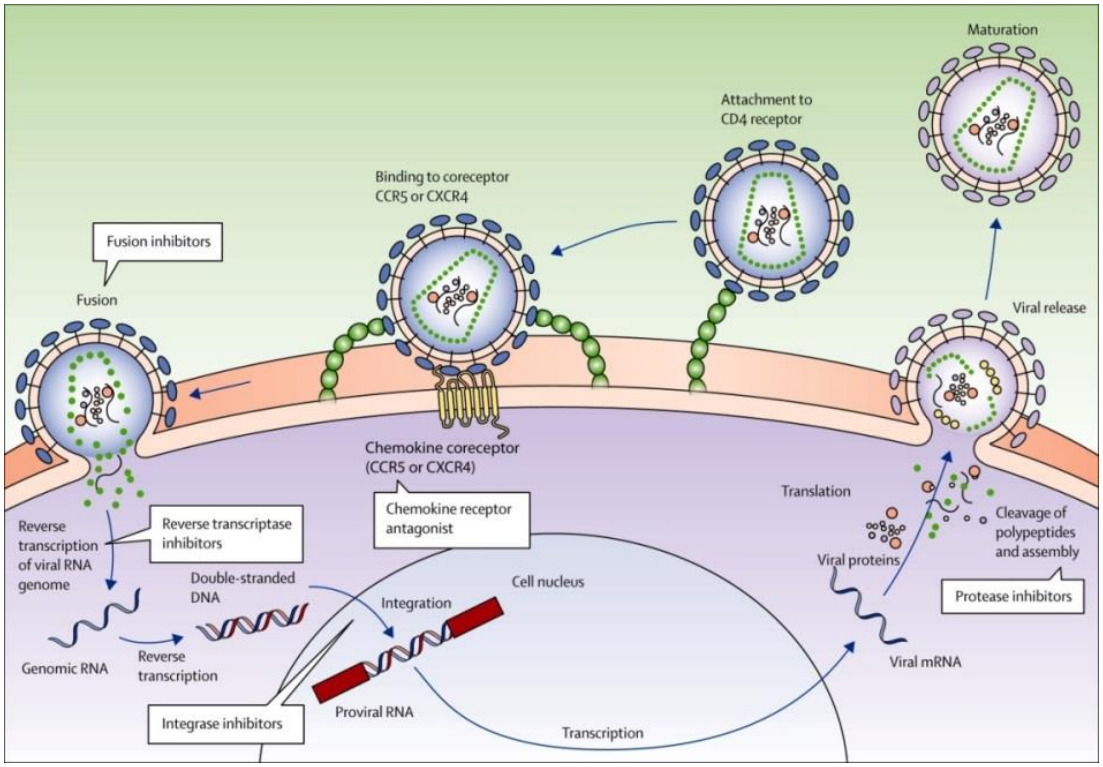

Figure 1.6 Sites of action of available classes of antiretroviral drugs

(adapted from Maartens G. et al. 2014, The Lancet).

The first antiretroviral drug to be licensed in 1987 was the NRTI zidovudine, which was soon followed by other compounds with similar mechanism of action (e.g., lamivudine, stavudine and didanosine). Following the disappointing result of monotherapy and dual therapy with NRTIs, a milestone was achieved in the second half of the 90s with the introduction of the PIs saquinavir and indinavir, and then the NNRTI nevirapine. In 1995-1996 it was demonstrated that it was possible to fully suppress virus replication using a combination of three drugs with two different mechanisms of action, which for many years consisted of two NRTIs plus either a PI or an NNRTI. In more

recent years, INSTIs have emerged as the preferred third agent in triple ART combinations. In addition, studies have explored the use of PI monotherapy and dual therapy with a PI as second agent as shown in 2015 guidelines by European AIDS Clinical Society (EACS Guidelines, 2015). In 2015, 25 antiretroviral drugs were available and they are described in following sections.

1.3.1 Entry inhibitors: CCR5 antagonists and fusion inhibitors

As discussed above, HIV-1 enters the cells via a multistep process that includes: engagement of the CD4 receptor and CCR5 or CXCR4 co-receptors by gp120 and conformational changes of the gp41 envelope protein that leads to fusion between the viral and host membrane.

Maraviroc is the only co-receptor antagonist available. It binds to the transmembrane region of CCR5 (Dorr et al., 2005) on the host cell, and induces a conformational change that inhibits the interaction between the co-receptor and gp120. Given its specific action, patients are tested for viral tropism before starting such treatment.

Enfuvirtide (T-20) is the only fusion inhibitor available. It is a peptide that mimics components of the HIV-1 fusion machinery and displaces them. Specifically, it binds the heptad repeat region 1 (HR1) in the N-terminal domain and prevents the formation of the six helical bundle that is needed to allow fusion.

1.3.2 Reverse transcriptase inhibitors

The RT enzyme is essential for the HIV-1 replication because it allows the transcription of the viral RNA into double stranded DNA prior to integration into the host genome. Blocking this step of the virus cycle is a key aspect of successful treatment. At present,

the RT enzyme can be targeted by either by competitive (NRTIs) or allosteric (NNRTIs) inhibition.

1.3.2.1 NRTIs

Nucleoside and nucleotide RT inhibitors are analogues of the natural deoxy-nucleotides that normally compose DNA molecules. These agents bind the active site of RT competing with the natural substrate and are incorporated by RT into the growing DNA chain. However, NRTIs lack the 3'-hydroxyl group on the deoxyribose, and once incorporated do not allow formation of the phosphodiester bound that is needed for the next nucleotide to be incorporated, resulting in premature chain termination (Parker et al., 1991, Zdanowicz, 2006). There are currently 7 available NRTIs: Abacavir (ABC), Emtricitabine (FTC), Lamivudine (3TC), Zidovudine (AZT), Tenofovir disoproxil (TDF), Didanosine (DDI), Stavudine (d4T). Some of them can be administrated in combined fixed doses such as: Kivexa (ABC plus 3TC), Trizivir (ABC, 3TC, AZT), Truvada (FTC, TDF), Descovy (FTC, Tenofovir alafenamide TAF), Combivir (3TC, AZT).

1.3.2.2 NNRTIs

The NNRTIs do not bind directly to the active site of RT to block its functionality. They bind to a pocket in the p66 subdomain of RT that is near the enzyme active site, causing a conformational change that inhibits the enzyme polymerization activity. Currently licensed NNRTIs comprise Efavirenz (EFV), Etravirine, Nevirapine (NVP), and Rilpivirine (RPV).

1.3.3 Protease inhibitors (PI)

PIs are competitive inhibitors that bind to the active site of the viral protease enzyme preventing binding of Gag and Gag-pol precursor, the natural substrate of the enzyme. Of note, Rabi *et al.* 2013 showed that PIs do not only affect virion maturation, but also block entry, reverse transcription, and post-reverse transcription step: the independent inhibition of multiple distinct steps in the virus replication cycle makes this drug uniquely effective. Currently licensed PIs comprise: Atazanavir (ATV), Darunavir (DRV), Indinavir, Fosamprenavir, Lopinavir (LPV), Nelfinavir (NFV), Ritonavir (RTV), Saquinavir (SQV), and Tipranavir (TPV). PIs have low and variable bioavailability and relatively short plasma elimination half-life; these limits can be compensated by multiple daily administrations, even though this practice may reduce the patient's adherence to the regimen (Cooper et al., 2003). An alternative procedure is to use a small dose of RTV, not for its direct antiviral activity but to inhibit the metabolism of co-administered PIs, thus boosting their concentration and improving their pharmacokinetics, with greatly enhanced activity and more patient-friendly dosing schedules. Recently cobicistat has been introduced as an alternative booster. Co-formulations include ATV and DRV with cobicistat and LPV with RTV.

1.3.4 Integrase inhibitors

The integrase strand transfer inhibitors (INSTIs) block the action of the integrase by binding to its active site and preventing divalent cationic ions from binding to the enzyme catalytic site. To date, 3 INSTIs have been approved: Dolutegravir (DTG), Elvitegravir (EVG), and Raltegravir (RAL). EVG is boosted by co-formulated cobicistat (EVG/c).

In Table 1.1 a list of regimens that are recommended for starting ART in HIV-positive adults is given.

Table 1.1 Regimens recommended for starting ART in HIV-positive adults.

EACS 2016[a]	DHSS 2016	
ABC 3TC DTG		*HLA-B*5701 negative*
TDF FTC DTG		
TDF FTC RAL		
TDF FTC EVG/c		*Pre-treatment estimated CrCl ≥70 mL/min*
TAF FTC EVG/c		*Pre-treatment estimated CrCl ≥30 mL/min*
TDF FTC DRV/r		
TDF FTC RPV		*CD4 count >200 cells and VL <100,000 cps*

[a] *to be released in autumn 2016. EACS= European AIDS clinical society; DHSS= Department of Health and Human Service (USA). CrCl= creatinine clearance.*

The introduction of the multidrug combination therapy for HIV-1 has notably increased life expectancy of HIV-infected individuals. HIV-1 replication is controlled significantly by continuous and uninterrupted therapy. However, if ART is stopped virus replication resumptions quickly. Virological rebound is driven by a pool of infectious HIV-1 provirus within $CD4^+$ T cells and monocytes that populate sanctuary sites located in various body compartments including gut associated lymphoid tissue, peripheral lymphoid tissue, peripheral blood and brain (Chun et al., 2015). This virus reservoir represents a substantial obstacle to an HIV cure, it is established early after initial infection and its levels remain stable during treatment from when patients start therapy and during the chronic phase (Ruggiero et al., 2015, Josefsson et al., 2013). Nonetheless, it has been shown that initiation of ART during the acute phase considerably reduces the size of the viral reservoir (Zhang et al., 1999, Chun et al., 2007). The establishment of the HIV-1 reservoir and the mechanisms that have been proposed to support the viral persistence will be discussed in the following sections.

1.4 HIV-1 persistence during ART

In 1997, Perelson and colleagues demonstrated that HIV-1 RNA concentration in plasma dropped by 99% in the first two weeks of antiretroviral therapy (Perelson et al., 1997). This first decay reflects the combined effect of inhibition of active virus replication with immune-mediated clearance of free plasma virus, which is known to have a short half-life (less than 6 hours). A second, slower phase of viral decay follows as a reflection of the turnover of chronically infected cells. Initial estimates calculated that based on the typical life-span of HIV-infected cells, 3.1 years of suppressive ART would eliminate HIV-1. In the same year, Chun TW (Chun et al., 1997b) demonstrated the presence of a latent HIV reservoir in resting memory CD4 T cells. Two years later, Finzi and colleagues (Finzi et al., 1999) described a model by which a stable reservoir could be established when infected activated CD4 T-cells rather than die as a result of HIV infection return to a resting state, maintaining integrated HIV-1 DNA. They estimated that the mean life of such latent viral reservoir was around 44 months and that viral eradication could have been achieved in 60 years of ART. To date, it is widely demonstrated that plasma HIV-1 RNA and cellular HIV-1 DNA can still be detected even after long period of effective and suppressive ART (Palmer et al., 2008). The source of this persistence has been identified in a pool of latently long-lived infected cells that present integrated HIV-1 DNA at stable levels and with little genetic evolution during treatment (Josefsson et al., 2013).

1.4.1 Latently infected cells: a long-lived viral reservoir

The term ‘viral latency’ indicates a type of persistent viral infection defined as ‘a state of reversibly non-productive infection of individual cell’ (Siliciano and Greene, 2011). In the case of HIV, the ‘individual cells’ are represented primarily by resting memory CD4 T-cells (Finzi et al., 1997). Memory cells include memory stem cells (T_{SCM}) (Gattinoni et al., 2011), defined as $CD45RA^{+}CCR7^{+}CD28^{+}CD95^{+}CD62L^{+}$), central memory cells (T_{CM}, defined as $CD45RA^{-}CD95^{+}CCR7^{+}CD62L^{+}$), transitional memory cells (T_{TM}, defined as $CD45RA^{-}CD95^{+}CCR7^{+}CD62L^{-}$), and effector memory cells (T_{EF}, defined as $CD95^{+}CCR7^{-}CD62L^{-}$) (Sallusto et al., 2004). T_{SCM} and T_{CM} are long-

lived and in a resting state (Buzon et al., 2014b); upon activation after T cell receptor (TRC) triggering (Sallusto et al., 1999), transitional memory cells start proliferating prior to differentiating into T_{EF} (Geginat et al., 2003). *In vitro* studies have shown that activated CD4 T-cells are highly susceptible to HIV infection, whereas resting cell need are significantly less susceptible (Buzon et al., 2014b) in the absence of direct stimulation (Buzon et al., 2014b, Swiggard et al., 2005). Two pathways are proposed to explain the establishment of the viral reservoir. In the dominant pathways, a fraction of infected activated T-cells survive the infection and revert to a resting G_0 state (Siliciano and Greene, 2011) (T_{CM}) while carrying integrated HIV-1 provirus. In the second pathway HIV can directly infect cells in a resting state (Chavez et al., 2015). The two models are not mutually exclusive. In both cases, resting cells create a favourable environment for viral persistence, including a pattern of gene expression that enables long-term survival, and the ability to respond to antigenic stimulation (Siliciano and Greene, 2011). Under these conditions, HIV can persist for a long period in a transcriptionally silent state that protects it from both immune responses and antiretroviral therapy. Of note, *in vitro* studies have demonstrated that these cells can express at least some viral protein in absence of (Pace et al., 2012) virus production. This suggest potential for ongoing stimulation of HIV-specific immune responses during suppressive ART; however, this hypothesis has not been consistently demonstrated and is in conflict with the decrease of anti-HIV CD8 T-cell responses observed over time in treated patients.

The latent reservoir is established early after primary infection (Finzi et al., 1997) and it is refractory to treatment. Interestingly, emerging evidence showed that treatment initiation during primary HIV infection may reduce viral reservoir formation (Ngo-Giang-Huong et al., 2001) and accelerate immune restoration by preserving T and B cell function (Oxenius et al., 2000). In particular, one study identified 14 individuals that were able to control plasma viremia after the interruption of prolonged ART initiated during acute infection (Saez-Cirion et al., 2013).

1.4.2 Mechanisms of persistence

1.4.2.1 Cell proliferation

Memory T-cells can proliferate upon antigenic (antigen-driven proliferation) or cytokine-mediated (homeostatic proliferation) stimulation (Bosque et al., 2011). Antigen-driven proliferation induces cell activation and the cells differentiate into T_{EF}. Activated T-cells can both produce new virus if infected, and become susceptible to infection if uninfected. Both immune recognition and effective ART can block both outcomes, providing a rational for HIV eradication strategies that aim to induce T-cell activation and viral gene expression as a way of reducing the size of the viral reservoir. Several observations support the hypothesis that newly produced virus originating from latently infected cells is unable to produce ongoing rounds of replication. These include the key observation that in stably suppressed patients, any detectable plasma HIV-1 RNA is generally detected at very low copies (1-3 copies/ml) and is typically represented by a few clones (reflecting origin from a relatively small source) that are genetically stable (Josefsson et al., 2013).

Homeostatic proliferation is a natural process aimed at keeping the T-cell count at physiological levels. It is independent of antigenic stimulation and mediated by IL-7 (Boyman et al., 2007, Kondrack et al., 2003) and the proliferating cells can be identified by the expression of the surface marker Ki67 (Coiras et al., 2016). The cells undergoing homeostatic proliferation do not actively produce virus due to low NF-κB induction. However, by multiplying the integrated provirus they provide effective expansion of the viral reservoir (Bosque et al., 2011).

Two independent studies (Maldarelli et al., 2014, Wagner et al., 2014) recently investigated the influence of HIV integration sites on cell proliferation during long-term suppressive ART (>10 years). Integration preferentially occurs within oncogenic genes,

such as MKL2 and BACH2, and can be found to recur within clonally expanded cells. These observations suggest that HIV can promote cell proliferation independently of antigenic or homeostatic proliferation.

1.4.2.2 Ongoing viral replication

Several putative markers of recent virus replication can be measured in subjects receiving seemingly effective ART, including low levels of plasma RNA, intracellular RNA forms, and 2-LTR circular HIV-1 DNA. Whether detection equals ongoing virus replication is debated. However, it is possible to propose that at least a subset of treated patients has low grade virus production ongoing in compartments where drug penetration or activity are suboptimal. Work from Fletcher *et al.* 2014 demonstrated variable drug concentrations in lymphoid tissue relative to peripheral blood, with evidence of viral persistence in tissues with low drug exposure. Deposition of collagen can cause fibrosis (Schacker et al., 2006) and disruption of the lymphoid architecture which may favour the formation of pockets of viral persistence. Intensification with the INSTI raltegravir has also been shown to cause an increase in intracellular episomal HIV-1 DNA (Buzon et al., 2010), which indirectly reflects ongoing virus replication.

HIV-1 also invades the central nervous system (CNS) and HIV-1 RNA levels remain detectable in the cerebrospinal fluid (CSF) despite ART. Some studies have found that HIV-1 RNA levels in the CSF can be higher than those in plasma, a phenomenon called CSF/plasma discordance (Eden et al., 2010, Nightingale et al., 2016) and that it is present in 12% of HIV-1 infected patients that are periodically examined by lumbar puncture. Such evidences have proposed that the CNS can act as a site for viral reservoir, ongoing viral replication and evolution of drug resistance (Garvey et al., 2009, Canestri et al., 2010).

1.4.2.3 Cell to cell virus transmission

HIV can also be disseminated by direct cell-to-cell contact. This process occurs via the assembly of supra-molecular complexes called virological synapses (VS) that ensure contact between the virus-donor cell and the target cell (Jolly and Sattentau, 2005). The VS formation starts with the actin-dependent polarization of the viral proteins Env and Gag to the plasma membrane at the site of the cell-to-cell contact where the CD4 receptor from the uninfected cells has been recruited (Alvarez et al., 2014). Cell-to-cell adhesion is promoted by Env-CD4 interactions and stabilized by cellular adhesion molecules (eg. LFA-1 and ICAM-1,3). Once the interaction between virus donor and target cell is stable, virus is assembled and released into the synaptic cleft before fusing with the target cell (Agosto et al., 2015). This mechanism has been described in the context of virus spread promoted by interaction between dendritic cells and T cells, or between infected and uninfected T cells (Sattentau, 2008) and generally is associated with virus burden in lymphoid tissue where cells density is very high. Of note, macrophages are also able to transmit virus to CD4 T-cells via VS (Kumar et al., 2014); interestingly it has been shown that HIV infected macrophages can attract lymphocytes in their vicinity by secretion of specific cytokines/chemokines (e.g. MIP-1β, MCP-1 and CCL-5) and further promote viral transfer (Herbein et al., 2010). Moreover, other studies have suggested that HIV-1 Nef may alter the physiologic characteristic of the infected macrophages in a way that enhances viral dissemination (Swingler et al., 2003) to CD4 T-cells.

By experimental-mathematical investigation, Iwami S. *et al.* 2015 demonstrated that more than half or virus infections are produced by cell-to-cell infection and this is also reflected in higher viral fitness. Of note, Sigal *et al*. 2013 demonstrated *in vitro* that cell-to-cell virus spread is considerably less sensitive to the action of the RT inhibitors. Similar results were found also by Titanji B.K. *et al.* 2013, who progressed previous work by demonstrating that PIs appeared particularly effective in blocking cell-to-cell transmission. Taken together these findings indicated that different drug classes impact

on the cell-to-cell virus dissemination and potentially on the maintenance of the viral reservoir.

1.4.3 Tools to measure the HIV reservoir

Measuring the viral reservoir, including HIV-1 RNA in plasma and HIV-1 DNA in cells, is paramount to understand viral persistence and to test innovative therapy strategies. Patients with persistent virological suppression, defined as plasma HIV-1 RNA levels below the cut-off of the clinical assay (50 HIV-1 RNA copies/ml), have traces of plasma viral RNA copies (herein referred to as 'residual HIV-1 RNA') that can be measured by ultrasensitive quantitative PCR assay. However, whether detection of so few HIV-1 RNA copies in plasma reflects ongoing viral replication as supported by the integrated HIV-1 reservoir despite suppressive ART, it is still debate. Of note, quantitative PCR assays quantify HIV-nucleic acids without necessarily addressing their integrity and functionality. Not all integrated HIV-1 DNA is replication-competent. Different outgrowth assays have been developed, sharing the common feature that resting CD4 T-cells are isolated from peripheral blood, stimulated to induce global T cell activation, and virus expression, with subsequent infection of CD4 T-cells. Virus production in culture is then measured as p24 concentration or RT activity. Resting CD4 T-cells are broadly defined as cells that do not express the HLA-DR activation marker. They are typically purified from whole CD4 T-cell populations and can generally be defined by the following expression profiles: $CD4^{+}HLA\text{-}DR^{-}CD25^{-}CD69^{-}$ (Laird et al., 2013) or $CD4^{+}HLA\text{-}DR^{-}CD38^{-}$ T cells (Buzon et al., 2014b).

In recent work from an international collaboration (Eriksson et al., 2013), integrated HIV-1 DNA load measured in peripheral blood mononuclear cells showed good correlation with the viral outgrowth assay.

1.4.3.1 Intracellular HIV-1 nucleic acid quantification

Intracellular HIV-1 nucleic acids comprise unintegrated (Sloan and Wainberg, 2011) and integrated (Graf and O'Doherty, 2013, Liszewski et al., 2009) forms of HIV-1 DNA that together constitute the total HIV-1 DNA, and cell-associated RNA (Pasternak et al., 2013). Two quantitative PCR technologies are currently used for quantification: real-time quantitative PCR (qPCR) (Bustin et al., 2009) and digital droplet PCR (ddPCR). The two methodologies show important differences.

In qPCR, the amplification of the target DNA is monitored in real-time: each sample is amplified when the forward and reverse primers alongside a specific probe bind to the target DNA molecule. The probe is a single stranded DNA sequence complementary to the target sequence, flanked by one fluorescent reporter and one quencher molecule. In absence of amplification, the quencher prevents fluorescent emission by the reporter; when target DNA is amplified, the polymerase moves along the template and the quencher is cleaved from the reporter and emits a signal (Figure 1.7a, Taqman chemistry). Fluorescent signal increases by each cycle and reflects the abundance of the target DNA. The number of cycles at which the fluorescence from the amplified samples is higher than the background signals is called threshold cycle (Ct) (Bustin et al., 2009). Higher sample concentration will allow the signal to exceed the threshold sooner, resulting in smaller Ct values (Figure 1.7b). Sample to sample variation resulting from pipetting errors is controlled by adding a passive reference dye that is not amplified during the qPCR: if a well does not present the required amount of passive reference, the reaction is not valid. Quantification of samples is calculated by interpolation of Ct values obtained from known concentration of a validated standard.

a)

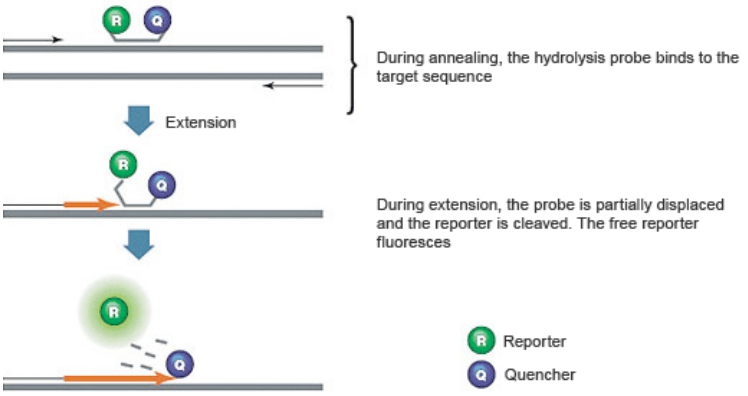

b)

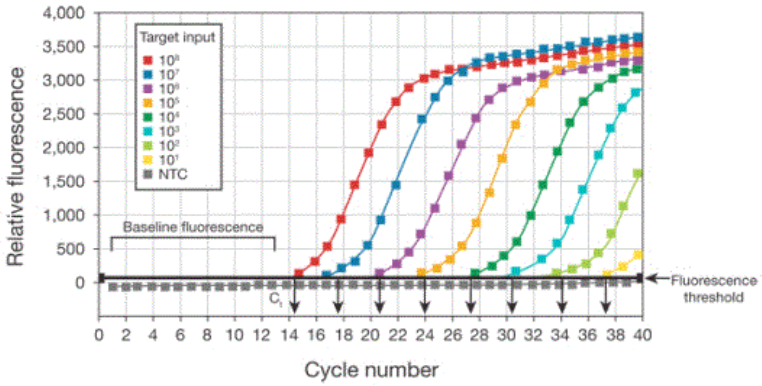

Figure 1.7 Illustration of qPCR principles

a) Adapted from Taqman comics, Real-Time PCR Handbook. Each PCR cycle includes an annealing phase during which the probe binds a specific sequence on the DNA target; an extension phase while the polymerase proceeds with the amplification of the DNA target meanwhile cuts the reporter molecule from the TaqMan hydrolysis probe allowing fluorescent signal to be emitted. b) Adapted from Life Technologies, Real-Time PCR Handbook. Amplification plots depicting fluorescent signal from known quantity of samples. Higher concentrations are reflected by greater amplification that corresponds to lower Ct values.

In ddPCR, a single sample is partitioned into thousands of nano-sized droplets that independently undergo PCR reaction by using a TaqMan hydrolysis probe technology as seen for qPCR; the end-point PCR product is then analysed with a fluorescent reader that scores each single individual droplet as positive or negative for fluorescent signal (Figure 1.8a and b). The fraction of positive droplets (*p*) is inputted into the formula [1.1] that applies Poisson statistics to allow absolute quantification of the target and its Poisson-based 95% confidence interval (CI).

[1.1] copies/droplet= -ln (1-*p*)

a)

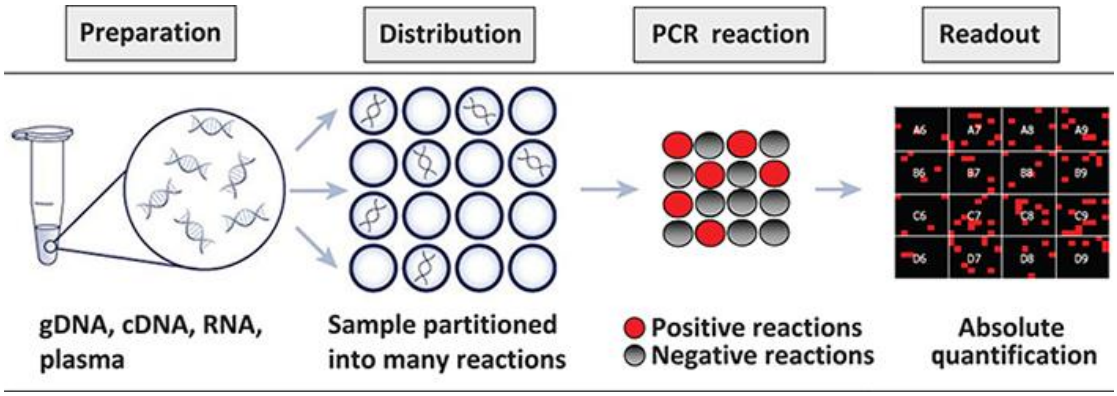

b)

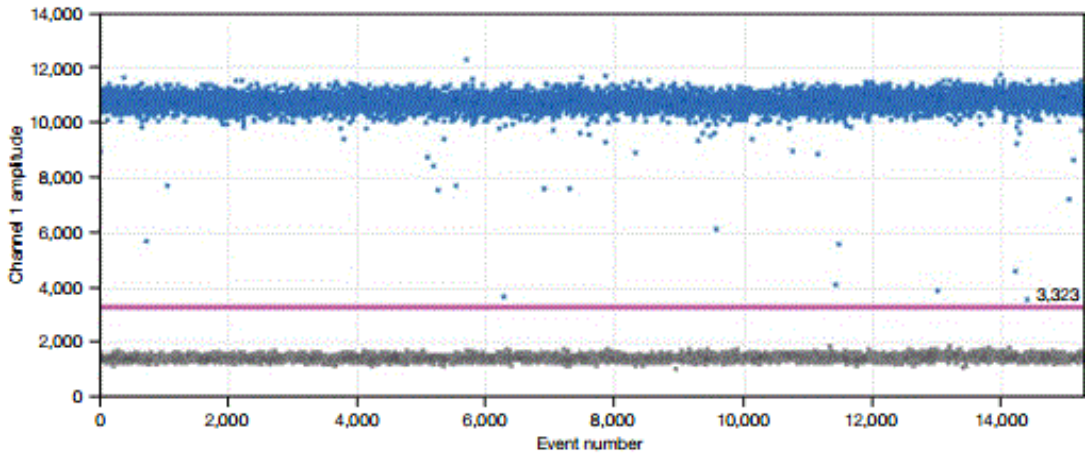

Figure 1.8 Illustration of ddPCR principle

a) Adapted from Thermofisher scientific, Digital PCR system introduction. Cartoon depicting the different steps of the protocol: sample is portioned into single droplets; then qPCR is run and fluorescent signals are red with a fluorescent reader to identify positive (red dots) and negative (grey dots). b) Adapted from Biorad ddPCR Bullettin 6407. Graph showing each droplet (x axis, event number) from one sample that is plotted vs fluorescent intensity (y axis, channel 1 amplitude). Positive droplets are those above the threshold line (pink line here).

The main difference between the two methods is that the ddPCR provides an absolute quantification without requiring an external standard. Both qPCR and ddPCR are currently used to quantify intracellular HIV-1 DNA and RNA, whereas only qPCR assays have been developed for integrated HIV-1 DNA quantification so far.

Una O'Doherty and colleagues developed the Alu-gag PCR assay which can quantify 0.6 proviruses for each 100,000 cells (Liszewski et al., 2009). Integrated HIV-1 DNA is amplified using primers that bind to the human genome and the HIV-1 gag sequence. Following PCR amplification (PCR1), qPCR (qPCR2) is run to produce sample quantification. A standard that contains a known quantity of integrated HIV-1 DNA is run in parallel to determine integrated HIV-1 DNA load in the samples. De Spiegelaere W. and colleagues recently described a variation of the method that uses Ct values obtained by qPCR to calculate absolute number of HIV-1 integration based upon Poisson statistics (De Spiegelaere et al., 2014).

1.4.3.2 Detection of plasma HIV-1 RNA load and virological suppression threshold

With the introduction of highly active triple antiretroviral therapy in the 90s, the HIV-1 RNA levels in plasma ("viral load") became established as the key surrogate marker of treatment efficacy. As described above, viral load spontaneously decline within 6 months of the initial infection to a certain set-point that is a powerful predictor of the rate of CD4 count decline and the risk of disease progression and mortality among untreated patients. Upon ART initiation, viral load is suppressed and the risk of disease progression is reduced. Based on this close relationship with clinical outcomes, continuous viral load suppression below the detection limit of commercially available assays is the key goal of ART. The threshold indicating optimal virological suppression

has changed over time, reflecting the technical evolution of viral load assays (Doyle et al., 2012). First generation assays had a lower limit of detection of 400 HIV-1 RNA copies/ml. Second generation assays had a lower limit of detection at 50 HIV-1 RNA copies/ml. One example of such an assay is the Amplicor v1.5 assay which was used extensively in clinical trials of triple ART and introduced the concept of <50 copies/ml as the desirable level of suppression. With the advent of real-time PCR, third generation assays were developed with lower limits of quantification below 50 HIV-1 RNA copies/ml, which can also qualitatively report HIV-1 RNA detection below the quantification limit (Doyle and Geretti, 2012). Within this group the most widely used are the Roche COBAS TaqMan HIV-1 Test Version 2.0 and the Abbott RealTime HIV-1 VL assay with lower limits of detection of 20 and 40 HIV-1 copies/ml, respectively.

In the research setting, various techniques have been employed to increase the sensitivity of detection down to a few HIV-1 RNA copies/ml in order to measure the 'residual' HIV-1 RNA. These assays have helped elucidate the kinetics of HIV-1 RNA decline in plasma after starting ART. The prototype "single copy" HIV-1 RNA assay was developed by Palmer *et. al* in 2003. In this method, 7 ml plasma volume was ultracentrifuged at 170,000xg for 30' in a Sorvall T-1270 rotor prior to manual RNA extraction. Purified RNA was then reverse transcribed into cDNA and this was amplified by quantitative real time PCR (qPCR), by binding the HIV-1 gag region. To control for the whole process, an internal virion standard consisting of the replication-competent avian sarcoma-leukosis retroviral vector RCAS BP(A) (RCAS) was added to the plasma sample prior to ultracentrifugation and quantified by qPCR in parallel to the HIV-1 RNA. In parallel, known quantity of an HIV-1 and RCAS RNA were run to allow quantification. Results showed viral RNA detection as low as 1 copy/ml in patients on antiretroviral therapy and in that period represented a confirmation of previous predictions (Dornadula et al., 1999) that viremia can persist at low levels that cannot be detected by routine screening.

1.5 Aims of the thesis

Current therapies are effective to drastically reduce HIV-1 replication and to decrease levels of immune activation. However, HIV-1 persists in sanctuary sites and the host immune system functionality appears altered when compared to healthy individuals. A relationship between levels of viral persistence and the host immune system has been proposed, however it warrants further investigation.

In relation to this question, I believed there was scope to quantify levels of the HIV-1 reservoir, measured as residual HIV-1 RNA in plasma and the different HIV-1 DNA forms in cells, in a population of patients that maintained continuous virological suppression while being on 1NNRTI and 2NRTIs for up to 15 years. Furthermore, I explored associations between the different forms of the HIV-1 reservoir and various markers of cellular and immune activation that were previously described as markers of disease progression in the absence of treatment.

I also had the occasion to participate in a clinical trial of patients switching from an EFV based regimen (Atripla) to a non-EFV based regimen (Eviplera) due to cytotoxicity. In this context, I explored the impact of the switch on the virological suppression measured as levels of residual HIV-1 RNA in plasma by an ultrasensitive assay that I first optimized.

Finally, I also worked to optimise the assays used to study the HIV-1 persistence. In particular, I developed a more sensitive technique used to measure the integrated HIV-1 DNA that represents the cellular HIV-1 reservoir. Furthermore, I set up a novel *in vitro* assay that could be used for testing novel drug formulations.

Chapter 2: Materials and Methods

2.1 Study populations and sampling

1) Population of subjects switching from Atripla (coformulated tenofovir, emtricitabine, efavirenz) to Eviplera (coformulated tenofovir, emtricitabine, rilpivirine). The trial was based at the Chelsea and Westminster Hospital in London, but recruitment involved different hospitals as listed in Table 2.1. All subjects had received Atripla for ≥12 weeks, and showed plasma HIV-1 RNA suppression <50 copies/ml, a CD4 count > 50 cells/mm^3, and persistent central nervous system (CNS) toxicity attributed to efavirenz. The treatment regimen was switched to Eviplera and improved CNS tolerability was the primary end-point. Plasma samples were collected immediately before switching (baseline) and at week 4, 12, and 24 after switching and stored on site at -80C until ready for shipment frozen to the University of Liverpool on dry ice (Table 2.1 an overview of available samples is given). Ethics was approved by local authorities; EudraCT registration number was 2012-002205-22 and the study was registered at clinicaltrial.gov (identifier number NCT017701882). All patients provided written informed consent.

Table 2.1 Breakdown of patient's recruitment and samples available for testing for the study on switching Atripla to Eviplera

Hospital, responsible	N patients	Samples available for			
		BL	W4	W12	W24
Chelsea and Westminster Hospital	9	9	9	9	9
Brighton Hospital	15	15	14	15	15
St Mary's Hospital	5	5	5	5	5
Mortimer Market Centre	8	8	8	8	5
Total	37	37	36	37	34

BL= baseline

2) The ERAS population included subjects on first-line ART with two NRTIs plus efavirenz or nevirapine (NNRTI), and showed continuous viral load suppression (<50 copies/ml) from the first six months of therapy up to sampling date, while undergoing ≥2 viral load measurements per year, without transient elevations above 50 copies/ml or treatment interruptions. No patients underwent a change in NNRTI, whereas changes in NRTI were permitted. Recruitment was stratified by duration of ART to range from 1 to over ≥10 years and it was carried out at different centres across the United Kingdom as listed in Table 2.2. Blood samples (40-50 ml) of venous were collected in EDTA tubes and plasma and peripheral blood mononuclear cells (PBMC) were isolated as described below. Until use, plasma samples were stored at -80^{o}C and PBMC in liquid nitrogen. The study was approved by National Research Ethics Service (London-Dulwich) and was included in the National Institute for Health Research Clinical Research Network (NIHR CRN) Portfolio. All patients provided written informed consent.

Table 2.2 Breakdown of recruitment for the ERAS study.

Hospital	ERAS
Royal free Hospital	46
N. Middlesex Hospital	14
St Mary's Hospital	20
Mortimer Market Centre	4
St Thomas' Hospital	3
King College Hospital	4
Royal Liverpool University Hospital	57
Total	148

3) Healthy volunteers with HLA-A2 positive or negative pseudo-type were recruited at the Institute of Infection and Global health (IGH). These cells were used to set up in vitro assay (chapter 7) were the HLA-A2 negative PBMCs were directly infected with free HIV-1 particles (donor cells) and used to infect HLA-A2 positive cells (target cells). The HLA-A2 expression was used to discriminate between donor and target cells. Up to 50 ml of venous blood samples were collected in Heparin tubes and PBMC were isolated as described below and stored in Liquid Nitrogen until use. The University of Liverpool Interventional Ethics Committee approved the study (no. RETH000685). All subjects gave written informed consent.

2.2 Cell separation

2.2.1 PBMC

Venous blood samples collected in EDTA or heparin tubes were processed within 2 hours of collection by density gradient centrifugation with Histopaque®-1077 (Sigma Aldrich, Poole Dorset UK) to allow PBMC isolation. Blood was first centrifuged at 1000xg for 10' at 18^0C (acceleration 4, break 0) to isolate plasma. Remaining blood

was further diluted 1:1 in PBS and layered over Ficoll in pre-labelled 50 ml tubes (20 ml of diluted blood onto 15 ml of Histopaque®-1077). Tubes were placed into centrifuge buckets with extreme care to avoid disruption of the layer to be spun at 500xg for 30' at 18-20°C (acceleration 4, brake 0). After centrifugation, the following layers will be visible from top to bottom of the tube: plasma and PBS, PBMC, Ficoll and blood. The PBMC layer was collected with sterile plastic Pasteur pipettes and transferred into pre-labelled 50 ml tubes. PBS (Thermofisher, Leicestershire UK) was added up to 50 ml and cells were washed by 8' centrifugation at 500xg, 18-20°C (acceleration and brake = 4). After the first wash, supernatant was discarded and the cell pellet was re-suspended in 10 ml of PBS; 5 µl of cell suspension was taken for the cell count and the remaining cells were washed as described above. For cell count, 45 µl of trypan blue 0.4% (Thermofisher, UK) were added to cell suspension to allow visualization of dead cells. Ten microliters of cell-trypan blue suspension was applied to a hemocytometer slide chamber. By using a microscope with a 10X objective, alive and dead cells could be discriminated and live cells (unstained by trypan blue) on one set of 4 corner squares were counted. The total number of cells was then calculated with the following formula [2.1] multiplied by the dilution factor, in this case equal to 10:

[2.1] cells/ml= (number of counted cells/4) * 10^4

Dead cells (stained by trypan blue therefore of blue color) were also counted to calculate cell viability. Only samples with >90% viable cells were used. Up to $25x10^6$ cells were used fresh for CD4 T-cell isolation, whereas remaining cells were frozen as follows. Up to 10^7 cells were re-suspended in freezing medium containing 90% of heat-inactivated FBS (Sigma, Poole Dorset UK) and 10% DMSO (Sigma, UK) and transferred to pre-labelled cryogenic vials. Tubes were transferred into a cooling box containing pure iso-propanol (Mr Frosty Nalgene, Thermofisher), and placed into the -80°C freezer to allow a cooling rate of 1°C/min. When cells were frozen (after at least

one night), cryovials were moved to Liquid Nitrogen tank (-135ºC to -190ºC) for long storage period.

2.2.2 CD4 T-cell subsets

Freshly isolated PBMC were used to obtain highly purified resting and non-resting CD4 T-cells by using a two-step protocol as described in Laird GM *et al.* and summarised in Figure 2.1. PBMC (20-25x10^6 cells) were washed twice by re-suspending cell pellet in 5 ml of wash/staining buffer (WS buffer) containing PBS with 5% bovine serum albumin (BSA, Sigma Aldrich UK) and 2 mM EDTA 0.5 M pH 8.0 (ThermoFisher scientific UK) prior to centrifugation at 300xg for 5' at RT. After the second wash, cell pellet was resuspended in WS buffer (40 µl each 10^7 cells) and the $CD4^+$ T Cell Biotin-Antibody Cocktail ($CD4^+$T cell isolation kit Miltenyi Biotec Ltd., Bisley UK) (20 µl each 10^7 cells) was added to the cells. The cocktail contained biotin-conjugated antibodies binding non CD4 T-cells and specifically: CD8 T-cells, monocytes, neutrophils, eosinophils, B cells, NK cells, granulocytes, γ/δ T cells, and erythroid cells. After 5' incubation at 4°C, $CD4^+$ T Cell MicroBead cocktail ($CD4^+$T cell isolation kit Miltenyi Biotec Ltd, UK) (20 µl each 10^7 cells) was added in order to magnetically label the non-target cells and incubated for 10' at 4^0C (Figure 2.1a). During the incubation, LS columns (Miltenyibiotec, Bisley UK) were activated by rising with 2 ml of WS buffer while they were placed in the magnetic separator. Once the incubation with the $CD4^+$T cell isolation kit was finished, the cell suspension volume was adjusted to 500 µl and loaded onto the activated LS column in the magnetic separator (Figure 2.1b). Unbound cells ($CD4^+$T cells) passed through the column and were collected in a pre-labelled 15 ml tube; the LS columns were washed twice with 1 ml of WS buffer and the total effluent was gathered to maximise yield of obtained $CD4^+$T cells. The obtained CD4 T-cells were then resuspended in WS buffer (40 µl per 10^7 cells) and anti-CD69 biotin-conjugated antibody (CD69 MicroBead Kit II Miltenyi Biotec Ltd, UK) was added (10 µl per 10^7 cells). After 15' incubation at 4^0C, anti-Biotin beads (20

µl per 10^7 cells, CD69 MicroBead Kit II Miltenyi Biotec Ltd, UK), anti-CD25 conjugated beads (20 µl per 10^7 cells, CD25 MicroBead II Miltenyi Biotec Ltd, UK) and anti-HLA-DR conjugated beads (20 µl per 10^7 cells, CD25 MicroBeads Miltenyi Biotec Ltd, UK) were added and incubated for an additional 15' at 4°C (Figure 2.1c). After the incubation, cells were washed by adding 1 ml of WS buffer prior to centrifugation at 300xg for 7'. After centrifugation, cell pellet was resuspended in 500 µl and loaded onto the pre-activated column (prepared as described above) for magnetic separation. Resting CD4 T-cells were collected in the flow-through together with the total effluent raised to wash the column, as described previously (Figure 2.1d), whereas the complementary population containing the $CD4^+CD26^+/CD69^+/HLA\text{-}DR^+$ T-cells remained linked to the LS columns. Differently from Siliciano lab, these cells were isolated from the columns as follow. LS columns were removed from the magnetic rack and placed on a suitable collection tube; 3 ml of WS buffer were pipette onto the LS columns and the volume containing the cells was collected after pulling it out with a syringe. Resting and non-resting CD4 T-cells were count and one aliquot (5-10 $x10^5$ upon cell availability) was used for flow cytometry analysis performed as described below in this chapter. For each population, a minimum $5x10^6$ cells were frozen as described above.

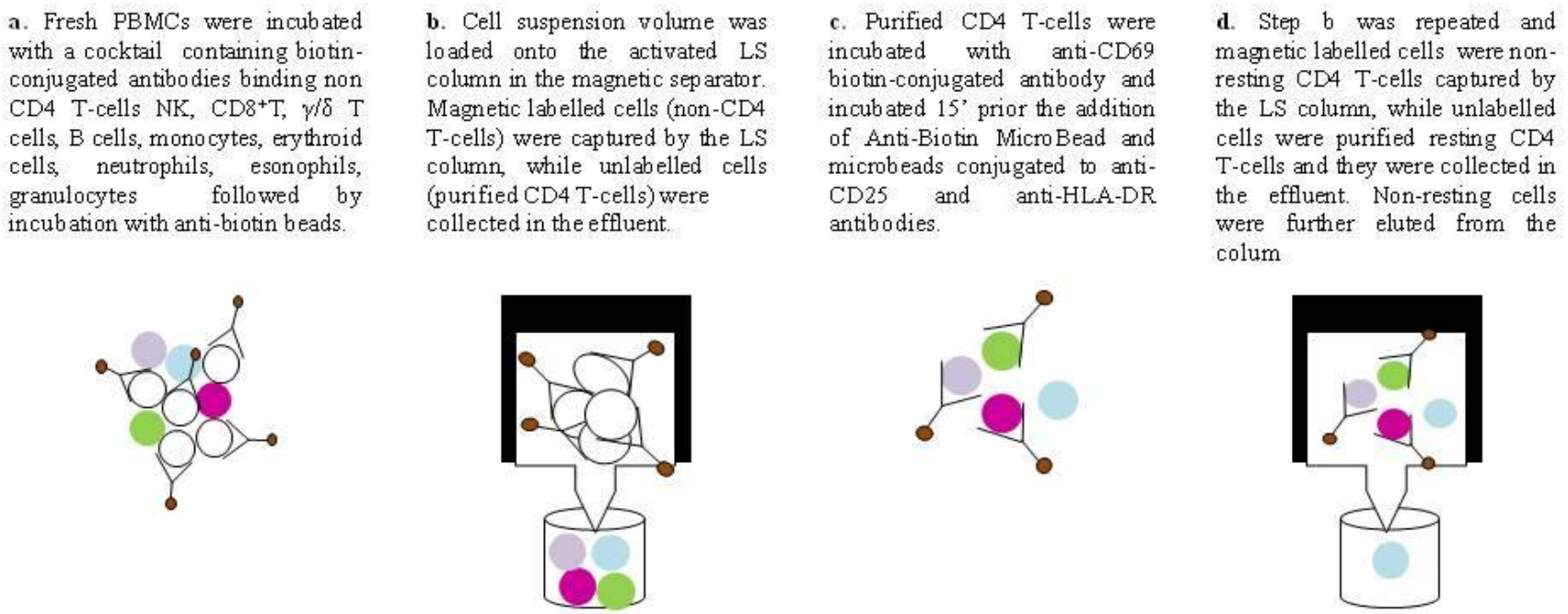

Figure 2.1 CD4 T-cell subsets isolation protocol

Figure depicting the two-step protocol that was used for CD4 T-cell subsets isolation. First step: CD4 T-cells isolation (a,b); second step: resting and non-resting CD4 T-cells isolation. Coloured circles represent: non-CD4 T-cells (white); $CD4^+CD69^+$T-cells (purple); $CD4^+CD25^+$T-cells (magenta); $CD4^+HLA\text{-}DR^+$T-cells (green); $CD4^+$ $CD69^-$ $CD25^-$ $HLA\text{-}DR^-$ T-cells (blue). Black square: magnetic rack. NK= natural killer cells.

2.3 Virological assays

2.3.1 HIV-1 RNA quantification

An alternative version (herein referred to as "ultrasensitive assay") of the Abbott Real Time HIV-1 assay (Doyle et al., 2012) (Abbott, Maidenhead UK) was used to quantify residual plasma HIV-1 RNA. The original assay showed quantification at 40 HIV-1 RNA copies/ml and 20 HIV-1 RNA copies/ml with 100% and 95% probability, respectively; with the ultrasensitive assay we were able to achieve quantification of 3 HIV-1 copies/ml and 1 HIV-1 copy/ml with 95% and 50% probability, respectively. In the ultrasensitive assay 8 ml of plasma sample containing HIV-1 RNA were used for the assay instead of 1ml as for the standard assay. Plasma was concentrated by ultracentrifugation of plasma samples at 215,000xg for 45' at 4°C in polycarbonate tubes (Beckman Coulter, High Wycombe UK) by using Beckman SW41 swinging bucket rotor (Beckman Coulter, UK) prior to RNA extraction. Pellet was resuspended in 1 ml of basematrix (Seracare, Milford USA) and it was used as input for automated RNA extraction onto the m2000sp™ instrument (Abbott) according to manufacturer instruction as for the standard assay. Abbott *m*™ Sample Preparation System solutions (Abbott) were loaded onto the m2000sp™: this technology uses magnetic particle beads to allow selective RNA isolation. Out of the 1 ml concentrated plasma RNA, 600 µl was used for extraction and RNA was eluted in 88 µl of which 50 µl were dispensed into an Abbott 96-well optical plate for the real-time PCR reaction. Following this step, Abbott real-time amplification reagents kit (Abbott) containing primers, probe and polymerase enzyme was loaded into the m2000sp™ which generated the mastermix and dispensed it into the Abbott 96-well optical plate containing the eluted RNA. The plate was then ready, after manual application of the optical seal, for transfer to the Abbott m2000rt (Abbott) for the real time reaction. Results were automatically analysed by the Abbott ROW Software (Abbott) and three types of results could be obtained: target quantified, target detected but not quantified, target not detected.

In the first case, the concentration of the sample HIV-1 RNA was automatically calculated by the software by using the following formula:

[2.2] $\log_{10}$ copies/ml of target = (Ct-intercept)/slope

The Ct indicated the threshold cycle obtained by the qPCR of the sample; whereas the intercept and the slope were obtained by running two calibrators that produced a standard curve. Given that the two calibrators were run under the same extraction and qPCR conditions described above for the samples, this formula expressed the $\log_{10}$ HIV-1 copies/ml when the extraction input volume was 1 ml, the elution volume was 88 µl, and the real-time PCR input volume was 50 µl. For results that were target detected but not quantified, the calculation was carried out manually by using the same formula [2.2]. Further, target not detected were not quantifiable.

According to Abbott recommendation, each run was validated as follows. An HIV-1 unrelated sequence was introduced at the beginning of the process and simultaneously quantified; further, three controls were added in each run: one high positive (CONTROL H), one low positive (CONROL L) and one negative (CONTROL NEG). Moreover, the two calibrators were run in triplicate each time reagents lots were changed to ensure consistency between runs. Primers used for this automated assay are specific for Group M, subtypes A-D, CRF01_AE, CRF02_AG, subtypes FH, group N and O as indicated in the manufacturer's instructions (Abbott).

2.3.1.1 Validation of the ultrasensitive assay

Ultrasensitive assay for detection of low levels of HIV-1 RNA in plasma was validated in the context of another study by spiking 8 ml of HIV-negative plasma with four

dilutions of the 3rd World Health Organisation (WHO) HIV-1 international standard (NIBSC code: 10/152, Hertfordshire UK). The International Standard (IS) has been assigned an International Unit (IU) value of 185,000 IU/ml by NIBSC. When tested with Abbott real time PCR assay, 1 ml contained 117,489 copies (NIBSC). The standard was prepared as recommended from the manufacturer. One ampule was resuspended in 1 ml of ddH20 and vortexed for 15'. Upon reconstitution, 13.7 µl of standard suspension was mixed with 986.3 µl of basematrix (Seracare, Massachusetts USA) and vortexed for 15' to produce a 2534 IU/ml stock solution. Stock was diluted 1:31.7 to make up 80 IU/ml concentration aliquots which were stored at -80°C for future use. Alternatively, stock solution was further diluted in 8 ml of basematrix to achieve following concentrations: 15.8 IU/ml (10 copies/ml), 7.9 IU/ml (5 copies/ml), 4.7 I/ml (3 copies/ml) and 1.6 IU/ml (1 copy/ml). Dilutions were run with Abbott assay following ultracentrifugation as described above and results showed 95% detection rate of 3 copies HIV-1 RNA/ml and a 50% detection rate of 1 copy HIV-1 RNA/ml.

In the context of this thesis, sensitivity of an alternative ultrasensitive assay which started with reduced plasma input (2 ml) was explored. Manual and automated HIV-1 RNA extraction methods were tested and results from validation runs are shown in Chapter 3. All runs were performed by using frozen 80 IU/ml aliquots of IS for consistency. After thawing, 80 IU/ml stock was diluted in basematrix to make 40 IU/ml, 20 IU/ml, 10 IU/ml and 5 IU/ml concentration.

2.3.2 HIV-1 DNA quantification

2.3.2.1 DNA isolation from PBMC and CD4 T-cell subsets

Frozen cells were quickly thawed in water bath at 37°C and washed twice by adding PBS prior to centrifugation at 400xg to eliminate the DMSO. Cell pellet was then resuspended in 400 µl of PBS and used as input for DNA isolation. The QIAamp DNA mini kit (Qiagen, Manchester UK) was used as follow. Lysis buffer (400 µl) and proteinase K (40 µl) were mixed to cell suspension and first incubated at 56°C for 30', therefore at 100°C for 40' as described in Geretti et *al.* Purified DNA was eluted in 100 µl of elution buffer containing 10 mM Tris-Cl plus 0.5 mM EDTA at a pH of 9.0 (TE buffer). Extracted DNA was quantified by spectrophotometry (Nanodrop, Labtech, Uckfield, UK).

2.3.2.2 Total HIV-1 DNA quantification

Total HIV-1 DNA in PBMC was quantified via qPCR using the Applied Biosystems 7500 Real-Time PCR system, as described in Geretti *et al.* (2013). A total of 1 µg of cellular DNA (equivalent to 150,000 cells) was input in each reaction, along with a 1:10 sample dilution to detect inhibition. The standard curve incorporated four quantities of input HIV-1 DNA at 6,000, 600, 60 and 6 copies per reaction. Although a commercial kit was available (the Generic HIV DNA cell kit Biocentric, Bandol France) having an in-house quantification method was desirable for cost savings. Therefore, a standard curve was produced using cloned HIV-1 LTR DNA plasmid and it was measured in every run to allow quantification. All runs were performed in a 50 µl volume containing DNA extract (1 µg of eluted DNA), 200 nM of primers and 400 nM of probe (listed in Table 2.4), 1X qPCR SuperMix with 50 nM of ROX passive reference dye (Thermofisher). Thermocycling conditions were 2' at 50°C and 10 min at 95°C, followed by 50 cycles at 95°C for 15 sec, and 60°C for 1'. HIV-1 DNA copies/µg

quantification was calculated by the software and then converted into HIV-1 DNA copies/10^6 PBMC using the formula [2.3]:

[2.3] HIV-1 DNA copies/10^6 PBMC = HIV-1 DNA copies/µg x 10^6/150,000

The sensitivity for this assay was 40 and 20 HIV-1 DNA copies/10^6 PBMC at 95% and 50% detection rate, respectively as previously described (Avettand-Fenoel et al., 2009). The validation for this assay was determined in the context of another study by comparing the consistency of the standard curve produced with the HIV-1 LTR plasmid versus the one produced using the commercial Generic HIV DNA cell kit (Biocentric, Bandol France). Results from five independent experiments showed a strong linear relation between input HIV-1 DNA and Ct values with R^2>0.9, where the R^2 was a statistical measure of how close the data were to the regression line that fitted the Ct values per each input concentrations. Coefficients of variations were <1% per each replicate.

2.3.2.3 Integrated HIV-1 DNA quantification

Integrated HIV DNA was quantified by a repetitive-sampling Alu-gag method published by Spiegelaere *et al.* 2014. This protocol included two steps: a first amplification PCR step (PCR1) is followed by a second quantification real-time PCR step (qPCR2) that measures the HIV-1 DNA load. During the first step, PCR was performed using one reverse primer targeting the HIV gag sequence and a forward primer targeting the human *Alu* sequence on 40 replicates (primers are listed in Table 2.3). This step allowed the exponential amplification of integrated HIV-1 DNA when both primers bind the target, the linear amplification of the unintegrated HIV-1 DNA when only gag primers binds the target sequence along, and of the human genome when only Alu is capable of binding (

Figure 2.2a). While amplification of human genome could not be quantified by qPCR2, linear amplification of unintegrated HIV-1 DNA can be measured and this generates difficulties for discrimination of the unintegrated vs integrated HIV-1 DNA. To correct for this linear amplification, 30 replicates with only HIV-1 gag primers were run to allow linear amplification of unintegrated HIV-1 DNA ("gag" control). All the reaction contained 200 nM of primers, 1X Promega GoTaq mix and 0.5 U/µl GoTaq polymerase (Promega, Southampton UK), 10nM dNTPs (Promega), DNA extract ranging from 50-250 ng/reaction depending on total HIV-1 copies, water to reach 50 µl of final volume reaction. Thermocycling conditions were 2' at 95°C; 40 cycles of the following steps: 95°C for 15''- 50°C for 15''- 70°C for 3.30'; followed by 15' at 70°C. Following amplification, 2 µl of PCR product was employed for the qPCR containing 400 nM of primers, 200 nM of probe, 1X qPCR SuperMix with ROX (Invitrogen UK, cat # 11743500), water to a final volume of 10 µl. qPCR was performed on 2 machines following validation of the systems: Roche qPCR System (supported by LightCycler 480 SW 1.5 software) and AB 7900HT System. Thermocycling conditions were 2' at 50°C and 5' at 95°C, followed by 45 cycles at 95°C for 15'', and 60°C for 1'. The integrated HIV-1 DNA copy number was obtained by input of the Ct value into pre-designed computational template (Microsoft Excel), which applies Poisson's principles for quantification (http://www.integratedhivpcr.ugent.be). Within the Alu-gag replicates, each reaction well was scored as positive for integrated HIV-1 DNA if the Ct value was lower than the average Ct values produced by the "gag" control (threshold). Number of positive wells was divided by number of Alu-gag replicates to calculate the percent positive (p) reaction per well. This value was input into the formula [1.1] to allow quantification of the integrated HIV-1 DNA per each replicate. Results were divided by "0.1" to take into account the limit of quantification for this assay that is 10% of the total integration events. The assay was valid only when at least 4 reaction wells were scored as positive. Figure 2.2 provides an illustration of the method.

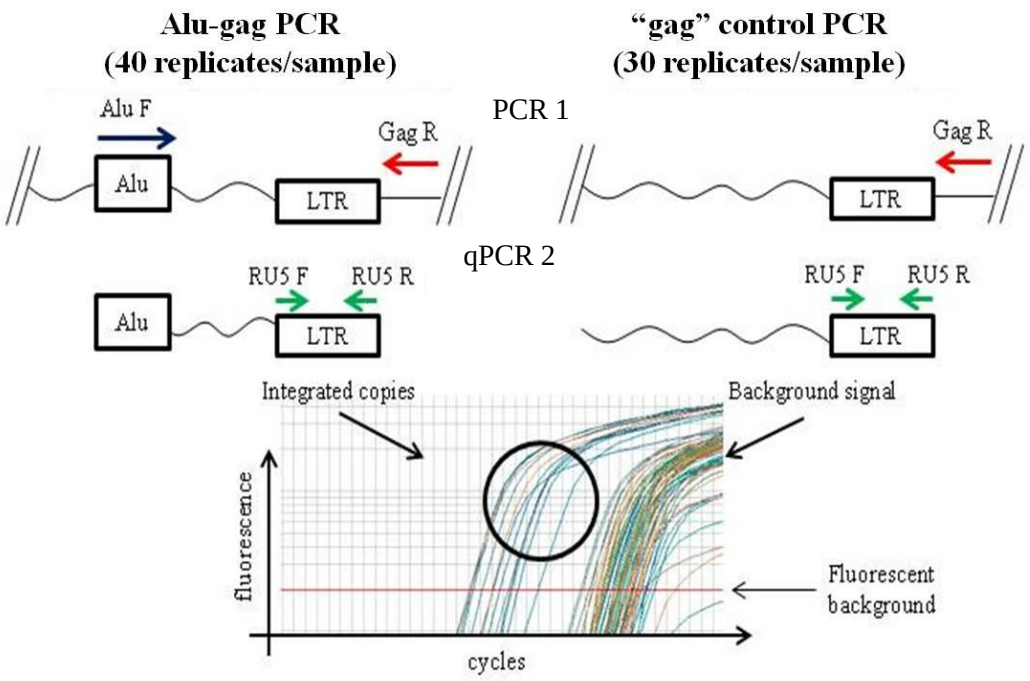

Integrated HIV-1 DNA copies/10^6 PBMCs quantification

Input			Output			
Correction for standard	0,1	(measured/expected)*100 =10% sensitivity				
# Alu-Gag replicates:	40		number of positive wells:	7		
# cells per replicate:	38051,7		percent positives	0,175		
	Cq values		Poisson calculation			
replicates	Alu gag PCR	Gag only		estimate	CI+	CI-
1	33,02	32,09	Integrations /Replicate	1,923718	3,849317	0,915157
2	33,19	34,84	Integrations/ Cell	5,1 E-05	0,00010	2,4E-05
3	31,58	34,49	Integrations/ 10^6 cells	50,555	101,160	24,050
4		32,73				
5	33,88	32,54				

Figure 2.2 Alu-gag assay

F= forward primer; R=reverse primer; qPCR=quantitative PCR; CI= confidence interval.

In the context of this thesis, we explored alternative primer combination to optimize the detection limit of this method. The primers that we used are listed in Table 2.43 and the results we obtained are shown in chapter 7.

2.3.2.4 2-LTR circular HIV-1 DNA quantification

2-LTR circular HIV-1 DNA was quantified in collaboration with prof. Douglas Richman research group by digital droplet PCR (ddPCR) as described in M.C. Strain *et al.* 2013 Primers and probe were listed in Table 2.4.

Table 2.3 List of all primers used in this thesis

Assay	Target		Primer sequence (5' – 3')
Total HIV-1 DNA assay	HIV-1 NEC005 (sense)		GCCTCAATAAAGCTTGCC
	HIV-1 NEC131 (anti-sense)		GGCGCCACTGCTAGAGATTTT
	HIV-1 probe		FAM/AAGTRGTGTGTGCCC/MGB -NFQ
Alu-gag assay for integrated HIV-1 DNA	PCR1	Alu sense	GCCTCCCAAAGTGCTGGGATTACAG
		Gag anti-sense	GTTCCTGCTATGTCACTTCC
	qPCR2	RU5 sense	TTAAGCCTCAATAAAGCTTGCC
		RU5 anti-sense	GTTCGGGCGCCACTGCTAGA
		RU5 probe	FAM/CCAGAGTCA/ZEN/CACAACAGAC GGCACA/3IABKFQ/
Alu-5LTR assay for integrated HIV-1 DNA	PCR1	Alu sense	GCCTCCCAAAGTGCTGGGATTACAG
		RU5 sense	GTTCGGGCGCCACTGCTAGA
	qPCR2	HIV-1 NEC005 (sense)	GCC TCA ATA AAG CTT GCC
		HIV-1 NEC131 (anti-sense)	GGC GCC ACT GCT AGA GAT TTT
		HIV-1 probe	FAM/CCAGAGTCA/ZEN/CACAACAGAC GGCACA/3IABKFQ/
2-LTR circular HIV-1 DNA assay	HIV-1 MH535 (sense)		AAC TAG GGA ACC CAC TGC TTA AG
	HIV-1 MH536 (antisense)		TCC ACA GAT CAA GGA TAT CTT GTC
	HIV-1 probe		FAM/ACACTACTTGAAGCACTCAAGGC AAGCTTT/MGB

2.3.3 HIV-1 p24 ELISA

In the setting up of an in vitro system to study HIV-1 persistence, HIV-1 p24 protein was quantified in the supernatant of infected cells to estimate viral titre, by using sandwich Lenti-X™ p24 Rapid Titer Kit (Clontech/Takara Bio Europe, Saint-Germain-en-Laye France) as recommended by the manufacturer. The rational of the sandwich ELISA is depicted in Figure 2.3.

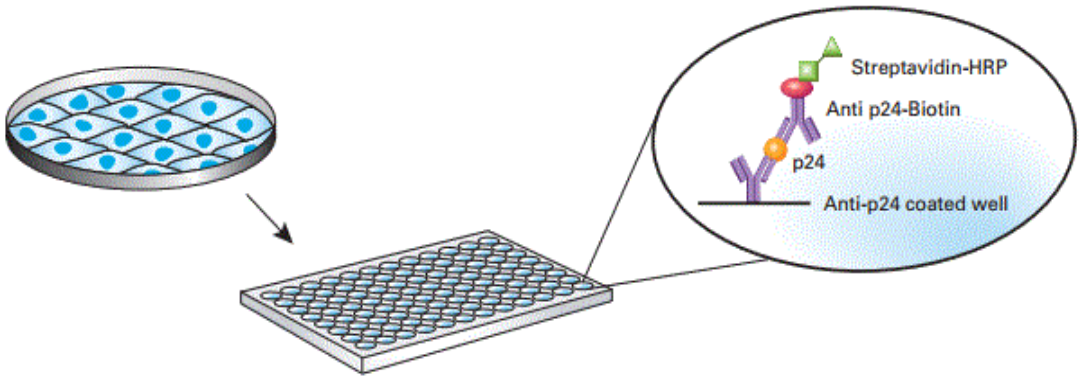

Figure 2.3 Sandwich ELISA

Adapted by Clonotech Lenti-X™ p24 Rapid Titer Kit User Manual. Anti-p24 coated=capture antibody that is bound to a well of the microtiter plate; p24= HIV-1 p24 protein; anti p24-Biotin= antibody binding the protein of interest that was biotin conjugated; streptavidin-HRP= anti biotin antibody that carried HRP.

The sandwich ELISA method measured a protein of interest between two layers of antibody (capture and detection). Capture antibody was coated to the wells in the microtiter well plate and quantitatively binds the target protein (in this case HIV-1 p24) in the sample. Specifically-bound target is detected using a biotinylated anti-p24

secondary antibody which is further bound by streptavidin conjugate to the horseradish peroxidise (HRP). When the HRP-substrate is added, it develops colour intensity in proportion to the quantity of the target protein concentration

After equilibration of all reagents at RT, lysis buffer (20 µl/well of a 96 well plate) was disposed into the selected wells that were pre-coated with anti-p24 capture antibody. Sample and standard dilutions were added in duplicates (200 µl/well) and plate was incubated at 37°C for 1 hr. After incubation plates were washed 5 times by aspirating the content of each well and by filling it with wash buffer (300 µl/well); plates were tapped dried before adding the anti-p24 biotin conjugate detector antibody (100 µl/well). After 30' incubation at RT, plate were washed 5 times as described before and substrate solution was added (100 µl/well) and incubated for 20' at RT. Stop solution (100 µl/well) was added prior to acquisition by microtiter plate reader at 450 nm to obtain the optical density values (OD_{450}). Average of OD_{450} obtained from the standard dilutions were plotted in y-axis and concentrations in x-axis to obtain a regression line equation for quantification. Only equations with R^2 value>0.9 were accepted. To calculate p24 concentration (x) in each sample, average OD_{450} values (y) were inserted into the obtained equation. This sandwich ELISA approach allowed quantification down to 6 pg/ml p24.

2.4 Immunology

2.4.1 Flow cytometry

In the context of the ERAS study (Chapter 4 and 6 of this thesis), cellular markers of immune activation were measured by flow cytometry on fresh blood at the Department of Clinical Immunology, Royal Free Hospital London under the supervision of Mrs Tahami Fariba. The Multitest IMK Kit (Becton Dickinson BD, Oxford UK) was used for lymphocyte counts according to manufacturer instructions; events were acquired by

using BD FACSCalibur and the analysis was performed by using CellQuest program. Markers of immune activation were measured as follows. Blood pellet was resuspended in 1X Hoffman's lysis buffer (100 ml of solution contained 8.3 g NH_4Cl, 1.0 g $KHCO_3$, 37 mg disodium EDTA dissolved in water, stock solution 10X) and incubated for 10' at RT to allow cell lysis. Cells were then added into the 96 well plate (round bottom) and incubated with the relevant antibody as listed in Table 2.4 for 15' at RT; following incubation, cells were washed 4 times where 1 wash was perfomed as follows: centrifuge the plate, flick out supernatant, add 150 µl PBSA buffer (PBS containing 0.2% albumin and 0.2% Sodium Azide), dry plate, cover with sealer, centrifuge the plate. Cells were resuspended in 1% paraformaldehyde (PFA) and incubated for 30' prior to acquisition with BD FACSCalibur; analysis was performed by using CellQuest program.

For the integrated HIV-1 DNA load in CD4 T-cell sub-populations study (Chapter 5 of this thesis), flow cytometry was used for the detection of markers of cellular immune activation including HLA-DR, CD25 and CD69 expression on CD4 T-cells. Cell suspension ($5x10^5$ cells in 40 µl of WS buffer previously described) was stained with the relevant antibody; all antibodies used were diluted 1:5 as recommended from manufacturer (Biolegend, London UK). After 30' incubation at RT, cells were washed twice in 1ml of PBS and centrifugation at 300xg for 5' at RT. After the last wash cells were resuspended in 100 µl of 2% PFA solution and acquired within 24 hrs. BD Accurri C6 Facs Machine (BD) was used to record 10,000 events for each sample and data analysis was performed by using C Flow Plus (BD) software.

For the development of *in vitro* assays to study HIV-1 persistence during ART, flow cytometry was used to measure HLA-A2 expression on $CD4^+$ T-cells and to quantify intracellular HIV-1 p24 protein as measure of infection, as described in Chapter 7.

All antibodies used in this thesis were listed in Table 2.4.

Table 2.4 List of all antibodies used in flow cytometry assays in this thesis

Study	Target (fluorocrome)	Company (Cat #)
Chapters 4 and 6	CD3 (Cy5)	BD (555341)
	CD8 (FITC)	BD (345772)
	CD4 (FITC)	BD (555346)
	CD4 (Cy5)	BD (555348)
	CD38 (PE	BD (555460)
	CD26 (PE)	BD (555437)
	CD69 (PE)	BD (555531)
	HLA-DR, P, Q (PE)	Serotec (MCA477PE)
Chapter 5	CD4 (PE)	Biolegend (317410)
	HLA-DR (APC)	Biolegend (307610)
	CD25 (APC)	Biolegend (302609)
	CD69 (FITCH)	Biolegend (310904)
Chapter 7	HLA-A2 (PE)	Biolegend (551285)
	HIV p24 (FITCH)	Beckman (6604665)

2.4.2 ELISA assays

Different commercially available ELISA kits were employed to measure plasma levels of the following soluble markers of immune activation: CD14, CD27, CD30, hsCRP, IL6, D-Dimer. An overview with the different kit and correspondent sensitivity is provided in Table 2.5. All kits used a sandwich ELISA approach as described in Figure 2.3. All kits provided plates that were pre-coated with relevant antibody and instructions from the manufacturer were followed. Samples were diluted as indicated in Table 2.5 and added to the wells. For CD27, CD30, IL6, soluble standard curve dilutions were already present in dedicated wells in the plate and they only need to be reconstituted by addition of water (100 µl); furthermore the detection antibody was already contained in all the wells. For these kits, 3 hrs incubation guaranteed the binding of the relevant markers contained in the plasma to both the capture and the detector antibody. Conversely, for the CD14, D-Dimer, and hsCRP kits the standard was provided in

powder form that needed to be re-constituted in water and diluted. Sample and standard dilutions were first incubated with capture antibody for 1-3 hrs (depending on the kit) at RT; following this incubation the plate was washed as described for the p24 ELISA kit and the relevant conjugate detection antibody was added and incubated for 1 hr. Following incubation with the detector antibody, all kits were washed as described above and the substrate solution was added and incubated for 10'-30' depending on the kit. Stop solution was added before acquisition by microtiter plate reader at 450 nm. Raw data were produced by research technicians and analysed in the context of this thesis according to manufacturer instructions. For CD27, CD30, IL-6, hsCRP pre-designed calculation sheet was available. For CD14, OD_{450} and p24 pg/ml standard concentration were log transformed and plotted with OD_{450} in y-axis and p24 pg/ml in x-axis prior to generate the linear regression curve equation that was used for quantification as done for the p24 ELISA. For D-Dimer, OD_{450} values were plotted in x-axis and $\log_{10}$p24 pg/ml in x-axis prior to analysing the data to fit a polynomial curve with order 2.

Table 2.5 List of all ELISA assay kits used to measure soluble markers of immune activation in this thesis

Soluble marker	Sample dilutions	Sensitivity	Company
CD14	1:200-1:400	125 pg/ml	R&D system, UK
D-Dimer	1:2	23.7 ng/ml	USCN, China
hsCRP	1:100	0.02 µg/ml	Demeditec, Germany
CD27	1:50	0.2 U/ml	EBiosciences, UK
CD30	1:4	0.33 ng/ml	EBiosciences, UK
IL6	None	0.92 pg/ml	EBiosciences, UK

2.5 Statistical Method

Different statistical approaches were used throughout the thesis as specified in the single chapters. Generally, non-parametric Wilcoxon-Mann-Witney test was used to compare continuous variables and chi-squared (X^2) test was used to compare un-paired categorical variables. When variables were paired, Wilcoxon matched-pairs signed rank test or McNemar X^2 test were used for continuous variables or categorical variables, respectively. Where the analyses required variables to be expressed as medians, undetectable results were generally assigned an arbitrary midpoint value between zero and the median lower limit of detection of the assay used for quantification, as specified in each chapter.

For the ERAS studies, characteristics of the study population were stratified into groups based upon duration of suppressive antiretroviral therapy. The mean differences (with 95% confidence interval, CI) over 10 years of suppressive ART of virologic and immunologic factors were analysed by univariate linear regression analysis after log transformation of the variables. Spearman's test was used to explore association between integrated HIV-1 DNA and immunological and virological factors. The

association between markers of HIV-1 persistence and the other immunological and virological variables was characterised further by univariate and multivariable linear regression modelling. For the ERAS study (Chapter 4), variables to be included in the multivariable linear regression models were selected based upon univariate analysis results and only factors with $p<0.1$ were included. For the integrated HIV-1 DNA study (Chapter 6), a 'best subset' approach and the Mallow Cp test were used for the selection of variables to be included in the multivariable model. This method is applied to find the best model involving a subset of input predictors. An example of a Mallow Cp output is given in Figure 2.4. The analyses were performed with SAS 9.4 in collaboration with Dr. Alessandro Cozzi-Lepri at University College London.

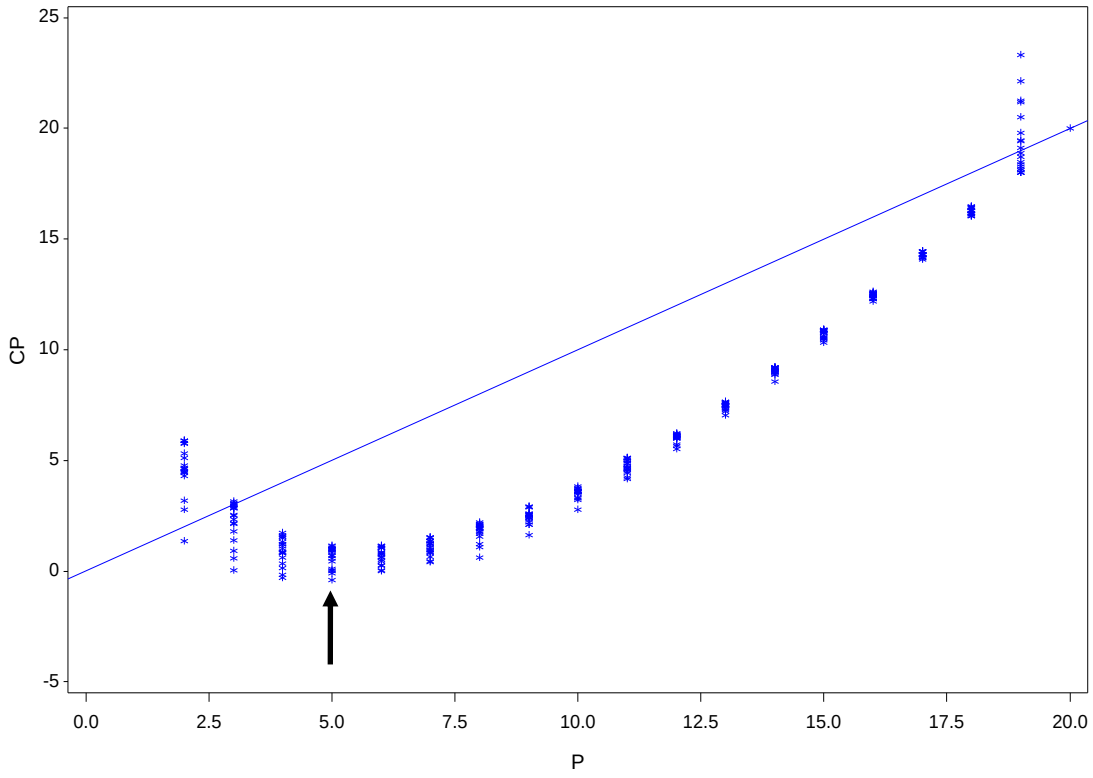

Figure 2.4 Example of Mallow statistic approach for variable selection

Cp= Cp value, with lower values being the most powerful; p= parameters included into the selection.

2.6 Mammalian cell lines maintenance

MT-4 and Human Embryonic Kidney 293 (HEK-293) cells were provided by Prof. Andew Owen, University of Liverpool. MT-4 cells are human T-cells transformed by co-cultivation with leukaemia lymphocytes harbouring HTLV-1. MT-4 cells are persistently infected with HTLV-1 and may shed HTLV-1 in culture (Pauwels et al., 1987). HEK-293 cells are a widely used cell line generated by transformation of human embryonic kidney cells with defective adenovirus 5 (HadV-5) (Graham et al., 1977). Rev-CEM cells were purchased from the National Institute of Health (NIH) AIDS Research & Reference Reagent Program (cat. # 11467). This is a reporter human T-cell lymphoma cell line engineered to contain the green fluorescent protein (GFP) gene. As

GFP is coupled to a Rev Responsive Element (RRE), the cells only express GFP upon expression of the Rev gene during HIV infection (Wu et al., 2007).

Upon arrival from external sources, MT-4 and Rev-CEM cell were quickly thawed at 37°C and resuspended in 10 ml of cool Roswell Park Memorial Institute medium (RPMI-1640), containing L-glutamine (Thermo Fisher scientific) complemented with 10% FBS (Thermo Fisher scientific). Cell pellet was harvested by centrifugation at 200xg for 5' and resuspended in 10 ml of pre-warmed complemented RPMI-1640, transferred to a culture flask, and placed in the incubator to allow cell growth. Cells were generally split 1:4 twice a week depending on growth rate. HEK-293 cells were thawed as described above, but Dulbecco's Modified Eagle Medium (DMEM, Thermo Fisher scientific, UK) complemented with 10% FBS (Thermo Fisher scientific, UK), 5% penicillin/streptomycin (Thermo Fisher scientific, UK) and 5 nM of L-Glutamine (Thermo Fisher scientific, UK) was used instead of complemented RPMI-1640. Once thawed, cell suspension was added to 10 ml of pre-warmed supplemented DMEM. Cell pellet was harvested by centrifugation at 400xg for 5', resuspended in 10 ml of pre-warmed supplemented DMEM, transferred to a culture flask, and place in the incubator to allow cell growth. Being adherent cells, flasks were placed horizontally in the incubator.

MT-4 and Rev-CEM cells are grown in suspension and each passage was performed by diluting cell suspension 1:5 in supplemented RPMI-1640 every 4-5 days depending on cell density and growth rate. HEK-293 cells were split 1:4 to 1:6 every 4-5 days depending on cell density as follow. When confluent, cells were washed with PBS (Fisher thermoscientific) and cells were incubated with trypsin-EDTA solution (Fisher thermoscientific) for 2-5' at 37°C to allow cell detachment from the flask. Following incubation, cells were resupended in complemented DMEM and split as needed. All cells types were frozen at a concentration of 10^7 cells/ml as described for PBMC above in this chapter.

Chapter 3: Residual plasma HIV-1 RNA detection in patients switching from a single-tablet regimen of co-formulated tenofovir/emtricitabine/efavirenz to one containing co-formulated tenofovir/emtricitabine/rilpivirine

3.1 INTRODUCTION

Co-formulated tenofovir/emtricitabine/efavirenz (Atripla) and tenofovir/emtricitabine/rilpivirine (Eviplera) are triple single tablet regimens (STRs) approved for once daily HIV-1 treatment. Both consist of one non-nucleoside reverse transcriptase inhibitor (NNRTI, efavirenz or rilpivirine) plus the nucleosides/nucleotide reverse transcriptase inhibitors (NRTIs) tenofovir disoproxil fumarate (TDF) and emtricitabine (FTC). Until recently, efavirenz (EFV)-based triple ART was the preferred combination for starting therapy in the United Kingdom (UK) (Asboe et al., 2012, Geretti and Tsakiroglou, 2014), and the majority of treated individuals achieved plasma HIV-1 RNA ("viral load") suppression (Gulick et al., 2006, Cassetti et al., 2007). However, EFV can induce central nervous system (CNS) toxicity (Sanchez Martin et al., 2013), which results in people discontinuing therapy both in the context of clinical trials and in routine clinical practice (reviewed in Geretti and Tsakiroglou, 2014) . The STR formulation of rilpivirine (RPV) with TDF and FTC has been compared with Atripla in the context of a randomised clinical trial (STAR), where it showed superior overall efficacy in patients with pre-ART plasma HIV-1 RNA <100,000 copies/ml. The better performance relative to EFV reflected improved tolerability and fewer discontinuations due to side effects. RPV however showed reduced potency in subjects with viral loads >100,000 copies/ml, which resulted in an increased number of virological failures compared with EFV (Cohen et al. AIDS 2014). As a result, Eviplera is only recommended for the initial treatment of subjects with pre-

ART viral load <100,000 copies/ml. The improved CNS safety profile, small tablet size, and good virological activity at low viral load make Eviplera an attractive option for patients who are already established on suppressive EFV-based ART but experience poor tolerability and therefore require a switch of therapy.

Third generation viral load assays reliably quantify HIV-1 RNA below the previously established cut-off of 50 copies/ml (e.g., 40 copies/ml with the Abbott RealTime assay and 20 copies/ml with the Roche TaqMan v.2 assay) and also report qualitative HIV-1 RNA detection below these thresholds. For example, with the Abbott RealTime assay, the manufacturer indicates that with 30, 20, and 10 HIV-1 RNA copies/ml detection rates were 96%, 88%, and 68%, respectively. Investigators have interrogated cohort data to determine whether a lower cut-off than 50 copies/ml should be introduced to define optimal viral suppression. Data produced using the Abbott Real-Time assay demonstrated that treated patients with detectable HIV-1 RNA between 40 and 49 copies/ml and those with qualitative detection below 40 copies/ml were more likely to experience viral rebound above 50 and 400 copies/ml over 12 months of follow-up relative to subjects with undetectable HIV-1 RNA (Doyle et al., 2012). Importantly, the effect of HIV-1 RNA detection below 50 copies/ml was independent of other known predictors of viral rebound including adherence levels (Doyle and Geretti, 2012, Doyle et al., 2012). Similar findings have been reported with the TaqMan assay v1 and v2 (Alvarez Estevez et al., 2013, Henrich et al., 2012). Moreover, in patients with HIV-1 RNA levels <50 copies/ml while receiving triple ART, a switch to a simplified atazanavir/ritonavir monotherapy regimen was associated with a progressive increase in HIV-1 RNA levels prior to virologic rebound >50 copies/ml (Wilkin et al., 2009).

The above findings indicate that monitoring plasma HIV-1 RNA loads with increased sensitivity can help predict viral load rebound (Wilkin et al., 2009) during ART. In order to explore this concept further, we investigated subjects receiving suppressive (HIV-1 RNA <50 copies/ml) first-line ART with Atripla who switched to Eviplera in

the context of a clinical trial. Following assay optimisation, ultrasensitive HIV-1 RNA measurements were made using stored plasma samples collected at the time of the switch (baseline) and at regular time points over the subsequent 24 weeks of follow-up.

3.2 METHODS

3.2.1 Study population

The trial was a phase III, open-label, multi-centre, pilot study. Eligible subjects had received Atripla for at least 12 weeks, showed a viral load <50 copies/ml and a CD4 count >50 cells/mm^3, had never previously received RPV or experienced virological failure, and were experiencing grade 2-4 CNS toxicity considered to be related to EFV. A total of 37 patients switched from Atripla to Eviplera and underwent follow-up for 24 weeks. The study-related standard viral load was measured at the centre of care using either the Versant HIV RNA v3.0 bDNA assay or the Roche TaqMan v2 assay. Plasma samples collected at baseline and at week 4, 12, and 24 after switching were stored at -80°C prior to shipping to the University of Liverpool on dry ice. Ethics was approved by local authorities and the study was registered at clinicaltrial.gov (identifier number NCT017701882) and the EudraCT registration number was 2012-002205-22.

3.2.2 Assay optimisation

As described in Chapter 2, our group developed an ultrasensitive HIV-1 RNA quantification assay that detected 1-3 copies/ml with an input of 8 ml of plasma. However, in this study the volume of plasma available for testing at each sampling point was ≤2 ml. Therefore, an alternative assay needed to be tested with a reduced plasma input in order to assess which was the higher sensitivity that could be achieved. The first step was virus concentration by ultracentrifugation of the sample at 215,000xg for 45' at 4°C as described in Chapter 2. We then compared two different RNA extraction

methods: the Abbott manual extraction kit and the automated m2000sp extractor, as detailed in the methods chapter. For manual extraction, following ultracentrifugation the pellet was resuspended in 600 µl of basematrix and used as input for the RNA extraction. After 20' incubation at 50°C with 100 µl of magnetic micro particle beads and 2.4 ml of lysis buffer, RNA was eluted in 66 µl volume. For automated extraction, pellets were resuspended in 1ml of basematrix and loaded onto the Abbott m2000sp instrument which eluted the RNA in 88 µl volume. With both methods, 50 µl of eluate was used as input in the Abbott m2000rt instrument. As described in Chapter 2, quantification results obtained from the Abbott software were based on an input volume for RNA extraction of 1 ml and an elution volume of 88 µl. For the manual extraction assay those volumes were modified and we therefore had to calculate the results manually. In particular, raw data produced by the software were divided by 1.7 and by 1.3 to correct for 600 µl plasma input and 66 µl elution volumes, respectively. Assay sensitivity was tested using dilutions of the World Health Organisation (WHO) 3rd International Standard for HIV-1 RNA in HIV-1 negative plasma. The dilutions were: 40 IU/ml (26 copies/ml), 20 IU/ml (13 copies/ml), 10 IU/ml (7 copies/ml), 5 IU/ml (3.5 copies/ml), and 1 IU/ml (1 copy/ml). The WHO recommended conversion factor for the Abbott RealTime assay was used to convert IU/ml into copies/ml, whereby 1 copy/ml = 1.4 IU/ml.

3.2.3 Sample processing

Plasma samples were ultracentrifuged as described above; pellet was resuspended in 1 ml of basematrix and loaded onto Abbott m2000sp instrument for the automated Abbot Real-Time assay (Maidenhead, UK). When plasma input volumes were smaller than 2 ml, the lower limit of detection was calculated based on specific plasma input using the Abbott detection rates for 1.0 ml. Median plasma input volume was 1.5 with a median lower limit of detection of 17 copies/ml. Levels of viral load suppression after switching were categorized as follows: improved suppression was defined as HIV-1 RNA >10

copies/ml at baseline followed by consistent suppression ≤10 cps/ml; reduced suppression was defined as HIV-1 RNA measurements ≤10 copies/ml at baseline followed by ≥2 consecutive HIV-1 RNA measurements >10 copies/ml or ≥1 HIV-1 RNA measurement >50 copies/ml during follow-up; loss of suppression was defined as HIV-1 RNA >50 copies/ml at week 12 and/or week 24.

3.2.4 Statistical analysis

For the validation tests, the coefficient of variation (CV) was calculated to describe the amount of variability relative to the mean of each standard dilution point within the same experiment; furthermore CV of each run was averaged to produce the overall CV per each standard dilution. CV>20% were considered unacceptable. Input plasma volumes were compared by non-parametric unpaired Mann Whitney test. HIV-1 RNA levels between baseline and other time points were compared by non-parametric paired-sample Wilcoxon signed rank test for continuous variables and by McNemar Chi-2 test for categorical variables. All values were log-transformed prior to analysis. Where the analyses required variables to be expressed as medians, undetectable HIV-1 RNA results were assigned an arbitrary midpoint value between zero and the median lower limit of detection (= 9 cps/ml).

3.3 RESULTS

3.3.1 Validation of the ultrasensitive viral load assay

Our initial aim was to validate an HIV-1 RNA quantification assay capable of utilising 2 ml of plasma as assay input. To do so, we compared assay sensitivities following either manual or automated RNA extraction of serial dilutions of WHO 3rd International Standard for HIV-1 RNA.

3.3.1.1 Manual extraction

A total of five independent experiments were performed (Table 3.1 and Table 3.2). The WHO Standard was tested at 40 IU/ml (26 copies/ml) in two experiments (4 replicates); at 20 IU/ml (13 copies/ml) in three experiments (6 replicates); at 10 IU/ml (7 copies/ml) in five independent experiments (19 replicates); at 5 IU/ml (3.5 copies/ml) in three experiments (7 replicates). HIV-1 RNA detection rates were 4/4 replicates (100%) at 40 IU/ml, 6/6 (100%) at 20 IU/ml, 14/19 (74%) at 10 IU/ml, and 4/7 (57%) at 5 IU/ml. Median HIV-1 RNA levels were 34 copies/ml (IQR 27-38, range 10-42) for 40 IU/ml input; 34 copies/ml (IQR 25-42, range: 7-63) for 20 IU/ml input; 24 copies/ml (IQR 14-29, range: 6-282) for 10 IU/ml input; and 10 copies/ml (IQR 5-18, range 5-29) for 5 IU/ml input. Abbott controls were run in each of the five independent experiments and median values were 5 $\log_{10}$ copies/ml (range: 2-5) and 3 $\log_{10}$ copies/ml (range: 3-3) for control H and L respectively, as expected. In one run, control H showed lower quantifications at 2 $\log_{10}$ copies/ml. In two independent runs, input values at 13 copies/ml and 7 copies/ml were read at 63 and 282 copies/ml, respectively (Table 3.2). Averages of coefficients of variation calculated for each run were all above acceptable threshold of 20% and are shown in Table 3.2.

Table 3.1 Validation of manual RNA extraction

Standard IU/ml (copies/ml)	Total replicates tested (runs)	HIV-1 RNA		
		Detected n (%)	Median copies/ml (IQR)	Range copies/ml
40 (26)	4 (2)	4/4 (100)	34 (27-38)	10-42
20 (13)	6 (3)	6/6 (100)	34 (25-42)	7-63
10 (7)	19 (5)	14/19 (74)	24 (14-29)	6-282
5 (3.5)	7 (3)	4/7 (57)	10 (5-18)	5-29
Abbott Control H, $\log_{10}$ cps/ml[a]	6 (5)	6/6 (100)	5.0 (4.9-5.0)	2.0-5.0
Abbott Control L, $\log_{10}$ cps/ml[b]	6 (5)	6/6 (100)	3.0 (3.0-3.0)	3.0-3.0

[a]5.0 $\log_{10}$ cps/ml; [b]3.0 $\log_{10}$ cps/ml.

Table 3.2 Individual runs performed to validate the manual RNA extraction assay

		HIV-1 input IU/ml (copies/ml)			
		40 (26)	20 (13)	10 (7)	5 (3.5)
RUN 1	Individual results (copies/ml)	40	22	24	4
		10	63	6	15
	CV between replicates, %	85	69	88	75
RUN 2	Individual results (copies/ml)	37	33	12	UD
		32	7	282	5
	CV between replicates, %	9.3	94	130	NA
RUN 3	Individual results (copies/ml)		34	39	UD
			45	26	UD
				UD	29
	CV between replicates, %		19	29	NA
RUN 4	Individual results (copies/ml)			22	
				21	
				UD	
				24	
				6	
				30	
				11	
	CV between replicates, %			47	
RUN 5	Individual results (copies/ml)			37	
				UD	
				UD	
				23	
				UD	
	CV between replicates, %			32	
Avarage of CV between replicates, %		47	81	65	NA

CV= coefficient of variation= (SD/average); UD= under limit of detection; NA= not available

3.3.1.2 Automated extraction

One experiment was run (Table 3.3) using the WHO International Standard in 3 replicates of 20 IU/ml (13 copies/ml), 8 replicates of 10 IU/ml (7 copies/ml), and 4 replicates of 1 IU/ml (<1 copy/ml). HIV-1 RNA detection rates were 3/3 (100%) at 20 IU/ml, 7/8 (88%) at 10 IU/ml, and 0/4 (0%) at 1 IU/ml. Median levels of detection were 15 copies/ml (IQR 13-16, range 11-16) for 20 IU/ml input and 14 copies/ml (IQR 8-16, range: 5-24) for 10 IU/ml input. The coefficient of variation between replicates was below 20% for the 13 copies/ml input and above 20% for the 7 copies/ml input.

Table 3.3 Validation of automated RNA extraction

Standard IU/ml (copies/ml)	Total replicates (runs)	HIV-1 RNA			CV between replicates (%)
		Detected n (%)	Median cps/ml (IQR)	Range cps/ml	
20 (13)	3 (1)	3/3 (100)	15 (13-16)	11 – 16	19
10 (7)	8 (1)	7/8 (88)	14 (8-16)	5 - 24	75
1 (0.7)	4 (1)	0/4 (0)	-	-	NA
Abbott Ctrl H[a], log_{10} cps/ml	1 (1)	1 (100)	-	-	
Abbott Ctrl L[b] , log_{10} cps/ml	1 (1)	1 (100)	-	-	

[a]=5.0 log_{10} cps/ml; [b]= 3.0 log_{10} cps/ml. CV= coefficient of variation= (SD/average).

Taken together the results indicated that the automated extraction method provided better results demonstrated by lower coefficient of variation between replicates compared with the manual RNA extraction method for the 13 copies/ml dilution. Based upon these results we proceeded with sample testing by using the automated extraction.

3.3.2 Study population at baseline

The cohort included 37 patients (33 male, 89%) with median duration of ART of 4 years (IQR 2-8) (Table 3.4). Overall 21/37 patients (57%) received only Atripla as treatment, whereas 16/37 (43%) patients had experienced median 3 drug changes (IQR 1-3) before receiving Atripla. For the whole population the median duration of receiving Atripla was 3 years (2-4).

Table 3.4 Baseline characteristics of the study population

Total, n (%)	37 (100)
Male gender, n (%)	33 (89)
Duration of ART, median years (IQR)	4 (2-8)
Atripla as the only regimen, n (%)	21 (57%)
Treatment changes prior to Atripla, median (IQR)	3 (1-3)
Duration of Atripla, median years (IQR)	3 (2-4)

3.3.3 Plasma HIV-1 RNA levels after the switch

Overall plasma samples from 37 subjects were tested (n=144) using the automated extraction protocol as described above and the results are shown in Table 3.5. The input volume was smaller than 2.0 ml in the majority of the patients with a median volume of 1.5 ml. This lower volume affected the lower limit of detection, which was median 17 copies/ml and ranged between 36 and 13 for the four time points. In particular, volumes was significantly smaller at week 4 (median 1.3, IQR 1.2-1.6) when compared with baseline (median 1.5, IQR 1.3-1.8) (p=0.03), but with no difference in volumes

tested at other time points (Table 3.5). The lower volume at week 4 compared to baseline was associated with a reduced rate of HIV-1 detection (p=0.001 Table 3.5). Among the samples tested, 134/144 (93%) yielded a valid result and overall 48/134 (36%) of them showed detectable HIV-1 RNA. An increase in HIV-1 RNA detections rates was observed from baseline to week 24 and detection rates were 11/37 (30%) at baseline, 7/31 (23%) at week 4, 15/36 (42%) at week 12, and 15/30 (50%) at week 24 (Table 3.5). The majority of test had HIV-1 RNA load<50 copies/ml (129, 96%) and within those, no-one had detectable HIVA-RNA between 40-49 copies, whereas 26 (54%) tests yielded levels between 10 and 40 copies (Table 3.5). Nevertheless, 2/36 (6%) and 3/30 (10%) of tests had HIV-1 RNA load > 50 at week 12 and 24 respectively.

The kinetics of plasma HIV-1 RNA load over 24 weeks indicate that overall 33 patients maintained HIV-1 RNA levels <50 copies/ml for the whole period (Figure 1.1 a) and within this group, four subjects showed improved virus suppression after switching (Figure 3.1 b). Overall seven subjects showed reduced suppression (Figure 3.1 c), including 4/37 (10%) subjects that showed viral load rebound >50 copies/ml at week 12 and/or week 24 (Figure 3.1 c points A, B, C, D). In 2 patients with viral load rebound >50 copies/ml, we were able to observe a progressive increase in HIV-1 RNA levels prior to the rebound at week 12 or 24 (Table 3.1c points: C and D). Median HIV-1 RNA load was 9 copies/ml at each time point (Table 3.5), but a trend for significant increase of HIV-RNA load was observed starting at week 12 after baseline (Table 3.2, p=0.06).

Table 3.5 Plasma HIV-1 RNA levels before and over 24 weeks after switching from Atripla to Eviplera

			HIV-1 RNA				
Time point	N	Median plasma volume, ml (IQR)	Detected n (%)	Detected between 10-40 copies/ml n (%)	Median cps/ml (IQR)[a]	<50 copies/ml n (%)	>50 copies/ml, n (%)
Baseline	37	1.5 (1.3-1.8)	11 (30)	4/11 (36)	9 (9-9)	37 (100)	0 (0)
Week 4	31	1.3 (1.2-1.6)[c*]	7 (23)[d**]	4/7 (57)	9 (9-9)	31 (100)	0 (0)
Week 12	36	1.4 (1.2-1.7)	15 (42)	9/15 (60)	9 (9-15)	34 (94)	2 (6)
Week 24	30	1.6 (1.3-1.7)	15 (50)	9/15 (60)	9 (9-14)	27 (90)	3 (10)[c]
Total	134	1.5 (1.2-1.7)	48 (36)	26/48 (54)	9 (9-12)	129 (96)	5 (4)

[a]samples with undetectable HIV-1 RNA were assigned an arbitrary value of 9 copies/ml; [c] p=0.04 vs. Baseline (Mann-Withney test);[d]** p=0.001 vs Baseline (McNemar Chi-2 test). [c]one patients experienced virologic rebound at weeks 12 and week 24.*

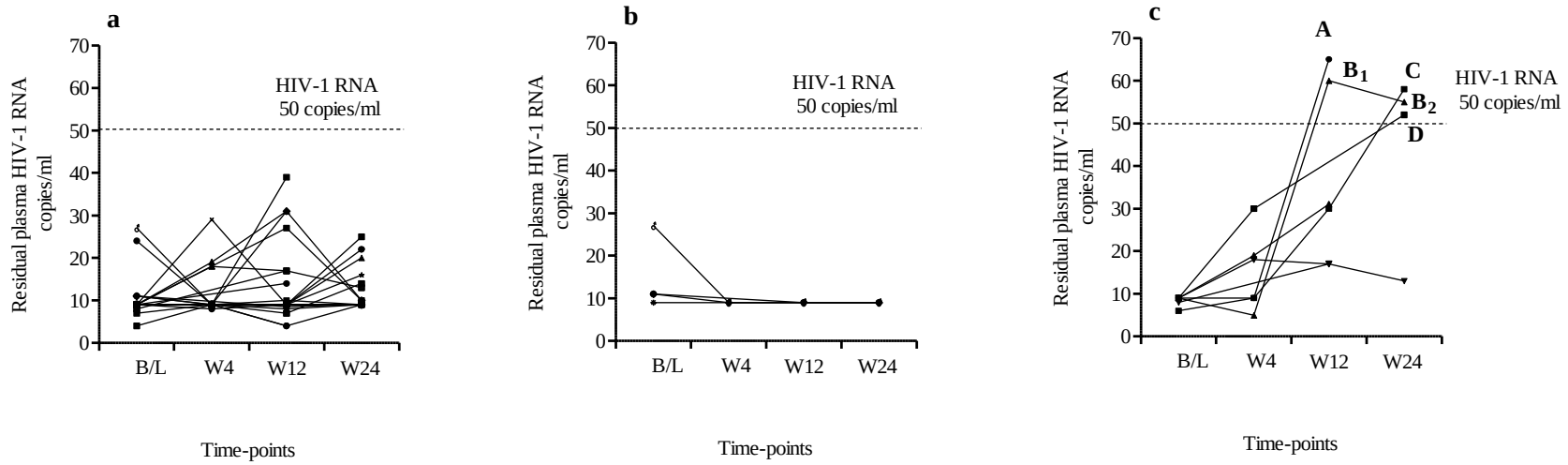

Figure 3.1 Kinetics of plasma HIV-1 RNA from baseline (B/L) to week24 after the switch from Atripla to Eviplera

a) 33 patients showed HIV-1 RNA copies/ml stably below 50 copies/ml during the whole study period with levels ranging from <9 to 39 copies/ml. b) 4 patients showed improved viral suppression after switching. c) 7 patients showed reduced suppression after switching; within this group, 4 patients showed HIV-1 RNA >50 copies/ml at week 12 and/or week 24. A= 185 HIV-1 RNA cps/ml; B_1= 124 HIV-1 RNA cps/ml; B_2= 78 HIV RNA cps/ml; C= 113 HIV-1 RNA cps/ml; D= 69 HIV-1 RNA cps/m. X Axis represented the 4 time points: B/L= baseline; W4= week 4 after the switch; W12= week 12 after the switch; W24= week 24 after the switch; y axis represented residual plasma HIV-1 RNA copies/ml.

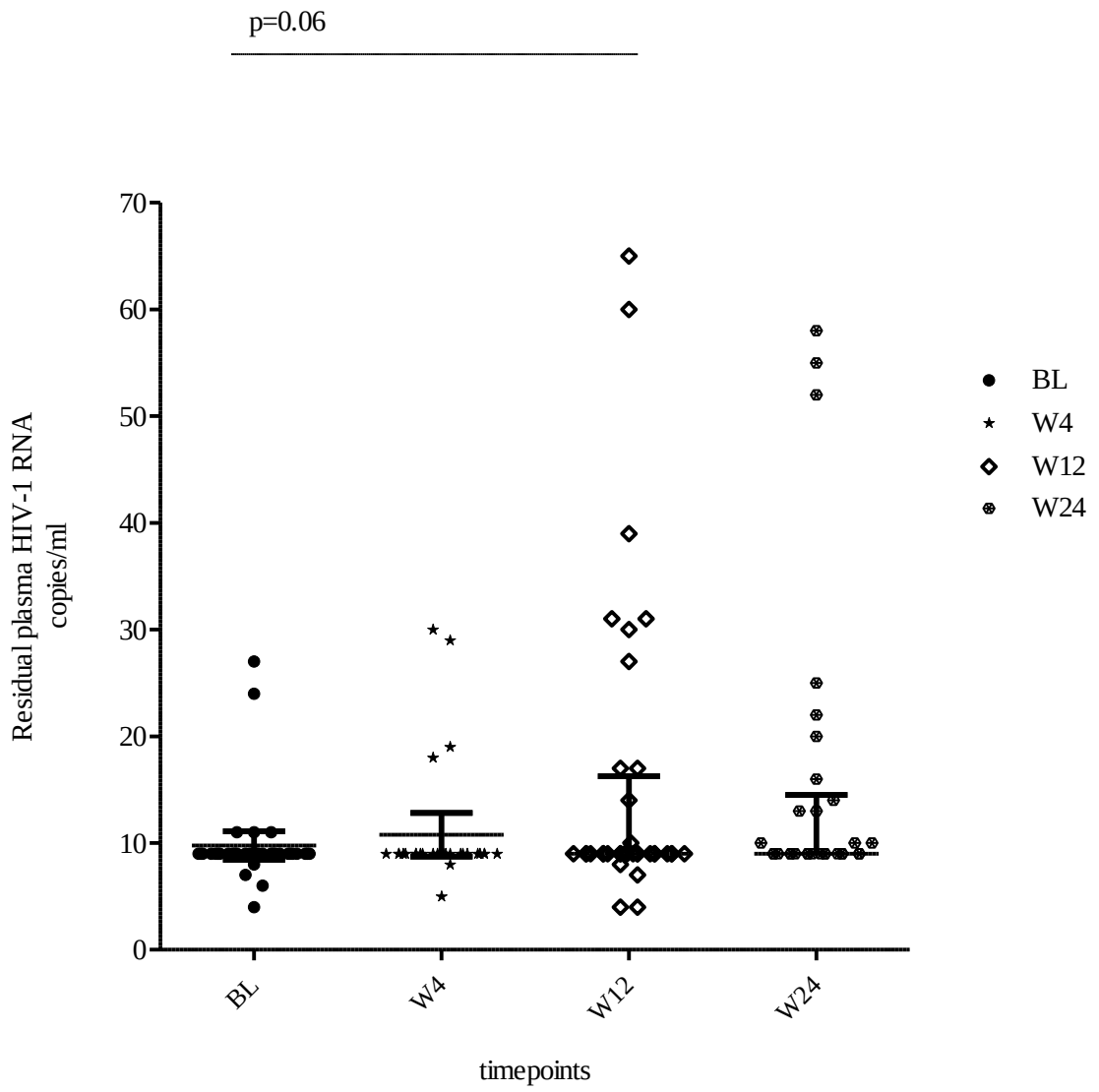

Figure 3.2 Plasma HIV-1 RNA levels measured in the whole cohort over time

For each time point, horizontal lines indicated median values of HIV-1 RNA and the vertical lines defined the interquartile range (IQR). Non-parametric paired-sample Wilcoxon signed rank p value is shown. Number of total test for each time point was: baseline=37, week 4=31, week 12=36; week 24=30.

3.4 DISCUSSION

In this study, residual plasma HIV-1 RNA below 50 copies/ml was measured over 24 weeks in 37 patients that switched suppressive ART with Atripla to Eviplera. Following optimisation of the ultrasensitive viral load assay, we showed that whilst the majority of patients maintained viral load suppression after the switch, seven subjects experienced reduced suppression and four had a viral load rebound >50 copies/ml. Importantly, in two subjects we were able to demonstrate a gradual increase in residual HIV-1 RNA levels prior to viral load rebound >50 copies/ml, which indicates the importance of the ultrasensitive assay as a predictive tool for viral load rebound.

Previous studies described ultrasensitive assays for quantifying residual HIV-1 RNA levels during suppressive ART that require input of large plasma volumes at 8 ml (Palmer et al., 2003). In our lab, we validated an ultrasensitive assay that allowed us to detect down to 1-3 copies/ml starting from 8 ml of plasma input (Chapter 2). In this study we had smaller quantities of plasma available for testing and the highest sensitivity we could expect with the automated procedure was around 13 HIV-1 RNA copies/ml. Although this threshold was acceptable based on previous observations that nearly HIV-1 RNA detection below 10 copies/ml is common in subjects that maintain long-term suppression <50 copies/ml (Maldarelli et al., 2007, Kiselinova et al., 2015), we decided to explore alternative procedures in order to optimise the assay to perform with improved sensitivity relative to the standard method. One previous study proposed a modified version of the Abbott RealTime assay with lower limit of quantification down to 5 copies/ml starting from 3 ml of plasma input (Amendola et al., 2011). The researchers used an *open mode protocol* which allowed the design of a standard curve with one point as low as 10 copies/ml ensuring robust quantification of very low concentrated samples. This option was not available for this study and we tested a manual RNA extraction protocol with reduced input volume from 1 ml to 600 µl and reduced elution volume from 88 µl to 66 µl. Such modifications aimed to further concentrate the extracted RNA and to reflect this in the final calculation of the results, the raw data produced by the software were adjusted dividing by 1.7 and 1.3 to correct for input and elution volumes, respectively. Our results demonstrated

a high variability between replicates when testing either serial dilutions of the WHO 3rd International Standard for HIV-1 RNA or the Abbott assay positive controls. With the automated standard procedure, variability between replicates was reduced. Discordance between the two procedures could be explained by the modifications we introduced within the manual protocol, as well as by an intrinsic inter-operator variability that manual procedure carries, as described by others (Scott et al., 2011). Based on these results we established to use the automated procedure with a sensitivity of quantification at 13 HIV-1 RNA copies/ml for further testing.

Previous reports have demonstrated that patients on suppressive ART show levels of HIV-1 RNA between 1-10 copies/ml and which normally do not associate with viral rebound (Doyle and Geretti, 2012). In this study we did not have the assay sensitivity to explore viral kinetics at HIV-1 RNA levels below 10 copies/ml and we largely focused on HIV-1 loads ranging between 10 and 50 copies/ml. Previous work also showed that around 50% of patients on stable ART with the same NNRTI for median of 6 years had detectable HIV-1 load (Palmer et al., 2008, Ruggiero et al., 2015, Kiselinova et al., 2015) whilst showing persistent viral load suppression confirmed by 2 HIV-1 VL test per year (Chapter 4 of this thesis). In the cohort presented here, before the switch to Eviplera all patients had HIV-1 RNA<50 copies/ml and 50% of those were on stable ART with Atripla for median 4 years. After the switch, patients maintained stable viral load suppression during the whole study period, whereas 7 patients showed a reduced suppression with HIV-1 RNA levels between 10-40 and >50 HIV-1 RNA copies/ml at week 12 or 24 after starting Eviplera. One previous study by Doyle and colleagues demonstrated that patients on ART with detectable HIV-1 RNA <40 copies/ml had 11.3% and 3.8% to experience virologic rebound at HIV-1 RNA levels above 50 and 400 copies/ml over 12 months of follow up, respectively. In our study we found that 4/7 patients with reduced suppression experienced a lack of suppression with HIV-1 RNA>50 copies by the end of study. Moreover, within the 4 “rebounders”, overall 2/4 showed levels between 10-40 HIV-1 RNA copies/ml at the time point prior to lack of suppression. Our findings confirmed both the Doyle study and another work on therapy simplification (Doyle et al., 2012, Swindells et al., 2006)

demonstrating that viral rebound was predicted by a progressive increase in HIV-1 RNA levels. The virologic rebound observed in our study could be explained by different factors including pharmacological drug characteristics as well as psychological aspects associated with therapy switch. It has been demonstrated that EFV half-life averages around 40-55 hours (Boffito et al., 2009, Smith et al., 2001), which means that a missed dose will not necessarily reflect a viral rebound. RVP half-life is around 50 hrs as well, but it needs to be taken with an abundant meal in order to achieve maximal concentration when orally administrated (Hoetelmans et al., 2005, Crauwels et al., 2013, Lamorde et al., 2015). Switching therapy regimes already modify patient compliance due to psychological as well as logistical reasons; in this case new administration criteria are also present and this could have had a potential impact on the adherence resulting in lack of viral suppression.

This study has a number of limitations, with the main being the lack of longer patient follow-up, which could have strengthened the analysis, particularly for the 7 patients who showed reduced viral load suppression. Moreover, there was limited information available on the patient's characteristics including factors such as the pre-ART viral load. Furthermore, the study was not powered to demonstrate virological non-inferiority between EFV and RPV and therefore it is difficult to achieve firm conclusions regarding the apparent risk of viral load rebound after switching away from EFV. In previous works RPV/FTC/TDF was considered a safe option to switch from EFV in case CNS toxicity, even though a small proportion of patients could experience virologic rebound at 48 weeks after switching (Mills et al., 2013). In line with these results, our data demonstrate that 33 out of 37 patients switching from Atripla to Eviplera were able to maintain viral load suppression with plasma HIV-1 RNA levels below 40 copies/ml. Four patients showed virologic rebound and using our ultrasensitive testing we were able to predict the rebound for 2 of them. Our results confirmed the importance of routine monitoring HIV-1 RNA loads with an ultrasensitive assay with the aim of improving clinical management and preventing viral rebounds.

The results from this chapter have raised important questions around the debate as to what significance residual HIV-1 RNA levels have on HIV-1 persistence. In the following chapters we study a population of 104 patients treated with either EFV or NVP based ART for 1-15 years and who demonstrate persistent viral load suppression (HIV-1 RNA <50 copies/ml) and characterize viral as well as immunologic factors that associate with HIV-1 persistence.

Chapter 4: Factors associated with HIV-1 persistence in a population of stable suppressed individuals

4.1 INTRODUCTION

Initiation of antiretroviral therapy (ART) causes a robust suppression of HIV replication, which results in a rapid decrease of plasma HIV-1 RNA below the limit of detection of commonly used diagnostic assays (20-50 copies/ml). Viral load undetectability defines the success of ART. However, research-based ultrasensitive assays can detect HIV-1 RNA at low levels in plasma of most treated patients, even after many years of seemingly suppressive ART. Other markers of HIV replication, including intracellular forms of HIV-1 RNA and unintegrated HIV-1 DNA (e.g., 2 long-terminal-repeat [LTR] circles), similarly decrease when ART is started (Mexas et al., 2012, Koelsch et al., 2008), but can remain detectable in the long-term despite undetectable levels of viral load in the plasma (Besson et al., 2014, Kiselinova et al., 2015, Palmer et al., 2008). Long-lived resting $CD4^{+}$T cells carry integrated HIV-1 DNA (Siliciano et al., 2003, Chomont et al., 2009) as a viral reservoir which is established early after infection and is unresponsive to ART. This stable integrated reservoir fuels resumption of plasma viremia if ART is stopped (Ruiz et al., 2000, Siliciano and Siliciano, 2015, Nicastri et al., 2008).

Current research efforts aim to identify the source of plasma HIV-1 RNA and unintegrated HIV-1 DNA during seemingly suppressive ART, and to unravel the association between these markers and the integrated viral reservoir, as key to our understanding of how HIV infection may be eradicated (Chun, 2013, Chun et al., 2011). Such studies must take into account the complex interplay between the virus and the host immune system (Hatano, 2013, Klatt et al., 2013). HIV-1 infection induces a state of chronic immune activation and inflammation that plays a key role in disease pathogenesis. Various soluble markers such as sCD14, D-dimers, highly sensitive C-reactive protein (hsCRP), IL-6, sCD30, and sCD27 have been found to be predictive of disease progression in untreated HIV-positive patients (Sandler et al., 2011, Pizzolo et al., 1994, Hazenberg et al., 2003). In addition, levels of sCD14, IL-6 and D-dimers have been associated with the risk of non-AIDS HIV-related morbidity, including

cardiovascular, renal and neurological disease and an increased risk of cancer (Sandler et al., 2011) .

Abnormal levels of cellular and soluble markers of immune activation and inflammation improve substantially with ART, although abnormalities may persist (Klatt et al., 2013, Hatano, 2013). The aim of this study was to investigate the relationship between virological markers of HIV-1 persistence and markers of immune activation and inflammation during stably suppressive ART. In order to minimise confounding factors, a cohort of patients was selected with the exact characteristics overall indicative of highly stably suppressive first-line treatment with two nucleoside/nucleotide reverse transcriptase inhibitors (NRTIs) plus one non-nucleoside reverse transcriptase inhibitor (NNRTI).

4.2 METHODS

4.2.1 Study population

Study subjects were recruited within the ERAS cohort study described in details in Chapter 2. Briefly, eligible patients started first-line ART with two NRTIs plus either efavirenz (EFV) or nevirapine (NVP), achieved plasma HIV-1 RNA suppression <50 copies/ml within the first 6 months of therapy, and during subsequent follow-up showed continuous viral load suppression (<50 copies/ml) without viral load elevations >50 copies/ml or treatment interruptions, while undergoing ≥2 viral load measurements per year and remaining on the initial NNRTI. Changes of the initial NRTIs (e.g., for toxicity) were allowed provided they were not associated with a treatment interruption or viral load rebound >50 copies/ml.

4.2.2 Quantification of residual HIV-1 RNA in plasma

Plasma HIV-1 RNA was quantified using a modified version of the Abbott RealTime HIV-1 assay (Maidenhead, UK) starting from 8ml of plasma that was ultracentrifuged at 215,000xg for 45’ at 4^{o}C. The assay 50% and 95% detection rates were 1 and 3 HIV-1 RNA copies/ml, respectively.

4.2.3 Drug concentration

Plasma concentration of EFV or NVP was measured by pharmacology department of University of Liverpool using standard methodology. The concentrations were measured in untimed samples.

4.2.4 Quantification of total and 2-LTR circular HIV-1 DNA in peripheral blood mononuclear cells (PBMC)

Total HIV-1 DNA in PBMC was quantified by real-time PCR; the assay 50% and 95% detection rates were 20 and 40 HIV-1 DNA copies/10^6 PBMC, respectively (Geretti et al., 2013) as previously reported. 2-LTR circular HIV-1 DNA was measured by digital PCR; the assay lower limit of detection was median 5 copies/10^6 PBMC (interquartile range, IQR 4-6).

4.2.5 Markers of immune activation

Cellular markers of immune activation were measured on fresh blood by flow cytometry at the Immunology Diagnostic Service of the Royal Free Hospital, in London as described in Chapter 2. PBMC were stained with labelled antibodies against CD4 plus CD26, CD38, or CD69, and against CD8 plus either CD38 or HLA-DR/DP/DQ. Soluble markers of immune activation and inflammation were measured by plate enzyme-linked immune-enzymatic assay (ELISA) and analysed according to the manufacturers' recommendations as described in Chapter 2.

4.2.6 Statistical analysis

The characteristics of the study population were summarised after stratification into three groups based upon duration of suppressive ART (0-4 years, 4-7 years, >7 years). Duration of suppressive ART was defined as the length of time following the first viral load measurement <50 copies/ml, which was recorded within six months of starting ART. Where the analyses required variables to be expressed as medians, undetectable results were given a midpoint value between zero and the lower limit of detection of each assay. Plasma drug concentrations for each patient were categorized as being above or below the recommended therapeutic dose for

wild-type virus (1000 ng/ml for EFV and 3400 ng/ml for NVP). For residual plasma HIV-1 RNA, total and 2-LTR circular HIV-1 DNA, cellular and soluble markers of immune activation, the mean difference (with 95% confidence interval, CI) over 10 years of suppressive ART was analysed by univariate linear regression analysis after log transformation of the variables. Associations between variables were tested by univariate and multivariable linear regression analysis, using as outcomes residual plasma HIV-1 RNA, 2-LTR circular HIV-1 DNA, and total HIV-1 DNA. Based upon results from the univariable models, all variables with $p \leq 0.20$ were included into the multivariable models. In the main multivariate analysis, only factors that had a number of observations >25 were considered, and as a result NNRTI used, gender, and ethnicity were excluded. Moreover, when age and duration of suppressive ART were eligible for inclusion into the same model, age was excluded due to the high co-linearity between the two variables. Separate models explored a) the effects of including ethnicity, which excluded four subjects of Asian origin; and b) the effect of excluding two outliers with HIV-1 RNA levels >11 copies/ml; c) the effect of including continuous levels of EFV, which excluded eighteen patients on NVP. When modelling for total HIV-1 DNA, the 2-LTR circular DNA level was not included due to strong co-linearity, and vice versa. Separate analyses described total HIV-1 DNA/10^6 CD4 T-cells (rather than PBMC); this was calculated after adjusting the load for the proportion of $CD3^+CD4^+$ cells in the sample as determined by flow cytometry; these analyses excluded the CD4 cell count and CD4/CD8 ratio. All statistical analyses were performed with IBM SPSS statistic v 22.0.

4.3 RESULTS

4.3.1 Study population

A total of 104 patients who were receiving two NRTIs plus either EFV (n=86; 83%) or NVP (n=18; 17%) and had experienced plasma HIV-1 RNA suppression <50 copies/ml for median 5 years were recruited and analysed cross-sectionally. Of these, 81/104 (78%) were men and 59/104 (57%) were of white ethnicity (Table 4.1). Patients with longer duration of suppressive ART were predictably older (p=0.04), had a marginally higher current CD4 cell count (p=0.06) but a lower nadir CD4 cell count (p<0.001) and a higher pre-ART viral load (p=0.01), and were more likely to have experienced changes in the composition of the NRTI backbone after

starting therapy ($p<0.001$). Overall 48/104 patients (48%) changed one or more component of the NRTI backbone, with median 1 drug change per subject (IQR 1-2). At the time of sampling, NRTI backbones were tenofovir/emtricitabine (76/104, 73%), tenofovir/ lamivudine (2/104, 2%) abacavir/emtricitabine (1/104, 1%), abacavir/lamivudine (21/104, 20%), zidovudine/lamivudine (4/104, 4%). Median levels of EFV and NVP were 1531 ng/ml (IQR 846-2235) and 5889 ng/ml (3096-7416), respectively. Overall, 33/104 (32%) individuals had suboptimal plasma therapeutic drug concentration, defined as a level below the recommended cut-off for wild-type virus.

4.3.2 Virological and immunological parameters

Residual plasma HIV-1 RNA was detected in 52/104 (50%) patients; median levels were 2 copies/ml and ranged between 1 and 35 copies/ml (Table 4.2). Among subjects with detectable HIV-1 RNA, 50/52 (96%) had levels ≤11 copies/ml. In PBMC, total HIV-1 DNA was detected in all subjects, with median levels of 2.5 $\log_{10}$ copies/10^6 PBMC and ranging between 1.3 and 2.5 $\log_{10}$ copies/10^6 PBMC; 2-LTR circular HIV-1 DNA was detected in 24/104 (23%) patients at median levels of 3 copies/10^6 PBMC levels and ranging between 4 and 119 copies/10^6 PBMC.

The difference in virological and immunological parameters over 10 years of suppressive ART was initially analysed by univariate linear regression analysis (Table 4.3). Levels of residual HIV-1 RNA and 2-LTR circular HIV-1 DNA were lower with longer treatment duration, whilst HIV-1 DNA levels did not show a significant difference. Longer treatment duration was also characterised by a higher CD4 cell count and a lower percentage of CD4 and CD8 cells expressing the CD38 and the HLA-DR/DP/DQ activation markers, respectively. Soluble markers showed no significant trends, with the exception of a marginally significant decline in sCD27 levels.

Table 4.1 General characteristics of the study population at the time of recruitment

Characteristic		Total (n=104)	Duration of suppressive ART stratum, years		
			<4 (n=34)	4-7 (n=35)	>7 (n=35)
Duration of suppressive ART[a], median years (IQR)		5 (3-8)	2 (2-3)	5 (5-6)	9 (8-10)
Age, median years (IQR)		47 (40-53)	44 (36-49)	49 (39-53)	48 (43-55)
Male, n (%)		81 (78)	29 (85)	29 (83)	23 (66)
Ethnicity, n (%)	White	59 (57)	20 (59)	22 (63)	17 (48.5)
	Black	41 (39)	13 (38)	11 (31)	17 (48.5)
	Asian	4 (4)	1 (3)	2 (6)	1 (3)
Pre-ART HIV-1 RNA, median $\log_{10}$ copies/ml (IQR)		4.9 (4.6-5.3)	4.7 (4.1-5.1)	4.9 (4.6-5.3)	5.1 (4.8-5.6)
Nadir CD4 count, median cells/mm^3 (IQR)		201 (110-270)	279 (216-365)	166 (126-238)	118 (79-215)
Efavirenz as NNRTI, n (%)		86 (83)	30 (88)	32 (89)	24 (69)
NNRTI concentration, median ng/ml (IQR)	EFV	1531 (846-2235)	1492 (735-2130)	1496 (866-2154)	1966 (855-2626)
	NVP	5889 (3096-7419)	4545 (2798-6147)	2734 (2539-5743)	6311 (4390-7603)
NNRTI concentration <target MEC[b], n (%)		33 (32)	12 (35)	11 (31)	10 (29)
Changed the initial NRTI backbone n (%)		48 (46)	4 (12)	13 (37)	31 (89)

[a] defined as the length of time after the first plasma HIV-1 RNA load <50 copies/ml; [b]MEC= minimum effective concentration recommended for wild-type virus; cuts off were 1000 ng/ml for EFV (Poeta et al., 2011) and 3400 ng/ml for NVP (Havlir et al., 1995). ART= antiretroviral therapy; NNRTI= non-nucleoside reverse transcriptase inhibitor; NRTI= nucleoside/nucleotide reverse transcriptase inhibitor.EFV= efavirenz, NVP= nevirapine.

Table 4.2 Virological and immunological profile of the study population at the time of recruitment

Parameter	Total (n=104)	Duration of suppressive therapy, years		
		<4 (n=34)	4-7 (n=35)	>7 (n=35)
Detectable residual plasma HIV-1 RNA, n (%)	52 (50)	21 (62)	18 (51)	13 (37)
Residual HIV-1 RNA, median cps/ml (IQR)[a]	2 (2-4)	2 (2-4)	2 (2-4)	2 (2-2)
Detectable 2-LTRc HIV-1 DNA, n (%)	24 (23)	12 (35)	7 (20)	5 (14)
2-LTRc HIV-1 DNA, median cps/10^6 PBMC (IQR)[b]	3 (3-3)	3 (3-7)	3 (3-3)	3 (3-3)
Total HIV-1 DNA, median $\log_{10}$ cps/10^6 PBMC (IQR)	2.5 (2.1-2.8)	2.6 (2.3-3.0)	2.4 (1.7-2.8)	2.5 (2.1-2.8)
Total HIV-1 DNA, median $\log_{10}$ cps/10^6 CD4 T-cells (IQR)	3.0 (2.6-3.4)	3.3 (2.8-3.5)	2.8 (2.4-3.3)	3.0 (2.6-3.4)
CD4 count, median cells/mm^3 (IQR)	581 (474-722)	548 (427-629)	580 (509-720)	632 (503-796)
CD8 count, median cells/mm^3 (IQR)	798 (656-1047)	808 (596-1060)	818 (685-1024)	679 (496-929)
$CD4^+$ $CD38^+$, median percentage (IQR)	24 (16-34)	32 (23-36)	21 (15-31)	22 (15-28)
$CD4^+CD26^+$, median percentage (IQR)	58 (46-64)	56 (47-67)	59 (49-63)	58 (44-64)
$CD4^+CD69^+$, median percentage (IQR)	1 (1-2)	2 (1-3)	1 (1-2)	2 (1-2)
$CD8^+CD38^+$, median percentage (IQR)	5 (3-7)	6 (4-8)	4 (3-6)	4 (3-6)
$CD8^+$HLA-DR/DP/DQ^+, median percentage (IQR)	35 (24-42)	37 (27-47)	35 (26-40)	30 (20-39)
sCD14, median µg/ml (IQR)	2.2 (1.8-2.5)	2.2 (1.8-2.4)	2 (1.8-2.5)	2.3 (1.9-2.5)
D-Dimer, median µg/ml (IQR)	2.2 (0.8-3.2)	1.4 (0.7-3.2)	2.5 (0.9-3.2)	2.1 (0.8-3.1)
hsCRP, median µg/ml (IQR)	1.4 (0.7-3.6)	1 (0.4-3.4)	1.9 (0.8-2.8)	2.1 (0.8-4)
IL6 median pg /ml (IQR)	0.8 (0.5-2.1)	0.5 (0.5-1.2)	1.1 (0.5-2.3)	0.8 (0.5-2.1)
sCD27, median U /ml (IQR)	61.8 (48.5-76.1)	64 (52.4-79.5)	61.1 (53.7-76.2)	59.6 (46.4-71.4)
sCD30, median ng /ml (IQR)	11 (9-15.2)	10.7 (8.9-14.8)	11.9 (9.5-16.8)	10.9 (8.8-13.4)

[a] Samples with undetectable HIV-1 RNA were assigned an arbitrary value of 1.5 copies/ml. [b]Samples with undetectable 2-LTRc HIV-1 DNA were assigned an arbitrary value of 2.5 copies/10^6 PBMC. IQR= interquartile range; cps= copies; PBMC= peripheral blood mononuclear cells; 2-LTRc= 2-LTR circular HIV-1 DNA.

Table 4.3 Univariate linear regression analysis of mean difference in log-transformed virological and immunological parameters per 10 years of suppressive antiretroviral therapy

Parameter	Mean difference	95% CI	P
Residual HIV-1 RNA, copies/ml	-0.19	-0.38; -0.01	0.04
2-LTRc HIV-1 DNA, copies/10^6 PBMC	-0.19	-0.39; 0.02	0.08
Total HIV-1 DNA, copies/10^6 PBMC	0.02	-0.35, 0.39	0.92
CD4 count, cells/mm^3	0.14	0.04, 0.25	0.01
CD8 count, cells/mm^3	-0.07	-0.19, 0.08	0.43
$CD4^+CD38^+$ percentage	-0.21	-0.34, -0.09	0.001
$CD4^+CD26^+$ percentage	-0.03	-0.11, 0.05	0.44
$CD4^+CD69^+$ percentage	-0.10	-0.28, 0.08	0.26
$CD8^+CD38^+$ percentage	-0.14	-0.31, 0.04	0.13
$CD8^+$HLA-DR/DP/DQ^+ percentage	-0.14	-0.27, -0.01	0.04
sCD14 μg/ml	0.02	-0.04, 0.01	0.51
D-Dimer ng/ml	-0.03	-0.33, 0.14	0.49
hsCRP μg/ml	0.01	-0.50, 0.52	0.79
IL-6 pg/ml	0.10	-0.18, 0.39	0.46
sCD27 U/ml	-0.09	-0.18, 0.001	0.06
sCD30 ng/ml	-0.05	-0.19, 0.09	0.45

[a]*All variables were log-transformed. CI= Confidence interval*

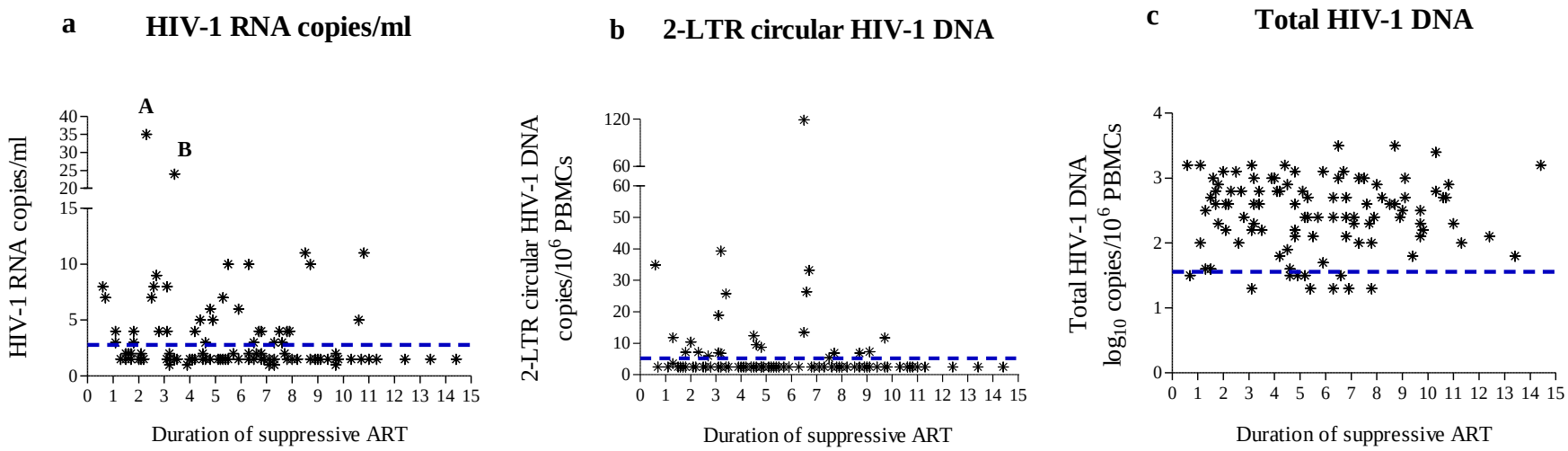

Figure 4.1 Markers of HIV-1 persistence in patients with 1-15 years of duration of suppressive ART

Dot plots representing a) HIV-1 RNA, b) 2-LTR circular HIV-1 DNA in PBMC, c) total HIV-1 DNA in PBMC in patients with 1-15 years of suppressive ART. Each dot represents patients with same x and y coordinates. Blue dotted lines indicate lower limit of detection: a) for HIV-1 RNA ultrasensitive assay=3 copies/ml; b) for the 2-LTR HIV-1 DNA assay that is 5 copies/10^6 PBMC; c) for the total HIV-1 DNA assay that is 1.6 $log_{10}/10^6$ PBMC. A=34 HIV-1 RNA copies/ml of one patient on EFV/ABC/3TC; B=24 HIV-1 RNA copies/ml of one patient on EFV/TDF/FTC. Y axis in a) and b) were split into two segments for a better visualization of the data.

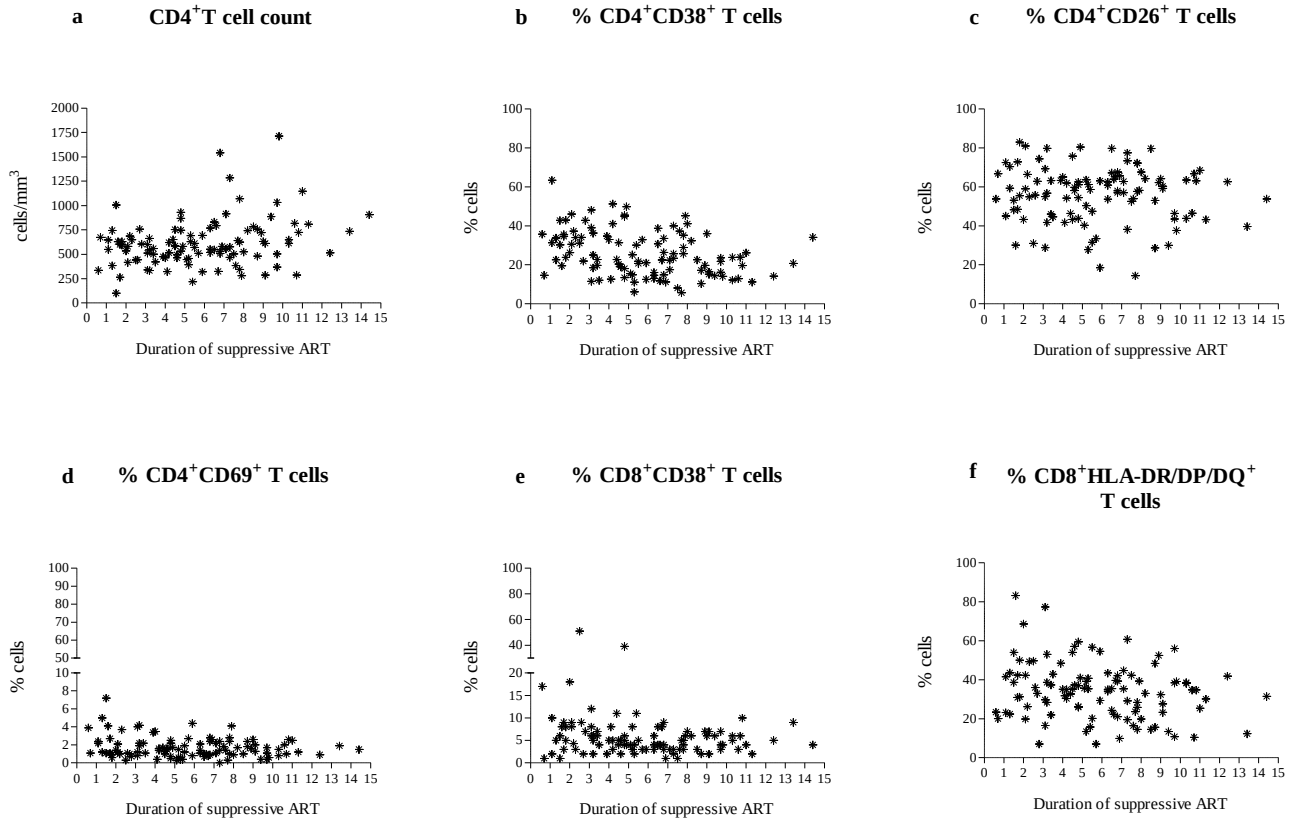

Figure 4.2 Markers of cellular immune activation in patients with 1-15 years of duration of suppressive ART

Dot plots representing a) % CD4 T-cells, b) % $CD4^+$ $CD38^+$T-cells, c) % $CD4^+$ $CD26^+$T-cells, d) % $CD4^+$ $CD69^+$T-cells, e) % $CD8^+$ $CD38^+$T-cells, f) % $CD8^+$HLA-DR/DP/DQ^+T-cell, in patients with 1-15 years of suppressive ART. Each dot represents patients with same x and y coordinates. Blue line in plot a) indicates 200 CD4 T-cells/mm^3. Y axis in plots d and e were spitted into two segments for better visualization. d) lower segment=up to 10 % $CD4^+$ $CD69^+$T-cells, higher segment from 50% to 100 % $CD4^+$ $CD69^+$T-cells; e) lower segment=up to 20 % $CD8^+$ $CD38^+$T-cells, higher segment from 30% to 100 % $CD8^+$ $CD38^+$T-cells.

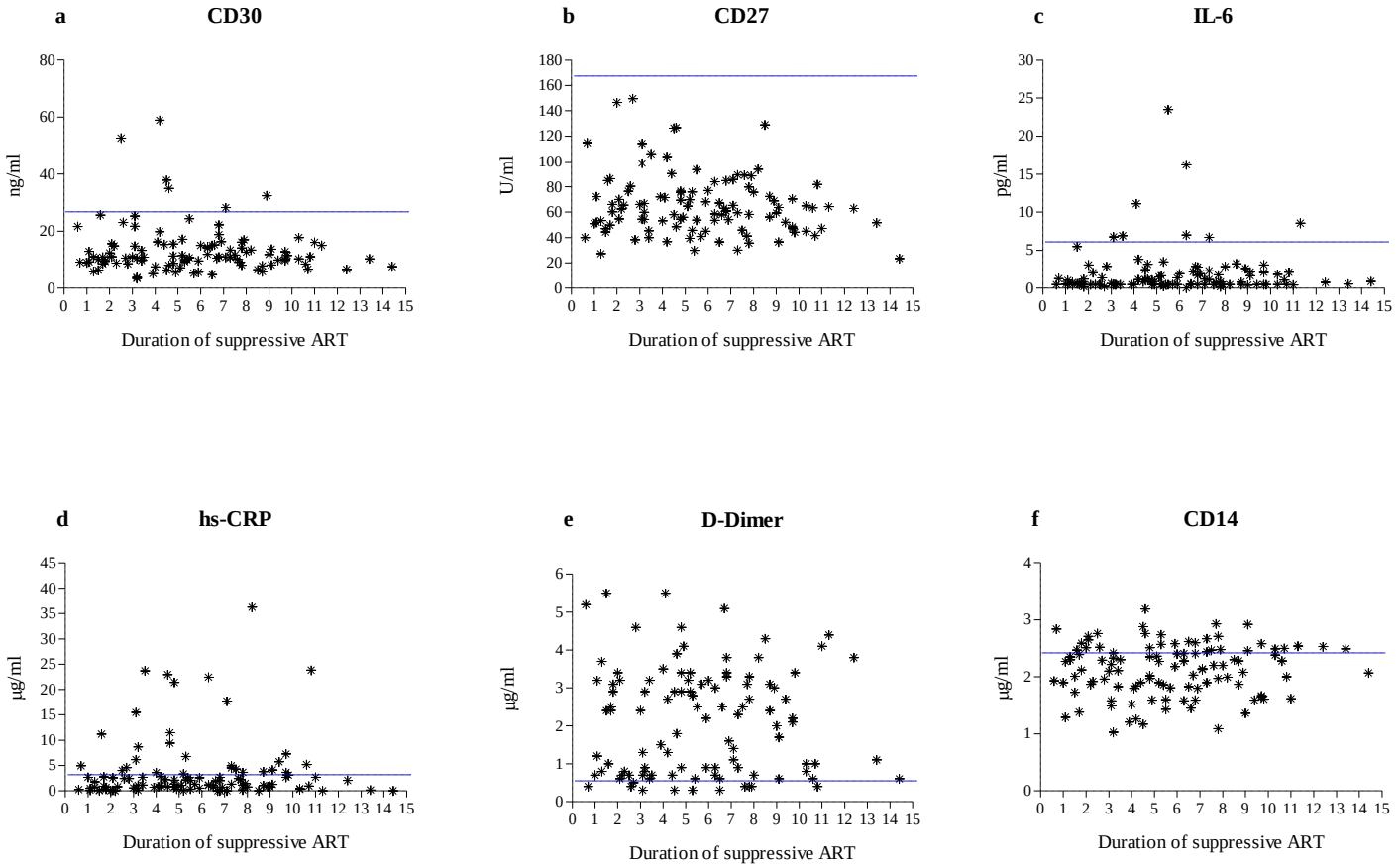

Figure 4.3 Soluble markers of cellular immune activation in patients with 1-15 years of duration of suppressive ART

Cross-sectional analysis of levels of sCD30, sCD27, IL-6, hs-CRP, D-dimers, and sCD14 in patients with 1-15 years of suppressive ART. Each dot represents one patient. Blue lines indicate the reference levels for healthy individuals that were : (a) sCD30 (Gao et al., 2015)= 25 ng/ml; (b) sCD27=164 U/ml (De Milito et al., 2002); c) IL6 (Tenorio et al., 2014)= 6pg/ml; d) hs-CRP= 3µg/ml (McBride and Cooper, 2008); e) D-Dimer= 0.5µg/ml (Lichtfuss et al., 2011); f) sCD14=2.5pg/ml (Sandler et al., 2011).

Factors associated with virological markers of HIV persistence

By univariate analysis, residual HIV-1 RNA levels were lower with longer duration of suppressive ART, and were also positively associated with sCD27 levels; however the strength of the association was reduced after adjustment (Table 4.4). A sensitivity analysis that excluded the two outliers with HIV-1 RNA levels >11 copies/ml confirmed an independent positive association between residual HIV-1 RNA levels and sCD27 levels, but detected no evidence of a difference in HIV-1 RNA levels by duration of suppressive ART (Table 4.5). There was also no evidence of an association with total and 2-LTR circular HIV-1 DNA levels and with other markers of immune activation and inflammation.

By univariate analysis, 2-LTR circular HIV-1 DNA levels were lower with longer duration of suppressive ART. After adjustment for duration of suppressive ART, $CD4^+CD26^+$ T-cells, pre-ART HIV-1 RNA, hsCRP and sCD27, higher levels of 2-LTR circular HIV-1 DNA remained associated with duration of suppressive ART (Table 4.6).

By univariate analysis, higher HIV-1 DNA levels in PBMC were associated with higher pre-ART HIV-1 RNA. In the analysis adjusted for age, nadir CD4 T-cell, pre-ART HIV-1 RNA, $CD8^+CD38^+$ T-cells, $CD8^+$HLA-DR/DP/DQ^+ T-cells, sCD14, IL6, and CD30, higher levels of total HIV-1 DNA were strongly associated with higher pre-ART HIV-1 RNA and frequencies of $CD8^+$HLA-DR/DP/DQ^+ T-cells, and to younger age (Table 4.7). A sensitivity analysis was run on total HIV-1 DNA load in CD4 T-cells and this confirmed the positive association with pre-ART HIV-1 RNA load and $CD8^+$HLA-DR/DP/DQ^+ T-cells both in univariate and multivariable analysis (Table 4.8).

The univariate analysis on patients with white or black ethnicity showed that levels of residual HIV-1 RNA and total HIV DNA load were similar in white compared with black, whereas a trend for association between ethnicity and 2-LTR circular HIV-1 DNA and total HIV-1 DNA in CD4 T-cells (Table 4.9). Based on these observations, we analysed factors associated with 2-LTR circular HIV-1 DNA and total HIV-1 DNA in CD4 T-cells when ethnicity was included into the multivariable model. Results confirmed the association between 2-LTR circular HIV-1 DNA and duration of suppressive ART (Table 4.10); further higher levels of total HIV-1 DNA in CD4 T-cells were found in patients with higher levels of pre-ART HIV-1 RNA and

%$CD8^+$DR-DP-DQ^+ T-cell as observed in previous analysis that was not adjusted for ethnicity (Table 4.11).

Furthermore we analyzed if plasma levels of EFV were associated with HIV-1 persistence. In 86 patients with EFV we found that drug levels were not associated with any marker of viral persistence; however, univariable analysis showed that levels EFV levels were eligible for inclusion in the multi-variable analysis when modelling for residual HIV-1 RNA levels in patient (N=84) with HIV-1 RNA<11 copies/ml (Table 4.12). Based upon these data we explored factors associated with residual HIV-1 RNA copies/ml when levels of EFV when included into the multivariable model. Results confirmed the association between residual HIV-1 RNA and sCD27 even though with weaker effect as observed in previous analysis without adjustment for EFV drug levels (Table 4.13).

Table 4.4 Univariate and multivariable linear regression analysis of factors associated with the mean difference in residual plasma HIV-1 RNA load

Characteristic	Univariate			Multivariable		
	Mean difference	95% CI	P	Mean difference	95% CI	P
Age, per 10 years higher	-0.01	-0.08, 0.05	0.67			
Nadir CD4 count per 100 cell/mm^3 higher	0.02	-0.02, 0.07	0.29			
Pre-ART HIV-1 RNA per log_{10} copies/ml higher	0.01	-0.08, 0.09	0.86			
Duration of suppressive ART per 10 years longer	-0.19	-0.38, -0.01	0.04*	-0.16	-0.34, 0.03	0.10
NNRTI concentration below the MEC "yes" vs "no"	0.08	0.04, 0.21	0.18*	0.04	-0.09, 0.17	0.56
CD4 count per 100 cells/mm^3 higher	0.001	-0.02, 0.03	0.95			
CD4/CD8 ratio per 1 unit higher	0.01	-0.16, 0.15	0.89			
2-LTRc DNA per log_{10} cps/10^6 PBMC cells higher	0.06	-0.12, 0.24	0.47			
Total HIV-1 DNA per log_{10} cps/10^6 PBMC higher	0.02	-0.08, 0.12	0.74			
$CD4^+CD38^+$ per 50% higher	0.09	-0.16, 0.37	0.47			
$CD4^+CD26^+$ per 50% higher	0.05	-0.16, 0.26	0.64			
$CD4^+CD69^+$ per 50% higher	0.24	-2.33, 2.8	0.85			
CD8 count per 100 cells/mm^3 higher	0.004	-0.01, 0.02	0.45			
$CD8^+CD38^+$ per 50% higher	0.25	-0.21, 0.72	0.28			
$CD8^+$HLA-DR/DP/DQ^+ per 50% higher	-0.02	-0.22, 0.19	0.87			
sCD14 per log_{10} µg/ml higher	0.22	-0.35, 0.79	0.22			
D-Dimer per log_{10} µg/ml higher	-0.08	-0.25, 0.08	0.33			
hs-CRP per log_{10} ng/ml higher	0.06	-0.09, 0.21	0.43			
IL6 per log_{10} pg/ml higher	0.08	-0.12, 0.29	0.41			
sCD27 per log_{10} U/ml higher	0.45	0.08, 0.82	0.02 *	0.31	-0.11, 0.72	0.15
sCD30 median per log_{10} ng/ml higher	0.20	-0.07, 0.46	0.15 *	0.09	-0.19, 0.37	0.50

**only variables with p≤0.2 were included in the multivariable analysis*

Table 4.5 Univariate and multivariable linear regression analysis of factors associated with the mean difference in residual plasma HIV-1 RNA load in patients with residual plasma load ≤11 copies/ml (N=102)

	Univariate			Multivariable		
Characteristic	Mean difference	95% CI	P	Mean difference	95% CI	P
Age, per 10 years higher	-0.01	-0.07, 0.05	0.78			
Nadir CD4 count per 100 cell/mm^3 higher	0.01	-0.06, 0.05	0.58			
Pre-ART HIV-1 RNA per log_{10} copies/ml higher	0.00	-0.08, 0.08	0.99			
Duration of suppressive ART per 10 years longer	-0.13	-0.29, 0.03	0.12*	-0.07	-0.24, 0.09	0.39
NNRTI concentration below the MEC "yes" vs "no"	0.12	0.01, 0.23	0.04*	0.06	-0.05, 0.18	0.25
CD4 count per 100 cells/mm^3 higher	-0.001	-0.02, 0.02	0.92			
CD4/CD8 ratio per 1 unit higher	0.04	-0.11, 0.17	0.62			
2-LTRc DNA per log_{10} cps/10^6 PBMC cells higher	0.05	-0.11, 0.20	0.57			
Total HIV-1 DNA per log_{10} cps/10^6 PBMC higher	-0.01	-0.09, 0.08	0.87			
$CD4^+CD38^+$ per 50% higher	0.08	-0.14, 0.30	0.47			
$CD4^+CD26^+$ per 50% higher	0.08	-0.10, 0.27	0.37			
$CD4^+CD69^+$ per 50% higher	-0.61	-2.97, 1.75	0.60			
CD8 count per 100 cells/mm^3 higher	0.002	-0.01, 0.01	0.70			
$CD8^+CD38^+$ per 50% higher	0.32	-0.11, 0.75	0.16*	0.25	-0.19, 0.67	0.26
$CD8^+$HLA-DR/DP/DQ^+ per 50% higher	-0.03	-0.21, 0.15	0.76			
sCD14 per log_{10} μg/ml higher	0.26	-0.24, 0.75	0.31			
D-Dimer per log_{10} μg/ml higher	-0.08	-0.22, 0.07	0.28			
hs-CRP per log_{10} ng/ml higher	0.07	-0.05, 0.20	0.24			
IL6 per log_{10} pg/ml higher	0.13	-0.05, 0.30	0.15*	0.12	-0.05, 0.29	0.18
sCD27 per log_{10} U/ml higher	0.49	0.17, 0.81	0.003*	0.37	0.01, 0.73	0.05
sCD30 median per log_{10} ng/ml higher	0.21	-0.02, 0.45	0.07*	0.02	-0.25, 0.28	0.90

**only variables with p≤0.2 were included in the multivariable analysis*

Table 4.6 Univariate and multivariable linear regression analysis of factors associated with the mean difference in 2-LTR circular HIV-1 DNA load in PBMC.

	Univariate			Multivariable		
Characteristic	Mean difference	95% CI	P	Mean difference	95% CI	P
Age, per 10 years higher	-0.08	-0.15, -0.02	0.01[a]			
Nadir CD4 count per 100 cell/mm^3 higher	0.002	-0.04, 0.05	0.92			
Pre-ART HIV-1 RNA per log_{10} copies/ml higher	0.06	-0.03, 0.16	0.17*	0.09	-0.01, 0.18	0.06
Duration of suppressive ART per 10 years longer	-0.19	-0.39, 0.02	0.08*	-0.25	-0.47, -0.04	0.02
NNRTI concentration below the MEC "yes" vs "no"	-0.01	-0.15, 0.13	0.91			
CD4 count per 100 cells/mm^3 higher	-0.13	-0.04, 0.01	0.33			
CD4_CD8 ratio per 1 unit higher	-0.04	-0.21, 0.14	0.69			
Residual HIV-1 RNA per log_{10} cps/ml higher	0.08	-0.14, 0.29	0.47			
Total HIV-1 DNA per log_{10} cps/10^6 PBMC higher	0.14	0.03, 0.25	0.01[b]			
$CD4^+CD38^+$ per 50% higher	0.07	-0.21, 0.35	0.62			
$CD4^+CD26^+$ per 50% higher	0.19	-0.04, 0.42	0.10*	0.15	-0.07, 0-38	0.44
$CD4^+CD69^+$ per 50% higher	-0.16	-3.01, 2.70	0.91			
CD8 count per 100 cells/mm^3 higher	-0.01	-0.02, 0.01	0.45			
$CD8^+CD38^+$ per 50% higher	0.19	-0.33, 0.71	0.45			
$CD8^+$HLA-DR/DP/DQ^+ per 50% higher	0.02	-0.22, 0.23	0.98			
CD14 per log_{10} μg/ml higher	0.25	-0.39, 0.88	0.44			
D-Dimer per log_{10} ng/ml higher	-0.06	-0.24, 0.12	0.51			
hs-CRP per log_{10} μg/ml higher	-0.01	-0.26, 0.05	0.19*	-0.06	-0.22, 0.09	0.44
IL6 per log_{10} pg/ml higher	-0.05	-0.27, 0.17	0.65			
CD27 per log_{10} U/ml higher	-0.30	-0.72, 0.11	0.15*	-0.29	-0.73, 0.14	0.18
CD30 per log_{10} ng/ml higher	-0.19	-0.49, 0.11	0.21			

**only variables with p≤0.2 were included in the multivariable analysis; [a] age was excluded from the multivariable analysis due to colinearity with duration of suppressive ART; [b] excluded from the multivariable analysis due to colinearity with 2-LTR circular HIV-1 DNA.cps=copies*

Table 4.7 Univariate and multivariable linear regression analysis of factors associated with the mean difference in total HIV-1 DNA load in PBMC

	Univariate			Multivariable		
Characteristic	Mean difference	95% CI	P	Mean difference	95% CI	P
Age, per 10 years higher	-0.08	-0.20, 0.04	0.18*	-0.14	-0.25, -0.2	0.03
Nadir CD4 count per 100 cell/mm^3 higher	0.06	-0.02, 0.14	0.14*	0.40	-0.43, 0.12	0.34
Pre-ART HIV-1 RNA per log_{10} copies/ml higher	0.22	0.06, 0.37	0.01*	0.29	0.14, 0.40	<0.001
Duration of suppressive ART per 10 years longer	0.02	-0.35, 0.39	0.91			
NNRTI concentration below the MEC "yes" vs "no"	0.01	-0.24, 0.25	0.97			
CD4 count per 100 cells/mm^3 higher	0.001	-0.05, 0.05	0.96			
CD4/CD8 ratio per 1 unit higher	0.15	-0.17, 0.46	0.35			
Residual HIV-1 RNA per log_{10} copies/ml higher	0.06	-0.32, 0.44	0.74			
2-LTRc HIV-1 DNA per log_{10} copies/10^6 PBMC	0.43	0.10, 0.76	0.01[a]			
$CD4^+CD38^+$ per 50% higher	0.08	-0.42, 0.57	0.74			
$CD4^+CD26^+$ per 50% higher	-0.09	-0.51, 0.31	0.63			
$CD4^+CD69^+$ per 50% higher	-0.80	-5.7, 4.20	0.75			
CD8 count per 100 cells/mm^3 higher	-0.01	-0.03, 0.02	0.65			
$CD8^+CD38^+$ per 50% higher	0.59	-0.31, 1.50	0.20*	0.77	-0.14, 1.66	0.09
$CD8^+HLA\text{-}DR/DP/DQ^+$ per 50% higher	0.32	-0.07, 0.71	0.10*	0.53	0.13, 0.92	0.01
CD14 per log_{10} µg/ml higher	0.71	-0.40, 1.81	0.20*	0.49	-0.54, 1.5	0.35
D-Dimer per log_{10} ng/ml higher	-0.08	-0.41, 0.23	0.59			
hs-CRP per log_{10} µg/ml higher	-0.14	-0.42, 0.14	0.32			
IL6 per log_{10} pg/ml higher	-0.29	-0.67, 0.10	0.14*	-0.24	-0.61, 0.14	0.21
CD27 per log_{10} U/ml higher	0.21	-0.53, 0.95	0.57			
CD30 median per log_{10} ng/ml higher	-0.34	-0.87, 0.18	0.19*	-0.45	-0.97, 0.08	0.09

**only variables with p≤0.2 were included in the multivariable analysis; [a] excluded from the multivariable analysis due to the high co-linearity with total HIV-1 DNA*

Table 4.8 Univariate and multivariable linear regression analysis of factors associated with the mean difference in total HIV-1 DNA load in CD4 T-cells

	Univariate			Multivariable		
Characteristic	Mean difference	95% CI	P	Mean difference	95% CI	P
Age, per 10 years higher	-0.06	-0.18, 0.07	0.38			
Nadir CD4 count per 100 cell/mm^3 higher	0.04	-0.05, 0.12	0.40			
Pre-ART HIV-1 RNA per log_{10} copies/ml higher	0.22	0.06, 0.39	0.01*	0.25	0.09, 0.40	0.002
Duration of suppressive ART per 10 years longer	-0.09	-0.47, 0.28	0.62			
NNRTI concentration below the MEC "yes" vs "no"	0.05	-0.20, 0.31	0.67			
Residual HIV-1 RNA per log_{10} copies/ml higher	0.11	-0.28, 0.50	0.57			
2-LTRc HIV-1 DNA per log_{10} copies/10^6 PBMC	0.42	0.07, 0.76	0.02[a]			
$CD4^+CD38^+$ per 50% higher	0.10	-0.41, 0.61	0.69			
$CD4^+CD26^+$ per 50% higher	-0.22	-0.63, 0.19	0.30			
$CD4^+CD69^+$ per 50% higher	2.59	-2.5, 7.69	0.32			
CD8 count per 100 cells/mm^3 higher	-0.007	-0.02, 0.03	0.57			
$CD8^+CD38^+$ per 50% higher	0.47	-0.47, 1.40	0.32			
$CD8^+$HLA-DR/DP/DQ^+ per 50% higher	0.43	0.04, 0.83	0.03*	0.53	0.15, 0.92	0.002
CD14 per log_{10} μg/ml higher	0.54	-0.61, 1.67	0.36			
D-Dimer per log_{10} ng/ml higher	-0.04	-0.37, 0.28	0.79			
hs-CRP per log_{10} μg/ml higher	-0.14	-0.43, 0.15	0.33			
IL6 per log_{10} pg/ml higher	-0.27	-0.67, 0.13	0.18*	-0.28	-0.66, 0.10	0.15
CD27 per log_{10} U/ml higher	0.19	-0.59, 0.95	0.62			
CD30 median per log_{10} ng/ml higher	-0.41	-0.97, 0.12	0.13*	-0.39	-0.91, 0.12	0.14

**only variables with p≤0.2 were included in the multivariable analysis; [a]excluded from the multivariable analysis due to the high co-linearity with total HIV-1 DNA*

Table 4.9 Influence of Black and White ethnicity on markers of HIV-1 persistence (N=100)

Characteristic	N tot	Univariate (Black ethnicity "yes" or "no")		
		Mean difference	95% CI	P
Residual HIV-1 RNA per $\log_{10}$ cps/ml higher	100	0.25	0.30, 0.15	0.67
Residual HIV-1 RNA <11 cps/ml per $\log_{10}$ copies/ml higher	98[b]	0.20	-0.09, 0.13	0.72
2-LTRc HIV-1 DNA per $\log_{10}$ cps/10^6 PBMC	100	-0.12	-0.25, 0.17	0.09
Total HIV-1 DNA per $\log_{10}$ cps/10^6 PBMC	100	0.10	-0.09, 0.25	0.35
Total HIV-1 DNA per $\log_{10}$ cps/10^6 CD4 T-cells	100	0.14	-0.25, 0.31	0.09

[b]*two patients had HIV-1 RNA>12 cps/ml and one had white and the other black ethnicity.*

Table 4.10 Univariate and multivariable linear regression analysis of factors associated with the mean difference in 2-LTR circular HIV-1 DNA load in PBMC in 100 patients with white or black ethnicity

Characteristic	Univariate			Multivariable		
	Mean difference	95% CI	P	Mean difference	95% CI	P
Age, per 10 years higher	-0.09	-0.16, -0.02	0.01[a]			
Ethnicity black "yes" vs "no"	-0.12	-0.25, 0.17	0.09*	-0.08	-0.23, 0.05	0.22
Nadir CD4 count per 100 cell/mm^3 higher	0.003	-0.05, 0.05	0.89			
Pre-ART HIV-1 RNA per log_{10} copies/ml higher	0.07	-0.03, 0.17	0.16*	0.08	-0.01, 0.17	0.08
Duration of suppressive ART per 10 years longer	-0.19	-0.40, 0.02	0.08*	-0.25	-0.47, -0.03	0.03
NNRTI concentration below the MEC "yes" vs "no"	-0.02	-0.16, 0.13	0.81			
CD4 count per 100 cells/mm^3 higher	-0.01	-0.04, 0.01	0.29			
CD4_CD8 ratio per 1 unit higher	0.04	-0.22, 0.15	0.69			
Residual HIV-1 RNA per log_{10} cps/ml higher	0.08	0.15, 0.30	0.49			
Total HIV-1 DNA per log_{10} cps/10^6 PBMC higher	0.14	0.03, 0.26	0.02[b]			
$CD4^+CD38^+$ per 50% higher	0.09	-0.21, 0.38	0.55			
$CD4^+CD26^+$ per 50% higher	0.20	-0.04, 0.49	0.09*	0.13	-0.11, 0.37	0.29
$CD4^+CD69^+$ per 50% higher	-0.17	-3.08, 2.73	0.90			
CD8 count per 100 cells/mm^3 higher	-0.01	-0.02, 0.01	0.40			
$CD8^+CD38^+$ per 50% higher	0.18	-0.35, 0.71	0.49			
$CD8^+$HLA-DR/DP/DQ^+ per 50% higher	0.001	-0.23, 0.23	0.99			
CD14 per log_{10} µg/ml higher	0.26	-0.40, 0.91	0.44			
D-Dimer per log_{10} ng/ml higher	-0.07	-0.26, 0.13	0.49			
hs-CRP per log_{10} µg/ml higher	-0.12	-0.28, 0.05	0.16*	-0.04	-0.21, 0.13	0.62
IL6 per log_{10} pg/ml higher	-0.06	-0.28, 0.17	0.60			
CD27 per log_{10} U/ml higher	-0.32	-0.75, 0.12	0.15*	-0.26	-0.72, 0.20	0.27
CD30 per log_{10} ng/ml higher	-0.24	-0.56, 0.08	0.14*	-0.16	-0.49, 0.18	0.36

**only variables with p≤0.2 were included in the multivariable analysis; [a] age was excluded from the multivariable analysis due to colinearity with duration of suppressive ART; [b] excluded from the multivariable analysis due to colinearity with 2-LTR circular HIV-1 DNA. cps=copies*

Table 4.11 Univariate and multivariable linear regression analysis of factors associated with the mean difference in total HIV-1 DNA load in CD4 T-cells in 100 patients with white or black ethnicity

	Univariate			Multivariable		
Characteristic	Mean difference	95% CI	P	Mean difference	95% CI	P
Age, per 10 years higher	-0.06	-0.18, 0.07	0.35			
Ethnicity black "yes" vs "no"	0.14	-0.25,0.31	0.09*	0.15	-0.08,3.69	0.19
Nadir CD4 count per 100 cell/mm^3 higher	0.04	-0.04, 0.13	0.31			
Pre-ART HIV-1 RNA per log_{10} copies/ml higher	0.22	0.05, 0.39	0.01*	0.24	0.09,0.40	0.003
Duration of suppressive ART per 10 years longer	-0.12	-0.49, 0.25	0.52			
NNRTI concentration below the MEC "yes" vs	0.04	-0.21, 0.29	0.73			
Residual HIV-1 RNA per log_{10} copies/ml higher	0.13	-0.26, 0.52	0.51			
2-LTRc HIV-1 DNA per log_{10} copies/10^6 PBMC	0.39	0.05, 0.73	0.02			
$CD4^+CD38^+$ per 50% higher	0.16	-0.35, 0.67	0.54			
$CD4^+CD26^+$ per 50% higher	-0.17	-0.58, 0.24	0.42			
$CD4^+CD69^+$ per 50% higher	2.5	-2.50, 7.40	0.33			
CD8 count per 100 cells/mm^3 higher	-0.01	-0.02, 0.03	0.60			
$CD8^+CD38^+$ per 50% higher	0.47	-0.45, 1.40	0.31			
$CD8^+$HLA-DR/DP/DQ^+ per 50% higher	0.49	0.09, 0.88	0.02*	0.65	0.27, 1.02	0.001
CD14 per log_{10} μg/ml higher	0.46	-0.67, 1.59	0.42			
D-Dimer per log_{10} ng/ml higher	-0.03	-0.30, 0.36	0.87			
hs-CRP per log_{10} μg/ml higher	-0.19	-0.47, 0.09	0.18*	-0.19	-0.47,0.07	0.15
IL6 per log_{10} pg/ml higher	-0.29	-0.60, 0.10	0.15*	-0.32	-0.69, 0.05	0.09
CD27 per log_{10} U/ml higher	0.07	-0.68, 0.82	0.86			
CD30 median per log_{10} ng/ml higher	-0.54	-1.08, 0.002	0.05*	-0.41	-0.95, 0.13	0.13

**only variables with p≤0.2 were included in the multivariable analysis.*

Table 4.12 Influence of EFV levels on markers of HIV-1 persistence (N=86)

Characteristic	N tot	Univariate EFV levels for log_{10} ng/ml higher		
		Mean difference	95% CI	P
Residual HIV-1 RNA per log_{10} cps/ml higher	86	-0.11	-0.31,0.09	0.30
Residual HIV-1 RNA ≤11cps/ml per log_{10} copies/ml higher	84[b]	-0.13	-0.29, 0.05	0.17
2-LTRc HIV-1 DNA per log_{10} cps/10^6 PBMC	86	-0.10	-0.33, 0.13	0.39
Total HIV-1 DNA per log_{10} cps/10^6 PBMC	86	-0.08	-0.46, 0.31	0.69
Total HIV-1 DNA per log_{10} cps/10^6 CD4 T-cells	86	-0.15	-0.54, 0.24	0.46

[b]*two patients had HIV-1 RNA>11 cps/ml and they were excluded from the analysis*

Table 4.13 Univariate and multivariable linear regression analysis of factors associated with the mean difference in residual plasma HIV-1 RNA load in 84 patients on EFV

	Univariate			Multivariable		
Characteristic	Mean	95% CI	P	Mean	95% CI	P
Age, per 10 years higher	-0.30	-0.09,0.03	0.31			
Nadir CD4 count per 100 cell/mm^3 higher	0.13	-0.03,0.06	0.57			
Pre-ART HIV-1 RNA per log_{10} copies/ml higher	-0.03	-0.09,0.08	0.94			
Duration of suppressive ART per 10 years longer	-0.11	-0.33, 0.10	0.30			
EFV concentration per log_{10} ng/ml higher	-0.13	-0.29, 0.05	0.17*	-0.06	-0.24,0.12	0.52
CD4 count per 100 cells/mm^3 higher	0.08	-0.02, 0.03	0.55			
CD4_CD8 ratio per 1 unit higher	0.43	0.13,0.21	0.62			
2-LTRc HIV-1 DNA per log_{10} cps/10^6 PBMC higher	0.04	-0.13,0.20	0.66			
Total HIV-1 DNA per log_{10} cps/10^6 PBMC higher	-0.02	-0.12,0.08	0.73			
$CD4^+CD38^+$ per 50% higher	0.06	-0.18,0.3	0.63			
$CD4^+CD26^+$ per 50% higher	0.08	-0.13,0.29	0.44			
$CD4^+CD69^+$ per 50% higher	-1.08	-3.52,1.37	0.38			
CD8 count per 100 cells/mm^3 higher	0.01	-0.01,0.2	0.40			
$CD8^+CD38^+$ per 50% higher	0.01	-0.59,0.62	0.97			
$CD8^+$HLA-DR/DP/DQ^+ per 50% higher	0.05	-0.26, 0.16	0.64			
CD14 per log_{10} μg/ml higher	0.23	-0.34,0.79	0.42			
D-Dimer per log_{10} ng/ml higher	-0.04	-0.20, 0.11	0.58			
hs-CRP per log_{10} μg/ml higher	0.09	-0.07,0.25	0.29			
IL6 per log_{10} pg/ml higher	0.18	-0.07,0.31	0.22			
CD27 per log_{10} U/ml higher	0.52	0.15, 0.88	0.01*	0.44	-0.03,0.84	0.04
CD30 per log_{10} ng/ml higher	0.20	-0.07,0.47	0.15*	0.08	-0.19,0.37	0.54

**only variables with p≤0.2 were included in the multivariable analysis*.

4.4 DISCUSSION

This study provides an in-depth characterization of the relationship between virological markers of HIV-1 persistence and immunological characteristic in a well-defined population which included 104 patients on stably suppressive ART for up to 14 years with the same NNRTI plus two NRTI. Patients with longer duration of treatment showed improved immune reconstitution and lower HIV-1 RNA loads and to a lesser extent lower 2-LTR circular HIV-1 DNA in PBMC; meanwhile total DNA loads did not vary between patients with short vs long duration of suppressive ART. Pre-ART HIV-1 RNA load was associated with total HIV-1 DNA but not with plasma residual viremia or 2-LTR circular HIV-1 DNA. Plasma levels of soluble CD27 showed association with residual plasma viremia, whereas cellular markers of immune activation including $CD8^{+}$HLA-DR/DP/DQ^{+} T showed association with total HIV-1 DNA.

Previous studies consistently demonstrated HIV-1 detection in populations with heterogeneous treatment history and duration (Palmer et al., 2008, Siliciano et al., 2003, Maldarelli et al., 2007, Lorenzo-Redondo et al., 2016). In our population where patient treatment history was overall homogenous and the viral load suppression was continuous at HIV-1 RNA<50 copies/ml from the first six months of starting therapy, we also detected plasma RNA and intracellular HIV-1 DNA. In plasma, half of patients had detectable HIV-1 RNA levels in line with previous reports (Maldarelli et al., 2007, Kiselinova et al., 2015) and the majority of patients had HIV-1 RNA levels <11 copies/ml as found by others (Kiselinova et al., 2015). In cells, 2-LTR circular HIV-1 DNA was detected in 23% of patients at low levels as also reported by another study (Besson et al., 2014) that measured 2-LTR circular HIV-1 DNA levels in long-term virological suppressed individuals (with HIV-1 RNA<50 copies/ml within first 32 weeks of starting therapy) with a low detection limit of 5 copies/10^6 PBMC similar to our case. Moreover overall levels of 2-LTR circular DNA that we found were comparable to what were found in the previous study (Besson et al., 2014) and in others (Kiselinova et al., 2015). Total HIV-1 DNA was detected in all patients at around 2-2.5 log10 copies/10^6 PBMC as also found by others (Besson et al., 2014, Malatinkova et al., 2015).

The significance of HIV-1 detection in plasma and the cellular source is still debated. Residual HIV-1 RNA has been proposed to be the product of ongoing viral replication in sanctuary sites unrelated to peripheral blood (Eriksson et al., 2013). If this is true, residual plasma viral HIV-1 could lack of association with the cellular HIV-1 reservoir. In line with this, our data did not show association between residual viral load and the total HIV-1 or 2-LTR circular HIV-1 DNA. This data was both in accordance and discordance with one previous study (Kiselinova et al., 2015) that showed that residual HIV-1 RNA was associated with total HIV-1 DNA but not with 2-LTR circular HIV-1 DNA. However in that study, patients also on PI were observed and it still need to be determined if treatment composition can influence total HIV-1 DNA. Moreover methods for total HIV-1 DNA and 2-LTR circular HIV-1 DNA quantification were different and this could also explain such discrepancies.

When looking at levels of markers of HIV-1 persistence during ART, we found that patients with longer treatment showed a trend for lower levels of plasma HIV-1 RNA and of 2-LTR circular HIV-1 DNA loads that are the biological products of viral replication and infection. Of note, when two patients with levels of residual HIV-1 RNA>11 with less than 3 years of ART were excluded from the analysis, similar levels of residual plasma HIV-1 at very low levels (≤11 copies/ml) were found in patients with different duration of suppressive ART. Taken together these findings could be a simple reflection of the success of the therapy over time in our virological suppressed population. Conversely, total HIV-1 DNA levels were similar in patients with different duration of suppressive ART and they were highly predicted by the pre-ART HIV-1 RNA. This finding is in line with previous reports demonstrating that the HIV-1 reservoir is established early after viral infection and it is insufficiently responsive to treatment (Williams et al., 2014, Josefsson et al., 2013, Siliciano et al., 2003, Hocqueloux et al., 2013, Buzon et al., 2014a). Overall levels of HIV-1 DNA or RNA did not significantly vary between patients with white vs black ethnicity. Previous literature debated regarding the influence of ethnicity on virological outcome in ART-treated patients. Some studies that looked at patients with a wide range of different ART regimen found a higher rate of virological failure in Black compared with White (Hodder et al., 2012, Fourie et al., 2011, Svedhem-Johansson et al., 2013). However one study reported no significant effect of race when comparing efficacy of EFV and

NVP at early stage of treatment (Keiser et al., 2002). Our data adds onto this by showing that in patients on stable suppressive ART with continuous follow up (at least one visit every six months) ethnicity is not a factor associated with greater HIV-1 persistence.

The mechanisms that support viral persistence are still unclear, although growing evidence is currently focussing the attention on host environment as central player in the viral persistence (Cockerham et al., 2016, Crowell and Hatano, 2015, Hatano, 2013) during suppressive therapy.

One recent work (Riddler et al., 2016) studied factors associated with residual plasma viremia in patients with 4 years of ART and demonstrated a strong association between residual HIV-1 RNA and pre-ART HIV-1 RNA alongside a lack of association with patient's characteristics such as age and ethnicity. Our results add onto this by saying that the lack of association between residual HIV-1 RNA and patients characteristics persists even after longer suppressive therapy. Conversely, we did not find an association with pre-ART HIV-1 RNA in accordance with others that studied patients on ART for median 6-7 years (Kiselinova et al., 2015). Moreover, we expanded the previous literature, by looking at a wide range of cellular and soluble markers of immune activation. As described by others (Hatano et al., 2013), we found that residual HIV-1 RNA was not associated with cellular markers of immune activation. On the other hand, our data showed a trend for a positive association between residual HIV-1 RNA and levels of soluble CD27 (sCD27), a marker of T cell activation. This has been identified as a marker of immune dysfunction in different disease (De Milito et al., 2002) such as rheumatoid arthritis, systemic lupus erythematosus, and AIDS-associated lymphoma (Widney et al., 1999). In HIV-1 patients on ART, sCD27 has been identified as a marker of chronic immune activation and it was defined a predictor of virologic rebound in case of treatment interruption (De Milito et al., 2002). The association we found seems unlikely to be an indication of viral replication in blood as discussed above. Conversely, it could reflect CD4 T-cell activation at peripheral as well as lymphoid tissue where infected CD4 T-cell could drive levels of replication (Chun et al., 2008). Our data did not show any association between residual HIV-1 DNA and markers of CD4 T-cell activation in plasma, whereas we could not conclude about lymphoid cell activation. Of note, this association appeared to be unrelated to levels of

EFV drugs in plasma; however previous reports (Fletcher et al., 2014, Lorenzo-Redondo et al., 2016) showed that suboptimal drug concentration in lymphoid tissue was unrelated to levels of drug concentration in plasma. The association between residual HIV-1 RNA in plasma, sCD27 and drug levels warrants further investigation and possibly expansion to lymphoid tissue analysis.

Overall our population did not show abnormal levels of soluble makers of inflammation (Tenorio et al., 2014, Gao et al., 2015, De Milito et al., 2002, Sandler et al., 2011, McBride and Cooper, 2008) compared to healthy individuals with the only exception being the D-Dimer (Lichtfuss et al., 2011). Whilst 2-LTR circular HIV-1 DNA and total HIV-1 DNA did not show any association with soluble markers of immune activation, we found a positive association between markers of cellular immune activation, in particular $CD8^{+}$HLA-DR/DP/DQ^{+} T-cells and total HIV-1 DNA both in PBMC and in CD4 T-cell as also observed by others (Cockerham et al., 2016, Hatano et al., 2013). We could speculate that this association could reflect clonal expansion of activated cells carrying HIV-1 DNA as a response to stimuli that could induce simultaneous activation of the CD8 T-cells and HIV-1 CD4 T-cells that would result in an association between higher levels of activated CD8 T-cells and HIV-1 DNA load. Alternatively HIV-1 virus particles themselves could trigger the immune system leading to CD8 T-cell activation against HIV-1: in this case, plasma HIV-1 RNA could be associated with higher levels of activation. Nonetheless, our data did not show evidence of association between CD8 T-cell activation and plasma HIV-1 RNA, as observed also by others (Hatano et al., 2013). We could propose that this data indicate that virus particles may not be triggering a CD8 T-cell response. Further studies aimed at the characterization of the CD8 T-cell antigen-specificity could provide useful information to solve such a conundrum.

This study has its limitations. First the cross-sectional design did not allow us to conclude for causality. Furthermore, we did not have a gender-age matched uninfected control population as reference for the immunological results as we only compared our results with existing literature, with possible bias derived from population heterogeneity as well as quantification methods. Moreover, due to the limited amount of blood obtained from the study subjects, we could not determine the specificity of the immunological response; for the same reason, we used PCR-based assay instead of

functional *in vitro* assay to determine HIV-1 load, even though quantification by PCR could not discriminate between replication competent and non-competent viruses.

Nonetheless we confirmed that HIV-1 is still detected in plasma and cells a population of patients on first-line ART that achieved virological suppression after the first 6 months of starting therapy and maintained the suppression while being on ART with 2 NRTI and with 1 NNRTI. We also showed association of some markers of HIV-1 persistence and immune activation. Our findings may confirm the importance of the host environment in HIV-1 persistence and question the relevance and significance of markers of immune activation as prognostic factors for HIV-1 persistence during suppressive therapy.

In this chapter we studied the total HIV-1 DNA as a surrogate for the cellular HIV-1 reservoir. Although in stably suppressed patients, most of the intracellular viral DNA was found to be integrated (Chomont et al., 2009), we thought there was scope to explore factors associated with the integrated HIV-1 DNA in a study group of 50 people with similar characteristics to the one described in this chapter. In the next chapters we will describe the optimization of the method used to quantify the integrated HIV-1 DNA. Furthermore we will present the results we obtained from univariate and multivariable linear regression analysis on factors associated with integrated HIV-1 DNA. Such study was published in 2015 in EBiomedicine journal.

Chapter 5: Establishing an assay for measuring integrated HIV-1 DNA load in peripheral blood mononuclear cells and purified CD4 T-cell subsets

5.1 INTRODUCTION

HIV-1 eradication has not yet been achieved mainly because the integrated virus reservoir that is established in CD4 T-cells early after infection (Pierson et al., 2000) is unresponsive to antiretroviral drugs. Viral persistence during seemingly effective antiretroviral therapy (ART) can be sustained by at least two mechanisms, which are not mutually exclusive. Resting T-cell biology includes homeostatic proliferation, which amplifies integrated provirus without requiring resumption of virus replication. Further, latently infected resting CD4 T-cells can become activated upon antigenic stimulation, which leads to resumed expression of integrated provirus and virus (Chun et al., 1995, Chun et al., 1997a) production. The latter mechanism requires the integrated provirus to be replication-competent, e.g. to carry no major genome defects. This proposed model of HIV-1 persistence implies that integrated provirus can be found in both activated and resting CD4 T-cells (Chun et al., 2005) and that its quantification can provide a measure of the viral pool that can give rise to infectious virus (Chun et al., 1997a, Finzi et al., 1999, Siliciano et al., 2003, Laird et al., 2013).

One methodology to quantify replication-competent virus within resting CD4 T-cells is the viral outgrowth assay (VOA). In this assay, resting CD4 T-cells purified from peripheral blood of HIV-positive patients are stimulated *in vitro* in order to induce activation and virus production. The frequency of cells producing virus is obtained and results are expressed as infectious unit per million (IUMP) (Mexas et al., 2012, Siliciano and Siliciano, 2005). The assay (Laird et al., 2013) is labour-intensive and expensive, and has been suggested to be lacking in sensitivity as it appears to underestimate the

replication-competent fraction (Hatano et al., 2013). Several PCR-based methods have been developed to measure integrated HIV-1 DNA, including gel separation, linker ligation PCR, inverse PCR, and *Alu-gag* PCR (Liszewski et al., 2009). Among these, the *Alu-gag* method shows a good correlation with the VOA (Eriksson et al., 2013). In this assay, 40 replicates of cellular DNA isolated from HIV-infected individuals undergo a first PCR amplification which targets both human *Alu* and HIV-1 *gag* sequences. At this stage, both integrated and unintegrated HIV-1 DNA forms are amplified in exponential and linear fashion respectively. In the next step, a HIV-1 specific real-time PCR (qPCR) is used for quantification of HIV-1 DNA. To discriminate between integrated and unintegrated amplicons, 30 additional replicates are run in parallel with only the *gag* primer to produce linear amplification of unintegrated HIV-1 DNA alone. The read out from this "*gag* control" provides the background signal that is use to set the threshold above which one sample can be defined as positive for integration. This technique presents a potential drawback: the requirement for a reliable standard for quantification (Liszewski et al., 2009). Preparation of the standard is costly and time consuming, and requires periodic infection of CEM-ss cells with green fluorescent protein (GFP)-labelled HIV-1 viruses capable of only one-round infection. Infected cells are then sorted based upon the GFP expression and DNA is extracted, quantified and checked for integration site variety. A desirable standard should mimic the natural variation of integration sites observed in patients (Brady et al., 2013). However, Ward De Spiegelaere and colleagues at University of Ghent in Belgium described a modified *Alu-gag* method that obviates the need a standard (De Spiegelaere et al., 2014), whereby the integrated HIV-1 DNA copy number is obtained by Poisson's principles that allow absolute quantification (Chapter 2).

In this chapter we sought to adopt the novel assay developed in Ghent, optimise its use on different assay platforms, and apply it to the quantification of integrated HIV-1 DNA in peripheral blood of HIV-positive patients receiving suppressive ART. In order to

optimise the assay, we also investigated the yield of integrated HIV-1 DNA in separated CD4 T-cell subsets comprising resting and activated CD4 T-cells.

5.2 METHODS

5.2.1 Study population

Peripheral blood anticoagulated with EDTA was obtained from patients recruited within the ERAS cohort studies described in Chapter 2. All patients started first-line ART with two NRTIs plus efavirenz or nevirapine, achieved a plasma HIV-1 RNA level <50 copies/ml within six months, and showed all subsequent viral load measurements <50 copies/ml without transient elevations above 50 copies/ml while maintaining the initial NNRTI. The duration of uninterrupted suppressive therapy ranged between 1 and 15 years. ERAS 1 subjects were tested in Ghent and ERAS 2 subjects were tested in Liverpool.

5.2.2 Isolation of CD4 T subsets

CD4 T-cells and resting and non-resting CD4 T-cells were isolated from fresh peripheral blood mononuclear cells (PBMC) using magnetic beads in a two-steps protocol as described by Laird et.al 2013 and as described in details in Chapter 2. Briefly, CD4 T-cells were enriched by depleting PBMC of CD8 and γ/δ T cells, B cells, NK cells, monocytes, neutrophils and other granulocytes, eosinophils, and erythrocytes using relevant antibodies described in Chapter 2. Resting CD4 T-cells were then obtained by depletion of CD4 T-cells expressing markers of immune activation that included CD25, CD69 and HLA-DR. Obtained resting and non-resting CD4 T-cell subsets were counted by haemocytometer as described in Chapter 2 and the purity was assessed by flow cytometry. Resting CD4 T-cells purity was first tested by CD25, CD69, and HLA-DR expression to set up purification conditions; following setting up,

cell separation purity was only tested for HLA-DR expression (Laird et al., 2013) and only fractions where HLA-DR positive cells represented <0.5% were considered suitable for further analysis of integrated HIV-1 DNA load. Non-resting CD4 T-cells were defined as the fraction complementary to the resting CD4 T-cells, therefore positive for the expression of CD25, CD69, and HLA-DR. Due to reduced sample availability, only HLA-DR expression was tested regularly.

5.2.3 Integrated HIV-1 DNA assay

The two-steps Alu-gag PCR assay was first practiced in Ghent and then established in Liverpool. To ensure reproducibility of the assay, validation tests were performed. Based upon sample availability, 4 patients were tested at 10 copies/replicate of total HIV-1 DNA both in Gent and in Liverpool and results were compared. Furthermore, for 1 out of the 4 patient, 20 copies of total HIV-1 DNA copy input was further tested in Liverpool. All the quantitative PCR were tested on different platforms and results were compared. PCR1 in Ghent and Liverpool were performed with the Gene Amp PCR system 2700 (Applied Bio Systems, USA) and Verity® Thermal Cycler (Applied Bio Systems) platforms, respectively. For the real time qPCR, the LightCycler 480 platform (Roche, Belgium) was used in Ghent, whereas the ABI 7500 or ABI 7900HT platforms (Applied Bio Systems, UK) were used in Liverpool. Integrated HIV-1 DNA load was calculated by inputting the Ct values obtained by qPCR assay into a pre-defined computational sheet (available on: http://www.integratedhivpcr.uGhent.be) as described in Chapter 2. Briefly, mean Ct values obtained from unintegrated HIV-1 DNA replicates were used to calculate the threshold above which each single reaction was identified as positive for the presence of integrated HIV-1 DNA replicates. A minimum number of 4 positive reactions was required to allow the calculation of integrated HIV-1 copies/replicate by Poisson statistics. In the computational sheet, input number of cells was included to obtain integrated HIV-1 DNA load per 10^6 cells.

Integrated HIV-1 DNA in PBMC and CD4 T-cell subsets was measured. Load in PBMC was measured by Mrs Lydia Ritter (MRes student).

5.2.4 Quantification of total HIV-1 DNA

Total DNA was measured in PBMC with the in house assay described in Chapter 2 by research technicians and by Dr. Maria Tsakiroglou. Briefly, DNA was extracted from frozen cells by using the QIAamp DNA mini kit (Qiagen, UK), measured by NanoDrop, and amplified by quantitative real-time PCR. One µg of cellular DNA (equivalent to 150,000 cells) was tested in duplicate, for a total of 300,000 cells tested for each patient. In order to detect inhibition, a 1:10 dilution of the extracted DNA was tested in parallel. Assay 50% and 95% detection rates were 20 and 40 HIV-1 DNA copies/10^6 PBMC, respectively. A standard curve with 6, 60, 600, 6000 HIV-1 DNA copies/10^6 cells was produced by using a cloned HIV-1 LTR DNA plasmid. In some assays, the Generic HIV DNA Cell kit (Biocentric,France) was employed according to manufacturer instructions. The in house-assay had been previously calibrated against the commercial kit ensuring comparable performance as shown in the Chapter 2.

5.3 RESULTS

5.3.1 Study population

Table 5.1 summarises the characteristics of the cross-sectional cohort. Overall, the 41 patients (73% male) were receiving combined ART with two NRTIs plus either efavirenz (85%) or nevirapine and had a median duration of viral load suppression (plasma HIV RNA <50 copies/ml) of seven years. Median nadir and current CD4 cell count were 204 cells/mm^3 (IQR 127-240) and 592 cells/mm^3 (IQR 497-725) respectively. All subjects had detectable HIV-1 DNA at median 2.5 $\log_{10}$ copies/10^6 PBMC (IQR 2.2-2.9).

Table 5.1 Characteristic of the ERAS study population

Characteristic	
Individuals, N total	41
Male n (%)	30 (73%)
Age median years (IQR)	45 (35-51)
Nadir CD4 count median cells/mm^3 (IQR)	204 (127-240)
Duration of ART median years (IQR)	7 (3-10)
Duration of suppressive ART median years (IQR)[a]	7 (3-10)
CD4 count median cells/mm^3 (IQR)	592 (497-725)
Efavirenz as initial NNRTI n (%)	35 (85%)
Changed NRTI backbone n (%)	15 (37%)
Median NRTI backbone change (IQR)	1 (1-2)
Pre-ART HIV-1 RNA median $\log_{10}$ cps/ml (IQR)	4.9 (4.6-5.1)
Detectable residual plasma HIV-1 RNA n (%)	16 (40%)
Residual HIV-1 RNA median cps/ml (IQR)[b]	2 (2-3)
Total HIV-1 DNA median $\log_{10}$ cps/10^6 PBMC (IQR)	2.5 (2.2-2.9)

[a]Defined as the length of time following the first viral load <50 copies/ml. [b] Samples with undetectable HIV-1 RNA were assigned an arbitrary value of 1.5 copies/ml. IQR= interquartile range; ART= antiretroviral therapy; NRTI= nucleoside/nucleotide reverse transcriptase inhibitor; NNRTI= non-nucleoside reverse transcriptase inhibitor; PBMC= peripheral blood mononuclear cells; cps=copies. ERAS population included ERAS1 and ERAS2.

5.3.2 Isolation of CD4 T subsets

Purity of the resting CD4 T-cell fraction was first assessed by testing expression of activation markers CD25, CD69, and HLA-DR and a representative example is given in Figure 5.1.

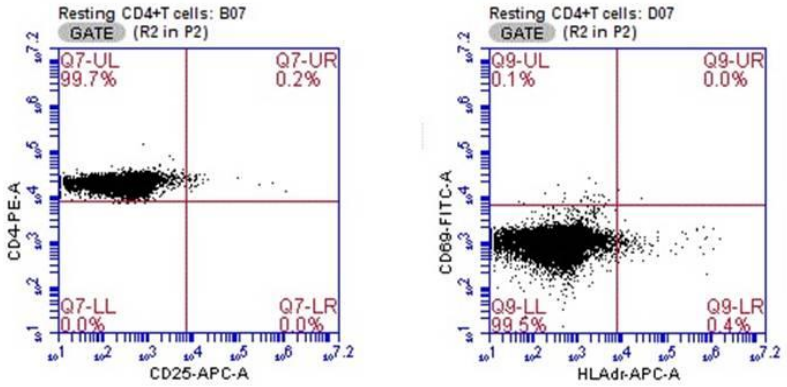

Figure 5.1 Representative example of resting CD4 T-cell purity

a) Representative dot plot indicating CD4 and CD25 expression. b) Representative dot plot indicating CD69 and HLA-DR expression.

Our experimental procedure was able to produce resting CD4 T-cells that had contamination of 0.2% cells expressing CD25, 0.1% cells expressing for CD69, and 0.4% cells expressing HLA-DR. The data showed that overall the protocol was able to produce a highly pure resting CD4 T-cell fraction. Cell fractions from the whole population were further tested only for HLA-DR expression that was mean 0.2% (range 0.1%-0.6%) in the resting CD4 T-cells and mean 5% (range 1%-12%) in the non-resting CD4 T-cells (

Table 5.2). With this method we were able to isolate resting CD4 T-cell fraction with purity levels ranging between 99.4 % and 99.9% across all experiments.

Table 5.2 Recovery and purity of resting and non-resting CD4 T-cells

Parameters	
Total TEST	30
PBMC 10^6 cells/ml of blood mean (range)	2 (3-1)
CD4 T-cell 10^6 cells/ml of blood mean (range)	0.4 (0.2-0.6)
Resting CD4 T-cells 10^6 cells/ml of blood mean (range)	0.2 (0.1-0.4)
Non-resting CD4 T-cells 10^6 cells/ml of blood mean (range)	0.1 (0.1-0.3)
% Resting CD4 T-cells expressing HLA-DR mean (range)	0.2 (0.1-0.6)
% Activated CD4 T-cells expressing HLA-DR mean (range)	5 (1-12)

Overall, mean $2x10^6$ (range 3-1) PBMC and mean $0.4x10^6$ (range 0.2-0.6) CD4 T-cells were recovered per each ml of whole blood; within the CD4 T-cell population, mean $0.2x10^6$ (range 0.1-0.4) and $0.1x10^6$ (range 0.1-0.3) were resting or non-resting $CD4^+$ T-cell, respectively.

5.3.3 Establishment of the integrated HIV-1 DNA assay

The assay was established by running three sets of experiments (Table 5.3). First, four plates (from one patient each) with PCR1 products that had been amplified in Ghent were quantified in Liverpool with the AB 7500 qPCR equipment (test 1-2-3-4, Table 5.3). With samples from three of four patients, the number of positive wells and background Ct values were reproduced. With one patient, there were a lower number of detected wells than measured in Ghent (23 instead of 17, test 2, Table 5.3). Further, we tested the same four samples by performing both PCR1 and qPCR2 in Liverpool. Results showed good reproducibility in number of positive wells and background Ct values. In addition, qPCR2 was run using two AB qPCR platforms, with similar results. Finally, one sample was tested using an input of 20 HIV-1 copies instead of 10, which doubled the detection of integrated HIV-1 DNA as expected (test 4_{II}, Table 5.3). These data provided reassurance about assay performance.

Table 5.3 Setting up of the integrated HIV-1 DNA method in Liverpool

Test (platform)[a]	HIV-1	N positive wells[b]			Average Ct value[c]			Cut-off Ct value		
		Ghent	Liv^{I}	Liv^{II}	Ghent	Liv^{I}	Liv^{II}	Ghent	Liv^{I}	Liv^{II}
1 (AB7500)	10 cps	7	7	7	34	35	35	31	32	32
2 (AB7500)	10 cps	23	17	23	34	34	35	32	31	32
3 (AB7500)	10 cps	5	5	4	35	36	35	33	34	32
3 (AB7900)	10 cps	---	---	5	---	---	36	---	---	34
4 (AB7500)	10 cps	9	8	8	36	35	37	33	33	35
4 (AB7900)	10 cps	---	---	7	---	36	36	---	---	32
4_{II} (AB7500)	20 cps	---	---	16	---	---	34	---	---	33

[a]platform= qPCR platform; [b]wells that were scored positive for integrated HIV-1 DNA; [c]Avarage Ct values produced by the background. Ghent=PCR1 and PCR2 performed in Ghent; Liverpool I= PCR1 performed in Ghent, PCR2 in Liverpool; Liverpool II= PCR1 and PCR2 performed in Liverpool; Ct= cycle threshold; AB7500= Applied Biosystem model 7500 qPCR; AB 7900= Applied Biosystem model 7900HT qPCR; cps=copies.

Having successfully set up the assay, integrated HIV-1 DNA load was measured in PBMC from 41 ERAS patients and results are shown in Table 5.4.

Table 5.4 HIV-1 DNA loads in PBMC from ERAS1 and ERAS2 populations

	Total	ERAS1	ERAS2	P
Total test	41	24	17	---
Total HIV-1 DNA median log_{10} cps/10^6 PBMC (IQR)	2.5 (2.2-2.9)	2.6 (2.2-2.9)	2.4 (2.2-2.9)	0.64
Integrated HIV-1 DNA median log_{10} cps/10^6 PBMC (IQR)	2.1 (1.8-2.4)	2.0 (1.8-2.5)	2.1 (1.7-2.3)	0.57

Integrated HIV-1 DNA measurements from ERAS1 and ERAS2 populations are compared. Data for ERAS1 and ERAS2 data were obtained in Ghent and Liverpool respectively. Mann Whitney p test are shown. cps= copies

Overall, total HIV-1 DNA was median 2.5 log_{10} cps/10^6 PBMC (IQR 2.2-2.9); HIV-1 DNA loads in ERAS1 and ERAS2 subjects were 2.6 log_{10} cps/10^6 PBMC (2.2-2.9) and 2.4 log_{10} cps/10^6 PBMC (2.2-2.9), respectively (p=0.64, Mann Whitney). Integrated HIV-1 DNA was overall median 2.1 log_{10} cps/10^6 PBMC (IQR 1.8-2.4), whereas it was median 2.0 log_{10} cps/10^6 PBMC (1.8-2.5) and 2.1 (1.7-2.3) log_{10} cps/10^6 PBMC (2.2-2.9) in ERAS1 and ERAS2 subjects, respectively (p=0.57, Mann Whitney).

5.3.4 Integrated HIV-1 DNA load in resting and non-resting CD4 T-cells

In eight subjects, integrated HIV-1 DNA was measured in resting and non-resisting CD4 T-cells. In these subsets, less than 0.5% of resting CD4 T-cells and up to 12% of non-resting CD4 T-cells expressed HLA-DR. Results are shown in Table 5.5. Median integrated HIV-1 DNA levels were 2.3 $\log_{10}$/ 10^6 cells (IQR 1.9-2.6) and 2.5 $\log_{10}$/ 10^6 cells (IQR 2.2-2.6) for resting and non-resting CD4 T-cells, respectively and there was not significant loads difference (p=0.56, Mann Withney). This demonstrated that integrated HIV-1 DNA load in a population of resting CD4 T-cells containing <0.5% of HLA-DR^+ cells was not significantly different compared with non-resting CD4 T-cells containing up to 12% of HLA-DR^+ cells.

Table 5.5 Integrated HIV-1 DNA loads in resting and non-resting CD4 T-cells

	$CD4^+$ T-cells		
	Resting	Non-resting	P
Total test	8	8	---
Integrated HIV-1 DNA median $\log_{10}$ cps/10^6 PBMC (IQR)	2.3 (1.9-2.6)	2.5 (2.2-2.6)	0.56

Mann Withney p values are shown. cps= copies.

5.4 DISCUSSION

In the present chapter, the *Alu-gag* method described by De Spiegelaere et al. for measuring integrated HIV-1 DNA was established on a different platform in our laboratory and the yield in resting and non-resting CD4 T-cell fractions was evaluated. The assay was implemented with good reproducibility and then applied to the measurement of integrated HIV-1 DNA load in subjects receiving stably suppressive ART. All patients had detectable integrated HIV-1 DNA and levels were not significantly different in resting and non-resting CD4 T-cells.

The *Alu-gag* PCR is becoming established in research settings as a reliable methodology for measuring integrated HIV-1 DNA (De Spiegelaere et al., 2014, Eriksson et al., 2013, Graf and O'Doherty, 2013, Liszewski et al., 2009, Agosto et al., 2011). In this two-step method, an initial PCR is run to allow amplification of integrated HIV-1 DNA and a second quantitative PCR is employed for quantification of PCR1 products. A drawback of the technique in its original application is that it requires preparation of a quantification standard is time consuming and costly. De Spiegelaere and colleagues proposed an alternative method for quantification that uses the number of wells scored as positive for the presence of the integrated HIV-1 DNA to calculate the integrated HIV-1 DNA load with the use of the Poisson statistics. An extensive set of experiments were performed in order to ensure the assay would transfer reliably between laboratories. We were in the favourable position of having patient samples that could be tested both in the host laboratory and in Liverpool. In the first set of experiments, good reproducibility was demonstrated with samples that underwent testing at both laboratories. Two key elements were reproduced: number of positive wells detected, which represent integrated HIV-1 DNA load, and background Ct values, which reflect linear amplification of the non-integrated HIV-1 DNA. As a further indication of assay reliability, when the HIV-1 copies input was doubled the amount of integrated HIV-1 DNA measured was also doubled. We also found consistency when

integrated HIV-1 DNA was measured in subjects with similar treatment histories. We tested samples from patients that had been recruited within the ERAS1 and ERAS2 studies that were all on first-line ART with 2 NRTIs and one NNRTI and showed continuous viral load suppression <50 copies/ml starting from the first 6 months of ART until recruitment without blips while being on the same NNRTI. ERAS1 subjects were tested in Ghent and ERAS2 subjects were tested in Liverpool. Consistent with the highly stable treatment status, integrated HIV-1 DNA load was similar in the two groups. It should be noted that two groups also showed similar levels of total HIV-1 DNA. In stably suppressed patients, integrated HIV-1 DNA is believed to represent the major molecular form of intracellular HIV-1 DNA (Chomont et al., 2008).

Resting CD4 T-cells are believed to be the major site of HIV-1 persistence during suppressive ART and the major reservoir of replication competent HIV-1 provirus (Chun et al., 1995, Chun et al., 1997a, Murray et al., 2014). Therefore, we sought to define whether testing integrated HIV-1 DNA load in purified resting CD4 T-cells would improve the assay by eliminating variation due to PBMC composition. The important prerequisite was to obtain a cell fraction of high purity, and this was successfully demonstrated, with results consistent with those reported by Laird et al., who recommend that resting CD4 T-cell purity should be >99.5%, and the proportion of cells expressing HLA-DR activation markers in the resting fraction should not exceed 0.5%. We tested only resting CD4 T-cells that had less than 0.5% of cells expressing HLA-DR. Subsequently, we detected integrated HIV-1 DNA in both resting and non-resting CD4 T-cells, and the levels were similar. Whilst the definition of purity of the resting cells was straightforward and based upon levels of activation markers expression, the definition of non-resting CD4 T-cells needs further discussion. The methodology that we used is designed to positively isolate cells that express markers of immune activation and therefore should selectively binds only the activated non-resting cell fractions. However, contamination of the resting CD4 T-cells in the non-resting CD4 T-cell could not be checked given the absence of specific markers that define the resting CD4 T-cell, and therefore could not be excluded. Nonetheless, whilst our

finding may be at odds with the known biology of HIV infection, the infection of non-resting/activated CD4 T-cells as they are transitioning to a resting memory state may be the primary mechanism by which latency is established (Chun et al., 2005, Chavez et al., 2015). Furthermore, there is a close association between T-cell activation and HIV persistence, which is not entirely understood (Hatano, 2013).

Previous studies have investigated the presence of integrated HIV-1 DNA in activated T-cells with conflicting findings. In two studies from Murray and Chun, the integrated HIV-1 DNA was measured in both activated and resting cells (Chun et al., 2011, Murray et al., 2014), where activated CD4 T-cells were defined as HLA-$DR^{+}CD38^{+}$ or $CD25^{+}CD69^{+}$HLA-DR^{+}, and resting CD4 T-cells were defined by the absence of the same activation markers. However, only Tae-Wook Chun *et al.* reported differences in the integrated HIV-1 DNA levels when looking at CD4 T-cells fractions, in particular they found that highly purified (>99%) FACS-enriched activated ($CD25^{+}CD69^{+}$HLA-DR^{+}) CD4 T-cells presented higher integrated HIV-1 DNA loads compared with resting ($CD25^{-}CD69^{-}$HLA-DR^{-}) CD4 T-cells (Chun et al., 2005). The two studies were different between each other and different from our own in terms of study population that included 11 subjects in Chun *et al.*, 12 in the Murray *et al.*, and 8 in our study. Further treatment history was different and in particular the other two studies included PI, NNRTI, and integrase inhibitor (RAL) in addition to 2NRTIs; whereas our study population only included patients that were taking one NNRT plus 2 NRTIs. Furthermore, methods for cell fractions isolation were different in the three studies.

This study has limitations. In order to ensure comparability, resting and non-resting CD4 T-cells were defined here as previously reported by Laird *et al.* Other studies have used a variety of other definitions and therefore the data cannot be generalised. Nonetheless, we were able to demonstrate that limiting the measurement of integrated HIV-1 DNA to the resting CD4 T-cell fraction would exclude an additional source of integrated HIV-1 DNA, while adding considerable labour intensity and cost. Based upon these observations, further work on integrated HIV-1 DNA was planned using

PBMC. In a second stage, we undertook further work on assay development that may in the future improve sensitivity, as described in Chapter 7.

Chapter 6: Integrated HIV-1 DNA load in peripheral blood is associated with the frequency of CD8 cells expressing HLA-DR/DP/DQ in patients receiving long-term suppressive antiretroviral therapy

In this chapter, the integrated HIV-1 reservoir was studied in relation to virological and immunological factors in 50 patients on stably suppressive ART for 1-15 years. Data were published in EBiomedicine journal (Ruggiero et al., 2015) and the full paper is attached to this thesis as Appendix (Appendix 1). The present chapter was adapted from the paper to fit the University of Liverpool thesis submission requirements.

6.1 INTRODUCTION

HIV establishes a reservoir of replication-competent integrated provirus early after transmission (Hocqueloux et al., 2013). The provirus is found predominantly in memory CD4 T-cells; it is poorly responsive to antiretroviral therapy (ART), and supports virus replication upon treatment discontinuation (Ruelas and Greene, 2013, Soriano-Sarabia et al., 2014, Siliciano et al., 2003). Different mechanisms have been proposed to support HIV persistence during successful ART, which could be grouped into two based on presence or absence of virus production, respectively. In the presence of virus production, continuous replenishment of the reservoir may occur through ongoing virus production (Hatano et al., 2013, Buzon et al., 2010), perhaps in sites where ART penetration or activity is suboptimal (Fletcher et al., 2014). In the absence of virus production, maintenance of the reservoir can also occur through proliferation of latently infected CD4 T-cells, as a possibly key determinant of HIV persistence during ART (Maldarelli et al., 2014, Josefsson et al., 2013, Chomont et al., 2009, Wagner et al., 2014). These proposed models are not mutually exclusive.

HIV replication causes chronic immune activation and inflammation, typically accompanied by an expansion of CD8 T-cells, which improve but rarely resolve with ART (Klatt et al., 2013). Moreover, in treated patients, persistent HIV production or partial antigenic expression may drive ongoing immune activation. In turn, immune activation can promote T-cell proliferation, leading to HIV transcription and production (Klatt et al., 2013). Furthermore, early in the course of the infection, HIV induces gut damage, which allows translocation of gastrointestinal microbial products into the systemic circulation. As a results, immune activation is raised and causes further gut damage, establishing a self-perpetuating cycle that can become independent of virus production (Shan and Siliciano, 2014). In addition, other persistent infections, such as with cytomegalovirus (CMV), play a linked role in ongoing immune activation despite suppressive ART (Gianella et al., 2014).

How markers of immune activation correlate with parameters of HIV persistence during long-term suppressive therapy is still unclear. Available data are inconsistent, possibly a consequence of heterogeneous study populations and measures of HIV persistence, but also a reflection of complex bilateral interactions (Hatano et al., 2013, Chun et al., 2011, Cockerham et al., 2014). Further characterization of this relationship is needed in order to improve our understanding of HIV pathogenesis and design improved curative strategies.

The aim of this study was to investigate factors associated with the levels of integrated HIV-1 DNA measured in peripheral blood during stably suppressive ART, including the relationship with markers of immune activation. Heterogeneity of the study population was minimized, by exclusively selecting patients who started first-line ART with two NRTIs plus one NNRTI, achieved a plasma HIV-1 RNA ("viral") load <50 copies/ml within the first six months of therapy, and subsequently showed consistent viral load suppression <50 copies/ml over up to 14 years of continuous treatment on the same NNRTI.

6.2 METHODS

6.2.1 Study population

Study subjects were recruited within the ERAS1 cohort study described in Chapter 2 and 4. Briefly, eligible patients were on first-line ART with two NRTIs plus efavirenz or nevirapine, and showed continuous viral load suppression (<50 copies/ml) with no blips from the first six months of therapy up to sampling date. Only changes of the initial NRTI (e.g., for toxicity) were allowed provided they were not associated with a treatment interruption or viral load rebound >50 copies/ml. Recruitment was stratified by duration of ART to range from 1 to 14 years.

6.2.2 Quantification of residual HIV-1 RNA in plasma

Plasma HIV-1 RNA below 50 copies/ml was quantified using a modified version of the Abbott RealTime HIV-1 assay (Maidenhead, UK) as described in Chapter 2 and 4. The assay 50% and 95% detection rates for 8 ml input were 1 and 3 HIV-1 RNA copies/ml, respectively.

6.2.3 HIV-1 subtyping

The HIV-1 subtype was available prior to this study. Polymerase sequences were obtain from HIV-1 DNA recovered from PBMC, and the subtype was determined s previously described (16).

6.2.4 Quantification of total, integrated and 2-LTR circular HIV-1 DNA in peripheral blood mononuclear cells

Total and integrated HIV-1 DNA loads were measured as described in Chapter 2,4, and 5. Total HIV-1 DNA load in peripheral blood mononuclear cells (PBMC) was

determined by a qPCR as previously described (Geretti et al., 2013) and the assay 50% and 95% detection rates were 20 and 40 HIV-1 DNA copies/10^6 PBMC, respectively. Integrated HIV-1 DNA was quantified by repetitive-sampling Alu-gag as previously described (De Spiegelaere et al., 2014). The assay was set up in Ghent and validated in Liverpool prior to sample testing as described in Chapter 5. The 2-LTR circular HIV-1 DNA levels were measured in collaboration with Prof Douglas Richman group as previously described (Strain et al., 2013). Assay details are given in Chapter 2. The lower limit of detection was median 5 copies/10^6 PBMC (interquartile range, IQR 4-6).

6.2.5 Markers of immune activation

Cellular markers of immune activation were measured with flow cytometry at the Royal Free Hospital, London as described in Chapter 2 and 4. In brief, fresh blood was stained with relevant antibodies (Table 2.5). PE or FITC labelled antibodies against CD4 plus either CD26, CD38, or CD69, and against CD8 plus either CD38 or HLA-DR/DP/DQ. Cell suspensions were fixed with 1% paraformaldehyde (PFA) prior to acquisition using FACScan and analysis by CellQuest software version 3.3. Soluble CD14 (sCD14) as a marker of bacterial lipopolysaccharide (LPS)-induced monocyte/macrophage activation was measured in plasma by enzyme-linked immune-enzymatic assay (ELISA). Details were given in Chapter 2. Raw data were available prior to the study and analysed by using a pre-calculated excel file provided from the manufacturer.

6.2.6 Detection of cytomegalovirus and Epstein-Barr virus DNA

Plasma was tested for CMV and Epstein-Barr Virus (EBV) DNA with a real-time PCR assay targeting the viral UL123/UL55 and p143 regions, respectively. DNA was extracted from 800 µl of plasma using the Qiasymphony DSP Virus/Pathogen Midi kit on the Qiagen QiaSymphony automated platform according to the manufacturers' instruction (Qiagen). Eluted DNA was tested at the Royal Liverpool University

Hospital, Liverpool collaboration with Dr. Mark Hopkins. The lower limits of detection were 50 IU/ml for CMV DNA and 100 copies/ml for EBV DNA.

6.2.7 Statistical analysis

The characteristics of the study population were stratified into two groups based upon duration of suppressive ART, which was defined as the length of time following the first viral load measurement <50 copies/ml recorded after starting ART. To compare continuous and categorical variables from the database, the non-parametric Wilcoxon-Mann-Whitney and the Fisher's exact test were used respectively. Where the analyses required variables to be expressed in median levels, undetectable HIV-1 RNA results were given an arbitrary midpoint value between zero and the assay 95% detection rate (=1.5 copies/ml), whereas undetectable 2-LTR circular HIV-1 DNA results were assigned a midpoint value between zero and the assay median lower limit of detection (=2.5 copies/10^6 PBMC). For measured residual plasma HIV-1 RNA, 2-LTR circular HIV-1 DNA, total and integrated HIV-1 DNA, sCD14, and frequency of activated CD4 and CD8 cells, the mean differences (with 95% confidence interval, CI) over 10 years of suppressive ART were analysed by univariate linear regression analysis after log transformation of the variables. The correlation between integrated HIV-1 DNA load or frequency of $CD8^+$HLA-DR/DP/DQ^+ cells and other measured parameters was explored by the Spearman's test. The association between integrated HIV-1 DNA load and other variables was characterised further by univariate and multivariable linear regression modelling. A 'best subset' approach and the Mallow Cp test were used for the selection of variables to be included in the multivariable model as described in Chapter 2. All available variables were initially considered for inclusion, with the exception of gender and NNRTI use (due to predominance of males and efavirenz use: 40/50, 80% for both variables) and total HIV-1 DNA load (due to strong co-linearity with integrated HIV-1 DNA load). Pre-ART viral load (Cp value 3.5), duration of suppressive ART (3.6), residual plasma HIV-1 RNA load (3.6), frequency of $CD8^+$HLA-DR/DP/DQ^+ cells (0.4), and sCD14 levels (1.7) were identified for

inclusion in the multivariate model. The CD4 cell count was added to the multivariable model as a possible confounding factor. In a second multivariable model, nadir CD4 count was included instead of pre-ART viral load. A sensitivity analysis was also performed replacing integrated with total HIV-1 DNA as the outcome variable in the same two models. The analyses were performed with SAS 9.4 with the support of Dr. Alessandro Cozzi-Lepri at University College London.

6.3 RESULTS

6.3.1 Study population

Fifty patients, who were receiving two NRTIs plus either efavirenz (80%) or nevirapine for median duration of viral load suppression <50 copies/ml of 6.4 years (Table 6.1), were recruited. Patients with duration of suppressive ART above the median of 6.4 years were older and had a lower nadir CD4 cell count, a marginally higher current CD4 cell count, and lower frequencies of CD4 and CD8 cells expressing CD38 relative to subjects with shorter duration. They were also more likely to have experienced changes in the composition of the NRTI backbone after first starting ART. Overall 25/50 patients (50%) changed one or more component of the NRTI backbone, with median 1 drug change per subject (IQR 0-1). At the time of sampling, NRTI backbones were tenofovir/emtricitabine (37/50, 74%), abacavir/lamivudine (10/50, 20%), or zidovudine/lamivudine (3/50, 6%). Residual plasma HIV-1 RNA was detected in 29/50 patients (58%) at levels ranging between 1 and 35 copies/ml, whereas 2-LTR circular HIV-1 DNA was detected in 16/50 patients (32%) at levels ranging between 5 and 35 copies/10^6 PBMC. All subjects had detectable HIV-1 DNA, with total and integrated HIV-1 DNA levels of median 2.6 and 1.9 $\log_{10}$ copies/10^6 PBMC, respectively. None of the patients had detectable CMV DNA in plasma, whereas 3/50 patients (6%) had detectable EBV DNA.

Differences in measured parameters per 10 years of suppressive ART were determined by linear regression analysis of data obtained from the cross-sectional sampling (Table 6.2). Longer duration of suppressive ART was associated with higher CD4 cell counts and lower levels of CD38 expression on CD4 and CD8 cells. There were also lower 2-LTR circular HIV-1 DNA levels and a trend for lower residual HIV-1 RNA levels. A sub-analysis compared subjects with integrated HIV-1 DNA load either in the lowest quartile (<1.7 $\log_{10}$ copies/10^6 PBMC) or the highest quartile (>2.2 $\log_{10}$ copies/10^6

PBMC) (Table 6.3). Subsets in the lowest quartile showed significant lower levels of total HIV-1 DNA and sCD14, and lower frequency of $CD8^{+}$HLA-DR/DP/DQ^{+} cells.

Table 6.1 Characteristics of the study population overall, and stratified by duration of suppressive therapy as below (Group I) or above (Group II) the median of 6.4 years

Characteristic	Total (n=50)	Group I (n=25)	Group II (n=25)	P
Male n (%)	40 (80)	22 (88)	18 (72)	0.29
Age median years (IQR)	46 (40-53)	44 (36-49)	48 (43-55)	0.04
HIV-1 subtype B n (%)	32 (64)	18 (72)	14 (56)	0.38
Nadir CD4 count median cells/mm^3 (IQR)	206 (110-265)	246 (160-292)	176 (97-213)	0.007
Duration of ART median years (IQR)	6.7 (3.4-9.1)	3.4 (2.5-5.0)	9.2 (8.0-10.3)	<0.001
Duration of suppressive ART median years (IQR)[a]	6.4 (3.1-8.8)	3.1 (2.1-4.8)	9.0 (7.7-10.0)	<0.001
Efavirenz as initial NNRTI n (%)	40 (80)	22 (44)	18 (36)	0.29
Changed NRTI backbone n (%)	25 (50)	4 (16)	21 (84)	<0.001
Pre-ART HIV-1 RNA median log_{10} copies/ml (IQR)	5.0 (4.7-5.5)	4.8 (4.5-5.3)	5.1 (4.9-5.6)	0.09

Table 6.1 continue on next page

Table 6.1 (continued)

Characteristic	Total (n=50)	Group I (n=25)	Group II (n=25)	P
Detectable residual plasma HIV-1 RNA n (%)	29 (58)	15 (60)	14 (56)	1.00
Residual HIV-1 RNA median copies/ml (IQR)[b]	2 (2-4)	2 (2-7)	2 (2-4)	0.33
Detectable 2-LTR circular HIV-1 DNA n (%)	16 (32)	10 (40)	6 (25)	0.36
2-LTR circular HIV-1 DNA median copies/10^6 PBMC (IQR)[c]	3 (3-7)	3 (3-7)	3 (3-5)	0.28
Total HIV-1 DNA median $\log_{10}$ copies/10^6 PBMC (IQR)	2.6 (2.3-2.9)	2.6 (2.4-2.9)	2.5 (2.2-2.7)	0.36
Integrated HIV-1 DNA median $\log_{10}$ copies/10^6 PBMC (IQR)	1.9 (1.7-2.2)	1.9 (1.7-2.1)	1.8 (1.7-2.4)	0.91
CD4 count median cells/mm^3 (IQR)	572 (478-734)	552 (442-606)	640 (502-794)	0.05
$CD4^+CD26^+$ median percentage (IQR)	54 (43-63)	54 (42-63)	54 (44-63)	0.55
$CD4^+$ $CD38^+$ median percentage (IQR)	22 (17-34)	25 (21-35)	20 (14-24)	0.02
$CD4^+CD69^+$ median percentage (IQR)	2 (1 -2)	1 (1-3)	2 (1-2)	0.48
$CD8^+CD38^+$ median percentage (IQR)	5 (3-7)	6 (3-8)	4 (3-6)	0.04
$CD8^+$HLA-DR/DP/DQ^+ median percentage (IQR)	32 (20-48)	37 (22-53)	30 (16-42)	0.19
sCD14 median μg/ml (IQR)	2.2 (1.8-2.6)	2.0 (1.6-2.6)	2.2 (2.0-2.7)	0.16

[a]Defined as the length of time following the first viral load <50 copies/ml; it ranged between 0.7 and 6.4 years in Group 1, and between 6.4 and 14.4 years in Group II. [b]Samples with undetectable HIV-1 RNA were assigned an arbitrary value of 1.5 copies/ml. [c]Samples with undetectable 2-LTR circular HIV-1 DNA were assigned an arbitrary value of 2.5 copies/106 PBMC. IQR= interquartile range; ART= antiretroviral therapy; NRTI= nucleoside/nucleotide reverse transcriptase inhibitor; NNRTI= non-nucleoside reverse transcriptase inhibitor; PBMC= peripheral blood mononuclear cells; sCD14= soluble CD14.

Table 6.2 Univariate linear regression analysis of mean difference in log-transformed virological and immunological variables per 10 years of suppressive antiretroviral therapy

Variable[a]	Mean difference	95% CI	P
Residual HIV-1 RNA copies/ml	-0.27	-0.57, 0.03	0.08
2-LTR circular HIV-1 DNA copies/10^6 PBMC	-0.34	-0.59,-0.08	0.01
Total HIV-1 DNA copies/10^6 PBMC	-0.12	-0.56, 0.32	0.60
Integrated HIV-1 DNA copies/10^6 PBMC	0.22	-0.19, 0.62	0.28
CD4 count cells/mm^3	0.14	0.00, 0.27	0.05
$CD4^+CD26^+$ percentage	-0.03	-0.02, 0.10	0.69
$CD4^+CD38^+$ percentage	-0.23	-0.39,-0.07	0.01
$CD4^+CD69^+$ percentage	-0.11	-0.28, 0.07	0.22
$CD8^+CD38^+$ percentage	-0.30	-0.54, -0.07	0.01
$CD8^+$HLA-DR/DP/DQ^+ percentage	-0.15	-0.37, 0.07	0.17
sCD14 μg/ml	0.07	-0.03, 0.16	0.19

[a]*Variables in log10. CI= Confidence interval; PBMC= peripheral blood mononuclear cells; sCD14= soluble CD14.*

Table 6.3 Comparative analysis of subjects whose integrated HIV-1 DNA load fell within the lowest or the highest quartile

Characteristic	Lowest quartile[a] (n = 13)	Highest quartile (n = 13)	P
Male n (%)	9 (70)	11 (84)	0.64
Age median years (IQR)	40 (31-49)	47 (43-53)	0.07
HIV-1 subtype B n (%)	8 (61)	5 (38)	0.43
Nadir CD4 count median cells/mm^3 (IQR)	180 (80-240)	208 (118-260)	0.41
Duration of ART median years (IQR)	6.7 (5.7-8.2)	9.1 (3.0-10.7)	0.29
Duration of suppressive ART median years (IQR)	6.6 (5.7-7.7)	8.9 (2.7-10.6)	0.24
Efavirenz as initial NNRTI n (%)	13 (100)	10 (77)	0.22
Changed NRTI backbone n (%)	8 (61)	5 (38)	0.43
Pre-ART HIV-1 RNA median log_{10} copies/ml (IQR)	4.9 (4.6-5.5)	5.1 (5.0-5.5)	0.26

Table 6.3 continues on the next page

Table 6.3 (continued)

Characteristic	Lowest quartile[a] (n = 13)	Highest quartile (n = 13)	P
Detectable residual plasma HIV-1 RNA n (%)	9 (69)	6 (46)	0.43
Residual HIV-1 RNA median copies/ml (IQR)	2 (2-3)	2 (2-5)	0.89
Detectable 2-LTR circular HIV-1 DNA n (%)	4 (31)	6 (46)	0.68
2-LTR circular HIV-1 DNA median copies/10^6 PBMC (IQR)	3 (3-7)	3 (3-7)	0.65
Total HIV-1 DNA median $\log_{10}$ copies/10^6 PBMC (IQR)	2.4 (2.1-2.6)	2.8 (2.7-3.0)	0.003
CD4 count median cells/mm^3 (IQR)	721 (552-758)	513 (482-640)	0.25
$CD4^+CD26^+$ median percentage (IQR)	53 (34-60)	54 (44-59)	0.85
$CD4^+$ $CD38^+$ median percentage (IQR)	23 (17-34)	20 (16-24)	0.28
$CD4^+CD69^+$ median percentage (IQR)	2 (1-2)	2 (1-2)	0.64
$CD8^+CD38^+$ median percentage (IQR)	4 (3-7)	3 (2-7)	0.43
$CD8^+$HLA-DR/DP/DQ^+ median percentage (IQR)	24 (16-37)	35 (32-49)	0.01
sCD14 median μg/ml (IQR)	1.8 (1.6-2.3)	2.4 (2.1-2.7)	0.04

[a]*Quartile cut-offs= 1.7 and 2.2 log10 copies/106 PBMC. PBMC= peripheral blood mononuclear cells; IQR= interquartile range; ART= antiretroviral therapy; NNRTI= non-nucleoside reverse transcriptase inhibitor; sCD14= soluble CD14.*

6.3.2 Factors associated with integrated HIV-1 DNA load

Integrated HIV-1 DNA load was positively associated with total HIV-1 DNA load ($p<0.0001$), frequency of $CD8^+$HLA-DR/DP/DQ^+ cells ($p=0.01$), and sCD14 levels ($p=0.04$), but not with the levels of residual plasma HIV-1 RNA ($p=0.80$) and 2-LTR circular HIV-1 DNA ($p=0.50$), or the frequency of $CD8^+CD38^+$ cells ($p=0.33$) (Figure 6.1). The associations were also tested by univariate and multivariable linear regression analysis (Table 6.4). An initial model was built including pre-ART viral load, duration of suppressive ART, CD4 cell counts, residual plasma HIV-1 RNA levels, frequency of $CD8^+$HLA-DR/DP/DQ^+ cells, and sCD14 levels. In this adjusted model, integrated HIV-1 DNA load was a mean of 0.5 $\log_{10}$ copies higher for each 50% increment in the frequency of $CD8^+$HLA-DR/DP/DQ^+ cells (95% CI 0.2, 0.9; $p=0.01$) (Table 6.4). We also found that $CD8^+$HLA-DR/DP/DQ^+ cells were not associated with plasma HIV-1 RNA or intracellular 2-LTR circular HIV-1 DNA (Figure 6.2).

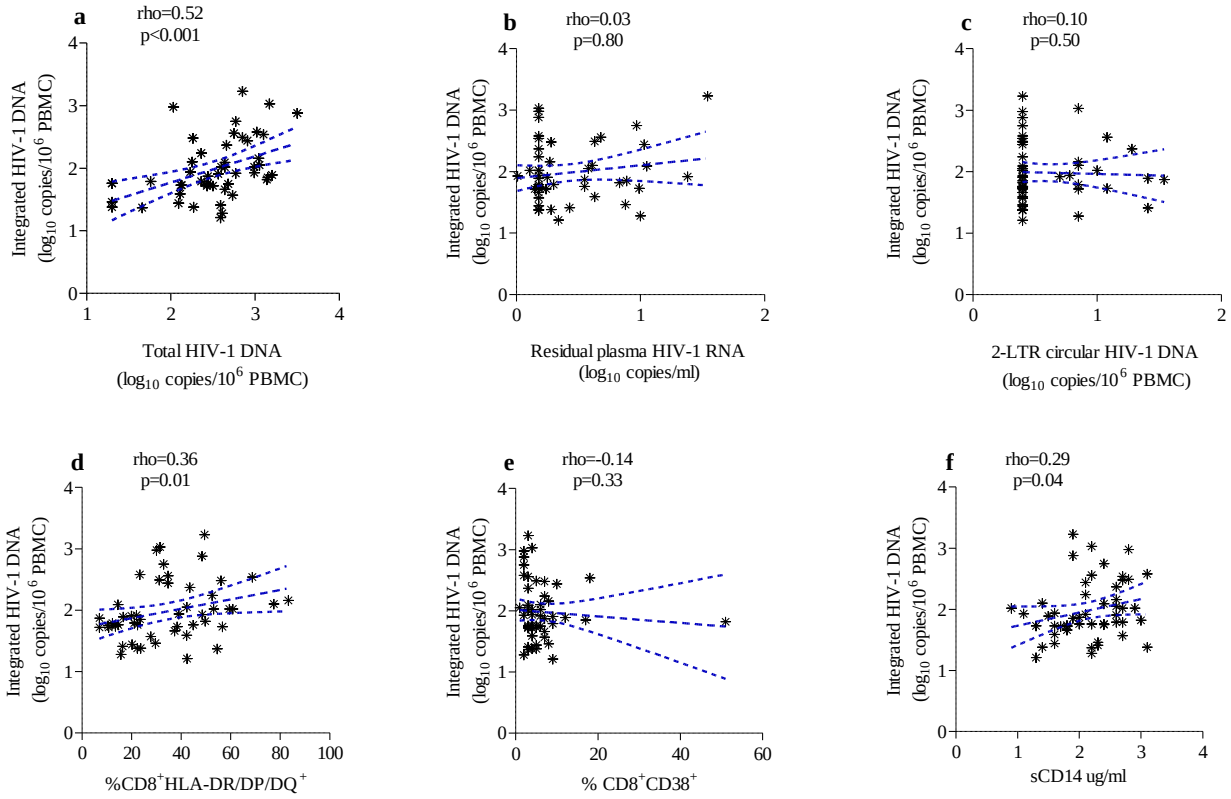

Figure 6.1 Association between integrated HIV-1 DNA and virological and immunological factors

Y axis: integrated HIV-1 DNA $log_{10}/10^6$ PBMC; x axis: a) total HIV-1 DNA load, b) residual plasma HIV-1 RNA levels, c) 2-LTR circular HIV-1 DNA levels, d) frequency of $CD8^+HLA\text{-}DR/DP/DQ^+$ cells, e) frequency of $CD8^+CD38^+$ cells, and f) levels of sCD14. Scatter plots with integrated HIV-1 DNA by the fitted fractional polynomial curves (with 95% confidence interval) and Spearman's rho (with p values) are shown.

Table 6.4 Univariate and multivariable linear regression analysis of factors associated with the mean difference in integrated HIV-1 DNA load

Factor	Univariate			Multivariable		
	Mean difference	95% CI	P	Mean difference	95% CI	P
Age, per 10 years higher	0.11	-0.03, 0.25	0.11			
HIV-1 subtype B vs. non B	0.11	-0.18, 0.39	0.46			
Nadir CD4 count per 100 cell/mm^3 higher	0.06	-0.04, 0.17	0.25			
Duration of suppressive ART per 10 years longer	0.22	-0.19, 0.62	0.28	0.23	-0.20, 0.66	0.30
Changed NRTI backbone yes vs. no	-0.14	-0.41, 0.13	0.30			
Pre-ART HIV-1 RNA per log_{10} copies/ml higher	0.10	-0.08, 0.28	0.27	0.13	-0.05, 0.30	0.15
Residual HIV-1 RNA per log_{10} copies/ml higher	0.20	-0.17, 0.57	0.28	0.27	-0.08, 0.62	0.13
2-LTR circular HIV-1 DNA per log_{10} copies/10^6 PBMC higher	0.04	-0.39, 0.46	0.85			
CD4 count per 100 cells/mm^3 higher	0.03	-0.02, 0.08	0.25	0.02	-0.03, 0.07	0.38
$CD4^+CD26^+$ per 50% higher	0.01	-0.44, 0.47	0.96			
$CD4^+CD38^+$ per 50% higher	-0.78	-2.11, 0.54	0.24			
$CD4^+CD69^+$ per 50% higher	1.02	-5.29, 7.33	0.75			
$CD8^+CD38^+$ per 50% higher	-0.27	-1.22, 0.67	0.57			
$CD8^+$HLA-DR/DP/DQ^+ per 50% higher	0.38	0.02, 0.74	0.04	0.51	0.15, 0.86	0.01
sCD14 per log_{10} μg/ml higher	0.97	-0.14, 2.08	0.09	0.90	-0.16, 1.97	0.10

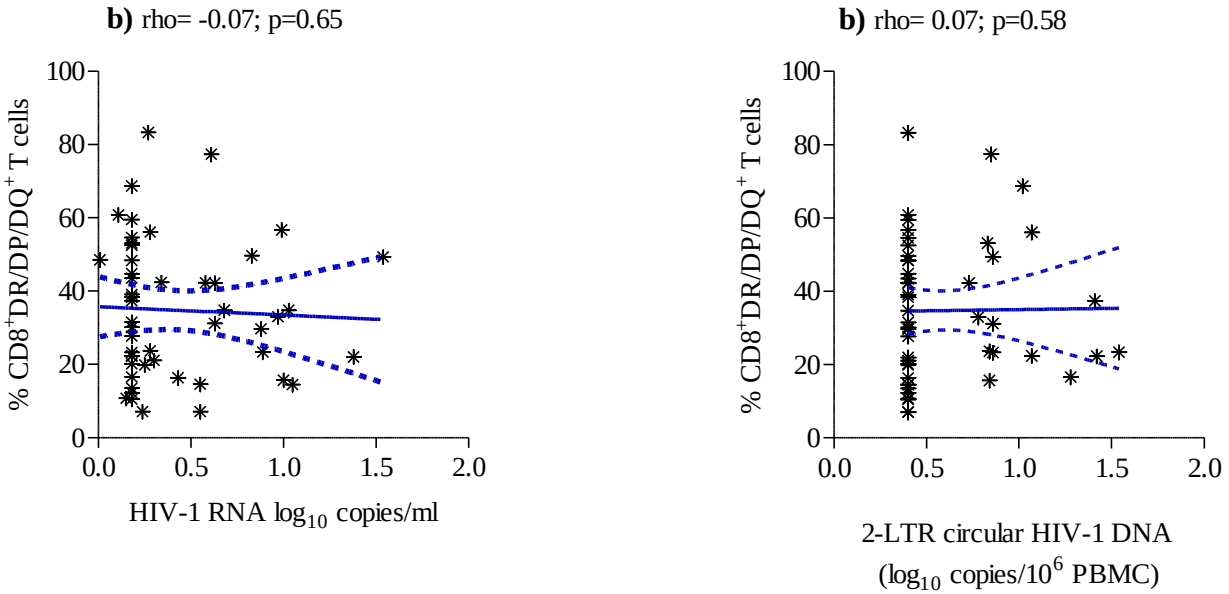

Figure 6.2 Association between residual plasma HIV-1 RNA levels and 2-LTR circular HIV-1 DNA levels and %CD8$^+$HLA-DR/DP/DQ$^+$

a) Residual plasma HIV-1 RNA levels, and b) 2-LTR circular HIV-1 DNA levels. Scatter plots with predicted CD8$^+$HLA-DR/DP/DQ$^+$ cells by the fitted fractional polynomial curves (with 95% confidence interval) and Spearman's rho (with p values) are shown.

The association between integrated HIV-1 DNA load and frequency of $CD8^+$HLA-DR/DP/DQ^+ cells was confirmed in a separate model including the nadir CD4 cell count in place of pre-ART viral load. In this second model integrated HIV-1 DNA load was mean 0.5 log_{10} copies higher for each 50% increase in the frequency of $CD8^+$HLA-DR/DP/DQ^+ cells (95% CI 0.1, 0.8; p=0.02) (Table 6.5). In a sensitivity analysis, integrated HIV-1 DNA was replaced with total HIV-1 DNA in the two multivariable models (Table 6.6). In the model including pre-ART viral load as one of variables, total HIV-1 DNA load was 0.4 log_{10} copies higher for each 50% increase in the frequency of $CD8^+$HLA-DR/DP/DQ^+ cells (95% CI -0.02, 0.8; p=0.06); in the model including the nadir CD4 cell count in place of pre-ART viral load, total HIV-1 DNA load was similarly 0.5 log_{10} copies higher for each 50% increase in the frequency of $CD8^+$HLA-DR/DP/DQ^+ cells (95% CI -0.1, 0.8; p=0.12).

Table 6.5 Multivariable linear regression analysis of factors associated with the mean difference in integrated HIV -1 DNA load over 10 years of suppressive antiretroviral therapy in a model including nadir CD4 cell count.

Factor	Mean difference[a]	95% CI	P
Nadir CD4 count per 100 cell/mm^3 higher	0.04	-0.09, 0.16	0.55
CD4 count per 100 cells/mm^3 higher	0.01	-0.04,0.06	0.60
Duration of suppressive ART per 10 years longer	0.37	-0.12, 0.86	0.13
Residual HIV-1 RNA per log_{10} copies/ml higher	0.26	-0.10, 0.62	0.15
$CD8^+$HLA-DR/DP/DQ^+ per 50% higher	0.45	0.08, 0.82	0.02
sCD14 per log_{10} μg/ml higher	0.76	-0.40, 1.92	0.19

[a]Mean difference in integrated HIV-1 DNA in log_{10} copies/10^6 PBMC. PBMC= peripheral blood mononuclear cells; ART= antiretroviral therapy.

Table 6.6 Sensitivity analysis replacing integrated with total HIV-1 DNA in the two multivariable models[a].

Factors	Model I			Model II		
	Mean difference	95% CI	P	Mean difference	95% CI	P
Nadir CD4 count per 100 cell/mm^3 higher	-	-	-	-0.02	-0.16, 0.13	0.83
CD4 count per 100 cells/mm^3 higher	-0.02	-0.08, 0.04	0.53	-0.02	-0.09, 0.04	0.43
Duration of suppressive ART per 10 years longer	-0.12	-0.62, 0.39	0.65	-0.01	-0.60, 0.58	0.98
Pre-ART HIV-1 RNA per log_{10}copies/ml higher	0.23	0.03, 0.43	0.03	-	-	-
Residual HIV-1 RNA per log_{10} copies/ml	0.14	-0.26, 0.55	0.48	0.14	-0.30, 0.57	0.53
$CD8^+$HLA-DR/DP/DQ^+ per 50% higher	0.39	-0.02, 0.80	0.06	0.35	-0.09, 0.80	0.12
sCD14 per log_{10} μg/ml higher	0.56	-0.68, 1.78	0.37	0.57	-0.83, 1.97	0.41

[a]Mean difference in log_{10} copies/10^6 PBMC. Model 1 included pre-ART viral load; model 2 replaced pre-ART viral load with nadir CD4 cell count. PBMC: peripheral blood mononuclear cells; ART: antiretroviral therapy.

6.4 DISCUSSION

This analysis of subjects receiving first-line NNRTI-based ART demonstrated that integrated HIV-1 DNA load did not differ by duration of suppressive therapy and was positively associated with the frequency of CD8 cells expressing HLA-DR/DP/DQ. Subjects with higher integrated HIV-1 DNA load also had higher levels of sCD14, although the association did not persist in adjusted analyses. While there was a predictable positive correlation with total HIV-1 DNA levels, integrated HIV-1 DNA load did not show a correlation with putative measures of recent HIV-1 replication (residual plasma HIV-1 RNA, 2-LTR circular HIV-1 DNA), or with the frequency of CD4 and CD8 cells expressing CD38.

Previous studies reported that during suppressive ART integrated HIV-1 DNA shows a constant load and little evidence of genetic evolution (Siliciano et al., 2003, von Stockenstrom et al., 2015, Josefsson et al., 2013, Besson et al., 2014). Our study adds to these previous analyses by demonstrating that the HIV-1 DNA load did not differ by duration of suppressive therapy in a population with a relatively homogenous treatment history and exact requirements in terms of evidence of plasma viral load suppression <50 copies/ml. There were indications that subjects treated for longer had lower levels of 2-LTR circular HIV-1 DNA and residual plasma HIV-1 RNA, accompanied by a reduction in the frequency of $CD4^+CD38^+$ and $CD8^+CD38^+$ cells, together suggesting that control of virus replication and resolution of immune dysfunction improve with longer duration of therapy. In contrast, the frequency of $CD8^+$HLA-DR/DP/DQ^+ cells was also not related to the duration of suppressive ART and we were able to quantify the association between two key parameters of virus persistence and immune activation, whereby integrated HIV-1 DNA load increased by 0.5 $\log_{10}$ copies/10^6 PBMC for each 50% increase in the frequency of $CD8^+$HLA-DR/DP/DQ^+ cells.

The function of $CD8^+$ cells expressing HLA-DR/DP/DQ^+ remains to be fully elucidated and may include both regulatory and effector functions (Arruvito et al., 2014, Saez-Cirion et al., 2007, Zubkova et al., 2014). In the context of suppressive ART, $CD8^+CD38^-$/HLA-DR^+ cells may be maintained by low-level expression of HIV or other persistent pathogens, including microbial translocation from the gut. It has been proposed that $CD8^+$ cells expressing HLA-DR without CD38 are preferentially

generated in response to low antigenic stimulation and that by retaining good effector function may play a role in suppressing HIV replication in elite controllers, as well as clearing hepatitis C infection (Zubkova et al., 2014, Saez-Cirion et al., 2007). It may seem therefore counterintuitive that $CD8^+$HLA-DR/DP/DQ^+ cells should have a positive (rather than inverse) correlation with integrated HIV-1 DNA load. Yet, in line with previous data (Hatano et al., 2013), our adjusted analyses showed a positive association between frequency of $CD8^+$HLA-DR/DP/DQ^+ cells and integrated HIV-1 DNA load. Several hypotheses may be proposed to explain the observed positive association. Firstly, low-level HIV production may both stimulate $CD8^+$HLA-DR/DP/DQ^+ cells and continuously replenish the integrated reservoir. Further to this, $CD8^+$HLA-DR/DP/DQ^+ cells may directly stimulate HIV-infected CD4 cells, causing their proliferation and expansion of the reservoir, which can be measured as increased integrated HIV-1 DNA load (Klatt et al., 2013). Thirdly, a stimulant or multiple stimulants may act simultaneously on $CD8^+$HLA-DR/DP/DQ^+ cells and HIV-infected CD4 cells, resulting in an indirect association between the two parameters.

The population we studied did not overall show evidence of ongoing HIV replication. Patients experienced no viral load rebound >50 copies/ml during follow-up (Doyle et al., 2012). In line with previous studies, just over half had traces of detectable plasma HIV-1 RNA (Palmer et al., 2008), whereas a third had detectable intracellular 2-LTR circular HIV-1 DNA. There was no association however between these two putative markers of recent HIV-1 replication and either integrated HIV-1 DNA load, or the frequency of $CD8^+$HLA-DR/DP/DQ^+ cells. While this indicates that HIV production was unlikely, the finding may also reflect insufficient sensitivity of the analytic systems and the limitation of assaying peripheral blood (Cockerham et al., 2014). It will be important to determine the antigenic specificity of $CD8^+$HLA-DR/DP/DQ^+ cells, for example against persistent viruses such as CMV and EBV (Gianella et al., 2014). As described in Chapter 1 of this thesis, CD8 T cells specific for those two herpes viruses have been found in ART-experienced HIV-1 infected individuals and activated CD8 T cells have been correlated with HIV-1 viral load (Doisne et al., 2004, Paiardini and Muller-Trutwin, 2013). Of note, the two viruses were not commonly detected in our population, which is consistent with containment by effective immune responses. One other aspect that warrants investigation is the relationship with levels of sCD14, which are an important predictor of disease progression and mortality in both treated and

untreated patients (Sandler et al., 2011, Marchetti et al., 2011, Hunt et al., 2014). Soluble CD14 is produced by monocytes in presence of microbial products and it can be defined as an indirect measurements of microbial translocation and GUT damage following HIV-1 infection. GUT damage sustains chronic immune activation that could drive T cells activation with consequent expansion of the viral reservoir. In this study, median sCD14 levels were within the range reported in healthy HIV-negative controls (Sandler et al., 2011). However, patients whose integrated HIV-1 DNA load fell within the highest quartile showed significantly higher sCD14 levels than those with integrated HIV-1 DNA load in the lowest quartile, a finding that warrants further investigation in larger cohorts.

A strong positive association was measured between total and integrated HIV-1 DNA, supporting the notion that integrated HIV-1 DNA is the most prevalent form of HIV-1 DNA during suppressive ART (Graf and O'Doherty, 2013), and total HIV-1 DNA was associated with the frequency of $CD8^{+}$HLA-DR/DP/DQ^{+} cells. Two previous studies have reported an association between the frequency of CD8 cells expressing HLA-DR and total HIV-1 DNA load in peripheral blood (Cockerham et al., 2014, Hatano et al., 2013). One study was unable to detect a consistent association between the expression of activation markers on CD8 cells and integrated HIV-1 DNA load among 19 subjects (Cockerham et al., 2014). The reasons for the discrepant findings are unclear, and may include a smaller and more heterogeneous study population relative to this cohort, as well as possible differences in the methods to quantify integrated HIV-1 DNA load.

This study also has limitations, including that parameters were measured cross-sectionally, albeit after stratifying recruitment according to duration of ART and causality of the observed associations cannot be concluded. Study size limited the number of variables included in the multivariable analysis of factors associated with integrated HIV-1 DNA load, and unmeasured variables may have contributed to the findings. Importantly, the cohort had received NNRTI-based ART exclusively, and findings may not necessarily be extrapolated to other treatment regimens. Further, we measured CD38 and HLA-DR/DP/DQ expression on CD8 cells separately. Unlike the frequency of $CD8^{+}$HLA-DR/DP/DQ^{+} cells however, the frequency of $CD8^{+}CD38^{+}$ cells declined with duration of suppressive ART and showed no statistical association with integrated HIV-1 DNA load. Further analyses are needed to confirm the

association between integrated HIV-1 DNA load and $CD8^+CD38^-HLA\text{-}DR/DP/DQ^+$ cells, characterise the antigenic specificity of $CD8^+HLA\text{-}DR/DP/DQ^+$ cells, and determine the direction of causality. Moreover, the data describe CD8 cells expressing HLA-DR/DP/DQ and it will be of interest to study the association between integrated HIV-1 DNA load and individual HLA isotypes. Meanwhile, our data add to the growing evidence indicating that a complex interplay between HIV-1 persistence and immune activation continues over many years of stably suppressive ART.

Chapter 7: Methodological development of experimental approaches to study HIV-1 persistence

7.1 Section A: Development of a new integrated HIV-1 DNA load assay

7.1.1 INTRODUCTION

The Alu-gag PCR assay for measuring integrated HIV-1 DNA has a good correlation with the IUMP (Eriksson et al., 2013) and provides a useful tool for investigating HIV persistence. The method comprises an initial first PCR reaction (PCR1) that amplifies integrated HIV-1 DNA and a second PCR reaction (qPCR2) that allows quantification of the first PCR products (De Spiegelaere et al., 2014, Liszewski et al., 2009). In PCR1, 42 replicates are run using one primer that binds the HIV-1 gag region and another that binds one of the Alu sequences randomly distributed within the human genome: this allows amplification of the integrated HIV-1 DNA (herein referred to as "integrated HIV-1 DNA replicates"). During this step, unintegrated HIV-1 DNA can also be linearly amplified by the binding of the gag primer only; to avoid bias in the quantification step, 30 replicates are run by using the gag primer only (herein referred to as "HIV-1 control") and the mean quantification cycle (Ct) obtained from these replicates is set as threshold above which an integrated HIV-1 DNA replicate is scored as positive. This test can detect 10% of the total integration events with a 7500-15000 cells input for each replicate (Liszewski et al., 2009, Swiggard et al., 2005). This limit of detection is a reflection of the efficiency of PCR1: integrated HIV-1 DNA that is situated at around 3.5 kb away from the human Alu sequence is amplified. This limit is partially compensated by running a large number of replicates for each sample, increasing the possibility of detecting the integrated HIV-1 DNA. This approach, however, makes the assay expensive and labour intensive, emphasizing the need for more sensitive and affordable assays.

In the Alu-gag PCR assay, the PCR1 step amplifies integrated HIV-1 DNA using one forward primer that is anchored to one of the Alu sequences that are randomly distributed within the human genome at approximately 5 kb distance from each other, and one reverse primer that binds the HIV-1 gag region located 1505 bp away from the 5'LTR end (

Figure **7.1**). This reaction is performed using the GoTaq polymerase enzyme (Promega, Southampton UK) that allows amplification of fragments that are maximum 5 kb long. Under these conditions, the 5kb long fragment would include 1505 bp on the viral genome plus 3495 bp on the human genome and this setting would therefore enable the amplification of all integrated HIV-1 DNA up to 3495 bp away from an Alu sequence. Published data indicated that this level of amplification represents 10% of the whole integration events.

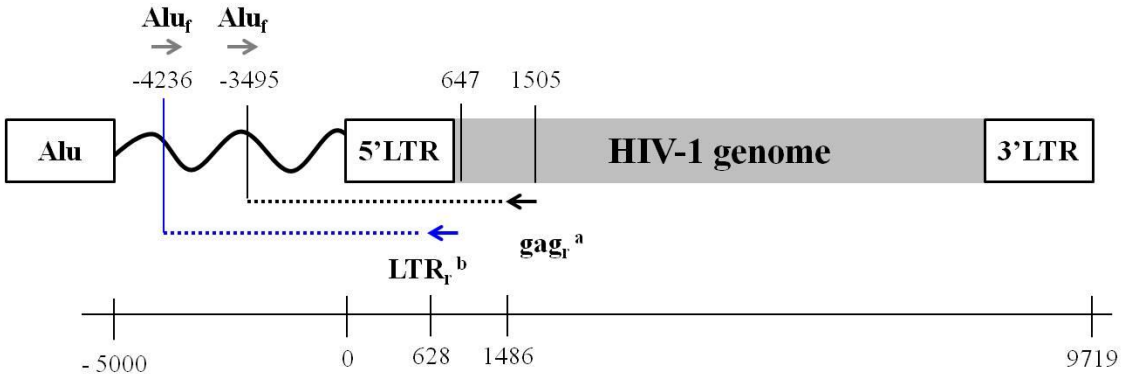

Figure 7.1 Primer combinations for Alu-gag and Alu-5LTR assays

Figure depicting the different primers used in the Alu-gag and in the Alu-5LTR assay for the PCR1 step. [a]gag reverse primer that binds HIV-1 genome at 1505-1486 bp; [b]5LTR reverse primer that binds HIV-1 genome at 647-628 bp. The black and the blue dashed lines represent 5kb long fragments. With the Alu-gag assay integration events that are up to 3495bp away from the human alu sequence can be amplified, whereas with the alu-5'LTR assay integration events that are up to 4236 bp from an alu sequence can be amplified. LTR= long terminal repeats.

In the study presented here we propose the use a different reverse primer for PCR1 that binds the HIV-1 genome 647 bp away from the 5'LTR end. By using the same GoTaq polymerase described above with these primer settings, the 5 kb long fragment would include 647 bp on the viral genome plus 4236 bp on the human genome. This would allow the amplification of all integration events that occur up to 4236 bp away from an Alu sequence. The new conditions will improve the previous method by amplifying integrated HIV-1 DNA genomes that are present between 3495 and 4236 bp away from the Alu sequence.

7.1.2 METHODS AND RESULTS

We set up experiments to test the use of a different PCR1 primer that binds to the 5'LTR region rather than the gag region of the HIV-1 genome. We also changed the primer and probe combination for the qPCR2, even if both settings targeted HIV-1 LTR region as described in Chapter 2. PCR cycles and mastermix conditions were kept constant. The quantification cycles (Ct) numbers obtained from the qPCR for each replicate (42 for the integrated HIV-1 DNA and 30 for the HIV-1 control) were used as input into a pre-designed worksheet for quantification (De Spiegelaere et al., 2014) as per the established methodology. We compared results between the two assays by testing samples from four patients of the ERAS1 cohort and the results are shown in Figure 7.2. The number of positive reactions within the integrated HIV-1 DNA replicates was three times greater when using the Alu-5LTR compared with Alu-gag assay (Figure 7.2a). Furthermore, we analysed Ct values for each replicate. Results showed that the overall mean Ct values obtained with Alu-5LTR assay were lower than the ones obtained by Alu-gag (Figure 7.2b), which indicates an increased load of the target DNA, in our case the integrated HIV-1 DNA. Moreover, the single fluorescent curves for each sample produced with the Alu-5LTR assay lay in a larger range of Ct values compared to the curves produced by the Alu-gag assay (Figure 7.2c). The Ct values reflect the quantity of the target DNA, and in this assay the initial target DNA input is greater if the pre-amplification in the PCR1 step is more efficient. Greater variety of Ct values means that the assay is detecting a larger number of integrated HIV-1 DNA generated

by PCR1. This data confirms that the new method can detect more integration events, which have a different PCR efficiency as expected.

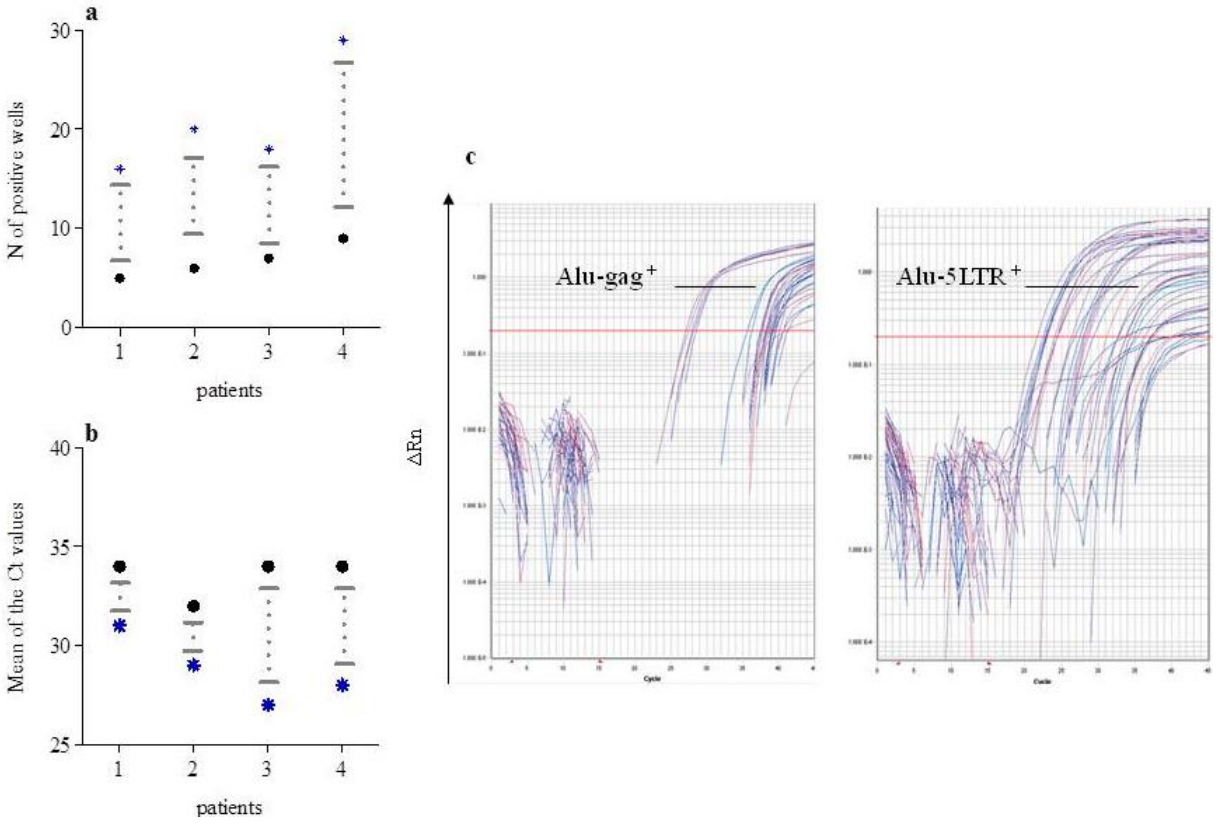

Figure 7.2 Results from the qPCR2 on the Alu-gag and Alu-5LTR PCR assays

Y axis represent number of positive wells (a) or mean Ct values obtained from the integrated HIV-1 DNA wells (b); X axis= patients. a) number of positive wells and b) mean Ct values over 40 replicates. Black diamond represents results from Alu-gag whereas blue stars indicate Alu-3LTR. c) Representative graph with fluorescence curve for patient 3. Axis: Y=ΔRn; X=Ct(cycle numbers).

We wanted to further determine whether the greater detection with the Alu-5LTR assay was only a reflection of the new setting for the PCR1 or also for the PCR2. Therefore, we ran the same sample with the two qPCR2 settings. Data showed that positive wells detection with the two methods was identical, and the average Ct and the CUT-OFF values were comparable (Table 7.1). This result indicates that the increased integrated HIV-1 DNA detection obtained with the Alu-5LTR assay is probably not produced by the different conditions used in the qPCR2 step, but is a reflection of the new primer set used in the PCR1.

Table 7.1 qPCR2 efficiency with Alu-gag and Alu-3LTR PCR assay settings

	PCR2 settings	
	Alu-gag	Alu-5LTR
Number of positive wells	8	8
Average Ct values	34.80	36.89
CUT-OFF	32.94	34.53

Collectively our preliminary data on a new method for measuring integrated HIV-1 DNA showed that we were able to achieve improved sensitivity of detection compared to the widely used Alu-gag assay. In our Alu-5LTR assay, we changed the settings for both PCR1 and qPCR2, whereas all the other conditions were kept as per the Alu-gag assay. Nonetheless, our data seems to indicate that the greater sensitivity was mostly driven by the changes in the PCR1 rather than the ones in the PCR2.

7.1.3 DISCUSSION

In this section we explored a new methodology to measure integrated HIV-1 DNA. In particular, we used an alternative primer set for the amplification PCR1 that binds HIV-1 genome towards the HIV-1 integration site. This modification allowed us to detect

integration events that occurred around 4kb from an Alu sequence compared to the previous Alu-gag method that could only detect integrated HIV-1 DNA situated up to 3kb distant from the Alu sequence. Our results were analysed with the Poisson distribution (De Spiegelaere et al., 2014) that calculates the copies of integrated HIV-1 DNA based on the number of wells scored as positive for the presence of the target DNA, which in our case was the integrated HIV-1 DNA. Data showed that with the new method, the number of positive wells was three times higher than with the previous method demonstrating improved sensitivity of detection.

De Spiegelaere and colleagues recently described a new method of quantification for the Alu-gag assay that enables absolute sample quantification without the use of serial dilution of a standard curve (De Spiegelaere et al., 2014). In this method, the Ct values obtained from a quantitative PCR (qPCR2) are inputted into a pre-designed calculation sheet that estimates the threshold Ct value above which one replicate is scored as positive (contains integrated HIV-1 DNA). The test is valid when at least 4 reactions are scored as positive. However this assay requires 70 replicates for each sample (with an estimated cost at around £80 per test) and considerable amounts of sample as reaction input. These two conditions are needed to compensate for the poor efficiency of the PCR1 that is ran prior to the quantitative PCR2 and its function is to amplify the region between the HIV-1 gag sequence and human Alu. In order to improve the PCR1 step we proposed a new primer combination that targets the 5' HIV-1 long terminal repeats (5'LTR) instead of the gag region. Consequently, we also had to change the primers for the quantitative qPCR2. Data produced by testing four patients on stable suppressive ART showed that we were able to detect greater number of wells that were scored as positive for the presence of the integrated HIV-1 DNA. This result indicated that the new primer set was able to amplify a greater number of integrated HIV-1 genomes and this was further confirmed by the analysis on the Ct values produced by qPCR2. These values indicate the PCR cycle number at which the fluorescent signal produced by the amplification of one sample is higher than the fluorescent signal emitted by the passive reference, therefore, smaller Ct values are indicative of greater

sample concentration. We found lower Ct values in the samples ran with the Alu-5LTR assay compared with the ones produced with the Alu-gag assay, which means that integrated HIV-1 DNA load was higher. Furthermore, we wanted to determine whether the greater amplification was engendered by the modifications we introduced in the PCR1 or in the qPCR2. We therefore ran the qPCR2 on the sample using the settings of the Alu-5LTR assay as opposed to the settings used for the Alu-gag assay. We found identical results and this data allowed us to assume that the greater amplification was a reflection of improved sensitivity in the PCR1.

The PCR1 serves to amplify specifically the integrated HIV-1 DNA. Integration sites are situated at heterogeneous distance from the Alu sequences that are randomly dispersed in the human genome at ~5kb distances from each other. Therefore, integrated HIV-1 may integrate up to 5kb from an Alu sequence. The polymerase used in this step can amplify up to 5kb long fragments and with the Alu-gag assay only integrations that are situated up to 3kb away from an Alu sequence can be amplified. We then thought to move this primer toward the end of the genome: in this way the 5kb long fragment produced by the polymerase could cover more human genome. As a result of this, we were able to detect integration events that occur up to 4kb away from an Alu sequence. A previous study described a two-step method for the quantification of integrated HIV-1 DNA where the PCR1 was ran with a primer binding one region of the HIV-1 LTR very close to the one we targeted (Brussel et al., 2005). However, in that study the achieved detection limit that was lower compared to the Alu-gag assay. The discrepancy could derive from the fact that they used two outward-facing primers targeting the Alu sequence. This choice could have increased the linear amplification of the Alu sequences that are more abundant with respect to the HIV-1 sequence with direct consequences on PCR1 efficiency. Our study is adding to this by demonstrating improved sensitivity when using an amplification PCR setting that includes one single primer biding the HIV-1 LTR sequence and one primer biding the Alu sequence. Furthermore, we used an innovative quantitative method that was originally developed

to analyse results generated by the Alu-gag assay and that avoids the use of a standard, rendering the assay more applicable to a larger scale.

Interestingly, we observed that samples ran with the Alu-5LTR assay had a greater heterogeneity in terms of Ct values obtained from each replicate. This data could be explained if we take into account that each single integration event carries its own efficiency of amplification (De Spiegelaere et al., 2014). Given that we are detecting more integration events it is likely that we were able to observe greater variety of PCR efficiency that is reflected by different Ct values between the replicates. We could also speculate that the different efficiency of amplification could be associated with different cell sub-populations within the PBMC that carry different amount of integrated HIV-1 DNA copies; however, this hypothesis needs further investigation and cannot be concluded from our results.

The results produced are preliminary and require further validation including running of a reference standard to determine assay sensitivity. Further assay modifications include evaluation of a reduced DNA input and consideration of reducing the number of replicates without affecting the Poisson statistics.

7.2 Section B: *In vitro* system to study cell-to-cell transmission

7.2.1 INTRODUCTION

The integrated HIV-1 DNA reservoir persists despite effective antiretroviral therapy (ART) and the underlying mechanisms are still debated. It has been proposed cell-to-cell virus transmission (Sigal et al., 2011) may contribute to the maintenance of the reservoir and potentially escape full suppression by ART. Retroviruses can initiate infection without requiring budding and extracellular release of free viral particles (Sato

et al., 1992), by transfer from the "donor" cell to the "target" cell via formation of a virological synapse (VS). This process has been described mainly in sites where cell density is high (Sigal et al., 2011), such as lymphoid tissue. Sigal and colleagues also proposed that cell-to-cell transmission is markedly less sensitive to the antiretroviral drugs tenofovir and efavirenz *in vitro* (Sigal et al., 2011) when compared to inhibition of cell-free virus. In the context of my research on HIV-1 persistence, there was scope to explore *in vitro* systems to study cell-to-cell HIV transmission *in vitro*.

The aim of this set of experiments was therefore to develop an *in vitro* system to study cell-free and cell-to-cell virus transmission. Such a system should include a population of virus-donor cells and one of target cells, where the two cell types could be discriminated with confidence. The read out for the target cells could be the quantification of a viral protein intracellularly, or alternatively a reporter gene which is expressed only upon HIV-1 infection. Sigal and colleagues described a method where donor cells were HLA-A2 negative peripheral mononuclear cells (PBMC) or fluorescent cells lines mCherry-MT4 cells, whereas target cells were HLA-A2 positive PBMC or Rev-CEM cells, which express green fluorescent protein (GFP) upon HIV-1 transcription (Iyer et al., 2009, Wu et al., 2007). We decided to use this system as a starting point for our assay to try and replicate the system proposed by Sigal. This project included genetically modified organisms and it was approved by local safety committee and notified to HSE prior to start the work (HSE approval number: GM99/09.1a).

7.2.2 METHODS AND RESULTS

7.2.2.1 Lentiviral vectors production

NL4-3 HIV (National Institute of Health (NIH) AIDS Research & Reference Reagent Program (cat# 114) and mCherry lentiviral vectors (provided by dr. Alex Sigal, PhD;

Division of Biology, California Institute of Technology) were produced by transfection of the relevant plasmids in HEK-293 that are listed in Table 7.2.

Table 7.2 Plasmids characteristics

Lentiviral vector	Plasmid used	Antibiotic selection (conc)	Restriction enzymes used for validation[a]
HIV-1 NL4-3	pNL4-3	Amp (0.1mg/ml)	PstI; EcoRI
mCherry lentivirus vector	pHAGE6-wtCMV-mCherry-W	Amp (0.1mg/ml)	HindIII; EcoRI
	HDM-Hpgm2	Amp (0.1mg/ml)	HindIII; BamHI
	HDM-VSVG	Amp (0.1mg/ml)	HindIII; EcoRI

The table summarizes the characteristics of the plasmid used to produce the lentiviral vectors. [a]all purchased by New England Biolabs, Hitchin, UK. conc=concentration.

First, virus plasmids were amplified by transformation in Dh5α bacterial cells (Thermo Fisher scientific, Loughborough UK): plasmid DNA (10ng) was added to Dh5α cells (100µl) and incubated as described below:

1. 30’ on ice;
2. 90’’ at 37ºC;
3. 2’ on ice;

30’ at 37ºC after the addition of 800 µl of pre-warmed SOC (Thermo Fisher scientific Loughborough, UK). After centrifugation at 2,000xg for 1’, cell pellet was re-suspended in ~100 µl prior to plate on LB agar plates (Sigma-Adrich, Poole Dorset UK) containing the relevant selective antibiotic as indicated in Table 7.2. After the overnight growth, the positive bacterial colonies were selected upon antibiotics resistance and

expanded by growing in LB broth (Sigma-Adrich, Poole Dorset UK) containing the relevant antibiotic selection. Plasmid DNA was then extracted with QIAprep spin minikit (Qiagen, Manchester UK) and each plasmid was treated with the relevant restriction enzyme (listed in Table 7.2) according to manufacturer instruction for validation Briefly, digestions reactions were performed by mixing 1 µg of DNA, 20 U of enzyme, 2 µl of enzyme buffer, and water to a final volume of 20 µl. Following digestion reaction for 1 hr at 37°C, the DNA fragments were separated by agarose gel electrophoresis and fragments sizes were compared to the ones obtained *in silico* by the analysis with NEBcutter v.02 free tool (a representative example is given in Figure 7.3).

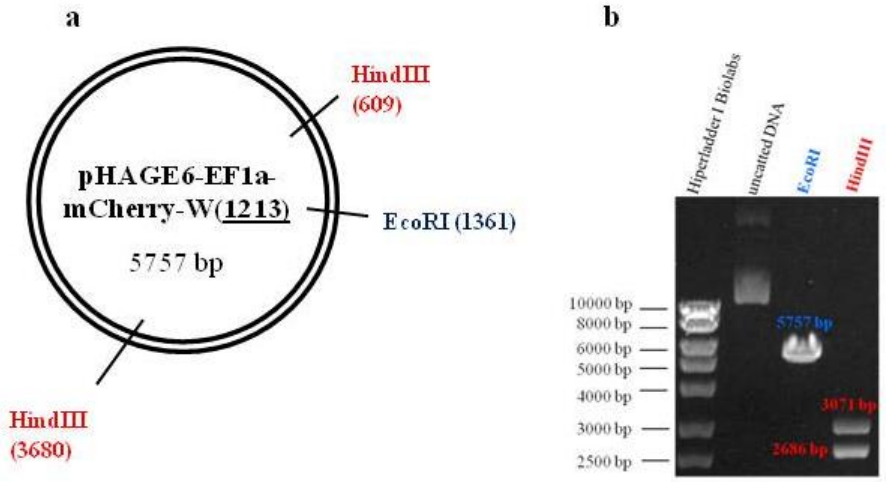

Figure 7.3 Example of validation of plasmid via restriction enzyme mapping

The figure shows the restriction map (a) and the agarose gel electrophoresis (b) of pHAGE-EF1a-mCherry-W (1213). Total length of the plasmid was 5757 base pair (bp). The full length linear form of the plasmid was obtained by cut with EcoRI, whereas HindIII produced two segments at 3071 bp and 2686 bp.

Verified plasmids were then transfected into HEK-293 cells by using Fugene HD transfection reagent (Promega, Southampton UK), as described in Sigal *et al.* Briefly, $0.2x10^6$ HEK-293 (provided by prof Andrew Owen, University of Liverpool) adherent cells were seeded in DMEM growing media made up as described in Chapter 2. The day after, the relevant plasmid mixes (Table 7.3) were added to FuGENE® HD in Opti-MEM® I Reduced Serum Medium (Thermo Fisher scientific, UK) and incubated for 15' at room temperature prior to being added to the cell for 5 hrs incubation at 37°C and 5% CO_2. After incubation, transfection media was replaced with fresh DMEM growing media.

Table 7.3 Transfection mixes

		Transfection mix[a]	
Lentiviral vector	Plasmid used	DNA	Fugene[b]
HIV-1 NL4-3	pNL4-3	5 µg	15 µl
mCherry lentivirus vector	pHAGE6-wtCMV-mCherry-W HDM-Hpgm2 HDM-VSVG	2.5 µg 0.9 µg 0.6 µg	12 µl

[a] for $0.2x10^6$ cells in 6 well plate. [b]DNA(µg)*:Fugene (*µl*)=1:3*

Virus was collected at 48 hours and virus titre was estimated by Lenti-X p24 Rapid titer kit as recommended from manufacturer (Takara Clonotech, Saint-Germain-en-Laye France) as described in Chapter 2. The results are shown in Table 7.4.

Table 7.4 Virus titre estimation by p24 Elisa assay

Recombinant virus	p24 (ng/ml)	Viral titre (lentiviral particles/ml)
Lentivirus mCherry	25	3.6×10^8
HIV-1 NL4-3[a]	200	2.5×10^9
HIV-1 NL4-3[b]	1000	10^{10}

[a] after transfection; [b] at week4 after virus growing.

We obtained p24 concentration of 25 ng/ml and 200 ng/ml for the mCherry lentivirus and NL4-3 HIV-1 virus, respectively; the results were in the range obtained from Sigal lab for the HIV-1 virus, but the mCherry lentivirus concentration was lower. The NL4-3 HIV-1 virus titre was further increased by passaging in Rev-CEM cells: 200 ng p24 and polybrene (8 µg/ml) (Pace et al., 2012) were added to the 2 ml of 10^7 cells and centrifuged at 1,000xg at room temperature (RT) for 2 hrs. After centrifugation, cell pellet was resuspended at a concentration of $2x10^6$ cells/ml. Five million of fresh cells at 10^6 cells/ml concentration were added every 3 days. At week 4, p24 concentration was 1000 ng/ml (Figure 7.4, plot) and such concentration was sufficient to run the desired assay (Sigal et al., 2011).

7.2.2.2 Co-culture system I: MT4-mCherry cell line as donor cells and Rev-CEM as target cells.

MT4 and Rev-CEM are T-cell lines; details on cell maintenance were given in Chapter 2. Briefly cells were grown in suspension in RPMI-1640 prepared as described in Chapter 2. They were split twice a week depending on growth rate.

MT4-mCherry cells were produced by infection of MT4 cells with mCherry lentivirus in order to produce $mCherry^+$ MT4 cells: 10^6 MT4 suspension cells were infected with

supernatant containing virus that has been previously diluted 1:4. At 48 hrs after the infection, cells were fixed with 3.7% PFA solution and proportion of mCherry positive MT4 cells was estimated by flow cytometry. Results showed that 3.6% of MT4 cells expressed mCherry protein (Figure 7.4a).

Rev-CEM cells are engineered to produce green fluorescent protein (GFP) upon HIV-1 infection. Prior to use in the assay, we first tested GFP production upon HIV-1 infection: this step was critical to allow discrimination between infected and non-infected target cells. Rev-CEM cells were infected with NL4-3 HIV ($1.7x10^5$ cells and 113 ng p24) (Sigal et al., 2011), or mock-infected with the same volume of growth medium. At 24, 48 and 52 hours post infection (Sigal et al., 2011), we checked cell viability and GFP expression by flow cytometry and microscopy. Cells were washed twice in 1 ml of PBS and centrifugation at 300xg for 5' at room temperature. After the last wash, cells were resuspended in 500 µl of 3.7% formaldehyde in PBS. Half of the volume was used for flow cytometry analysis, whereas the other half was processed for microscopy analysis. Briefly, cell suspension was centrifuged by Cytospin^{TM} 4 Cytocentrifuge (Thermo Fisher scientific, UK) to allow thin layer cell preparation on the slide. Vectashield mounting media (Vector Laboratories, Peterborough UK) was applied between cover slip and slide in order to minimize quenching and the slides were sealed with nail polish. Images were collected using a Zeiss LSM 510 META detector and analysed using the Zeiss AIM software (Zeiss, Germany) in collaboration with Dr. Marco Marcello at the centre for cell imaging at the University of Liverpool.

Results showed that cell viability was overall >90% and around 80% in mock-infected and HIV-1 infected cells, respectively (Figure 7.4b). We observed that the proportion of cells expressing GFP was 8.1% at 24 hours; 8.8% at 48 hrs; and 14.5% at 52 hours (Figure 7.4c), which indicated that GFP production increased with virus growing as expected. Furthermore we analysed cells by immunofluorescence and we observed that mock-infected cells had green and red fluorescence which was unexpected (Figure 7.5).

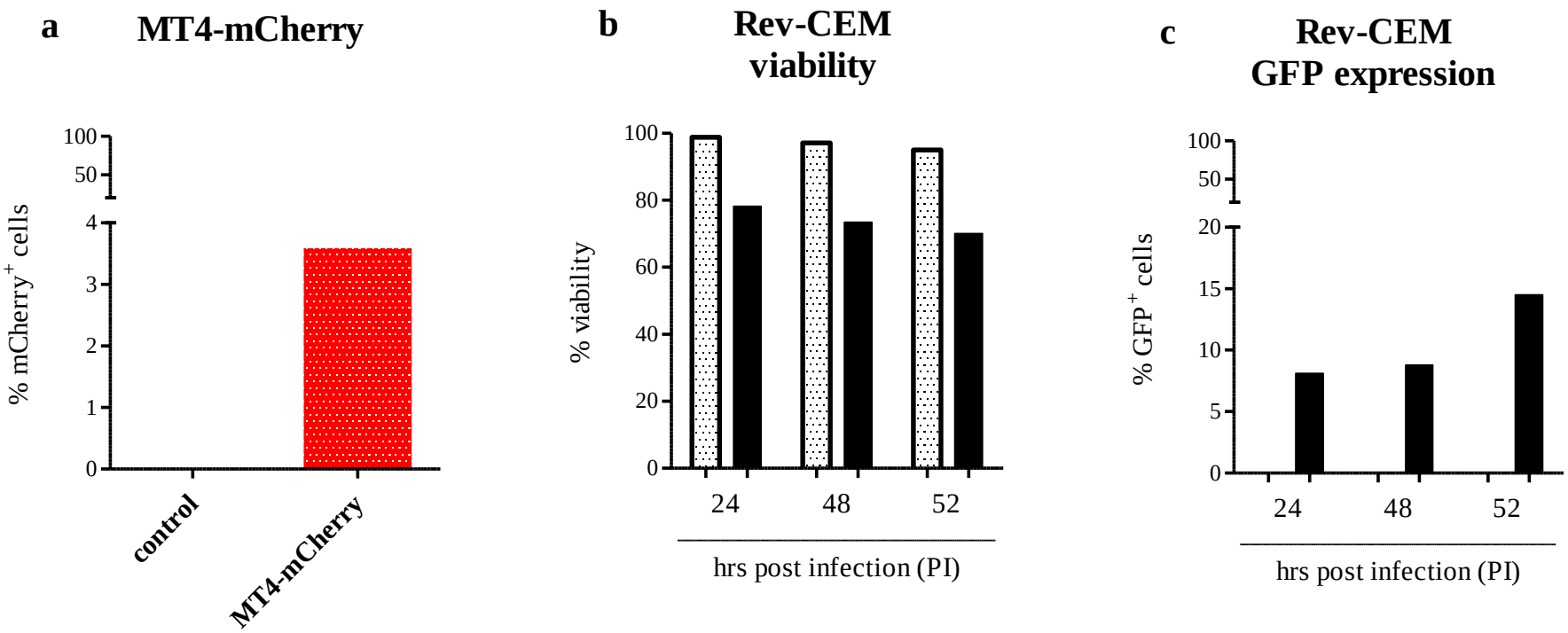

Figure 7.4 Validation of MT4-mCherry and Rev-CEM cell lines

Bar chart representing a) mCherry expression in MT4 cells at 48 hrs after infection with the mCherry lentivirus; b) Rev-CEM viability and c) GFP production at 24, 48, 52 hrs after infection with NL4-3 HIV-1 virus. Red pattern bars= MT4 cells that express mCherry; white pattern bars= mock infected cell; black bars= NL4-3 HIV-1 infected cells. One single experiment.

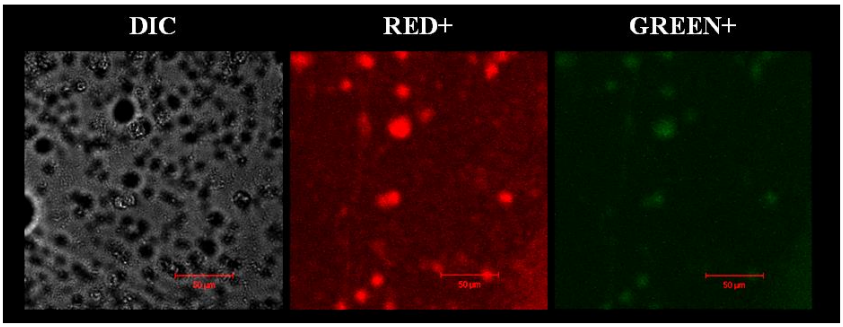

Figure 7.5 Characterization of Rev-CEM by immunofluorescence

DIC= Differential interference contrast; RED+= red channel; GREEN+= green channel. Bar= 50µm.

This data on the development of a co-culture system showed that we obtained 3.7% mCherry^{+} MT4 cells and we observed that Rev-CEM cells expressed GFP production upon virus infection by flow cytometry. However, microscopy analysis showed fluorescence signal in absence of infection in Rev-CEM, which meant that those cells could not be used for fluorescent assays because the read-out was biased by the auto-fluorescence produced by the cells *per se*.

7.2.2.3 Co-culture system II: HLA-A2 negative PBMC as donor cells and HLA-A2 positive PBMC as target cells.

We further used co-cultures of infected PBMC to induce cell-to-cell spread as described in Sigal *et al*. 2011. Donors with HLA-A2 positive and negative phenotypes were enrolled within the Institute of Infection and Global Health and signed written consent form prior to participate to the study. Blood was collected in Heparin tubes and processed fresh to isolate peripheral blood mononuclear cells (PBMC) as described in Methods. Isolate cells were then cultured for 3 days in RPMI growing media in the

presence of 5 µg/ml of Pha-p (Sigma, UK) to ensure cell activation and maintained in RPMI growing media supplemented with 100 U/ml of human interleukin-2 (IL-2, Miltenyi Biotec Ltd., Bisley UK). The co-culture assay was performed as described by Sigal et al. Briefly, 1.5 x 10^6 HLA-A2-negative PBMC were first infected with HIV-1 NL4-3 (700 ng of p24); at 2 days after the infection the HLA-A2-negative PBMC (donor cells) were washed, counted, diluted to 10^6 cells/ml and added to HLA-A2-positive PBMC (target cells) at an approximately 1:10 donor:target ratio. Target cells were also directly infected with NL4-3 (250 ng of p24). Two days after target-cell infection, the number of infected target cells was determined by flow cytometry by staining the intracellular p24 viral protein. Briefly, cells were first incubated with HLA-A2 PE-conjugated antibody, washed in PBS as described above and fixed in 3.7% PFA; following incubation cells underwent intracellular staining with anti p24 FITC-conjugate antibody. Donor and target cells were discriminated based upon HLA-A2 expression and cells that were PE positive were defined as target cells. HIV-1 infection was estimated upon intracellular p24 expression and FITC positive cells were considered as infected. Results are shown in Figure 7.6. At 2 days post infection, donor cells were 70% alive and we judged this viability to be good enough to proceed with the co-culture assay (Figure 7.6 a). Analysis of the target cells showed that target cell viability was 70% and 60% in direct infection and co-culture conditions, respectively (Figure 7.6b). Infection rate was 17% in cell-free infection condition compared to 7% in the co-culture assay (Figure 7.6c) which was in the range published by Sigal *et al.*

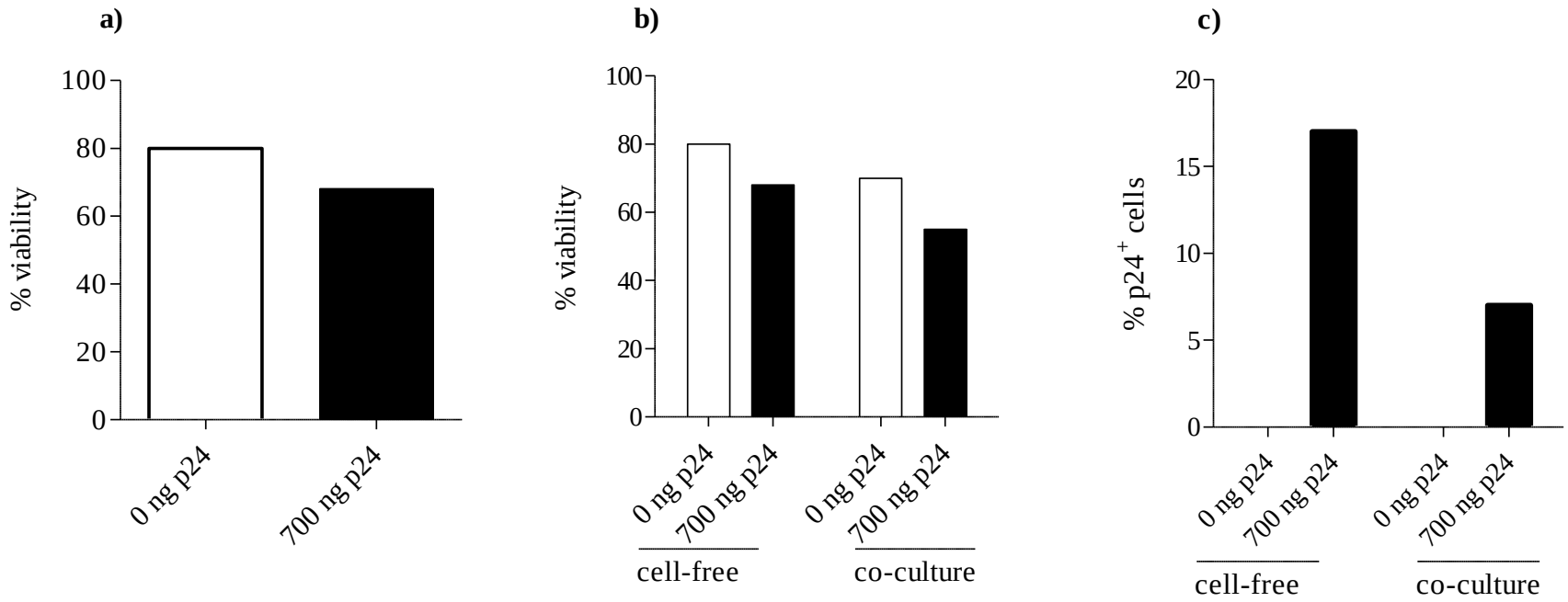

Figure 7.6 Co-culture assay in PBMC

a) viability of donor cell after 48 hr of infection with NL4-3 HIV prior to co-culture with target cells; b) Target cells viability after 48 hrs of co-culture; c) infection rate after co-culture or cell-free infection. White bars=infection with 0 ng p24 input; black bars=infection with 700 ng p24 input. One single experiment.

7.2.3 DISCUSSION

We present preliminary methodological developments for an *in vitro* assay to study cell-to-cell HIV-1 infection, based upon a publication from 2013 that proposed that commonly used antiretrovirals were less effective against cell-to-cell transmission when compared to inhibition of replication of cell free virus. In this previous study two systems were proposed for the cell-to-cell viral infection. One system used engineered cells lines to act as virus donor and target cells, whereas another used HLA-A2 pseudo-typed PBMC.

In the first system, MT4-mCherry cells were used as virus donor cells whereas Rev-CEM cells were used as target cells. We first produced the MT4-mCherry cells by the infection of the MT4 cells with a lentivirus that carries the fluorescent protein. Our data showed that only 3.7% of cells expressed mCherry protein and this result was not consistent with the Sigal paper where the proportion of $mCherry^{+}$ cells was higher at levels >90%. The discrepancy might have derived from different efficiencies of the infection with the lentivirus; we concluded that further optimization of the infection conditions was needed. We then tested the ability of the Rev-CEM to produce GFP upon viral infection. Data produced by flow cytometry showed that 7% of cells expressed GFP at 48 hrs after the infection and that the expression increased over time, in line with one previous study (Wu et al., 2007). Of note, we tested the Rev-CEM cells by microscopy and found that cells showed auto-fluorescence in the red and green channel in absence of any infection. This was not checked or reported by Sigal and colleagues. This finding needs further investigation including testing different fixing and mounting conditions that might affect the photo-bleaching of the slides. From this first set of data we concluded that Rev-CEM efficiently produced GFP upon virus infection at 48 hours after infection and that further optimization was needed for the production of the MT4-mCherry stable cell line.

We further developed the co-culture system by using HLA-A2 negative (donor cells) and positive (target cells) PBMC. We infected donor cells with the recommended viral dose and following assessment of viability we used them to infect the target cells. Results showed that target cells had 17% and 7% infection rate when cells were infected by cell-free virus or co-culture with donor cells, respectively. For the cell-free infection, we obtained higher levels of infection compared to Sigal *et al.*, which had 7.6% of infected cells, whereas cell-to-cell infection showed lower infection rate compared to Sigal *et al.* which obtained 8% of infected cells. Given the limited set of data we could draw limited conclusions; nonetheless we obtained cell-free and cell-to-cell virus transmission in a primary cell system. Further optimization is needed for this assay to be used for further testing.

Chapter 8: General discussion and future directions

Current ART is unable to eradicate HIV that persists in sanctuary sites such as lymphoid organs, and the nervous system as well as in peripheral blood (Sturdevant et al., 2015, Palmer et al., 2008, Chun et al., 2008). This virus reservoir contains a pool of competent viruses that can fuel viral rebound when ART is stopped (Finzi et al., 1997, Finzi et al., 1999, Wong et al., 1997, Alexaki et al., 2008, Chun et al., 1997b). The mechanisms that contribute to maintenance of the viral reservoir are still debated. Some previous studies showed the influence of immunological activation and inflammation (Hatano et al., 2013, Cockerham et al., 2014, Malatinkova et al., 2015), drugs levels (Fletcher et al., 2014), and patient's characteristics such as ethnicity (Keiser et al., 2002, Hodder et al., 2012) on virological outcome and HIV-1 persistence in patients with a wide range of different ART regimens. In this context, I studied the characteristics associated with HIV-1 persistence in blood measured as residual HIV-1 RNA, 2-LTR circular DNA and total HIV-1 DNA in a large population of patients with continuous viral load suppression (HIV-1 RNA<50 copies/ml) without evidence of transient elevations of viremia above 50 HIV-1 RNA copies/ml while on ART with 1NNRTI plus 2NRTIs.

We first studied levels of HIV-1 in plasma and PBMC and we found detection of both HIV-1 DNA and RNA in line with previous studies (Besson et al., 2014, Chomont et al., 2009, Palmer et al., 2008, Kiselinova et al., 2015, Malatinkova et al., 2015). The significance of residual HIV-1 RNA levels in stably suppressed patients is not clearly defined. It is still controversial as to whether detection of low HIV-1 RNA copies reflects ongoing virus replication (Palmer et al., 2008, Maldarelli et al., 2007) in sanctuary sites or if it arises from intermittent viral production which is quickly suppressed by ART (Kiselinova et al., 2015, Fourati et al., 2014). The two mechanisms are not mutually exclusive. Two previous studies showed a positive association between residual HIV-1 DNA and total HIV-1 DNA that could indicate the presence of virus replication in the blood. Conversely, Bailey *et al.* showed that residual HIV-1 RNA is dominated by viral clones that are profoundly unrepresented in peripheral blood cells indicating that an additional source of residual viremia might be present (Bailey

et al., 2006, Eriksson et al., 2013, Lorenzo-Redondo et al., 2016, Fletcher et al., 2014). Our study adds onto this by showing lack of association between residual HIV-1 RNA and levels of total or integrated HIV-1 DNA in PBMC. Our data may support the view that the source of residual HIV-1 RNA could not directly be represented by the viral reservoir contained in the blood.

In the context of the study of factors that may support the virus persistence, the immune system has been identified as a possible player. Previous studies have shown a positive association between cellular total HIV-1 DNA and markers of cellular immune activation in blood of patients with virologic suppression on heterogeneous ART treatments (Cockerham et al., 2014, Hatano et al., 2013). Our results showed a strong positive association between activated CD8 T-cells and both total and integrated HIV-1 DNA in a population of patients on ART with the same NNRTI plus 2 NRTIs. Further to this, residual HIV-1 RNA was not associated with any markers of cellular immune activation in line with previous studies (Hatano et al., 2013), but we found a positive association with plasma levels of sCD27, which is a marker of T cell activation (Lens et al., 1998, Huang et al., 2013). We could propose that similar mechanisms are driving CD8 and CD4 T-cells activation in peripheral blood and possibly reflects activation in lymphoid tissue. HIV-1 infected activated cells may expand in blood resulting in integrated HIV-1 DNA load increase; at the same time, activated cells may drive HIV-1 replication in sanctuary sites (Fletcher et al., 2014, Lorenzo-Redondo et al., 2016) resulting in an indirect association between markers of immune activation and HIV-1 DNA and RNA. In this context, it would be of extreme interest to study levels of soluble and cellular markers of immune activation in lymphoid tissues in relation to HIV-1 replication.

Furthermore it remains to be determined whether circulating CD4 T-cells carry replication competent or incompetent virus (Ananworanich and Mellors, 2015). Events of abortive virus integration following infection can be tracked by studying the unintegrated HIV-1 DNA forms including 2-LTR circular HIV-1 DNA. In our population, only a small proportion of patients showed low levels of 2-LTR circular HIV-1 DNA and this was in line with previous works (Besson et al., 2014, Malatinkova et al., 2015). Additionally, we found no association between 2-LTR circular HIV-1 DNA and any markers of immune activation or virus replication. Of note, 2-LTR

circular HIV-1 DNA was historically defined as a short-live marker of recent replication, but some studies (Agosto et al., 2011, Pace et al., 2013) questioned its stability. Whilst our data may indicate that HIV-1 replication is reduced in peripheral blood confirming viral control by ART, the role and significance of 2-LTR circular HIV-1 DNA during suppressive therapy needs further investigation.

In this thesis, the integrated HIV-1 reservoir load was significantly predicted by the pre-ART viral load which confirms previous studies demonstrating that the viral reservoir is established early after infection and it is stable during ART. In line with this, recent results from the START trial demonstrated that early treatment initiation limits the extent of the viral reservoir and generally improves therapy outcome (Group et al., 2015). Based on these results, it is likely that early treatment initiation will become the standard clinical practice in future to start ART irrespectively of CD4 T-count (Ryom et al., 2016). In this context, the identification of methodological tools capable of ultrasensitive detection of markers of HIV-1 persistence is needed.

The study on patients switching from Atripla to Eviplera that we performed, showed that monitoring residual HIV-1 RNA levels in plasma increases the possibility of detecting virologic rebound during treatment switch; therefore similar approaches could be taken into consideration in intervention strategies. Moreover, we proposed an innovative method to measure integrated HIV-1 DNA reservoir that showed higher sensitivity compared to all previous published assays. Of note, previous assays were not only less sensitive but also relatively expensive given the high number of replicates that was needed for each test to allow quantification. Greater sensitivity could be translated into a cheaper price with the possibility of reducing the number of replicates needed for testing. Furthermore, the assay could be tested with lower DNA input per reaction to reduce the amount of clinical specimen required for the test. The results presented in this thesis are promising and encourage further testing to ensure clinical applicability.

As discussed previously in this dissertation, lymphoid tissues play a central role in maintaining the HIV-1 reservoir supporting viral replication and cell-to-cell virus transmission in the context of sub-optimal drug penetration. Innovative drugs formulation, such as nanomedicines (McDonald et al., 2014, Tatham et al., 2015),

showed improved oral bioavailability. There could be scope to test whether the bioavailability is translated also into improved drug penetration in different tissues. In this scenario, the development of *in vitro* assays will be needed. Our preliminary results validated a set of useful tools that represent the potential starting point for the setting up of such systems.

Appendix 1: Published paper

During stably suppressive antiretroviral therapy integrated HIV-1 DNA load in peripheral blood is associated with the frequency of CD8 cells expressing HLA-DR/DP/DQ

Alessandra Ruggiero, MSc[1], Ward De Spiegelaere, PhD[2], Alessandro Cozzi-Lepri, PhD[3], Maja Kiselinova, MD[2], Georgios Pollakis, PhD[1], Apostolos Beloukas, PhD[1], Linos Vandekerckhove, MD[2], Matthew Strain, PhD[4], Douglas Richman, MD[4], Andrew Phillips, PhD[3], Anna Maria Geretti, MD[1] on behalf of the ERAS Study Group.

[1]Department of Clinical Infection, Microbiology and Immunology (CIMI), Institute of Infection and Global Health (IGH), University of Liverpool, 8 West Derby Street, Liverpool L697BE, United Kingdom; [2]HIV Translational Research Unit, Department of Internal Medicine, Ghent University and University Hospital Ghent, De Pintelaan 1859000, Ghent, Belgium; [3]Department of Infection and Population Health, University College London, Royal Free Campus, Rowland Hill Street, London, NW32PF, United Kingdom; [4]VA San Diego Healthcare System and Center for AIDS Research, University of California San Diego, La Jolla, CA 92093, USA.

STUDY GROUP

Paola Vitiello, Royal Free Hospital, London and The Royal Liverpool Hospital, Liverpool; Nicola Mackie, St Mary's Hospital, London; Jonathan Ainsworth and Anele Waters, North Middlesex Hospital, London; Frank Post, King's College Hospital, London; Simon Edwards, University College Hospital, London; and Julie Fox, St Thomas' Hospital, London, United Kingdom.

Corresponding author details:
Prof Anna Maria Geretti, MD, PhD

Department of Clinical Infection, Microbiology and Immunology, Institute of Infection and Global Health, University of Liverpool, 8 West Derby Street, Liverpool L69 7BE, United Kingdom. Email: geretti@liverpool.ac.uk. Tel: +44 (0)7581486481

Keywords: Suppression; Reservoir; Persistence; Integration; Activation

Running title: Integrated HIV-1 DNA and immune activation

Word count: 3,080

Abstract: 249

Tables: 4

Figures: 1

References: 30

Supplementary Tables: 3

Abbreviation list

HIV-1: Human Immunodeficiency Virus type 1; HIV-1 VL: HIV-1 viral load; ART: Anti-retroviral therapy; HIC: HIV-1 controllers; NNRTI: Non-nucleoside reverse-transcriptase inhibitors; NRTI: nucleoside/nucleotide reverse transcriptase inhibitors; VLS: Viral Load Suppression; PBMC: Peripheral blood mononuclear cells; 2-LTR: 2-long terminal repeats; sCD14: soluble CD14; HLA: Human Leukocyte Antigen; CMV: cytomegalovirus virus; EBV; Epstein-Bar virus; NIHR: National Institute for Health Research; CRN: Clinical Research Network; WHO: World Health Organisation; ELISA: enzyme-linked immune-enzymatic assay; PFA: paraformaldehyde; LPS: lipopolysaccharide; PCR: Polymerase chain reaction

ABSTRACT

Background: Characterising the correlates of HIV persistence improves understanding of disease pathogenesis and guides the design of curative strategies. This study investigated factors associated with integrated HIV-1 DNA load during consistently suppressive first-line antiretroviral therapy (ART).

Method: Total, integrated, and 2-long terminal repeats (LTR) circular HIV-1 DNA, residual plasma HIV-1 RNA, T-cell activation markers, and soluble CD14 (sCD14) were measured in peripheral blood of 50 patients that had received 1-14 years of efavirenz-based or nevirapine-based therapy.

Results: Integrated HIV-1 DNA load (per 10^6 peripheral blood mononuclear cells) was median 1.9 $\log_{10}$ copies (interquartile range 1.7-2.2) and showed a mean difference of 0.2 $\log_{10}$ copies per 10 years of suppressive ART (95% confidence interval -0.2, 0.6; p=0.28). It was positively correlated with total HIV-1 DNA load and frequency of $CD8^+$HLA-DR/DP/DQ^+ cells, and was also higher in subjects with higher sCD14 levels, but showed no correlation with levels of 2-LTR circular HIV-1 DNA and residual plasma HIV-1 RNA, or the frequency of $CD4^+CD38^+$ and $CD8^+CD38^+$ cells. Adjusting for pre-ART viral load, duration of suppressive ART, CD4 cell counts, residual plasma HIV-1 RNA levels, and sCD14 levels, integrated HIV-1 DNA load was mean 0.5 $\log_{10}$ copies higher for each 50% higher frequency of $CD8^+$HLA-DR/DP/DQ^+ cells (95% confidence interval 0.2, 0.9; p=0.01).

Conclusions: The observed positive association between integrated HIV-1 DNA load and frequency of CD8+HLA-DR/DP/DQ+ cells indicates that a close correlation between HIV persistence and immune activation continues during consistently suppressive therapy. The inducers of the distinct activation profile warrant further investigation.

Research into context

Evidence before this study. We searched PubMed for studies describing the relationship between integrated HIV-1 DNA load and markers of immune activation during antiretroviral therapy (ART). The last search was completed in April 2015. The search terms comprised combinations of [HIV, DNA, integrated] plus [CD8, activation, DR, HLA, CD38, CD14]. References cited in the selected papers were searched manually. The published data indicated that integrated HIV-1 DNA load remains constant in peripheral blood of subjects receiving long-term ART. Two studies described a positive association between total HIV-1 DNA load in peripheral blood mononuclear cells (PBMC) and frequency of CD8 cells expressing HLA-DR; one of the two studies also investigated integrated HIV-1 DNA load in relation to $CD8^+HLA\text{-}DR^+$ cells in 19 subjects, with inconsistent results.

Implications of all the available evidence. The mechanisms that prevent the decay of the integrated HIV-1 DNA reservoir during long-term suppressive ART remain unclear. Two main hypotheses are proposed. The first suggests that incomplete therapeutic efficacy allows ongoing virus replication and replenishment of the reservoir. The second hypothesis suggests that proliferation of infected CD4 T-cells causes expansion of integrated HIV-1 DNA, without requiring or leading to virus production. In the second model, factors that promote proliferation of infected CD4 T-cells favour HIV persistence.

Added value of this study. We studied a relatively homogenously treated population that was sampled cross-sectionally in recruitment strata defined by the duration of suppressive ART. Key eligibility criteria were continuation of the initial non-nucleoside reverse transcriptase inhibitor (NNRTI) and consistent plasma HIV-1 RNA suppression <50 copies/ml during follow-up ranging between one and 14 years. Confirming previous observations, integrated HIV-1 DNA load did not differ significantly according to the duration of suppressive ART. Integrated HIV-1 DNA load was also not associated with direct or indirect markers of virus replication, including levels of residual HIV-1 RNA in plasma and 2-long terminal repeats (LTR) circular HIV-1 DNA in PBMC, and frequency of CD4 and CD8 cells expressing the activation marker CD38 in peripheral blood. Rather, there was an independent, positive linear association between integrated HIV-1 DNA load and the frequency of CD8 cells expressing the activation marker HLA-DR/DP/DQ. These cells appear to have

important regulatory and effector function. Our findings add to growing evidence that immune activation sustains the HIV-1 reservoir during long-term suppressive ART.

INTRODUCTION

Early after transmission, HIV establishes a reservoir of replication-competent integrated provirus that resides predominantly within memory CD4 T cells, is unresponsive to antiretroviral therapy (ART), and rapidly fuels resumption of virus replication upon treatment discontinuation (Ruelas and Greene, 2013, Soriano-Sarabia et al., 2014, Siliciano et al., 2003). The mechanisms underlying HIV persistence have not been fully elucidated and proposed models are not mutually exclusive. Continuous replenishment of the reservoir may occur through ongoing virus production (Hatano et al., 2013, Buzon et al., 2010), perhaps in sites where ART penetration or activity is suboptimal (Fletcher et al., 2014). In the absence of virus production, maintenance of the reservoir can also occur through proliferation of latently infected CD4 T-cells, as a possibly key determinant of HIV persistence during ART (Maldarelli et al., 2014, Josefsson et al., 2013, Chomont et al., 2009, Wagner et al., 2014).

HIV replication causes chronic immune activation and inflammation, typically accompanied by an expansion of CD8 T-cells, which improve but rarely resolve with ART (Klatt et al., 2013). Persistent HIV production or partial antigenic expression may drive ongoing immune activation in treated patients. In turn, immune activation can promote T-cell proliferation, HIV transcription, and virus production (Klatt et al., 2013). Furthermore, early in the course of the infection, HIV-induced gut damage allows translocation of gastrointestinal microbial products into the systemic circulation, and the resulting immune activation causes further gut damage, establishing a self-perpetuating cycle that can become independent of virus production (Shan and Siliciano, 2014). Other persistent infections, for example with cytomegalovirus (CMV), have also been linked with ongoing immune activation despite suppressive ART (Gianella et al., 2014).

There are inconsistent data on how markers of immune activation correlate with parameters of HIV persistence during long-term suppressive therapy, possibly a consequence of heterogeneous study populations and measures of HIV persistence, but also a reflection of complex bilateral interactions (Hatano et al., 2013, Chun et al., 2011, Cockerham et al., 2014). There remains a need to characterise this relationship further in order to improve our understanding of HIV pathogenesis and design improved curative strategies. The aim of this study was to investigate factors associated with the

levels of integrated HIV-1 DNA measured in peripheral blood during stably suppressive ART, including the relationship with markers of immune activation. Efforts were taken to minimise heterogeneity of the study population, by exclusively selecting patients who started first-line ART with two nucleoside/nucleotide reverse transcriptase inhibitors (NRTIs) plus one non-nucleoside reverse transcriptase inhibitor (NNRTI), achieved a plasma HIV-1 RNA ("viral") load <50 copies/ml within six months of starting ART, and subsequently showed consistent viral load suppression <50 copies/ml over up to 14 years of continuous treatment on the same NNRTI.

METHODS

Study population

Study subjects were recruited at clinical centres across the United Kingdom (see study group). Eligible patients had started first-line ART with two NRTIs plus efavirenz or nevirapine, achieved viral load suppression <50 copies/ml within six months of starting therapy, and subsequently showed all viral load measurements <50 copies/ml while undergoing ≥2 viral load measurements per year, without transient elevations above 50 copies/ml or treatment interruptions. Changes of the initial NNRTI were not allowed. Changes of the initial NRTI (e.g., for toxicity) were allowed provided they were not associated with a treatment interruption or viral load rebound >50 copies/ml. Recruitment was stratified by duration of ART to range from 1 to over 10 years. The study was approved by National Research Ethics Service (London-Dulwich) and was included in the National Institute for Health Research Clinical Research Network (NIHR CRN) Portfolio. All patients provided written informed consent.

Quantification of residual HIV-1 RNA in plasma

Plasma HIV-1 RNA below 50 copies/ml was quantified using a modified version of the Abbott RealTime HIV-1 assay (Maidenhead, UK), following ultracentrifugation of 8 ml of plasma at 215,000g for 45' at 4^{o}C, and resuspension of the pellet in 1ml of basematrix (SeraCare, USA). Each run included negative, low positive, and high positive controls. Assay sensitivity was determined by spiking HIV-negative plasma with four dilutions of the World Health Organisation (WHO) 3rd International Standard for HIV-1 RNA in triplicate (NIBSC code:10/152, Hertfordshire, UK). The assay 50%

and 95% detection rates for 8 ml input were 1 and 3 HIV-1 RNA copies/ml, respectively.

HIV-1 subtyping

The HIV-1 subtype was determined using polymerase sequences obtain from HIV-1 DNA recovered from PBMC, as previously described (16).

Quantification of total, integrated and 2-LTR circular HIV-1 DNA in peripheral blood mononuclear cells

Total HIV-1 DNA load in peripheral blood mononuclear cells (PBMC) was determined by a quantitative real-time PCR targeting a conserved LTR region as previously described (Geretti et al., 2013). The assay 50% and 95% detection rates were 20 and 40 HIV-1 DNA copies/10^6 PBMC, respectively. Integrated HIV-1 DNA was quantified by repetitive-sampling Alu-PCR as previously described (De Spiegelaere et al., 2014) using the primers shown in Supplementary Table 1. Briefly, 42 replicate Alu-HIV-1 PCR amplifications were performed with gag reverse HIV-1 primer and Alu forward primer for integrated HIV-1 DNA, and 32 replicates with only HIV-1 gag primers for unintegrated HIV-1 DNA. After amplification, the first PCR product was subjected to a nested quantitative PCR targeting the HIV-1 LTR RU5 region. The integrated HIV-1 DNA copy number was calculated according to Poisson's principles with error estimation including the Wilson method (www.integratedhivpcr.ugent.be). Four Alu-HIV positive wells were required as output to allow reliable quantification. 2-LTR circular HIV-1 DNA levels were measured by droplet digital PCR as previously described (Strain et al., 2013); the lower limit of detection was median 5 copies/10^6 PBMC (interquartile range, IQR 4-6).

Markers of immune activation

Cellular markers were measured by staining freshly isolated PBMC with PE or FITC labelled antibodies against CD4 plus either CD26, CD38, or CD69, and against CD8 plus either CD38 or HLA-DR/DP/DQ (Serotec, Oxford, UK; Becton Dickinson, NJ, USA). Cell suspensions were fixed with 1% paraformaldehyde (PFA) prior to acquisition using FACScan and analysis by CellQuest software version 3.3 (Becton Dickinson NJ, USA). Soluble CD14 (sCD14) as a marker of bacterial

lipopolysaccharide (LPS)-induced monocyte/macrophage activation was measured in plasma by enzyme-linked immune-enzymatic assay (ELISA) (R&D System sCD14 ELISA, Abington, UK).

Detection of cytomegalovirus and Epstein-Barr virus DNA

Plasma was tested for CMV and Epstein-Barr Virus (EBV) DNA with a real-time PCR assay targeting the viral UL123/UL55 and p143 regions, respectively. The lower limits of detection were 50 IU/ml for CMV DNA and 100 copies/ml for EBV DNA.

Statistical analysis

Duration of suppressive ART was defined as the length of time following the first viral load measurement <50 copies/ml recorded after starting ART. The characteristics of the study population stratified into two groups based upon duration of suppressive ART, integrated HIV-1 DNA load, or frequency of $CD8^{+}HLA\text{-}DR/DP/DQ^{+}$ cells were compared using non-parametric Wilcoxon and Mann-Witney tests for continuous variables, and the Fisher's exact test for categorical variables. Where the analyses required variables to be expressed in median levels, undetectable HIV-1 RNA results were given an arbitrary midpoint value between zero and the assay 95% detection rate (=1.5 copies/ml), whereas undetectable 2-LTR circular HIV-1 DNA results were assigned a midpoint value between zero and the assay median lower limit of detection (=2.5 copies/10^6 PBMC). Mean differences (with 95% confidence interval, CI) in measured residual plasma HIV-1 RNA, 2-LTR circular HIV-1 DNA, total and integrated HIV-1 DNA, sCD14, and frequency of activated CD4 and CD8 cells over 10 years of suppressive ART were analysed by univariate linear regression analysis after log transformation of the variables. The correlation between integrated HIV-1 DNA load or frequency of $CD8^{+}HLA\text{-}DR/DP/DQ^{+}$ cells and other measured parameters was explored by the Spearman's test. The association between integrated HIV-1 DNA load and other variables was characterised further by univariate and multivariable linear regression modelling. A 'best subset' approach and the Mallow Cp test were used for the selection of variables to be included in the multivariable model. All available variables were initially considered for inclusion, with the exception of gender and NNRTI use (due to predominance of males and efavirenz use: 40/50, 80% for both variables) and total HIV-1 DNA load (due to strong co-linearity with integrated HIV-1 DNA load). Pre-ART viral load (Cp value 3.5), duration of suppressive ART (3.6),

residual plasma HIV-1 RNA load (3.6), frequency of $CD8^{+}HLA\text{-}DR/DP/DQ^{+}$ cells (0.4), and sCD14 levels (1.7) were identified for inclusion in the multivariate model. The CD4 cell count was added to the multivariable model as a possible confounding factor. In a second multivariable model, nadir CD4 count was included instead of pre-ART viral load. A sensitivity analysis was also performed replacing integrated with total HIV-1 DNA as the outcome variable in the same two models. The analyses were performed with SAS 9.4.

RESULTS

Study population

The cohort comprised 50 patients who at the time of sampling were receiving two NRTIs plus either efavirenz (80%) or nevirapine and had a median duration of viral load suppression <50 copies/ml of 6.4 years (Table 1). Patients with duration of suppressive ART above the median of 6.4 years were older and had a lower nadir CD4 cell count, a marginally higher current CD4 cell count, and lower frequencies of CD4 and CD8 cells expressing CD38 relative to subjects with shorter duration. They were also more likely to have experienced changes in the composition of the NRTI backbone after first starting ART. Overall 25/50 patients (50%) changed one or more component of the NRTI backbone, with median 1 drug change per subject (IQR 0-1). At the time of sampling, NRTI backbones were tenofovir/emtricitabine (37/50, 74%), abacavir/lamivudine (10/50, 20%), or zidovudine/lamivudine (3/50, 6%). Residual plasma HIV-1 RNA was detected in 29/50 patients (58%) at levels ranging between 1 and 35 copies/ml, whereas 2-LTR circular HIV-1 DNA was detected in 16/50 patients (32%) at levels ranging between 5 and 35 copies/10^6 PBMC. All subjects had detectable HIV-1 DNA, with total and integrated HIV-1 DNA levels of median 2.6 and 1.9 $\log_{10}$ copies/10^6 PBMC, respectively. None of the patients had detectable CMV DNA in plasma, whereas 3/50 patients (6%) had detectable EBV DNA.

Differences in measured parameters per 10 years of suppressive ART were determined by linear regression analysis of data obtained from the cross-sectional sampling (Table 2). Longer duration of suppressive ART was associated with higher CD4 cell counts and lower levels of CD38 expression on CD4 and CD8 cells. There were also lower 2-LTR circular HIV-1 DNA levels and a trend for lower residual HIV-1 RNA levels. A sub-analysis compared subjects with integrated HIV-1 DNA load either in the lowest quartile (<1.7 $\log_{10}$ copies/10^6 PBMC) or the highest quartile (>2.2 $\log_{10}$ copies/10^6 PBMC) (Table 3). Subsets in the lowest quartile showed significant lower levels of total HIV-1 DNA and sCD14, and lower frequency of $CD8^+$HLA-DR/DP/DQ^+ cells.

Table 1. Characteristics of the study population overall, and stratified by duration of suppressive therapy as below (Group I) or above (Group II) the median of 6.4 years

Characteristic	Total (n=50)	Group I (n=25)	Group II (n=25)	P
Male n (%)	40 (80)	22 (88)	18 (72)	0.29
Age median years (IQR)	46 (40-53)	44 (36-49)	48 (43-55)	0.04
HIV-1 subtype B n (%)	32 (64)	18 (72)	14 (56)	0.38
Nadir CD4 count median cells/mm^3 (IQR)	206 (110-265)	246 (160-292)	176 (97-213)	0.007
Duration of ART median years (IQR)	6.7 (3.4-9.1)	3.4 (2.5-5.0)	9.2 (8.0-10.3)	<0.001
Duration of suppressive ART median years (IQR)[a]	6.4 (3.1-8.8)	3.1 (2.1-4.8)	9.0 (7.7-10.0)	<0.001
Efavirenz as initial NNRTI n (%)	40 (80)	22 (44)	18 (36)	0.29
Changed NRTI backbone n (%)	25 (50)	4 (16)	21 (84)	<0.001
Pre-ART HIV-1 RNA median log_{10} copies/ml (IQR)	5.0 (4.7-5.5)	4.8 (4.5-5.3)	5.1 (4.9-5.6)	0.09
Detectable residual plasma HIV-1 RNA n (%)	29 (58)	15 (60)	14 (56)	1.00
Residual HIV-1 RNA median copies/ml (IQR)[b]	2 (2-4)	2 (2-7)	2 (2-4)	0.33
Detectable 2-LTR circular HIV-1 DNA n (%)	16 (32)	10 (40)	6 (25)	0.36
2-LTR circular HIV-1 DNA median copies/10^6 PBMC (IQR)[c]	3 (3-7)	3 (3-7)	3 (3-5)	0.28
Total HIV-1 DNA median log_{10} copies/10^6 PBMC (IQR)	2.6 (2.3-2.9)	2.6 (2.4-2.9)	2.5 (2.2-2.7)	0.36
Integrated HIV-1 DNA median log_{10} copies/10^6 PBMC (IQR)	1.9 (1.7-2.2)	1.9 (1.7-2.1)	1.8 (1.7-2.4)	0.91
CD4 count median cells/mm^3 (IQR)	572 (478-734)	552 (442-606)	640 (502-794)	0.05
$CD4^+CD26^+$ median percentage (IQR)	54 (43-63)	54 (42-63)	54 (44-63)	0.55
$CD4^+$ $CD38^+$ median percentage (IQR)	22 (17-34)	25 (21-35)	20 (14-24)	0.02
$CD4^+CD69^+$ median percentage (IQR)	2 (1 -2)	1 (1-3)	2 (1-2)	0.48
$CD8^+CD38^+$ median percentage (IQR)	5 (3-7)	6 (3-8)	4 (3-6)	0.04
$CD8^+$HLA-DR/DP/DQ^+ median percentage (IQR)	32 (20-48)	37 (22-53)	30 (16-42)	0.19
sCD14 median μg/ml (IQR)	2.2 (1.8-2.6)	2.0 (1.6-2.6)	2.2 (2.0-2.7)	0.16

[a]Defined as the length of time following the first viral load <50 copies/ml; it ranged between 0.7 and 6.4 years in Group 1, and between 6.4 and 14.4 years in Group II. [b]Samples with undetectable HIV-1 RNA were assigned an arbitrary value of 1.5 copies/ml. [c]Samples with undetectable 2-LTR circular HIV-1 DNA

were assigned an arbitrary value of 2.5 copies/10^6 PBMC. IQR= interquartile range; ART= antiretroviral therapy; NRTI= nucleoside/nucleotide reverse transcriptase inhibitor; NNRTI= non-nucleoside reverse transcriptase inhibitor; PBMC= peripheral blood mononuclear cells; sCD14= soluble CD14.

Table 2. Univariate linear regression analysis of mean difference in log-transformed virological and immunological variables per 10 years of suppressive antiretroviral therapy

Variable[a]	Mean difference	95% CI	P
Residual HIV-1 RNA copies/ml	-0.27	-0.57, 0.03	0.08
2-LTR circular HIV-1 DNA copies/10^6 PBMC	-0.34	-0.59, -0.08	0.01
Total HIV-1 DNA copies/10^6 PBMC	-0.12	-0.56, 0.32	0.60
Integrated HIV-1 DNA copies/10^6 PBMC	0.22	-0.19, 0.62	0.28
CD4 count cells/mm^3	0.14	0.00, 0.27	0.05
$CD4^+CD26^+$ percentage	-0.03	-0.02, 0.10	0.69
$CD4^+CD38^+$ percentage	-0.23	-0.39, -0.07	0.01
$CD4^+CD69^+$ percentage	-0.11	-0.28, 0.07	0.22
$CD8^+CD38^+$ percentage	-0.30	-0.54, -0.07	0.01
$CD8^+$HLA-DR/DP/DQ^+ percentage	-0.15	-0.37, 0.07	0.17
sCD14 μg/ml	0.07	-0.03, 0.16	0.19

[a]Variables in $\log_{10}$. CI= Confidence interval; PBMC= peripheral blood mononuclear cells; sCD14= soluble CD14.

Table 3. Comparative analysis of subjects whose integrated HIV-1 DNA load fell within the lowest or the highest quartile[a]

Characteristic	Lowest quartile (n = 13)	Highest quartile (n = 13)	P
Integrated HIV-1 DNA median log_{10} copies/10^6 PBMC (IQR)	1.4 (1.4-1.6)	2.6 (2.5-2.9)	<0.0001
Male n (%)	9 (70)	11 (84)	0.64
Age median years (IQR)	40 (31-49)	47 (43-53)	0.07
HIV-1 subtype B n (%)	8 (61)	5 (38)	0.43
Nadir CD4 count median cells/mm^3 (IQR)	180 (80-240)	208 (118-260)	0.41
Duration of ART median years (IQR)	6.7 (5.7-8.2)	9.1 (3.0-10.7)	0.29
Duration of suppressive ART median years (IQR)	6.6 (5.7-7.7)	8.9 (2.7-10.6)	0.24
Efavirenz as initial NNRTI n (%)	13 (100)	10 (77)	0.22
Changed NRTI backbone n (%)	8 (61)	5 (38)	0.43
Pre-ART HIV-1 RNA median log_{10} copies/ml (IQR)	4.9 (4.6-5.5)	5.1 (5.0-5.5)	0.26
Detectable residual plasma HIV-1 RNA n (%)	9 (69)	6 (46)	0.43
Residual HIV-1 RNA median copies/ml (IQR)	2 (2-3)	2 (2-5)	0.89
Detectable 2-LTR circular HIV-1 DNA n (%)	4 (31)	6 (46)	0.68
2-LTR circular HIV-1 DNA median copies/10^6 PBMC (IQR)	3 (3-7)	3 (3-7)	0.65
Total HIV-1 DNA median log_{10} copies/10^6 PBMC (IQR)	2.4 (2.1-2.6)	2.8 (2.7-3.0)	0.003
CD4 count median cells/mm^3 (IQR)	721 (552-758)	513 (482-640)	0.25
$CD4^+CD26^+$ median percentage (IQR)	53 (34-60)	54 (44-59)	0.85
$CD4^+$ $CD38^+$ median percentage (IQR)	23 (17-34)	20 (16-24)	0.28
$CD4^+CD69^+$ median percentage (IQR)	2 (1-2)	2 (1-2)	0.64
$CD8^+CD38^+$ median percentage (IQR)	4 (3-7)	3 (2-7)	0.43
$CD8^+$HLA-DR/DP/DQ^+ median percentage (IQR)	24 (16-37)	35 (32-49)	0.01
sCD14 median μg/ml (IQR)	1.8 (1.6-2.3)	2.4 (2.1-2.7)	0.04

[a]Quartile cut-offs= 1.7 and 2.2 $\log_{10}$ copies/10^6 PBMC. PBMC= peripheral blood mononuclear cells; IQR= interquartile range; ART= antiretroviral therapy; NNRTI= non-nucleoside reverse transcriptase inhibitor; sCD14= soluble CD14.

Factors associated with integrated HIV-1 DNA load

Integrated HIV-1 DNA load was positively correlated with total HIV-1 DNA load ($p<0.0001$), frequency of $CD8^+$HLA-DR/DP/DQ^+ cells ($p=0.01$), and sCD14 levels ($p=0.04$), but not with the levels of residual plasma HIV-1 RNA ($p=0.81$) and 2-LTR circular HIV-1 DNA ($p=0.50$), or the frequency of $CD8^+CD38^+$ cells ($p=0.33$) (Fig. 1). The associations were also tested by univariate and multivariable linear regression analysis (Table 4). A first model was built including pre-ART viral load, duration of suppressive ART, CD4 cell counts, residual plasma HIV-1 RNA levels, frequency of $CD8^+$HLA-DR/DP/DQ^+ cells, and sCD14 levels. In this adjusted model, integrated HIV-1 DNA load was a mean of 0.5 $\log_{10}$ copies higher for each 50% increment in the frequency of $CD8^+$HLA-DR/DP/DQ^+ cells (95% CI 0.2, 0.9; $p=0.01$) (Table 4).

The association between integrated HIV-1 DNA load and frequency of $CD8^+$HLA-DR/DP/DQ^+ cells was confirmed in a separate model including the nadir CD4 cell count in place of pre-ART viral load. In this second model integrated HIV-1 DNA load was mean 0.5 $\log_{10}$ copies higher for each 50% increase in the frequency of $CD8^+$HLA-DR/DP/DQ^+ cells (95% CI 0.1, 0.8; $p=0.02$) (Supplementary Table 2). In a sensitivity analysis, integrated HIV-1 DNA was replaced with total HIV-1 DNA in the two multivariable models (Supplementary Table 3). In the model including pre-ART viral load as one of variables, total HIV-1 DNA load was 0.4 $\log_{10}$ copies higher for each 50% increase in the frequency of $CD8^+$HLA-DR/DP/DQ^+ cells (95% CI -0.02, 0.8; $p=0.06$); in the model including the nadir CD4 cell count in place of pre-ART viral load, total HIV-1 DNA load was similarly 0.5 $\log_{10}$ copies higher for each 50% increase in the frequency of $CD8^+$HLA-DR/DP/DQ^+ cells (95% CI -0.1, 0.8; $p=0.12$). We found no evidence that the association between integrated HIV-1 DNA load and frequency of $CD8^+$HLA-DR/DP/DQ^+ cells varied by HIV-1 subtype (B vs. non-B) (not shown).

Table 4. Univariate and multivariable linear regression analysis of factors associated with the mean difference in integrated HIV-1 DNA load[a]

Factor	Univariate			Multivariable		
	Mean difference	95% CI	P	Mean difference	95% CI	P
Age, per 10 years higher	0.11	-0.03, 0.25	0.11			
HIV-1 subtype B vs. non B	0.11	-0.18, 0.39	0.46			
Nadir CD4 count per 100 cell/mm^3 higher	0.06	-0.04, 0.17	0.25			
Duration of suppressive ART per 10 years longer	0.22	-0.19, 0.62	0.28	0.23	-0.20, 0.66	0.30
Changed NRTI backbone yes vs. no	-0.14	-0.41, 0.13	0.30			
Pre-ART HIV-1 RNA per log_{10} copies/ml higher	0.10	-0.08, 0.28	0.27	0.13	-0.05, 0.30	0.15
Residual HIV-1 RNA per log_{10} copies/ml higher	0.20	-0.17, 0.57	0.28	0.27	-0.08, 0.62	0.13
2-LTR circular HIV-1 DNA per log_{10} copies/10^6 PBMC higher	0.04	-0.39, 0.46	0.85			
CD4 count per 100 cells/mm^3 higher	0.03	-0.02, 0.08	0.25	0.02	-0.03, 0.07	0.38
$CD4^+CD26^+$ per 50% higher	0.01	-0.44, 0.47	0.96			
$CD4^+CD38^+$ per 50% higher	-0.78	-2.11, 0.54	0.24			
$CD4^+CD69^+$ per 50% higher	1.02	-5.29, 7.33	0.75			
$CD8^+CD38^+$ per 50% higher	-0.27	-1.22, 0.67	0.57			
$CD8^+$HLA-DR/DP/DQ^+ per 50% higher	0.38	0.02, 0.74	0.04	0.51	0.15, 0.86	0.01
sCD14 per log_{10} μg/ml higher	0.97	-0.14, 2.08	0.09	0.90	-0.16, 1.97	0.10

DISCUSSION

This analysis of subjects receiving first-line NNRTI-based ART demonstrated that integrated HIV-1 DNA load did not differ by duration of suppressive therapy and was positively associated with the frequency of CD8 cells expressing HLA-DR/DP/DQ. Subjects with higher integrated HIV-1 DNA load also had higher levels of sCD14, although the association did not persist in adjusted analyses. While there was a predictable positive correlation with total HIV-1 DNA levels, integrated HIV-1 DNA load did not show a correlation with putative measures of recent HIV-1 replication (residual plasma HIV-1 RNA, 2-LTR circular HIV-1 DNA), or with the frequency of CD4 and CD8 cells expressing CD38.

Previous studies reported that during suppressive ART integrated HIV-1 DNA shows a constant load and little evidence of genetic evolution (Siliciano et al., 2003, von Stockenstrom et al., 2015, Josefsson et al., 2013, Besson et al., 2014). Our study adds to these previous analyses by demonstrating that HIV-1 DNA load did not differ by duration of suppressive therapy in a population with a relatively homogenous treatment history and exact requirements in terms of evidence of plasma viral load suppression <50 copies/ml. There were indications that subjects treated for longer had lower levels of 2-LTR circular HIV-1 DNA and residual plasma HIV-1 RNA, accompanied by a reduction in the frequency of $CD4^+CD38^+$ and $CD8^+CD38^+$ cells, together suggesting that control of virus replication and resolution of immune dysfunction improve with longer duration of therapy. In contrast, the frequency of $CD8^+$HLA-DR/DP/DQ^+ cells was also not related to the duration of suppressive ART and we were able to quantify the association between two key parameters of virus persistence and immune activation, whereby integrated HIV-1 DNA load increased by 0.5 $\log_{10}$ copies/10^6 PBMC for each 50% increase in the frequency of $CD8^+$HLA-DR/DP/DQ^+ cells.

The function of $CD8^+$ cells expressing HLA-DR/DP/DQ^+ remains to be fully elucidated and may include both regulatory and effector functions (Arruvito et al., 2014, Saez-Cirion et al., 2007, Zubkova et al., 2014). In the context of suppressive ART, $CD8^+CD38^-$/HLA-DR^+ cells may be maintained by low-level expression of HIV or, other persistent pathogens, including microbial translocation from the gut. It has been proposed that $CD8^+$ cells expressing HLA-DR without CD38 are preferentially generated in response to low antigenic stimulation and that by retaining good effector

function, may play a role in suppressing HIV replication in elite controllers, as well as clearing hepatitis C infection (Zubkova et al., 2014, Saez-Cirion et al., 2007). It may seem therefore counterintuitive that $CD8^+$HLA-DR/DP/DQ^+ cells should have a positive (rather than inverse) correlation with integrated HIV-1 DNA load. Yet, in line with previous data (4), our adjusted analyses showed a positive association between frequency of $CD8^+$38-HLA-DR/DP/DQ^+ cells and integrated HIV-1 DNA load. Several hypotheses may be proposed to explain the observed positive association. Firstly, low-level HIV production may both stimulate $CD8^+$HLA-DR/DP/DQ^+ cells and continuously replenish the integrated reservoir. Further, $CD8^+$HLA-DR/DP/DQ^+ cells may directly stimulate HIV-infected CD4 cells, causing their proliferation and expansion of the reservoir, which can be measured as increased integrated HIV-1 DNA load (Klatt et al., 2013). Thirdly, a stimulant or multiple stimulants may act simultaneously on $CD8^+$HLA-DR/DP/DQ^+ cells and HIV-infected CD4 cells, resulting in an indirect association between the two parameters.

The population we studied did not overall show evidence of ongoing HIV replication. Patients experienced no viral load rebound >50 copies/ml during follow-up (Doyle et al., 2012). In line with previous studies, just over half had traces of detectable plasma HIV-1 RNA (Palmer et al., 2008), whereas a third had detectable intracellular 2-LTR circular HIV-1 DNA. There was no association however between these two putative markers of recent HIV-1 replication and either integrated HIV-1 DNA load, or the frequency of $CD8^+$HLA-DR/DP/DQ^+ cells (data not shown). While this indicates that HIV production was unlikely, the finding may also reflect insufficient sensitivity of the analytic systems and the limitation of assaying peripheral blood (Cockerham et al., 2014). It will be important to determine the antigenic specificity of $CD8^+$HLA-DR/DP/DQ^+ cells, for example against persistent viruses such as CMV and EBV (Gianella et al., 2014). The two herpes viruses were not commonly detected in our population, which is consistent with containment by effective immune responses. One other aspect that warrants investigation is the relationship with levels of sCD14, which are an important predictor of disease progression and mortality in both treated and untreated patients (Sandler et al., 2011, Marchetti et al., 2011, Hunt et al., 2014). In this study, median sCD14 levels were within the range reported in healthy HIV-negative controls (Sandler et al., 2011). However, patients whose integrated HIV-1 DNA load fell within the highest quartile showed significantly higher sCD14 levels than those

with integrated HIV-1 DNA load in the lowest quartile, a finding that warrants further investigation in larger cohorts.

A strong positive association was measured between total and integrated HIV-1 DNA, supporting the notion that integrated HIV-1 DNA is the most prevalent form of HIV-1 DNA during suppressive ART (Graf and O'Doherty, 2013), and total HIV-1 DNA was associated with the frequency of $CD8^+$HLA-DR/DP/DQ^+ cells. Two previous studies have reported an association between the frequency of CD8 cells expressing HLA-DR and total HIV-1 DNA load in peripheral blood (Cockerham et al., 2014, Hatano et al., 2013). One study was unable to detect a consistent association between the expression of activation markers on CD8 cells and integrated HIV-1 DNA load among 19 subjects (Cockerham et al., 2014). The reasons for the discrepant findings are unclear, and may include a smaller and more heterogeneous study population relative to this cohort, as well as possible differences in the methods to quantify integrated HIV-1 DNA load.

This study has limitations. Parameters were measured cross-sectionally, albeit after stratifying recruitment according to duration of ART, and causality of the observed associations cannot be concluded. Study size limited the number of variables included in the multivariable analysis of factors associated with integrated HIV-1 DNA load, and unmeasured variables may have contributed to the findings. Importantly, the cohort had received NNRTI-based ART exclusively, and findings may not necessarily be extrapolated to other treatment regimens. Further, we measured CD38 and HLA-DR/DP/DQ expression on CD8 cells separately. Unlike the frequency of $CD8^+$HLA-DR/DP/DQ^+ cells however, the frequency of $CD8^+CD38^+$ cells declined with duration of suppressive ART and showed no statistical association with integrated HIV-1 DNA load. Further analyses are needed to confirm the association between integrated HIV-1 DNA load and $CD8^+CD38^-$HLA-DR/DP/DQ^+ cells, characterise the antigenic specificity of $CD8^+$HLA-DR/DP/DQ^+ cells, and determine the direction of causality. Moreover, the data describe CD8 cells expressing HLA-DR/DP/DQ and it will be of interest to study the association between integrated HIV-1 DNA load and individual HLA isotypes. Meanwhile, our data add to growing evidence indicating that a complex interplay between HIV-1 persistence and immune activation continues over many years of stably suppressive ART.

AUTHORS' CONTRIBUTION

AMG and AP designed the study. AMG managed study governance and patient recruitment. AR performed the laboratory work under AMG's supervision and with support from AB, GP, MK, WdS, and LV. MS contributed to the production and analysis of the 2-LTR circular HIV-1 DNA results under DR's supervision. ACL performed the statistical analysis. AMG and AR wrote the manuscript, which was reviewed by all authors. AMG, AB, and AR revised the manuscript with support from ACL. The Eras Study group members contributed to patient recruitment.

ACKNOWLEDGEMENTS

We are grateful to the staff and patients at participating centres for their support and contribution. We thank Dr Giorgio Calisti (while based at the Royal Free Hospital in London and the Institute of Infection and Global Health in Liverpool) for assistance with recruitment; Dr Mark Hopkins (Liverpool Specialist Virology Centre, Royal Liverpool University Hospital) for performing the CMV and EBV DNA assays; and Mr Stephen Lada (VA San Diego Healthcare System and Center for AIDS Research, University of California San Diego) for performing the 2-LTR circular HIV-1 DNA assays.

FUNDING

The study was supported by research awards from the European AIDS Treatment Network (NEAT), the British HIV Association, the Collaborator for AIDS Research on Eradication (CARE; U19 AI096113), the UCSD CFAR (AI306214), the Department of Veterans Affairs, and the James B. Pendleton Charitable Trust. The funding sources had no role in the writing of the manuscript or the decision to submit for publication. The corresponding author (AMG) had full access to all the data in the study and had the final responsibility for the decision to submit for publication.

The authors have no conflict of interest to declare.

REFERENCES

1. Ruelas DS, Greene WC. An integrated overview of HIV-1 latency. Cell. 2013;155:519-29.

2. Soriano-Sarabia N, Bateson RE, Dahl NP, Crooks AM, Kuruc JD, Margolis DM, et al. Quantitation of replication-competent HIV-1 in populations of resting CD4+ T cells. J Virol. 2014;88:14070-7.

3. Siliciano JD, Kajdas J, Finzi D, Quinn TC, Chadwick K, Margolick JB, et al. Long-term follow-up studies confirm the stability of the latent reservoir for HIV-1 in resting CD4+ T cells. Nat Med. 2003;9:727-8.

4. Hatano H, Jain V, Hunt PW, Lee TH, Sinclair E, Do TD, et al. Cell-based measures of viral persistence are associated with immune activation and programmed cell death protein 1 (PD-1)-expressing CD4+ T cells. J Infect Dis. 2013;208:50-6.

5. Buzon MJ, Massanella M, Llibre JM, Esteve A, Dahl V, Puertas MC, et al. HIV-1 replication and immune dynamics are affected by raltegravir intensification of HAART-suppressed subjects. Nat Med. 2010;16:460-5.

6. Fletcher CV, Staskus K, Wietgrefe SW, Rothenberger M, Reilly C, Chipman JG, et al. Persistent HIV-1 replication is associated with lower antiretroviral drug concentrations in lymphatic tissues. Proc Natl Acad Sci U S A. 2014;111:2307-12.

7. Maldarelli F, Wu X, Su L, Simonetti FR, Shao W, Hill S, et al. HIV latency. Specific HIV integration sites are linked to clonal expansion and persistence of infected cells. Science. 2014;345:179-83.

8. Josefsson L, von Stockenstrom S, Faria NR, Sinclair E, Bacchetti P, Killian M, et al. The HIV-1 reservoir in eight patients on long-term suppressive antiretroviral therapy is stable with few genetic changes over time. Proc Natl Acad Sci U S A. 2013;110:E4987-96.

9. Chomont N, El-Far M, Ancuta P, Trautmann L, Procopio FA, Yassine-Diab B, et al. HIV reservoir size and persistence are driven by T cell survival and homeostatic proliferation. Nat Med. 2009;15:893-900.

10. Wagner TA, McLaughlin S, Garg K, Cheung CY, Larsen BB, Styrchak S, et al. HIV latency. Proliferation of cells with HIV integrated into cancer genes contributes to persistent infection. Science. 2014;345:570-3.

11. Klatt NR, Chomont N, Douek DC, Deeks SG. Immune activation and HIV persistence: implications for curative approaches to HIV infection. Immunol Rev. 2013;254:326-42.

12. Shan L, Siliciano RF. Unraveling the relationship between microbial translocation and systemic immune activation in HIV infection. J Clin Invest. 2014;124:2368-71.
13. Gianella S, Massanella M, Richman DD, Little SJ, Spina CA, Vargas MV, et al. Cytomegalovirus replication in semen is associated with higher levels of proviral HIV DNA and CD4+ T cell activation during antiretroviral treatment. J Virol. 2014;88:7818-27.
14. Chun TW, Murray D, Justement JS, Hallahan CW, Moir S, Kovacs C, et al. Relationship between residual plasma viremia and the size of HIV proviral DNA reservoirs in infected individuals receiving effective antiretroviral therapy. J Infect Dis 2011;204:135-8.
15. Cockerham LR, Siliciano JD, Sinclair E, O'Doherty U, Palmer S, Yukl SA, et al. CD4+ and CD8+ T cell activation are associated with HIV DNA in resting CD4+ T cells. PloS One. 2014;9:e110731.
16. Geretti AM, Conibear T, Hill A, Johnson JA, Tambuyzer L, Thys K, Vingerhoets J, Van Delft Y; SENSE Study Group. Sensitive testing of plasma HIV-1 RNA and Sanger sequencing of cellular HIV-1 DNA for the detection of drug resistance prior to starting first-line antiretroviral therapy with etravirine or efavirenz. J Antimicrob Chemother. 2014;69:1090-7.
17. Geretti AM, Arribas JR, Lathouwers E, Foster GM, Yakoob R, Kinloch S, et al. Dynamics of cellular HIV-1 DNA levels over 144 weeks of darunavir/ritonavir monotherapy versus triple therapy in the MONET trial. HIV Clin Trials. 2013;14:45-50.
18. De Spiegelaere W, Malatinkova E, Lynch L, Van Nieuwerburgh F, Messiaen P, O'Doherty U, et al. Quantification of integrated HIV DNA by repetitive-sampling Alu-HIV PCR on the basis of Poisson statistics. Clin Chemistry. 2014;60:886-95.
19. Strain MC, Lada SM, Luong T, Rought SE, Gianella S, Terry VH, et al. Highly precise measurement of HIV DNA by droplet digital PCR. PloS One. 2013;8:e55943.
20. von Stockenstrom S, Odevall L, Lee E, Sinclair E, Bacchetti P, Killian M, et al. Longitudinal genetic characterization reveals that cell proliferation maintains a persistent HIV type 1 DNA pool during effective HIV therapy. J Infect Dis. 2015. Feb 23. [Epub ahead of print]
21. Besson GJ, Lalama CM, Bosch RJ, Gandhi RT, Bedison MA, Aga E, et al. HIV-1 DNA decay dynamics in blood during more than a decade of suppressive antiretroviral therapy. Clin Infect Dis. 2014;59:1312-21.

22. Arruvito L, Payaslian F, Baz P, Podhorzer A, Billordo A, Pandolfi J, et al. Identification and clinical relevance of naturally occurring human CD8+HLA-DR+ regulatory T cells. J Immunol. 2014;193:4469-76.
23. Saez-Cirion A, Lacabaratz C, Lambotte O, Versmisse P, Urrutia A, Boufassa F, et al. HIV controllers exhibit potent CD8 T cell capacity to suppress HIV infection ex vivo and peculiar cytotoxic T lymphocyte activation phenotype. Proc Natl Acad Sci U S A. 2007;104:6776-81.
24. Zubkova I, Duan H, Wells F, Mostowski H, Chang E, Pirollo K, et al. Hepatitis C virus clearance correlates with HLA-DR expression on proliferating CD8+ T cells in immune-primed chimpanzees. Hepatology. 2014;59:803-13.
25. Doyle T, Smith C, Vitiello P, Cambiano V, Johnson M, Owen A, et al. Plasma HIV-1 RNA detection below 50 copies/ml and risk of virologic rebound in patients receiving highly active antiretroviral therapy. Clin Infect Dis. 2012;54:724-32.
26. Palmer S, Maldarelli F, Wiegand A, Bernstein B, Hanna GJ, Brun SC, et al. Low-level viremia persists for at least 7 years in patients on suppressive antiretroviral therapy. Proc Natl Acad Sci U S A. 2008;105:3879-84.
27. Sandler NG, Wand H, Roque A, Law M, Nason MC, Nixon DE, et al. Plasma levels of soluble CD14 independently predict mortality in HIV infection. J Infect Dis. 2011;203:780-90.
28. Marchetti G, Cozzi-Lepri A, Merlini E, Bellistri GM, Castagna A, Galli M, et al. Microbial translocation predicts disease progression of HIV-infected antiretroviral-naive patients with high CD4+ cell count. AIDS. 2011;25:1385-94.
29. Hunt PW, Sinclair E, Rodriguez B, Shive C, Clagett B, Funderburg N, et al. Gut epithelial barrier dysfunction and innate immune activation predict mortality in treated HIV infection. J Infect Dis. 2014;210:1228-38.
30. Graf EH, O'Doherty U. Quantitation of integrated proviral DNA in viral reservoirs. Curr Opin HIV AIDS. 2013;8:100-5.

LEGEND TO FIGURE 1

Figure 1. Correlation between integrated HIV-1 DNA load and a) total HIV-1 DNA load, b) residual plasma HIV-1 RNA levels, c) 2-LTR circular HIV-1 DNA levels, d) frequency of $CD8^+HLA\text{-}DR/DP/DQ^+$ cells, e) frequency of $CD8^+CD38^+$ cells, and f) levels of sCD14. Scatter plots with predicted HIV-1 DNA by the fitted fractional polynomial curves (with 95% confidence interval) and Spearman's rho (with p values) are shown.

Fig. 1

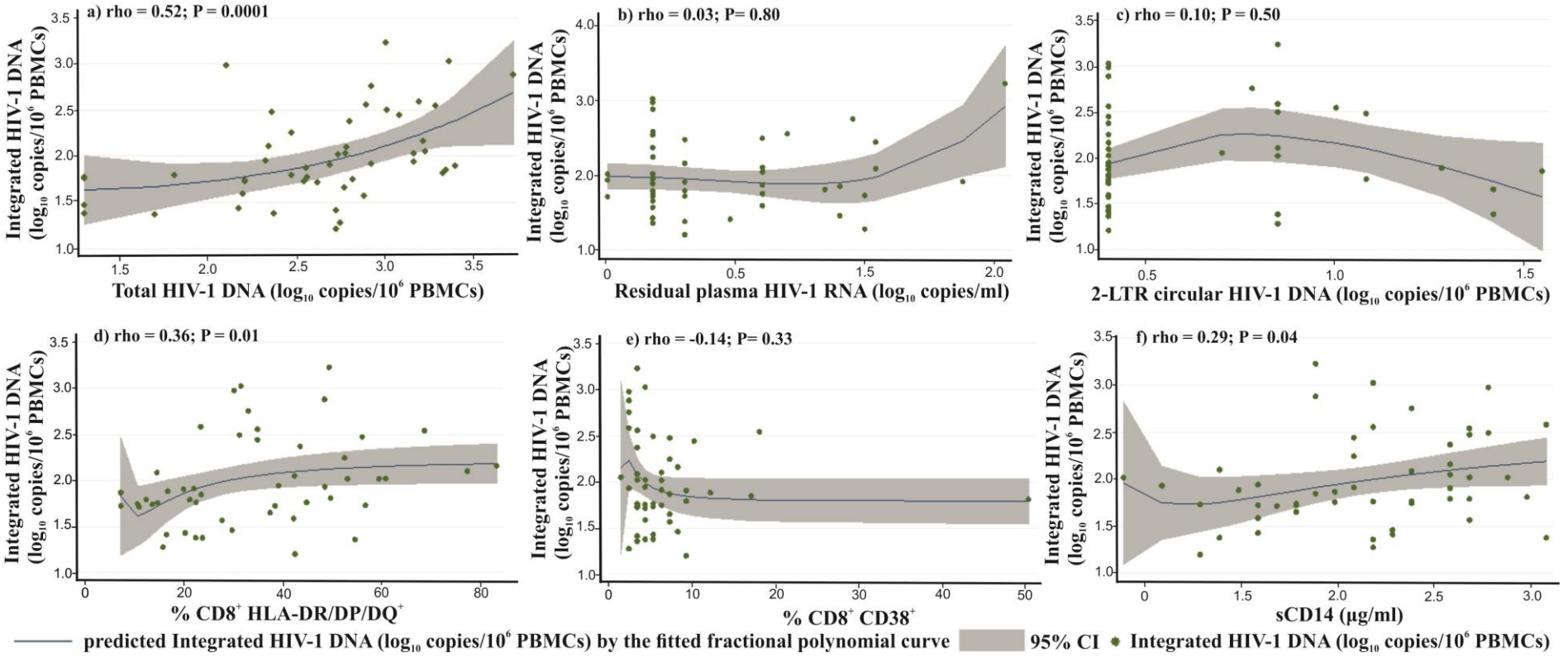
a) rho = 0.52; P = 0.0001
b) rho = 0.03; P= 0.80
c) rho = 0.10; P = 0.50
d) rho = 0.36; P = 0.01
e) rho = -0.14; P= 0.33
f) rho = 0.29; P = 0.04
Integrated HIV-1 DNA (log10 copies/10^6 PBMCs)
Total HIV-1 DNA (log10 copies/10^6 PBMCs)
Residual plasma HIV-1 RNA (log10 copies/ml)
2-LTR circular HIV-1 DNA (log10 copies/10^6 PBMCs)
% CD8+ HLA-DR/DP/DQ+
% CD8+ CD38+
sCD14 (µg/ml)
predicted Integrated HIV-1 DNA (log10 copies/10^6 PBMCs) by the fitted fractional polynomial curve
95% CI
Integrated HIV-1 DNA (log10 copies/10^6 PBMCs)

Supplementary Table 1. Primers used in the integrated HIV-1 DNA assay

	Target	Primer sequence (5' – 3')
PCR 1	Human Alu (sense)	GCCTCCCAAAGTGCTGGGATTACAG
	HIV-1 gag (anti-sense)	GTTCCTGCTATGTCACTTCC
PCR2	HIV-1 RU5 (sense)	TTAAGCCTCAATAAAGCTTGCC
	HIV-1 RU5 (anti-sense)	GTTCGGGCGCCACTGCTAGA
	HIV-1 RU5 (probe)	FAM/CCAGAGTCA/ZEN/CACAACAGACGGGCACA/3IABKFQ/

Supplementary Table 2. Multivariable linear regression analysis of factors associated with the mean difference in integrated HIV -1 DNA load over 10 years of suppressive antiretroviral therapy in a model including nadir CD4 cell count

Factor	Mean difference[a]	95% CI	P
Nadir CD4 count per 100 cell/mm^3 higher	0.04	-0.09, 0.16	0.55
CD4 count per 100 cells/mm^3 higher	0.01	-0.04, 0.06	0.60
Duration of suppressive ART per 10 years longer	0.37	-0.12, 0.86	0.13
Residual HIV-1 RNA per $\log_{10}$ copies/ml higher	0.26	-0.10, 0.62	0.15
$CD8^+$HLA-DR/DP/DQ^+ per 50% higher	0.45	0.08, 0.82	0.02
sCD14 per $\log_{10}$ µg/ml higher	0.76	-0.40, 1.92	0.19

[a]Mean difference in integrated HIV-1 DNA in $\log_{10}$ copies/10^6 PBMC. PBMC= peripheral blood mononuclear cells; ART= antiretroviral therapy.

Supplementary Table 3. Sensitivity analysis replacing integrated with total HIV-1 DNA in the two multivariable models[a].

	Model 1			Model 2		
Factor	**Mean difference**	**95% CI**	**P**	**Mean difference**	**95% CI**	**P**
Nadir CD4 count per 100 cell/mm^3 higher	-	-	-	-0.02	-0.16, 0.13	0.83
CD4 count per 100 cells/mm^3 higher	-0.02	-0.08, 0.04	0.53	-0.02	-0.09, 0.04	0.43
Duration of suppressive ART per 10 years longer	-0.12	-0.62, 0.39	0.65	-0.01	-0.60, 0.58	0.98
Pre-ART HIV-1 RNA per $\log_{10}$copies/ml higher	0.23	0.03, 0.43	0.03	-	-	-
Residual HIV-1 RNA per $\log_{10}$ copies/ml	0.14	-0.26, 0.55	0.48	0.14	-0.30, 0.57	0.53
$CD8^+$HLA-DR/DP/DQ^+ per 50% higher	0.39	-0.02, 0.80	0.06	0.35	-0.09, 0.80	0.12
sCD14 per $\log_{10}$ µg/ml higher	0.56	-0.68, 1.78	0.37	0.57	-0.83, 1.97	0.41

[a]Mean difference in $\log_{10}$ copies/10^6 PBMC. Model 1 included pre-ART viral load; model 2 replaced pre-ART viral load with nadir CD4 cell count. PBMC: peripheral blood mononuclear cells; ART: antiretroviral therapy.

BIBLIOGRAPHY

AGOSTO, L. M., LISZEWSKI, M. K., MEXAS, A., GRAF, E., PACE, M., YU, J. J., BHANDOOLA, A. & O'DOHERTY, U. 2011. Patients on HAART often have an excess of unintegrated HIV DNA: implications for monitoring reservoirs. *Virology,* 409**,** 46-53.

AGOSTO, L. M., UCHIL, P. D. & MOTHES, W. 2015. HIV cell-to-cell transmission: effects on pathogenesis and antiretroviral therapy. *Trends Microbiol,* 23**,** 289-95.

ALEXAKI, A., LIU, Y. & WIGDAHL, B. 2008. Cellular reservoirs of HIV-1 and their role in viral persistence. *Curr HIV Res,* 6**,** 388-400.

ALIMONTI, J. B., BALL, T. B. & FOWKE, K. R. 2003. Mechanisms of CD4+ T lymphocyte cell death in human immunodeficiency virus infection and AIDS. *J Gen Virol,* 84**,** 1649-61.

ALVAREZ ESTEVEZ, M., CHUECA PORCUNA, N., GUILLOT SUAY, V., PENA MONGE, A., GARCIA GARCIA, F., MUNOZ MEDINA, L., VINUESA GARCIA, D., PARRA RUIZ, J., HERNANDEZ-QUERO, J. & GARCIA GARCIA, F. 2013. Quantification of viral loads lower than 50 copies per milliliter by use of the Cobas AmpliPrep/Cobas TaqMan HIV-1 test, version 2.0, can predict the likelihood of subsequent virological rebound to >50 copies per milliliter. *J Clin Microbiol,* 51**,** 1555-7.

ALVAREZ, R. A., BARRIA, M. I. & CHEN, B. K. 2014. Unique features of HIV-1 spread through T cell virological synapses. *PLoS Pathog,* 10**,** e1004513.

AMBROSE, Z. & AIKEN, C. 2014. HIV-1 uncoating: connection to nuclear entry and regulation by host proteins. *Virology,* 454-455**,** 371-9.

AMENDOLA, A., BLOISI, M., MARSELLA, P., SABATINI, R., BIBBO, A., ANGELETTI, C. & CAPOBIANCHI, M. R. 2011. Standardization and performance evaluation of "modified" and "ultrasensitive" versions of the Abbott RealTime HIV-1 assay, adapted to quantify minimal residual viremia. *J Clin Virol,* 52**,** 17-22.

ANANWORANICH, J. & MELLORS, J. W. 2015. How Much HIV is Alive? The Challenge of Measuring Replication Competent HIV for HIV Cure Research. *EBioMedicine,* 2**,** 788-9.

ARRUVITO, L., PAYASLIAN, F., BAZ, P., PODHORZER, A., BILLORDO, A., PANDOLFI, J., SEMENIUK, G., ARRIBALZAGA, E. & FAINBOIM, L. 2014. Identification and clinical relevance of naturally occurring human CD8+HLA-DR+ regulatory T cells. *J Immunol,* 193**,** 4469-76.

ASBOE, D., AITKEN, C., BOFFITO, M., BOOTH, C., CANE, P., FAKOYA, A., GERETTI, A. M., KELLEHER, P., MACKIE, N., MUIR, D., MURPHY, G., ORKIN, C., POST, F., ROONEY, G., SABIN, C., SHERR, L., SMIT, E., TONG, W., USTIANOWSKI, A., VALAPPIL, M., WALSH, J., WILLIAMS, M., YIRRELL, D. & SUBCOMMITTEE, B. G. 2012. British HIV Association guidelines for the routine investigation and monitoring of adult HIV-1-infected individuals 2011. *HIV Med,* 13**,** 1-44.

AVETTAND-FENOEL, V., CHAIX, M. L., BLANCHE, S., BURGARD, M., FLOCH, C., TOURE, K., ALLEMON, M. C., WARSZAWSKI, J., ROUZIOUX, C. & FRENCH PEDIATRIC COHORT STUDY, A.-C. O. G. 2009. LTR real-time PCR for HIV-1 DNA quantitation in blood cells for early diagnosis in infants born to seropositive mothers treated in HAART area (ANRS CO 01). *J Med Virol,* 81**,** 217-23.

BAILEY, J. R., SEDAGHAT, A. R., KIEFFER, T., BRENNAN, T., LEE, P. K., WIND-ROTOLO, M., HAGGERTY, C. M., KAMIREDDI, A. R., LIU, Y., LEE, J., PERSAUD, D., GALLANT, J. E., COFRANCESCO, J., JR., QUINN, T. C., WILKE, C. O., RAY, S. C., SILICIANO, J. D., NETTLES, R. E. & SILICIANO, R. F. 2006. Residual human immunodeficiency virus type 1 viremia in some patients on antiretroviral therapy is dominated by a small number of invariant clones rarely found in circulating CD4+ T cells. *J Virol,* 80**,** 6441-57.

BARRE-SINOUSSI, F. 1996. HIV as the cause of AIDS. *Lancet,* 348**,** 31-5.

BARRE-SINOUSSI, F., CHERMANN, J. C., REY, F., NUGEYRE, M. T., CHAMARET, S., GRUEST, J., DAUGUET, C., AXLER-BLIN, C., VEZINET-BRUN, F., ROUZIOUX, C., ROZENBAUM, W. & MONTAGNIER, L. 1983. Isolation of a T-lymphotropic retrovirus from a patient at risk for acquired immune deficiency syndrome (AIDS). *Science,* 220**,** 868-71.

BESSON, G. J., LALAMA, C. M., BOSCH, R. J., GANDHI, R. T., BEDISON, M. A., AGA, E., RIDDLER, S. A., MCMAHON, D. K., HONG, F. & MELLORS, J. W. 2014. HIV-1 DNA decay dynamics in blood during more than a decade of suppressive antiretroviral therapy. *Clin Infect Dis,* 59**,** 1312-21.

BOFFITO, M., JACKSON, A., LAMORDE, M., BACK, D., WATSON, V., TAYLOR, J., WATERS, L., ASBOE, D., GAZZARD, B. & POZNIAK, A. 2009. Pharmacokinetics and safety of etravirine administered once or twice daily after 2 weeks treatment with efavirenz in healthy volunteers. *J Acquir Immune Defic Syndr,* 52**,** 222-7.

BORROW, P., LEWICKI, H., HAHN, B. H., SHAW, G. M. & OLDSTONE, M. B. 1994. Virus-specific CD8+ cytotoxic T-lymphocyte activity associated with control of viremia in primary human immunodeficiency virus type 1 infection. *J Virol,* 68**,** 6103-10.

BOSQUE, A., FAMIGLIETTI, M., WEYRICH, A. S., GOULSTON, C. & PLANELLES, V. 2011. Homeostatic proliferation fails to efficiently reactivate HIV-1 latently infected central memory CD4+ T cells. *PLoS Pathog,* 7**,** e1002288.

BOYMAN, O., PURTON, J. F., SURH, C. D. & SPRENT, J. 2007. Cytokines and T-cell homeostasis. *Curr Opin Immunol,* 19**,** 320-6.

BRADY, T., KELLY, B. J., MALE, F., ROTH, S., BAILEY, A., MALANI, N., GIJSBERS, R., O'DOHERTY, U. & BUSHMAN, F. D. 2013. Quantitation of HIV DNA integration: effects of differential integration site distributions on Alu-PCR assays. *J Virol Methods,* 189**,** 53-7.

BRENCHLEY, J. M., SCHACKER, T. W., RUFF, L. E., PRICE, D. A., TAYLOR, J. H., BEILMAN, G. J., NGUYEN, P. L., KHORUTS, A., LARSON, M., HAASE, A. T. & DOUEK, D. C. 2004. CD4+ T cell depletion during all stages of HIV disease occurs predominantly in the gastrointestinal tract. *J Exp Med,* 200**,** 749-59.

BRIEU, N., PORTALES, P., CARLES, M. J. & CORBEAU, P. 2011. Interleukin-7 induces HIV type 1 R5-to-X4 switch. *Blood,* 117**,** 2073-4.

BROSTROM, C., SONNERBORG, A., LINDBACK, S. & GAINES, H. 1998. Low relative frequencies of CD26(+) CD4(+) cells in long-term nonprogressing human immunodeficiency virus type 1-infected subjects. *Clin Diagn Lab Immunol,* 5**,** 662-6.

BRUSSEL, A., DELELIS, O. & SONIGO, P. 2005. Alu-LTR real-time nested PCR assay for quantifying integrated HIV-1 DNA. *Methods Mol Biol,* 304**,** 139-54.

BUSTIN, S. A., BENES, V., GARSON, J. A., HELLEMANS, J., HUGGETT, J., KUBISTA, M., MUELLER, R., NOLAN, T., PFAFFL, M. W., SHIPLEY, G. L., VANDESOMPELE, J. & WITTWER, C. T. 2009. The MIQE guidelines: minimum information for publication of quantitative real-time PCR experiments. *Clin Chem,* 55**,** 611-22.

BUTLER, S. L., JOHNSON, E. P. & BUSHMAN, F. D. 2002. Human immunodeficiency virus cDNA metabolism: notable stability of two-long terminal repeat circles. *J Virol,* 76**,** 3739-47.

BUZON, M. J., MARTIN-GAYO, E., PEREYRA, F., OUYANG, Z., SUN, H., LI, J. Z., PIOVOSO, M., SHAW, A., DALMAU, J., ZANGGER, N., MARTINEZ-PICADO, J., ZURAKOWSKI, R., YU, X. G., TELENTI, A., WALKER, B. D., ROSENBERG, E. S. & LICHTERFELD, M. 2014a. Long-term antiretroviral treatment initiated at primary HIV-1 infection affects the size, composition, and decay kinetics of the reservoir of HIV-1-infected CD4 T cells. *J Virol,* 88**,** 10056-65.

BUZON, M. J., MASSANELLA, M., LLIBRE, J. M., ESTEVE, A., DAHL, V., PUERTAS, M. C., GATELL, J. M., DOMINGO, P., PAREDES, R., SHARKEY, M., PALMER, S., STEVENSON, M., CLOTET, B., BLANCO, J. & MARTINEZ-PICADO, J. 2010. HIV-1 replication and immune dynamics are affected by raltegravir intensification of HAART-suppressed subjects. *Nat Med,* 16**,** 460-5.

BUZON, M. J., SUN, H., LI, C., SHAW, A., SEISS, K., OUYANG, Z., MARTIN-GAYO, E., LENG, J., HENRICH, T. J., LI, J. Z., PEREYRA, F., ZURAKOWSKI, R., WALKER, B. D., ROSENBERG, E. S., YU, X. G. & LICHTERFELD, M. 2014b. HIV-1 persistence in CD4+ T cells with stem cell-like properties. *Nat Med,* 20**,** 139-42.

CANESTRI, A., LESCURE, F. X., JAUREGUIBERRY, S., MOULIGNIER, A., AMIEL, C., MARCELIN, A. G., PEYTAVIN, G., TUBIANA, R., PIALOUX, G. & KATLAMA, C. 2010. Discordance between cerebral spinal fluid and plasma HIV replication in patients with neurological symptoms who are receiving suppressive antiretroviral therapy. *Clin Infect Dis,* 50**,** 773-8.

CARBONE, J., GIL, J., BENITO, J. M. & FERNANDEZ-CRUZ, E. 2003. Decreased expression of activation markers on CD4 T lymphocytes of HIV-infected long-term non-progressors. *AIDS,* 17**,** 133-4.

CASSETTI, I., MADRUGA, J. V., SULEIMAN, J. M., ETZEL, A., ZHONG, L., CHENG, A. K., ENEJOSA, J. & STUDY, E. T. 2007. The safety and efficacy of tenofovir DF in combination with lamivudine and efavirenz through 6 years in antiretroviral-naive HIV-1-infected patients. *HIV Clin Trials,* 8**,** 164-72.

CENTERS FOR DISEASE, C. 1981. Pneumocystis pneumonia--Los Angeles. *MMWR Morb Mortal Wkly Rep,* 30**,** 250-2.

CHAVEZ, L., CALVANESE, V. & VERDIN, E. 2015. HIV Latency Is Established Directly and Early in Both Resting and Activated Primary CD4 T Cells. *PLoS Pathog,* 11**,** e1004955.

CHOMONT, N., EL-FAR, M., ANCUTA, P., TRAUTMANN, L., PROCOPIO, F. A., YASSINE-DIAB, B., BOUCHER, G., BOULASSEL, M. R., GHATTAS, G., BRENCHLEY, J. M., SCHACKER, T. W., HILL, B. J., DOUEK, D. C., ROUTY, J. P., HADDAD, E. K. & SEKALY, R. P. 2009. HIV reservoir size and persistence are driven by T cell survival and homeostatic proliferation. *Nat Med,* 15**,** 893-900.

CHOMONT, N., HOCINI, H., GODY, J. C., BOUHLAL, H., BECQUART, P., KRIEF-BOUILLET, C., KAZATCHKINE, M. & BELEC, L. 2008. Neutralizing monoclonal antibodies to human immunodeficiency virus type 1 do not inhibit viral transcytosis through mucosal epithelial cells. *Virology,* 370**,** 246-54.

CHUN, T. W. 2013. Tracking replication-competent HIV reservoirs in infected individuals. *Curr Opin HIV AIDS,* 8**,** 111-6.

CHUN, T. W., CARRUTH, L., FINZI, D., SHEN, X., DIGIUSEPPE, J. A., TAYLOR, H., HERMANKOVA, M., CHADWICK, K., MARGOLICK, J., QUINN, T. C., KUO, Y. H., BROOKMEYER, R., ZEIGER, M. A., BARDITCH-CROVO, P. & SILICIANO, R. F. 1997a. Quantification of latent tissue reservoirs and total body viral load in HIV-1 infection. *Nature,* 387**,** 183-8.

CHUN, T. W., FINZI, D., MARGOLICK, J., CHADWICK, K., SCHWARTZ, D. & SILICIANO, R. F. 1995. In vivo fate of HIV-1-infected T cells: quantitative analysis of the transition to stable latency. *Nat Med,* 1**,** 1284-90.

CHUN, T. W., JUSTEMENT, J. S., MOIR, S., HALLAHAN, C. W., MAENZA, J., MULLINS, J. I., COLLIER, A. C., COREY, L. & FAUCI, A. S. 2007. Decay of the HIV reservoir in patients receiving antiretroviral therapy for extended periods: implications for eradication of virus. *J Infect Dis,* 195**,** 1762-4.

CHUN, T. W., MOIR, S. & FAUCI, A. S. 2015. HIV reservoirs as obstacles and opportunities for an HIV cure. *Nat Immunol,* 16**,** 584-9.

CHUN, T. W., MURRAY, D., JUSTEMENT, J. S., HALLAHAN, C. W., MOIR, S., KOVACS, C. & FAUCI, A. S. 2011. Relationship between residual plasma viremia and the size of HIV proviral DNA reservoirs in infected individuals receiving effective antiretroviral therapy. *J Infect Dis,* 204**,** 135-8.

CHUN, T. W., NICKLE, D. C., JUSTEMENT, J. S., LARGE, D., SEMERJIAN, A., CURLIN, M. E., O'SHEA, M. A., HALLAHAN, C. W., DAUCHER, M., WARD, D. J., MOIR, S., MULLINS, J. I., KOVACS, C. & FAUCI, A. S. 2005. HIV-infected individuals receiving effective antiviral therapy for extended periods of time continually replenish their viral reservoir. *J Clin Invest,* 115**,** 3250-5.

CHUN, T. W., NICKLE, D. C., JUSTEMENT, J. S., MEYERS, J. H., ROBY, G., HALLAHAN, C. W., KOTTILIL, S., MOIR, S., MICAN, J. M., MULLINS, J. I., WARD, D. J., KOVACS, J. A., MANNON, P. J. & FAUCI, A. S. 2008. Persistence of HIV in gut-associated lymphoid tissue despite long-term antiretroviral therapy. *J Infect Dis,* 197**,** 714-20.

CHUN, T. W., STUYVER, L., MIZELL, S. B., EHLER, L. A., MICAN, J. A., BASELER, M., LLOYD, A. L., NOWAK, M. A. & FAUCI, A. S. 1997b. Presence of an inducible HIV-1 latent reservoir during highly active antiretroviral therapy. *Proc Natl Acad Sci U S A,* 94**,** 13193-7.

CLAVEL, F., GUETARD, D., BRUN-VEZINET, F., CHAMARET, S., REY, M. A., SANTOS-FERREIRA, M. O., LAURENT, A. G., DAUGUET, C., KATLAMA, C., ROUZIOUX, C. & ET AL. 1986. Isolation of a new human retrovirus from West African patients with AIDS. *Science,* 233**,** 343-6.

COCKERHAM, L. R., HATANO, H. & DEEKS, S. G. 2016. Post-Treatment Controllers: Role in HIV "Cure" Research. *Curr HIV/AIDS Rep,* 13**,** 1-9.

COCKERHAM, L. R., SILICIANO, J. D., SINCLAIR, E., O'DOHERTY, U., PALMER, S., YUKL, S. A., STRAIN, M. C., CHOMONT, N., HECHT, F. M., SILICIANO, R. F., RICHMAN, D. D. & DEEKS, S. G. 2014. CD4+ and CD8+ T cell activation are associated with HIV DNA in resting CD4+ T cells. *PLoS One,* 9**,** e110731.

COIRAS, M., BERMEJO, M., DESCOURS, B., MATEOS, E., GARCIA-PEREZ, J., LOPEZ-HUERTAS, M. R., LEDERMAN, M. M., BENKIRANE, M. & ALCAMI, J. 2016. IL-7 Induces SAMHD1 Phosphorylation in CD4+ T Lymphocytes, Improving Early Steps of HIV-1 Life Cycle. *Cell Rep,* 14**,** 2100-7.

COOPER, C. L., VAN HEESWIJK, R. P., GALLICANO, K. & CAMERON, D. W. 2003. A review of low-dose ritonavir in protease inhibitor combination therapy. *Clin Infect Dis,* 36**,** 1585-92.

CRAUWELS, H. M., VAN HEESWIJK, R. P., BUELENS, A., STEVENS, M., BOVEN, K. & HOETELMANS, R. M. 2013. Impact of food and different meal types on the pharmacokinetics of rilpivirine. *J Clin Pharmacol,* 53**,** 834-40.

CROWELL, T. A. & HATANO, H. 2015. Clinical outcomes and antiretroviral therapy in 'elite' controllers: a review of the literature. *J Virus Erad,* 1**,** 72-77.

CULLEN, B. R. 1991. Regulation of HIV-1 gene expression. *FASEB J,* 5**,** 2361-8.

DAWSON, L. & YU, X. F. 1998. The role of nucleocapsid of HIV-1 in virus assembly. *Virology,* 251**,** 141-57.

DE MILITO, A., ALEMAN, S., MARENZI, R., SONNERBORG, A., FUCHS, D., ZAZZI, M. & CHIODI, F. 2002. Plasma levels of soluble CD27: a simple marker to monitor immune activation during potent antiretroviral therapy in HIV-1-infected subjects. *Clin Exp Immunol,* 127**,** 486-94.

DE SPIEGELAERE, W., MALATINKOVA, E., LYNCH, L., VAN NIEUWERBURGH, F., MESSIAEN, P., O'DOHERTY, U. & VANDEKERCKHOVE, L. 2014. Quantification of Integrated HIV DNA by Repetitive-Sampling Alu-HIV PCR on the Basis of Poisson Statistics. *Clinical Chemistry,* 60**,** 886-895.

DOISNE, J. M., URRUTIA, A., LACABARATZ-PORRET, C., GOUJARD, C., MEYER, L., CHAIX, M. L., SINET, M. & VENET, A. 2004. CD8+ T cells specific for EBV, cytomegalovirus, and influenza virus are activated during primary HIV infection. *J Immunol,* 173**,** 2410-8.

DOITSH, G. & GREENE, W. C. 2016. Dissecting How CD4 T Cells Are Lost During HIV Infection. *Cell Host Microbe,* 19**,** 280-91.

DORNADULA, G., ZHANG, H., VANUITERT, B., STERN, J., LIVORNESE, L., JR., INGERMAN, M. J., WITEK, J., KEDANIS, R. J., NATKIN, J., DESIMONE, J. & POMERANTZ, R. J. 1999. Residual HIV-1 RNA in blood plasma of patients taking suppressive highly active antiretroviral therapy. *JAMA,* 282**,** 1627-32.

DORR, P., WESTBY, M., DOBBS, S., GRIFFIN, P., IRVINE, B., MACARTNEY, M., MORI, J., RICKETT, G., SMITH-BURCHNELL, C., NAPIER, C., WEBSTER, R., ARMOUR, D., PRICE, D., STAMMEN, B., WOOD, A. &

PERROS, M. 2005. Maraviroc (UK-427,857), a potent, orally bioavailable, and selective small-molecule inhibitor of chemokine receptor CCR5 with broad-spectrum anti-human immunodeficiency virus type 1 activity. *Antimicrob Agents Chemother,* 49**,** 4721-32.

DOUEK, D. C., PICKER, L. J. & KOUP, R. A. 2003. T cell dynamics in HIV-1 infection. *Annu Rev Immunol,* 21**,** 265-304.

DOYLE, T. & GERETTI, A. M. 2012. Low-level viraemia on HAART: significance and management. *Curr Opin Infect Dis,* 25**,** 17-25.

DOYLE, T., SMITH, C., VITIELLO, P., CAMBIANO, V., JOHNSON, M., OWEN, A., PHILLIPS, A. N. & GERETTI, A. M. 2012. Plasma HIV-1 RNA detection below 50 copies/ml and risk of virologic rebound in patients receiving highly active antiretroviral therapy. *Clin Infect Dis,* 54**,** 724-32.

EDEN, A., FUCHS, D., HAGBERG, L., NILSSON, S., SPUDICH, S., SVENNERHOLM, B., PRICE, R. W. & GISSLEN, M. 2010. HIV-1 viral escape in cerebrospinal fluid of subjects on suppressive antiretroviral treatment. *J Infect Dis,* 202**,** 1819-25.

ERIKSSON, S., GRAF, E. H., DAHL, V., STRAIN, M. C., YUKL, S. A., LYSENKO, E. S., BOSCH, R. J., LAI, J., CHIOMA, S., EMAD, F., ABDEL-MOHSEN, M., HOH, R., HECHT, F., HUNT, P., SOMSOUK, M., WONG, J., JOHNSTON, R., SILICIANO, R. F., RICHMAN, D. D., O'DOHERTY, U., PALMER, S., DEEKS, S. G. & SILICIANO, J. D. 2013. Comparative analysis of measures of viral reservoirs in HIV-1 eradication studies. *PLoS Pathog,* 9**,** e1003174.

ESTE, J. A. & TELENTI, A. 2007. HIV entry inhibitors. *Lancet,* 370**,** 81-8.

FINKEL, T. H., TUDOR-WILLIAMS, G., BANDA, N. K., COTTON, M. F., CURIEL, T., MONKS, C., BABA, T. W., RUPRECHT, R. M. & KUPFER, A. 1995. Apoptosis occurs predominantly in bystander cells and not in productively infected cells of HIV- and SIV-infected lymph nodes. *Nat Med,* 1**,** 129-34.

FINZI, D., BLANKSON, J., SILICIANO, J. D., MARGOLICK, J. B., CHADWICK, K., PIERSON, T., SMITH, K., LISZIEWICZ, J., LORI, F., FLEXNER, C., QUINN, T. C., CHAISSON, R. E., ROSENBERG, E., WALKER, B., GANGE, S., GALLANT, J. & SILICIANO, R. F. 1999. Latent infection of CD4+ T cells provides a mechanism for lifelong persistence of HIV-1, even in patients on effective combination therapy. *Nat Med,* 5**,** 512-7.

FINZI, D., HERMANKOVA, M., PIERSON, T., CARRUTH, L. M., BUCK, C., CHAISSON, R. E., QUINN, T. C., CHADWICK, K., MARGOLICK, J., BROOKMEYER, R., GALLANT, J., MARKOWITZ, M., HO, D. D., RICHMAN, D. D. & SILICIANO, R. F. 1997. Identification of a reservoir for HIV-1 in patients on highly active antiretroviral therapy. *Science,* 278**,** 1295-300.

FIORENTINI, S., MARINI, E., CARACCIOLO, S. & CARUSO, A. 2006. Functions of the HIV-1 matrix protein p17. *New Microbiol,* 29**,** 1-10.

FISER, A. L., VINCENT, T., BRIEU, N., LIN, Y. L., PORTALES, P., METTLING, C., REYNES, J. & CORBEAU, P. 2010. High CD4(+) T-cell surface CXCR4 density as a risk factor for R5 to X4 switch in the course of HIV-1 infection. *J Acquir Immune Defic Syndr,* 55**,** 529-35.

FLETCHER, C. V., STASKUS, K., WIETGREFE, S. W., ROTHENBERGER, M., REILLY, C., CHIPMAN, J. G., BEILMAN, G. J., KHORUTS, A., THORKELSON, A., SCHMIDT, T. E., ANDERSON, J., PERKEY, K., STEVENSON, M., PERELSON, A. S., DOUEK, D. C., HAASE, A. T. &

SCHACKER, T. W. 2014. Persistent HIV-1 replication is associated with lower antiretroviral drug concentrations in lymphatic tissues. *Proc Natl Acad Sci U S A,* 111**,** 2307-12.

FOURATI, S., FLANDRE, P., CALIN, R., CARCELAIN, G., SOULIE, C., LAMBERT-NICLOT, S., MAIGA, A., AIT-ARKOUB, Z., TUBIANA, R., VALANTIN, M. A., AUTRAN, B., KATLAMA, C., CALVEZ, V. & MARCELIN, A. G. 2014. Factors associated with a low HIV reservoir in patients with prolonged suppressive antiretroviral therapy. *J Antimicrob Chemother,* 69**,** 753-6.

FOURIE, J., FLAMM, J., RODRIGUEZ-FRENCH, A., KILBY, D., DOMINGO, P., LAZZARIN, A., BALLESTEROS, J., SOSA, N., VAN DE CASTEELE, T., DEMASI, R., SPINOSA-GUZMAN, S. & LAVREYS, L. 2011. Effect of baseline characteristics on the efficacy and safety of once-daily darunavir/ ritonavir in HIV-1-infected, treatment-naive ARTEMIS patients at week 96. *HIV Clin Trials,* 12**,** 313-22.

FRANCIOLI, P., VOGT, M., SCHADELIN, J., CLEMENT, F., RUSSI, E., DELACRETAZ, F., PERRET, C. & GLAUSER, M. P. 1982. [Acquired immunologic deficiency syndrome, opportunistic infections and homosexuality. Presentation of 3 cases studied in Switzerland]. *Schweiz Med Wochenschr,* 112**,** 1682-7.

FREED, E. O. 2015. HIV-1 assembly, release and maturation. *Nat Rev Microbiol,* 13**,** 484-96.

FRENCH, M. A., KING, M. S., TSCHAMPA, J. M., DA SILVA, B. A. & LANDAY, A. L. 2009. Serum immune activation markers are persistently increased in patients with HIV infection after 6 years of antiretroviral therapy despite suppression of viral replication and reconstitution of CD4+ T cells. *J Infect Dis,* 200**,** 1212-5.

GAO, F., BAILES, E., ROBERTSON, D. L., CHEN, Y., RODENBURG, C. M., MICHAEL, S. F., CUMMINS, L. B., ARTHUR, L. O., PEETERS, M., SHAW, G. M., SHARP, P. M. & HAHN, B. H. 1999. Origin of HIV-1 in the chimpanzee Pan troglodytes troglodytes. *Nature,* 397**,** 436-41.

GAO, R., SUN, W., CHEN, Y., SU, Y., WANG, C. & DONG, L. 2015. Elevated Serum Levels of Soluble CD30 in Ankylosing Spondylitis Patients and Its Association with Disease Severity-Related Parameters. *Biomed Res Int,* 2015**,** 617282.

GARVEY, L. J., EVERITT, A., WINSTON, A., MACKIE, N. E. & BENZIE, A. 2009. Detectable cerebrospinal fluid HIV RNA with associated neurological deficits, despite suppression of HIV replication in the plasma compartment. *AIDS,* 23**,** 1443-4.

GATTINONI, L., LUGLI, E., JI, Y., POS, Z., PAULOS, C. M., QUIGLEY, M. F., ALMEIDA, J. R., GOSTICK, E., YU, Z., CARPENITO, C., WANG, E., DOUEK, D. C., PRICE, D. A., JUNE, C. H., MARINCOLA, F. M., ROEDERER, M. & RESTIFO, N. P. 2011. A human memory T cell subset with stem cell-like properties. *Nat Med,* 17**,** 1290-7.

GEGINAT, J., SALLUSTO, F. & LANZAVECCHIA, A. 2003. Cytokine-driven proliferation and differentiation of human naive, central memory and effector memory CD4+ T cells. *Pathol Biol (Paris),* 51**,** 64-6.

GERETTI, A. M. 2006. HIV-1 subtypes: epidemiology and significance for HIV management. *Curr Opin Infect Dis,* 19**,** 1-7.

GERETTI, A. M., ARRIBAS, J. R., LATHOUWERS, E., FOSTER, G. M., YAKOOB, R., KINLOCH, S., HILL, A., VAN DELFT, Y. & MOECKLINGHOFF, C.

2013. Dynamics of cellular HIV-1 DNA levels over 144 weeks of darunavir/ritonavir monotherapy versus triple therapy in the MONET trial. *HIV Clin Trials,* 14**,** 45-50.

GERETTI, A. M. & TSAKIROGLOU, M. 2014. HIV: new drugs, new guidelines. *Curr Opin Infect Dis,* 27**,** 545-53.

GIANELLA, S., MASSANELLA, M., RICHMAN, D. D., LITTLE, S. J., SPINA, C. A., VARGAS, M. V., LADA, S. M., DAAR, E. S., DUBE, M. P., HAUBRICH, R. H., MORRIS, S. R., SMITH, D. M. & CALIFORNIA COLLABORATIVE TREATMENT GROUP, T. 2014. Cytomegalovirus replication in semen is associated with higher levels of proviral HIV DNA and CD4+ T cell activation during antiretroviral treatment. *J Virol,* 88**,** 7818-27.

GRAF, E. H. & O'DOHERTY, U. 2013. Quantitation of integrated proviral DNA in viral reservoirs. *Curr Opin HIV AIDS,* 8**,** 100-5.

GRAHAM, F. L., SMILEY, J., RUSSELL, W. C. & NAIRN, R. 1977. Characteristics of a human cell line transformed by DNA from human adenovirus type 5. *J Gen Virol,* 36**,** 59-74.

GROUP, I. S. S., LUNDGREN, J. D., BABIKER, A. G., GORDIN, F., EMERY, S., GRUND, B., SHARMA, S., AVIHINGSANON, A., COOPER, D. A., FATKENHEUER, G., LLIBRE, J. M., MOLINA, J. M., MUNDERI, P., SCHECHTER, M., WOOD, R., KLINGMAN, K. L., COLLINS, S., LANE, H. C., PHILLIPS, A. N. & NEATON, J. D. 2015. Initiation of Antiretroviral Therapy in Early Asymptomatic HIV Infection. *N Engl J Med,* 373**,** 795-807.

GULICK, R. M., RIBAUDO, H. J., SHIKUMA, C. M., LALAMA, C., SCHACKMAN, B. R., MEYER, W. A., 3RD, ACOSTA, E. P., SCHOUTEN, J., SQUIRES, K. E., PILCHER, C. D., MURPHY, R. L., KOLETAR, S. L., CARLSON, M., REICHMAN, R. C., BASTOW, B., KLINGMAN, K. L., KURITZKES, D. R. & TEAM, A. C. T. G. A. S. 2006. Three- vs four-drug antiretroviral regimens for the initial treatment of HIV-1 infection: a randomized controlled trial. *JAMA,* 296**,** 769-81.

HAHN, B. H., SHAW, G. M., DE COCK, K. M. & SHARP, P. M. 2000. AIDS as a zoonosis: scientific and public health implications. *Science,* 287**,** 607-14.

HATANO, H. 2013. Immune activation and HIV persistence: considerations for novel therapeutic interventions. *Curr Opin HIV AIDS,* 8**,** 211-6.

HATANO, H., JAIN, V., HUNT, P. W., LEE, T. H., SINCLAIR, E., DO, T. D., HOH, R., MARTIN, J. N., MCCUNE, J. M., HECHT, F., BUSCH, M. P. & DEEKS, S. G. 2013. Cell-based measures of viral persistence are associated with immune activation and programmed cell death protein 1 (PD-1)-expressing CD4+ T cells. *J Infect Dis,* 208**,** 50-6.

HAVLIR, D., CHEESEMAN, S. H., MCLAUGHLIN, M., MURPHY, R., ERICE, A., SPECTOR, S. A., GREENOUGH, T. C., SULLIVAN, J. L., HALL, D., MYERS, M. & ET AL. 1995. High-dose nevirapine: safety, pharmacokinetics, and antiviral effect in patients with human immunodeficiency virus infection. *J Infect Dis,* 171**,** 537-45.

HAZENBERG, M. D., OTTO, S. A., VAN BENTHEM, B. H., ROOS, M. T., COUTINHO, R. A., LANGE, J. M., HAMANN, D., PRINS, M. & MIEDEMA, F. 2003. Persistent immune activation in HIV-1 infection is associated with progression to AIDS. *AIDS,* 17**,** 1881-8.

HENRICH, T. J., WOOD, B. R. & KURITZKES, D. R. 2012. Increased risk of virologic rebound in patients on antiviral therapy with a detectable HIV load <48 copies/mL. *PLoS One,* 7**,** e50065.

HERBEIN, G., GRAS, G., KHAN, K. A. & ABBAS, W. 2010. Macrophage signaling in HIV-1 infection. *Retrovirology,* 7**,** 34.

HERBEUVAL, J. P., GRIVEL, J. C., BOASSO, A., HARDY, A. W., CHOUGNET, C., DOLAN, M. J., YAGITA, H., LIFSON, J. D. & SHEARER, G. M. 2005. CD4+ T-cell death induced by infectious and noninfectious HIV-1: role of type 1 interferon-dependent, TRAIL/DR5-mediated apoptosis. *Blood,* 106**,** 3524-31.

HOCQUELOUX, L., AVETTAND-FENOEL, V., JACQUOT, S., PRAZUCK, T., LEGAC, E., MELARD, A., NIANG, M., MILLE, C., LE MOAL, G., VIARD, J. P., ROUZIOUX, C. & VIRALES, A. C. O. T. A. N. D. R. S. L. S. E. L. H. 2013. Long-term antiretroviral therapy initiated during primary HIV-1 infection is key to achieving both low HIV reservoirs and normal T cell counts. *J Antimicrob Chemother,* 68**,** 1169-78.

HODDER, S., ARASTEH, K., DE WET, J., GATHE, J., GOLD, J., KUMAR, P., MOHAPI, L., SHORT, W., CRAUWELS, H., VANVEGGEL, S. & BOVEN, K. 2012. Effect of gender and race on the week 48 findings in treatment-naive, HIV-1-infected patients enrolled in the randomized, phase III trials ECHO and THRIVE. *HIV Med,* 13**,** 406-15.

HOETELMANS, R., VAN HEESWIJK, R., KESTENS, D., MARIEN, K., STEVENS, M., PEETERS, M., WILLIAMS, P., BASTIAANSE, L., BUFFELS, R. & WOODFALL, B. Effect of food and multiple-dose pharmacokinetics of TMC278 as an oral tablet formulation. 3rd IAS Conference on HIV Pathogenesis and Treatment, 2005 Rio De Janeiro, Brazil. International AIDS Society.

HUANG, J., JOCHEMS, C., ANDERSON, A. M., TALAIE, T., JALES, A., MADAN, R. A., HODGE, J. W., TSANG, K. Y., LIEWEHR, D. J., STEINBERG, S. M., GULLEY, J. L. & SCHLOM, J. 2013. Soluble CD27-pool in humans may contribute to T cell activation and tumor immunity. *J Immunol,* 190**,** 6250-8.

HUNT, P. W., SINCLAIR, E., RODRIGUEZ, B., SHIVE, C., CLAGETT, B., FUNDERBURG, N., ROBINSON, J., HUANG, Y., EPLING, L., MARTIN, J. N., DEEKS, S. G., MEINERT, C. L., VAN NATTA, M. L., JABS, D. A. & LEDERMAN, M. M. 2014. Gut epithelial barrier dysfunction and innate immune activation predict mortality in treated HIV infection. *J Infect Dis,* 210**,** 1228-38.

HUTTER, G., NOWAK, D., MOSSNER, M., GANEPOLA, S., MUSSIG, A., ALLERS, K., SCHNEIDER, T., HOFMANN, J., KUCHERER, C., BLAU, O., BLAU, I. W., HOFMANN, W. K. & THIEL, E. 2009. Long-term control of HIV by CCR5 Delta32/Delta32 stem-cell transplantation. *N Engl J Med,* 360**,** 692-8.

HYMES, K. B., CHEUNG, T., GREENE, J. B., PROSE, N. S., MARCUS, A., BALLARD, H., WILLIAM, D. C. & LAUBENSTEIN, L. J. 1981. Kaposi's sarcoma in homosexual men-a report of eight cases. *Lancet,* 2**,** 598-600.

IORDANSKIY, S., SANTOS, S. & BUKRINSKY, M. 2013. Nature, nurture and HIV: The effect of producer cell on viral physiology. *Virology,* 443**,** 208-13.

IWAMI, S., TAKEUCHI, J. S., NAKAOKA, S., MAMMANO, F., CLAVEL, F., INABA, H., KOBAYASHI, T., MISAWA, N., AIHARA, K., KOYANAGI, Y. & SATO, K. 2015. Cell-to-cell infection by HIV contributes over half of virus infection. *Elife,* 4.

IYER, S. R., YU, D., BIANCOTTO, A., MARGOLIS, L. B. & WU, Y. 2009. Measurement of human immunodeficiency virus type 1 preintegration transcription by using Rev-dependent Rev-CEM cells reveals a sizable

transcribing DNA population comparable to that from proviral templates. *J Virol,* 83**,** 8662-73.

JACOBS, G. B., WILKINSON, E., ISAACS, S., SPIES, G., DE OLIVEIRA, T., SEEDAT, S. & ENGELBRECHT, S. 2014. HIV-1 subtypes B and C unique recombinant forms (URFs) and transmitted drug resistance identified in the Western Cape Province, South Africa. *PLoS One,* 9**,** e90845.

JAYAPPA, K. D., AO, Z. & YAO, X. 2012. The HIV-1 passage from cytoplasm to nucleus: the process involving a complex exchange between the components of HIV-1 and cellular machinery to access nucleus and successful integration. *Int J Biochem Mol Biol,* 3**,** 70-85.

JIAO, J., REBANE, A. A., MA, L., GAO, Y. & ZHANG, Y. 2015. Kinetically coupled folding of a single HIV-1 glycoprotein 41 complex in viral membrane fusion and inhibition. *Proc Natl Acad Sci U S A,* 112**,** E2855-64.

JOLLY, C. & SATTENTAU, Q. J. 2005. Human immunodeficiency virus type 1 virological synapse formation in T cells requires lipid raft integrity. *J Virol,* 79**,** 12088-94.

JOSEFSSON, L., VON STOCKENSTROM, S., FARIA, N. R., SINCLAIR, E., BACCHETTI, P., KILLIAN, M., EPLING, L., TAN, A., HO, T., LEMEY, P., SHAO, W., HUNT, P. W., SOMSOUK, M., WYLIE, W., DOUEK, D. C., LOEB, L., CUSTER, J., HOH, R., POOLE, L., DEEKS, S. G., HECHT, F. & PALMER, S. 2013. The HIV-1 reservoir in eight patients on long-term suppressive antiretroviral therapy is stable with few genetic changes over time. *Proc Natl Acad Sci U S A,* 110**,** E4987-96.

KARN, J. & STOLTZFUS, C. M. 2012. Transcriptional and posttranscriptional regulation of HIV-1 gene expression. *Cold Spring Harb Perspect Med,* 2**,** a006916.

KEELE, B. F., GIORGI, E. E., SALAZAR-GONZALEZ, J. F., DECKER, J. M., PHAM, K. T., SALAZAR, M. G., SUN, C., GRAYSON, T., WANG, S., LI, H., WEI, X., JIANG, C., KIRCHHERR, J. L., GAO, F., ANDERSON, J. A., PING, L. H., SWANSTROM, R., TOMARAS, G. D., BLATTNER, W. A., GOEPFERT, P. A., KILBY, J. M., SAAG, M. S., DELWART, E. L., BUSCH, M. P., COHEN, M. S., MONTEFIORI, D. C., HAYNES, B. F., GASCHEN, B., ATHREYA, G. S., LEE, H. Y., WOOD, N., SEOIGHE, C., PERELSON, A. S., BHATTACHARYA, T., KORBER, B. T., HAHN, B. H. & SHAW, G. M. 2008. Identification and characterization of transmitted and early founder virus envelopes in primary HIV-1 infection. *Proc Natl Acad Sci U S A,* 105**,** 7552-7.

KEISER, P., NASSAR, N., WHITE, C., KOEN, G. & MORENO, S. 2002. Comparison of nevirapine- and efavirenz-containing antiretroviral regimens in antiretroviral-naive patients: a cohort study. *HIV Clin Trials,* 3**,** 296-303.

KISELINOVA, M., GERETTI, A. M., MALATINKOVA, E., VERVISCH, K., BELOUKAS, A., MESSIAEN, P., BONCZKOWSKI, P., TRYPSTEEN, W., CALLENS, S., VERHOFSTEDE, C., DE SPIEGELAERE, W. & VANDEKERCKHOVE, L. 2015. HIV-1 RNA and HIV-1 DNA persistence during suppressive ART with PI-based or nevirapine-based regimens. *J Antimicrob Chemother,* 70**,** 3311-6.

KLATT, N. R., CHOMONT, N., DOUEK, D. C. & DEEKS, S. G. 2013. Immune activation and HIV persistence: implications for curative approaches to HIV infection. *Immunol Rev,* 254**,** 326-42.

KOELSCH, K. K., LIU, L., HAUBRICH, R., MAY, S., HAVLIR, D., GUNTHARD, H. F., IGNACIO, C. C., CAMPOS-SOTO, P., LITTLE, S. J., SHAFER, R.,

ROBBINS, G. K., D'AQUILA, R. T., KAWANO, Y., YOUNG, K., DAO, P., SPINA, C. A., RICHMAN, D. D. & WONG, J. K. 2008. Dynamics of total, linear nonintegrated, and integrated HIV-1 DNA in vivo and in vitro. *J Infect Dis,* 197**,** 411-9.

KONDRACK, R. M., HARBERTSON, J., TAN, J. T., MCBREEN, M. E., SURH, C. D. & BRADLEY, L. M. 2003. Interleukin 7 regulates the survival and generation of memory CD4 cells. *J Exp Med,* 198**,** 1797-806.

KUMAR, A., ABBAS, W. & HERBEIN, G. 2014. HIV-1 latency in monocytes/macrophages. *Viruses,* 6**,** 1837-60.

KVARATSKHELIA, M., SHARMA, A., LARUE, R. C., SERRAO, E. & ENGELMAN, A. 2014. Molecular mechanisms of retroviral integration site selection. *Nucleic Acids Res,* 42**,** 10209-25.

KWONG, P. D., WYATT, R., ROBINSON, J., SWEET, R. W., SODROSKI, J. & HENDRICKSON, W. A. 1998. Structure of an HIV gp120 envelope glycoprotein in complex with the CD4 receptor and a neutralizing human antibody. *Nature,* 393**,** 648-59.

LAIRD, G. M., EISELE, E. E., RABI, S. A., LAI, J., CHIOMA, S., BLANKSON, J. N., SILICIANO, J. D. & SILICIANO, R. F. 2013. Rapid quantification of the latent reservoir for HIV-1 using a viral outgrowth assay. *PLoS Pathog,* 9**,** e1003398.

LAMORDE, M., WALIMBWA, S., BYAKIKA-KIBWIKA, P., KATWERE, M., MUKISA, L., SEMPA, J. B., ELSE, L., BACK, D. J., KHOO, S. H. & MERRY, C. 2015. Steady-state pharmacokinetics of rilpivirine under different meal conditions in HIV-1-infected Ugandan adults. *J Antimicrob Chemother,* 70**,** 1482-6.

LAWN, S. D., BUTERA, S. T. & FOLKS, T. M. 2001. Contribution of immune activation to the pathogenesis and transmission of human immunodeficiency virus type 1 infection. *Clin Microbiol Rev,* 14**,** 753-77, table of contents.

LENS, S. M., TESSELAAR, K., VAN OERS, M. H. & VAN LIER, R. A. 1998. Control of lymphocyte function through CD27-CD70 interactions. *Semin Immunol,* 10**,** 491-9.

LI, X., KRISHNAN, L., CHEREPANOV, P. & ENGELMAN, A. 2011. Structural biology of retroviral DNA integration. *Virology,* 411**,** 194-205.

LICHTFUSS, G. F., HOY, J., RAJASURIAR, R., KRAMSKI, M., CROWE, S. M. & LEWIN, S. R. 2011. Biomarkers of immune dysfunction following combination antiretroviral therapy for HIV infection. *Biomark Med,* 5**,** 171-86.

LIN, Y. L., PORTALES, P., SEGONDY, M., BAILLAT, V., DE BOEVER, C. M., LE MOING, V., REANT, B., MONTES, B., CLOT, J., REYNES, J. & CORBEAU, P. 2005. CXCR4 overexpression during the course of HIV-1 infection correlates with the emergence of X4 strains. *J Acquir Immune Defic Syndr,* 39**,** 530-6.

LISZEWSKI, M. K., YU, J. J. & O'DOHERTY, U. 2009. Detecting HIV-1 integration by repetitive-sampling Alu-gag PCR. *Methods,* 47**,** 254-60.

LIU, J., BARTESAGHI, A., BORGNIA, M. J., SAPIRO, G. & SUBRAMANIAM, S. 2008. Molecular architecture of native HIV-1 gp120 trimers. *Nature,* 455**,** 109-13.

LLANO, A., BARRETINA, J., GUTIERREZ, A., BLANCO, J., CABRERA, C., CLOTET, B. & ESTE, J. A. 2001. Interleukin-7 in plasma correlates with CD4 T-cell depletion and may be associated with emergence of syncytium-inducing variants in human immunodeficiency virus type 1-positive individuals. *J Virol,* 75**,** 10319-25.

LORENZO-REDONDO, R., FRYER, H. R., BEDFORD, T., KIM, E. Y., ARCHER, J., KOSAKOVSKY POND, S. L., CHUNG, Y. S., PENUGONDA, S., CHIPMAN, J. G., FLETCHER, C. V., SCHACKER, T. W., MALIM, M. H., RAMBAUT, A., HAASE, A. T., MCLEAN, A. R. & WOLINSKY, S. M. 2016. Persistent HIV-1 replication maintains the tissue reservoir during therapy. *Nature,* 530**,** 51-6.

MALATINKOVA, E., DE SPIEGELAERE, W., BONCZKOWSKI, P., KISELINOVA, M., VERVISCH, K., TRYPSTEEN, W., JOHNSON, M., VERHOFSTEDE, C., DE LOOZE, D., MURRAY, C., KINLOCH-DE LOES, S. & VANDEKERCKHOVE, L. 2015. Impact of a decade of successful antiretroviral therapy initiated at HIV-1 seroconversion on blood and rectal reservoirs. *Elife,* 4**,** e09115.

MALDARELLI, F., PALMER, S., KING, M. S., WIEGAND, A., POLIS, M. A., MICAN, J., KOVACS, J. A., DAVEY, R. T., ROCK-KRESS, D., DEWAR, R., LIU, S., METCALF, J. A., REHM, C., BRUN, S. C., HANNA, G. J., KEMPF, D. J., COFFIN, J. M. & MELLORS, J. W. 2007. ART suppresses plasma HIV-1 RNA to a stable set point predicted by pretherapy viremia. *PLoS Pathog,* 3**,** e46.

MALDARELLI, F., WU, X., SU, L., SIMONETTI, F. R., SHAO, W., HILL, S., SPINDLER, J., FERRIS, A. L., MELLORS, J. W., KEARNEY, M. F., COFFIN, J. M. & HUGHES, S. H. 2014. HIV latency. Specific HIV integration sites are linked to clonal expansion and persistence of infected cells. *Science,* 345**,** 179-83.

MARCHETTI, G., BELLISTRI, G. M., BORGHI, E., TINCATI, C., FERRAMOSCA, S., LA FRANCESCA, M., MORACE, G., GORI, A. & MONFORTE, A. D. 2008. Microbial translocation is associated with sustained failure in CD4+ T-cell reconstitution in HIV-infected patients on long-term highly active antiretroviral therapy. *AIDS,* 22**,** 2035-8.

MARCHETTI, G., COZZI-LEPRI, A., MERLINI, E., BELLISTRI, G. M., CASTAGNA, A., GALLI, M., VERUCCHI, G., ANTINORI, A., COSTANTINI, A., GIACOMETTI, A., DI CARO, A., D'ARMINIO MONFORTE, A. & GROUP, I. F. S. 2011. Microbial translocation predicts disease progression of HIV-infected antiretroviral-naive patients with high CD4+ cell count. *AIDS,* 25**,** 1385-94.

MARSHALL, H. M., RONEN, K., BERRY, C., LLANO, M., SUTHERLAND, H., SAENZ, D., BICKMORE, W., POESCHLA, E. & BUSHMAN, F. D. 2007. Role of PSIP1/LEDGF/p75 in lentiviral infectivity and integration targeting. *PLoS One,* 2**,** e1340.

MCBRIDE, J. D. & COOPER, M. A. 2008. A high sensitivity assay for the inflammatory marker C-Reactive protein employing acoustic biosensing. *J Nanobiotechnology,* 6**,** 5.

MCDONALD, T. O., GIARDIELLO, M., MARTIN, P., SICCARDI, M., LIPTROTT, N. J., SMITH, D., ROBERTS, P., CURLEY, P., SCHIPANI, A., KHOO, S. H., LONG, J., FOSTER, A. J., RANNARD, S. P. & OWEN, A. 2014. Antiretroviral solid drug nanoparticles with enhanced oral bioavailability: production, characterization, and in vitro-in vivo correlation. *Adv Healthc Mater,* 3**,** 400-11.

MELIKYAN, G. B., MARKOSYAN, R. M., HEMMATI, H., DELMEDICO, M. K., LAMBERT, D. M. & COHEN, F. S. 2000. Evidence that the transition of HIV-1 gp41 into a six-helix bundle, not the bundle configuration, induces membrane fusion. *J Cell Biol,* 151**,** 413-23.

MELLORS, J. W., RINALDO, C. R., JR., GUPTA, P., WHITE, R. M., TODD, J. A. & KINGSLEY, L. A. 1996. Prognosis in HIV-1 infection predicted by the quantity of virus in plasma. *Science,* 272**,** 1167-70.

MEXAS, A. M., GRAF, E. H., PACE, M. J., YU, J. J., PAPASAVVAS, E., AZZONI, L., BUSCH, M. P., DI MASCIO, M., FOULKES, A. S., MIGUELES, S. A., MONTANER, L. J. & O'DOHERTY, U. 2012. Concurrent measures of total and integrated HIV DNA monitor reservoirs and ongoing replication in eradication trials. *AIDS,* 26**,** 2295-306.

MILLS, A. M., COHEN, C., DEJESUS, E., BRINSON, C., WILLIAMS, S., YALE, K. L., RAMANATHAN, S., WANG, M. H., WHITE, K., CHUCK, S. K. & CHENG, A. K. 2013. Efficacy and safety 48 weeks after switching from efavirenz to rilpivirine using emtricitabine/tenofovir disoproxil fumarate-based single-tablet regimens. *HIV Clin Trials,* 14**,** 216-23.

MONROE, K. M., YANG, Z., JOHNSON, J. R., GENG, X., DOITSH, G., KROGAN, N. J. & GREENE, W. C. 2014. IFI16 DNA sensor is required for death of lymphoid CD4 T cells abortively infected with HIV. *Science,* 343**,** 428-32.

MULLER, B., PATSCHINSKY, T. & KRAUSSLICH, H. G. 2002. The late-domain-containing protein p6 is the predominant phosphoprotein of human immunodeficiency virus type 1 particles. *J Virol,* 76**,** 1015-24.

MUNOZ-ARIAS, I., DOITSH, G., YANG, Z., SOWINSKI, S., RUELAS, D. & GREENE, W. C. 2015. Blood-Derived CD4 T Cells Naturally Resist Pyroptosis during Abortive HIV-1 Infection. *Cell Host Microbe,* 18**,** 463-70.

MURRAY, J. M., ZAUNDERS, J. J., MCBRIDE, K. L., XU, Y., BAILEY, M., SUZUKI, K., COOPER, D. A., EMERY, S., KELLEHER, A. D., KOELSCH, K. K. & TEAM, P. S. 2014. HIV DNA subspecies persist in both activated and resting memory CD4+ T cells during antiretroviral therapy. *J Virol,* 88**,** 3516-26.

NABEL, G. & BALTIMORE, D. 1987. An inducible transcription factor activates expression of human immunodeficiency virus in T cells. *Nature,* 326**,** 711-3.

NAEGER, D. M., MARTIN, J. N., SINCLAIR, E., HUNT, P. W., BANGSBERG, D. R., HECHT, F., HSUE, P., MCCUNE, J. M. & DEEKS, S. G. 2010. Cytomegalovirus-specific T cells persist at very high levels during long-term antiretroviral treatment of HIV disease. *PLoS One,* 5**,** e8886.

NGO-GIANG-HUONG, N., DEVEAU, C., DA SILVA, I., PELLEGRIN, I., VENET, A., HARZIC, M., SINET, M., DELFRAISSY, J. F., MEYER, L., GOUJARD, C., ROUZIOUX, C. & FRNECH, P. C. S. G. 2001. Proviral HIV-1 DNA in subjects followed since primary HIV-1 infection who suppress plasma viral load after one year of highly active antiretroviral therapy. *AIDS,* 15**,** 665-73.

NICASTRI, E., PALMISANO, L., SARMATI, L., D'ETTORRE, G., PARISI, S., ANDREOTTI, M., BUONOMINI, A., PIRILLO, F. M., NARCISO, P., BELLAGAMBA, R., VULLO, V., MONTANO, M., DI PERRI, G. & ANDREONI, M. 2008. HIV-1 residual viremia and proviral DNA in patients with suppressed plasma viral load (<400 HIV-RNA cp/ml) during different antiretroviral regimens. *Curr HIV Res,* 6**,** 261-6.

NIGHTINGALE, S., MICHAEL, B. D., FISHER, M., WINSTON, A., NELSON, M., TAYLOR, S., USTIANOWSKI, A., AINSWORTH, J., GILSON, R., HADDOW, L., ONG, E., LEEN, C., MINTON, J., POST, F., BELOUKAS, A., BORROW, R., PIRMOHAMED, M., GERETTI, A. M., KHOO, S. & SOLOMON, T. 2016. CSF/plasma HIV-1 RNA discordance even at low levels

is associated with up-regulation of host inflammatory mediators in CSF. *Cytokine,* 83**,** 139-46.

OKOYE, A. A. & PICKER, L. J. 2013. CD4(+) T-cell depletion in HIV infection: mechanisms of immunological failure. *Immunol Rev,* 254**,** 54-64.

OXENIUS, A., PRICE, D. A., EASTERBROOK, P. J., O'CALLAGHAN, C. A., KELLEHER, A. D., WHELAN, J. A., SONTAG, G., SEWELL, A. K. & PHILLIPS, R. E. 2000. Early highly active antiretroviral therapy for acute HIV-1 infection preserves immune function of CD8+ and CD4+ T lymphocytes. *Proc Natl Acad Sci U S A,* 97**,** 3382-7.

PACE, M. J., GRAF, E. H., AGOSTO, L. M., MEXAS, A. M., MALE, F., BRADY, T., BUSHMAN, F. D. & O'DOHERTY, U. 2012. Directly infected resting CD4+T cells can produce HIV Gag without spreading infection in a model of HIV latency. *PLoS Pathog,* 8**,** e1002818.

PACE, M. J., GRAF, E. H. & O'DOHERTY, U. 2013. HIV 2-long terminal repeat circular DNA is stable in primary CD4+T Cells. *Virology,* 441**,** 18-21.

PAIARDINI, M. & MULLER-TRUTWIN, M. 2013. HIV-associated chronic immune activation. *Immunol Rev,* 254**,** 78-101.

PALMER, S., MALDARELLI, F., WIEGAND, A., BERNSTEIN, B., HANNA, G. J., BRUN, S. C., KEMPF, D. J., MELLORS, J. W., COFFIN, J. M. & KING, M. S. 2008. Low-level viremia persists for at least 7 years in patients on suppressive antiretroviral therapy. *Proc Natl Acad Sci U S A,* 105**,** 3879-84.

PALMER, S., WIEGAND, A. P., MALDARELLI, F., BAZMI, H., MICAN, J. M., POLIS, M., DEWAR, R. L., PLANTA, A., LIU, S., METCALF, J. A., MELLORS, J. W. & COFFIN, J. M. 2003. New real-time reverse transcriptase-initiated PCR assay with single-copy sensitivity for human immunodeficiency virus type 1 RNA in plasma. *J Clin Microbiol,* 41**,** 4531-6.

PANCERA, M., MAJEED, S., BAN, Y. E., CHEN, L., HUANG, C. C., KONG, L., KWON, Y. D., STUCKEY, J., ZHOU, T., ROBINSON, J. E., SCHIEF, W. R., SODROSKI, J., WYATT, R. & KWONG, P. D. 2010. Structure of HIV-1 gp120 with gp41-interactive region reveals layered envelope architecture and basis of conformational mobility. *Proc Natl Acad Sci U S A,* 107**,** 1166-71.

PARKER, W. B., WHITE, E. L., SHADDIX, S. C., ROSS, L. J., BUCKHEIT, R. W., JR., GERMANY, J. M., SECRIST, J. A., 3RD, VINCE, R. & SHANNON, W. M. 1991. Mechanism of inhibition of human immunodeficiency virus type 1 reverse transcriptase and human DNA polymerases alpha, beta, and gamma by the 5'-triphosphates of carbovir, 3'-azido-3'-deoxythymidine, 2',3'-dideoxyguanosine and 3'-deoxythymidine. A novel RNA template for the evaluation of antiretroviral drugs. *J Biol Chem,* 266**,** 1754-62.

PASTERNAK, A. O., LUKASHOV, V. V. & BERKHOUT, B. 2013. Cell-associated HIV RNA: a dynamic biomarker of viral persistence. *Retrovirology,* 10**,** 41.

PAUWELS, R., DE CLERCQ, E., DESMYTER, J., BALZARINI, J., GOUBAU, P., HERDEWIJN, P., VANDERHAEGHE, H. & VANDEPUTTE, M. 1987. Sensitive and rapid assay on MT-4 cells for detection of antiviral compounds against the AIDS virus. *J Virol Methods,* 16**,** 171-85.

PEARL, L. H. & TAYLOR, W. R. 1987. A structural model for the retroviral proteases. *Nature,* 329**,** 351-4.

PERELSON, A. S., ESSUNGER, P., CAO, Y., VESANEN, M., HURLEY, A., SAKSELA, K., MARKOWITZ, M. & HO, D. D. 1997. Decay characteristics of HIV-1-infected compartments during combination therapy. *Nature,* 387**,** 188-91.

PERELSON, A. S., NEUMANN, A. U., MARKOWITZ, M., LEONARD, J. M. & HO, D. D. 1996. HIV-1 dynamics in vivo: virion clearance rate, infected cell life-span, and viral generation time. *Science,* 271**,** 1582-6.

PHILLIPS, R. E., ROWLAND-JONES, S., NIXON, D. F., GOTCH, F. M., EDWARDS, J. P., OGUNLESI, A. O., ELVIN, J. G., ROTHBARD, J. A., BANGHAM, C. R., RIZZA, C. R. & ET AL. 1991. Human immunodeficiency virus genetic variation that can escape cytotoxic T cell recognition. *Nature,* 354**,** 453-9.

PICKER, L. J. & WATKINS, D. I. 2005. HIV pathogenesis: the first cut is the deepest. *Nat Immunol,* 6**,** 430-2.

PIERSON, T., MCARTHUR, J. & SILICIANO, R. F. 2000. Reservoirs for HIV-1: mechanisms for viral persistence in the presence of antiviral immune responses and antiretroviral therapy. *Annu Rev Immunol,* 18**,** 665-708.

PIZZOLO, G., VINANTE, F., MOROSATO, L., NADALI, G., CHILOSI, M., GANDINI, G., SINICCO, A., RAITERI, R., SEMENZATO, G., STEIN, H. & ET AL. 1994. High serum level of the soluble form of CD30 molecule in the early phase of HIV-1 infection as an independent predictor of progression to AIDS. *AIDS,* 8**,** 741-5.

POETA, J., LINDEN, R., ANTUNES, M. V., REAL, L., MENEZES, A. M., RIBEIRO, J. P. & SPRINZ, E. 2011. Plasma concentrations of efavirenz are associated with body weight in HIV-positive individuals. *J Antimicrob Chemother,* 66**,** 2601-4.

POPOVIC, M., SARNGADHARAN, M. G., READ, E. & GALLO, R. C. 1984. Detection, isolation, and continuous production of cytopathic retroviruses (HTLV-III) from patients with AIDS and pre-AIDS. *Science,* 224**,** 497-500.

PRESTON, B. D., POIESZ, B. J. & LOEB, L. A. 1988. Fidelity of HIV-1 reverse transcriptase. *Science,* 242**,** 1168-71.

RABI, S. A., LAIRD, G. M., DURAND, C. M., LASKEY, S., SHAN, L., BAILEY, J. R., CHIOMA, S., MOORE, R. D. & SILICIANO, R. F. 2013. Multi-step inhibition explains HIV-1 protease inhibitor pharmacodynamics and resistance. *J Clin Invest,* 123**,** 3848-60.

RASAIYAAH, J., TAN, C. P., FLETCHER, A. J., PRICE, A. J., BLONDEAU, C., HILDITCH, L., JACQUES, D. A., SELWOOD, D. L., JAMES, L. C., NOURSADEGHI, M. & TOWERS, G. J. 2013. HIV-1 evades innate immune recognition through specific cofactor recruitment. *Nature,* 503**,** 402-5.

RATNER, L., GALLO, R. C. & WONG-STAAL, F. 1985. HTLV-III, LAV, ARV are variants of same AIDS virus. *Nature,* 313**,** 636-7.

RIDDLER, S. A., AGA, E., BOSCH, R. J., BASTOW, B., BEDISON, M., VAGRATIAN, D., VAIDA, F., ERON, J. J., GANDHI, R. T., MELLORS, J. W. & TEAM, A. A. P. 2016. Continued Slow Decay of the Residual Plasma Viremia Level in HIV-1-Infected Adults Receiving Long-term Antiretroviral Therapy. *J Infect Dis,* 213**,** 556-60.

RIZZARDI, G. P., BARCELLINI, W., TAMBUSSI, G., LILLO, F., MALNATI, M., PERRIN, L. & LAZZARIN, A. 1996. Plasma levels of soluble CD30, tumour necrosis factor (TNF)-alpha and TNF receptors during primary HIV-1 infection: correlation with HIV-1 RNA and the clinical outcome. *AIDS,* 10**,** F45-50.

ROCHE, J., LOUIS, J. M., ANIANA, A., GHIRLANDO, R. & BAX, A. 2015. Complete dissociation of the HIV-1 gp41 ectodomain and membrane proximal regions upon phospholipid binding. *J Biomol NMR,* 61**,** 235-48.

ROUX, K. H. & TAYLOR, K. A. 2007. AIDS virus envelope spike structure. *Curr Opin Struct Biol,* 17**,** 244-52.

ROZENBAUM, W., COULAUD, J. P., SAIMOT, A. G., KLATZMANN, D., MAYAUD, C. & CARETTE, M. F. 1982. Multiple opportunistic infection in a male homosexual in France. *Lancet,* 1**,** 572-3.

RUELAS, D. S. & GREENE, W. C. 2013. An integrated overview of HIV-1 latency. *Cell,* 155**,** 519-29.

RUGGIERO, A., DE SPIEGELAERE, W., COZZI-LEPRI, A., KISELINOVA, M., POLLAKIS, G., BELOUKAS, A., VANDEKERCKHOVE, L., STRAIN, M., RICHMAN, D., PHILLIPS, A., GERETTI, A. M. & GROUP, E. S. 2015. During Stably Suppressive Antiretroviral Therapy Integrated HIV-1 DNA Load in Peripheral Blood is Associated with the Frequency of CD8 Cells Expressing HLA-DR/DP/DQ. *EBioMedicine,* 2**,** 1153-9.

RUIZ, L., MARTINEZ-PICADO, J., ROMEU, J., PAREDES, R., ZAYAT, M. K., MARFIL, S., NEGREDO, E., SIRERA, G., TURAL, C. & CLOTET, B. 2000. Structured treatment interruption in chronically HIV-1 infected patients after long-term viral suppression. *AIDS,* 14**,** 397-403.

RYOM, L., BOESECKE, C., GISLER, V., MANZARDO, C., ROCKSTROH, J. K., PUOTI, M., FURRER, H., MIRO, J. M., GATELL, J. M., POZNIAK, A., BEHRENS, G., BATTEGAY, M., LUNDGREN, J. D. & BOARD, E. G. 2016. Essentials from the 2015 European AIDS Clinical Society (EACS) guidelines for the treatment of adult HIV-positive persons. *HIV Med,* 17**,** 83-8.

SACKETT, K., NETHERCOTT, M. J., SHAI, Y. & WELIKY, D. P. 2009. Hairpin folding of HIV gp41 abrogates lipid mixing function at physiologic pH and inhibits lipid mixing by exposed gp41 constructs. *Biochemistry,* 48**,** 2714-22.

SAEZ-CIRION, A., BACCHUS, C., HOCQUELOUX, L., AVETTAND-FENOEL, V., GIRAULT, I., LECUROUX, C., POTARD, V., VERSMISSE, P., MELARD, A., PRAZUCK, T., DESCOURS, B., GUERGNON, J., VIARD, J. P., BOUFASSA, F., LAMBOTTE, O., GOUJARD, C., MEYER, L., COSTAGLIOLA, D., VENET, A., PANCINO, G., AUTRAN, B., ROUZIOUX, C. & GROUP, A. V. S. 2013. Post-treatment HIV-1 controllers with a long-term virological remission after the interruption of early initiated antiretroviral therapy ANRS VISCONTI Study. *PLoS Pathog,* 9**,** e1003211.

SAEZ-CIRION, A., LACABARATZ, C., LAMBOTTE, O., VERSMISSE, P., URRUTIA, A., BOUFASSA, F., BARRE-SINOUSSI, F., DELFRAISSY, J. F., SINET, M., PANCINO, G., VENET, A. & AGENCE NATIONALE DE RECHERCHES SUR LE SIDA, E. P. H. I. V. C. S. G. 2007. HIV controllers exhibit potent CD8 T cell capacity to suppress HIV infection ex vivo and peculiar cytotoxic T lymphocyte activation phenotype. *Proc Natl Acad Sci U S A,* 104**,** 6776-81.

SALLUSTO, F., GEGINAT, J. & LANZAVECCHIA, A. 2004. Central memory and effector memory T cell subsets: function, generation, and maintenance. *Annu Rev Immunol,* 22**,** 745-63.

SALLUSTO, F., LENIG, D., FORSTER, R., LIPP, M. & LANZAVECCHIA, A. 1999. Two subsets of memory T lymphocytes with distinct homing potentials and effector functions. *Nature,* 401**,** 708-12.

SANCHEZ MARTIN, A., CABRERA FIGUEROA, S., CRUZ GUERRERO, R., HURTADO, L. P., HURLE, A. D. & CARRACEDO ALVAREZ, A. 2013. Impact of pharmacogenetics on CNS side effects related to efavirenz. *Pharmacogenomics,* 14**,** 1167-78.

SANDLER, N. G., WAND, H., ROQUE, A., LAW, M., NASON, M. C., NIXON, D. E., PEDERSEN, C., RUXRUNGTHAM, K., LEWIN, S. R., EMERY, S., NEATON, J. D., BRENCHLEY, J. M., DEEKS, S. G., SERETI, I., DOUEK, D. C. & GROUP, I. S. S. 2011. Plasma levels of soluble CD14 independently predict mortality in HIV infection. *J Infect Dis,* 203**,** 780-90.

SARAFIANOS, S. G., MARCHAND, B., DAS, K., HIMMEL, D. M., PARNIAK, M. A., HUGHES, S. H. & ARNOLD, E. 2009. Structure and function of HIV-1 reverse transcriptase: molecular mechanisms of polymerization and inhibition. *J Mol Biol,* 385**,** 693-713.

SATO, H., ORENSTEIN, J., DIMITROV, D. & MARTIN, M. 1992. Cell-to-cell spread of HIV-1 occurs within minutes and may not involve the participation of virus particles. *Virology,* 186**,** 712-24.

SATTENTAU, Q. 2008. Avoiding the void: cell-to-cell spread of human viruses. *Nat Rev Microbiol,* 6**,** 815-26.

SCHACKER, T. W., BRENCHLEY, J. M., BEILMAN, G. J., REILLY, C., PAMBUCCIAN, S. E., TAYLOR, J., SKARDA, D., LARSON, M., DOUEK, D. C. & HAASE, A. T. 2006. Lymphatic tissue fibrosis is associated with reduced numbers of naive CD4+ T cells in human immunodeficiency virus type 1 infection. *Clin Vaccine Immunol,* 13**,** 556-60.

SCHINDLER, M., MUNCH, J., KUTSCH, O., LI, H., SANTIAGO, M. L., BIBOLLET-RUCHE, F., MULLER-TRUTWIN, M. C., NOVEMBRE, F. J., PEETERS, M., COURGNAUD, V., BAILES, E., ROQUES, P., SODORA, D. L., SILVESTRI, G., SHARP, P. M., HAHN, B. H. & KIRCHHOFF, F. 2006. Nef-mediated suppression of T cell activation was lost in a lentiviral lineage that gave rise to HIV-1. *Cell,* 125**,** 1055-67.

SCOTT, L. E., CRUMP, J. A., MSUYA, E., MORRISSEY, A. B., VENTER, W. F. & STEVENS, W. S. 2011. Abbott RealTime HIV-1 m2000rt viral load testing: manual extraction versus the automated m2000sp extraction. *J Virol Methods,* 172**,** 78-80.

SHAN, L. & SILICIANO, R. F. 2014. Unraveling the relationship between microbial translocation and systemic immune activation in HIV infection. *J Clin Invest,* 124**,** 2368-71.

SHARKEY, M. 2013. Tracking episomal HIV DNA: implications for viral persistence and eradication of HIV. *Curr Opin HIV AIDS,* 8**,** 93-9.

SIGAL, A., KIM, J. T., BALAZS, A. B., DEKEL, E., MAYO, A., MILO, R. & BALTIMORE, D. 2011. Cell-to-cell spread of HIV permits ongoing replication despite antiretroviral therapy. *Nature,* 477**,** 95-8.

SILICIANO, J. D., KAJDAS, J., FINZI, D., QUINN, T. C., CHADWICK, K., MARGOLICK, J. B., KOVACS, C., GANGE, S. J. & SILICIANO, R. F. 2003. Long-term follow-up studies confirm the stability of the latent reservoir for HIV-1 in resting CD4+ T cells. *Nat Med,* 9**,** 727-8.

SILICIANO, J. D. & SILICIANO, R. F. 2005. Enhanced culture assay for detection and quantitation of latently infected, resting CD4+ T-cells carrying replication-competent virus in HIV-1-infected individuals. *Methods Mol Biol,* 304**,** 3-15.

SILICIANO, J. M. & SILICIANO, R. F. 2015. The Remarkable Stability of the Latent Reservoir for HIV-1 in Resting Memory CD4+ T Cells. *J Infect Dis,* 212**,** 1345-7.

SILICIANO, R. F. & GREENE, W. C. 2011. HIV latency. *Cold Spring Harb Perspect Med,* 1**,** a007096.

SLOAN, R. D. & WAINBERG, M. A. 2011. The role of unintegrated DNA in HIV infection. *Retrovirology,* 8**,** 52.

SMITH, P. F., DICENZO, R. & MORSE, G. D. 2001. Clinical pharmacokinetics of non-nucleoside reverse transcriptase inhibitors. *Clin Pharmacokinet,* 40**,** 893-905.

SORIANO-SARABIA, N., BATESON, R. E., DAHL, N. P., CROOKS, A. M., KURUC, J. D., MARGOLIS, D. M. & ARCHIN, N. M. 2014. Quantitation of replication-competent HIV-1 in populations of resting CD4+ T cells. *J Virol,* 88**,** 14070-7.

SOUSA, A. E., CARNEIRO, J., MEIER-SCHELLERSHEIM, M., GROSSMAN, Z. & VICTORINO, R. M. 2002. CD4 T cell depletion is linked directly to immune activation in the pathogenesis of HIV-1 and HIV-2 but only indirectly to the viral load. *J Immunol,* 169**,** 3400-6.

STEIN, B. S. & ENGLEMAN, E. G. 1990. Intracellular processing of the gp160 HIV-1 envelope precursor. Endoproteolytic cleavage occurs in a cis or medial compartment of the Golgi complex. *J Biol Chem,* 265**,** 2640-9.

STRAIN, M. C., LADA, S. M., LUONG, T., ROUGHT, S. E., GIANELLA, S., TERRY, V. H., SPINA, C. A., WOELK, C. H. & RICHMAN, D. D. 2013. Highly precise measurement of HIV DNA by droplet digital PCR. *PLoS One,* 8**,** e55943.

STURDEVANT, C. B., JOSEPH, S. B., SCHNELL, G., PRICE, R. W., SWANSTROM, R. & SPUDICH, S. 2015. Compartmentalized replication of R5 T cell-tropic HIV-1 in the central nervous system early in the course of infection. *PLoS Pathog,* 11**,** e1004720.

SVEDHEM-JOHANSSON, V., PUGLIESE, P., BROCKMEYER, N. H., THALME, A., MICHALIK, C., ESSER, S., BARLET, M. H., NAKONZ, T. & JIMENEZ-EXPOSITO, M. J. 2013. Long-term gender-based outcomes for atazanavir/ritonavir (ATV/r)- containing regimens in treatment-experienced patients with HIV. *Curr HIV Res,* 11**,** 333-41.

SWIGGARD, W. J., BAYTOP, C., YU, J. J., DAI, J., LI, C., SCHRETZENMAIR, R., THEODOSOPOULOS, T. & O'DOHERTY, U. 2005. Human immunodeficiency virus type 1 can establish latent infection in resting CD4+ T cells in the absence of activating stimuli. *J Virol,* 79**,** 14179-88.

SWINDELLS, S., DIRIENZO, A. G., WILKIN, T., FLETCHER, C. V., MARGOLIS, D. M., THAL, G. D., GODFREY, C., BASTOW, B., RAY, M. G., WANG, H., COOMBS, R. W., MCKINNON, J., MELLORS, J. W. & TEAM, A. C. T. G. S. 2006. Regimen simplification to atazanavir-ritonavir alone as maintenance antiretroviral therapy after sustained virologic suppression. *JAMA,* 296**,** 806-14.

SWINGLER, S., BRICHACEK, B., JACQUE, J. M., ULICH, C., ZHOU, J. & STEVENSON, M. 2003. HIV-1 Nef intersects the macrophage CD40L signalling pathway to promote resting-cell infection. *Nature,* 424**,** 213-9.

TATHAM, L. M., RANNARD, S. P. & OWEN, A. 2015. Nanoformulation strategies for the enhanced oral bioavailability of antiretroviral therapeutics. *Ther Deliv,* 6**,** 469-90.

TENORIO, A. R., ZHENG, Y., BOSCH, R. J., KRISHNAN, S., RODRIGUEZ, B., HUNT, P. W., PLANTS, J., SETH, A., WILSON, C. C., DEEKS, S. G., LEDERMAN, M. M. & LANDAY, A. L. 2014. Soluble markers of inflammation and coagulation but not T-cell activation predict non-AIDS-defining morbid events during suppressive antiretroviral treatment. *J Infect Dis,* 210**,** 1248-59.

TINCATI, C., DOUEK, D. C. & MARCHETTI, G. 2016. Gut barrier structure, mucosal immunity and intestinal microbiota in the pathogenesis and treatment of HIV infection. *AIDS Res Ther,* 13**,** 19.

TITANJI, B. K., AASA-CHAPMAN, M., PILLAY, D. & JOLLY, C. 2013. Protease inhibitors effectively block cell-to-cell spread of HIV-1 between T cells. *Retrovirology,* 10**,** 161.

VAN DER RYST, E. & WESTBY, M. 2007. Changes in HIV-1 co-receptor tropism for patients participating in the maraviroc Motivate 1 and 2 clinical trials. *Program and abstracts of the 47th Interscience Conference on Antimicrobial Agents and Chemotherapy.* Chicago, IL.

VILASECA, J., ARNAU, J. M., BACARDI, R., MIERAS, C., SERRANO, A. & NAVARRO, C. 1982. Kaposi's sarcoma and toxoplasma gondii brain abscess in a Spanish homosexual. *Lancet,* 1**,** 572.

VON STOCKENSTROM, S., ODEVALL, L., LEE, E., SINCLAIR, E., BACCHETTI, P., KILLIAN, M., EPLING, L., SHAO, W., HOH, R., HO, T., FARIA, N. R., LEMEY, P., ALBERT, J., HUNT, P., LOEB, L., PILCHER, C., POOLE, L., HATANO, H., SOMSOUK, M., DOUEK, D., BORITZ, E., DEEKS, S. G., HECHT, F. M. & PALMER, S. 2015. Longitudinal Genetic Characterization Reveals That Cell Proliferation Maintains a Persistent HIV Type 1 DNA Pool During Effective HIV Therapy. *J Infect Dis*.

WAGNER, T. A., MCLAUGHLIN, S., GARG, K., CHEUNG, C. Y., LARSEN, B. B., STYRCHAK, S., HUANG, H. C., EDLEFSEN, P. T., MULLINS, J. I. & FRENKEL, L. M. 2014. HIV latency. Proliferation of cells with HIV integrated into cancer genes contributes to persistent infection. *Science,* 345**,** 570-3.

WALZER, P. D., PERL, D. P., KROGSTAD, D. J., RAWSON, P. G. & SCHULTZ, M. G. 1974. Pneumocystis carinii pneumonia in the United States. Epidemiologic, diagnostic, and clinical features. *Ann Intern Med,* 80**,** 83-93.

WARD, M. J., LYCETT, S. J., KALISH, M. L., RAMBAUT, A. & LEIGH BROWN, A. J. 2013. Estimating the rate of intersubtype recombination in early HIV-1 group M strains. *J Virol,* 87**,** 1967-73.

WATTS, J. M., DANG, K. K., GORELICK, R. J., LEONARD, C. W., BESS, J. W., JR., SWANSTROM, R., BURCH, C. L. & WEEKS, K. M. 2009. Architecture and secondary structure of an entire HIV-1 RNA genome. *Nature,* 460**,** 711-6.

WEBER, J. 2001. The pathogenesis of HIV-1 infection. *Br Med Bull,* 58**,** 61-72.

WIDNEY, D., GUNDAPP, G., SAID, J. W., VAN DER MEIJDEN, M., BONAVIDA, B., DEMIDEM, A., TREVISAN, C., TAYLOR, J., DETELS, R. & MARTINEZ-MAZA, O. 1999. Aberrant expression of CD27 and soluble CD27 (sCD27) in HIV infection and in AIDS-associated lymphoma. *Clin Immunol,* 93**,** 114-23.

WILKIN, T. J., MCKINNON, J. E., DIRIENZO, A. G., MOLLAN, K., FLETCHER, C. V., MARGOLIS, D. M., BASTOW, B., THAL, G., WOODWARD, W., GODFREY, C., WIEGAND, A., MALDARELLI, F., PALMER, S., COFFIN, J. M., MELLORS, J. W. & SWINDELLS, S. 2009. Regimen simplification to atazanavir-ritonavir alone as maintenance antiretroviral therapy: final 48-week clinical and virologic outcomes. *J Infect Dis,* 199**,** 866-71.

WILLIAMS, J. P., HURST, J., STOHR, W., ROBINSON, N., BROWN, H., FISHER, M., KINLOCH, S., COOPER, D., SCHECHTER, M., TAMBUSSI, G., FIDLER, S., CARRINGTON, M., BABIKER, A., WEBER, J., KOELSCH, K. K., KELLEHER, A. D., PHILLIPS, R. E., FRATER, J. & INVESTIGATORS,

S. P. 2014. HIV-1 DNA predicts disease progression and post-treatment virological control. *Elife,* 3**,** e03821.

WONG, J. K., HEZAREH, M., GUNTHARD, H. F., HAVLIR, D. V., IGNACIO, C. C., SPINA, C. A. & RICHMAN, D. D. 1997. Recovery of replication-competent HIV despite prolonged suppression of plasma viremia. *Science,* 278**,** 1291-5.

WU, Y., BEDDALL, M. H. & MARSH, J. W. 2007. Rev-dependent indicator T cell line. *Curr HIV Res,* 5**,** 394-402.

YANG, H., NKEZE, J. & ZHAO, R. Y. 2012. Effects of HIV-1 protease on cellular functions and their potential applications in antiretroviral therapy. *Cell Biosci,* 2**,** 32.

YOUNAS, M., PSOMAS, C., REYNES, J. & CORBEAU, P. 2016. Immune activation in the course of HIV-1 infection: Causes, phenotypes and persistence under therapy. *HIV Med,* 17**,** 89-105.

ZDANOWICZ, M. M. 2006. The pharmacology of HIV drug resistance. *Am J Pharm Educ,* 70**,** 100.

ZHANG, L., RAMRATNAM, B., TENNER-RACZ, K., HE, Y., VESANEN, M., LEWIN, S., TALAL, A., RACZ, P., PERELSON, A. S., KORBER, B. T., MARKOWITZ, M. & HO, D. D. 1999. Quantifying residual HIV-1 replication in patients receiving combination antiretroviral therapy. *N Engl J Med,* 340**,** 1605-13.

ZUBKOVA, I., DUAN, H., WELLS, F., MOSTOWSKI, H., CHANG, E., PIROLLO, K., KRAWCZYNSKI, K., LANFORD, R. & MAJOR, M. 2014. Hepatitis C virus clearance correlates with HLA-DR expression on proliferating CD8+ T cells in immune-primed chimpanzees. *Hepatology,* 59**,** 803-13.

Additional Bibliography

INTERNATIONAL COMMITTEE ON TAXONOMY OF VIRUSES (2002). "61. Retroviridae". National Institutes of Health. Archived from the original on 2006-06-29. Retrieved 2012-06-25.

INTERNATIONAL COMMITTEE ON TAXONOMY OF VIRUSES (2002). "61.0.6. Lentivirus". National Institutes of Health. Archived from the original on 2006-04-18. Retrieved 2012-06-25.

UNAIDS, 2016 consulted on 03/07/2016. Available at http://www.unaids.org/sites/default/files/media_asset/UNAIDS_FactSheet_en.pdf.

HIV SEQUENCE DATABASE, last modified on 05/04/2016. Available at http://www.hiv.lanl.gov/content/sequence/HIV/CRFs/CRFs.html.

EACS GUIDELINES VERSION 8.0, 2015. Available at http://www.eacsociety.org/files/guidelines_8.0-english-revised_20160610.pdf